HYPERBRANCHED POLYMERS AND OTHER HIGHLY BRANCHED TOPOLOGIES IN THE MODIFICATION OF THERMALLY AND UV CURED EXPOXY RESINS

David Foix Tajuelo

Dipòsit Legal: T-1719-2011

David Foix Tajuelo

Hyperbranched Polymers and Other Highly Branched Topologies in the Modification of Thermally and UV Cured Epoxy Resins

PhD THESIS

Supervised by Dra. Àngels Serra i Albet and
Dr. Xavier Ramis Juan

Departament de Química Analítica i Química Orgànica

UNIVERSITAT ROVIRA I VIRGILI

Tarragona 2011

UNIVERSITAT ROVIRA I VIRGILI

Departament de Química Analítica i Química Orgànica
C/ Marcel·lí Domingo s/n
Campus Sescelades
43007, Tarragona
Telf. 977 559 769
Fax. 977 558 446

Àngels Serra Albet, Catedràtica del Departament de Química Analítica i Química Orgànica de la Universitat Rovira i Virgili; i Xavier Ramis Juan, Catedràtic del Departament de Màquines i Motors Tèrmics de la ETSEIB de la Universitat Politècnica de Catalunya,

FEM CONSTAR que el present treball, que porta per títol “Hyperbranched Polymers and Other Highly Branched Topologies in the Modification of Thermally and UV Cured Epoxy Resins”, que presenta David Foix Tajuelo per a l’obtenció del títol de Doctor, ha estat realitzat sota la nostra direcció i que compleix els requisits per a poder optar a la Menció Europea.

Tarragona, 20 de setembre de 2011

Dra. Àngels Serra i Albet

Dr. Xavier Ramis Juan

UNIVERSITAT ROVIRA I VIRGILI
HYPERBRANCHED POLYMERS AND OTHER HIGHLY BRANCHED TOPOLOGIES IN THE MODIFICATION OF THERMALLY AND UV CURED EXPOXY RESINS
David Foix Tajuelo
DL:T-1719-2011

En primer lloc vull donar les gràcies a la Dra. Àngels Serra per l'oportunitat que em va donar ara fa cinc anys de realitzar la tesi al seu grup, així com pel seu ajut en la realització de la mateixa, però sobretot per la paciència que ha tingut amb mi des del primer dia fins a l'últim. També vull agrair al Dr. Xavier Ramis per tota l'ajuda prestada durant el transcurs de la tesi, per les discussions sobre ciència i per haver estat disposat a donar un cop de mà en qualsevol cosa i en tot moment.

Vull donar les gràcies a tots els professors de l'àrea de Química Orgànica per haver estat disponibles a ajudar en tot moment.

Vull agrair al Dr. Francesc Ferrando del Departament 'Enginyeria Mecànica de la URV tota l'ajuda proporcionada en la realització d'assajos mecànics i haver estat sempre disposat a trobar solucions als problemes pràctics que ens hem anat trobant al llarg d'aquests anys. També vull agrair al Dr. Emilio Jiménez Piqué Departament de Ciència dels Materials i Enginyeria Metal·lúrgica de la UPC per la realització de les mesures de nanoindentació.

Vorrei ringraziare il Dr. Marco Sangermano, non solo per avermi dato l'opportunità di lavorare con lui (lasciandomi anche un pezzo del suo ufficio...), ma anche per essere stato sempre pronto ad aiutarmi in tutte le difficoltà. Ringrazio, inoltre, tutte le persone che ho conosciuto sia lavorando nel suo laboratorio (Fede, Enrica, Sophie, Lorenzo, etc.) che fuori (Manu, Simona, etc) per avermi aiutato ad avere una bel periodo di permanenza a Torino.

I would like to thank Prof. Brigitte Voit, for giving me the opportunity to work for one month in her group in Dresden, as well as to Dr. Albena Lederer. Also, I would like to thank the colleagues I met there (Michael, Susi, Anna) for the good times I had outside the laboratory and for being so nice with me even after Spain beat Germany in the final of the Eurocup.

També vull donar les gràcies als tècnics tant del departament (Juan Luis, Tere, Thaís) com del servei de recursos (Ramón, Miguel, Mercè, Rita, Lukas, etc.) i d'Enginyeria Mecànica (Josep) per que sense la seva feina aquesta tesi no hagués estat possible. Gràcies també a l'Avelina, l'Eulàlia i l'Olga, per fer-me més fàcil tota la burocràcia durant aquests anys.

Els bons moments que he passat durant aquesta tesi són en gran part deguts als companys que he tingut aquests anys. Alguns ja els coneixia abans de començar: Vanessa, y tanto si te conocía de antes, de muuuuucho antes, yo creo que casi que nos conocimos en blanco y negro; Isildur, segurament una de les millors persones que he conegut i de les més freaks també; Pep, un crack al laboratori i també de festa; la Vero i l'Ari, que sapigueu que jo no m'he posat ni la meitat de nerviós durant el tram final de la tesi, oi que fa ràbia.

Altres els vaig conèixer durant la tesi, espero no deixar-me'n a cap. Començo pels que ja estaven per la uni abans que jo comencés: els que estaven a "sucres": l'Omar, la Patri i el Benito; la Lidia, que quan ella acabava jo tot just començava i vam tenir moltes xerrades que ara entenc millor; la Mercé, tant callada com és; Lucas, del que no digo todos sus apellidos por no alargarme y que siente el metal; Aitor, pedazo de cocinero y cantante; Marta, una de las personas más trabajadoras que he visto nunca; Marisa, que era e imagino que seguirà siendo muy competitiva en los deportes; la Silvana amb qui em vaig barallar més d'una vegada però l'aprecio molt; la Míriam, la Pava pa' que ens entenguem, que és de lluny la més guai en el món dels científics; Asta y Marjorie que por su "culpa" y la del montón de chocolate que traen al laboratorio peso 10 kg más; Cristina la voz del laboratorio, que me ha amenizado estos últimos tiempos; Surya, que empezó la tesi soltero y la terminará como un padre de família responsable; Adrian, foc, fum y otras muchas palabras que todavia le quedan por aprender; la Lluch, que de tant bona xiqueta que és, és molt divertit gastar-li bromes perquè sempre pica; l'Isma, un paio molt serio al cafè, però que guarda les forces per a quan surt de festa; Rodolfo, que una vez, creo que por error, passo el balón jugando a futbol; Camilo, nunca pensé que existiera alguien más tranquilo que yo hasta que lo conocí; Maryluz, que nunca me quiere traer el souvenir típico de su país que quiero; l'Irene, l'organitzadora oficial del departament; la Mariam i el Xavi, que de tant en tant ens acompanyen en el cafè "psicològic"; tos els "nous" Emma, Guasch, Sebas, Montaner, Ignasi, Alev, Zeynep, podeu estar feliços, sou els que m'heu hagut d'aguantar menys temps; la Idoia, sempre contenta i que és molt més morena que jo; el Xavier Fernández, que ara el tenim per aquí a províncies, i amb qui he compartit molts congressos; la Jessi que va fer els seus pinets científics al nostre labo però en va saber escapar; Belén, que vino de tierras gallegas y fue durante unos meses mi compañera de mesa. I he deixat a la Mireieta pel final per a que anés llegint i s'enfadés per no veure el seu nom. Guapeta de cara, ja no serà res el mateix sense tenir-te a la taula del costat.

Tampoco quiero dejar de nombrar a la "gente de Ingeniería" que he conocido estos años: Anton, excelente; Vero, que es una chica muy maja, que da hasta un poco de rabia de lo maja que es; Susana, que me cae bien aún siendo del Madrid; Beteley, que diusssss; Luis, el político, Oscar, siempre tan correcto; Sven, que es un crack del Volley, etc.

També vull tenir un record pel meus amics de tota la vida, el Gerard, el Masgu, i sobretot pel Busi, que ens coneixem ja de tota una vida i que ha estat, a més, un gran company de pis durant tot aquest temps. Sense ell de ben segur la tapa no seria tan maca ni la tesi tindria un tipus de lletra tan bonic. Ah, i també vull donar les gracies a Marlotino, el meu gos, per no haver-se menjat aquesta tesi.

Debo agradecer, y con un párrafo aparte para no ser menos, al Dr. del Río y a Mayra, o como ella prefiere Señora del Río. A Kike lo conocí nada más empezar el doctorado y debo decir que por muy gañan que sea es un pedazo de doctor y un buen amigo. A Mayra la conocí un año después, y con sus locurones y frikadas hace que piense que yo en el fondo soy casi normal, una amiga así no tiene precio. Ah, y también quiero agradecer a sus gatos que me dejaran limpiarles la caja de arena unas cuantas veces sin agredirme. Total, que los cuatro son tan buenos tan buenos, que casi parece que no sean españoles!!!

Grazie Letizia, per avere fatto con me l'ultimo pezzo di strada che mi ha portato a finire il dottorato e per le strade che faremo insieme d'ora in poi.

Als meus pares i a la meva família a qui els hi dec tot.

Table of Contents

Chapter 1

General Introduction and Scope

1.1 Epoxy Thermosets and Curing Systems

Epoxy resins are a class of high-performance thermosetting polymers, which display a unique combination of properties. These outstanding physical properties exhibited by epoxy resins include:

- No volatiles given off during cure
- Compatibility with a great number of materials
- Strength and durability
- Adhesion
- Corrosion, thermal and chemical resistance
- Electrical insulation

Taking all of these into account is no wonder that this type of thermosets has been commercially available for more than a half-century.[1] The range of application of epoxy resin is so large that comprises industries going from the aerospace to electronics or textile. Table 1.1 shows some of these applications.

In 2006, the epoxy industry was estimated to be $5 billion in North America and about $16.1 billion worldwide. This market is made up of approximately 50-100 manufacturers of basic or commodity epoxy resins and hardeners.

Impacted by the global economic slump, the epoxy market size declined to $15.8 billion in 2009, almost to the level of 2005. In some regional markets it even decreased nearly 20%. The current epoxy market is experiencing a positive growth as the global economy revives. With an

[1] E. M. Petrie. *Epoxy adhesive formulations.* McGraw-Hill, New York, 2006.

annual growth rate of 3.5 - 4%, the epoxy market is expected to reach $17.7 billion by 2012 and $21.35 by 2015. Higher growth rate is foreseen thereafter due to stronger demands from epoxy composite market and epoxy adhesive market.[2]

Table 1.1 Common Applications for Epoxy Resins.

Aircraft and Aerospace:	Chemical:
Structural parts of aircraft, spacecraft and satellites	Linings for storage tanks
Adhesives	Chemical plant including coatings
Aircraft paints and coatings	Pipes and pipe linings
Automobile:	Filters
Automotive primers and primer surfaces	Electrical:
Sealers	Switchgear construction and insulation
Adhesives	Turbine alternator insulation
Structural components	Electric motor insulation
Racing car bodies	Cable jointing
Tooling compounds	Coatings for domestic electrical appliances
Ignition coil impregnators	Electronic:
Construction:	Printed-circuit boards
Industrial flooring	Packaging of components
Grouts for roads and bridges	Encapsulation
Antiskid road surfaces	Adhesives
Tooling compounds	Food and beverage:
Repair compounds	Can and drum coatings
Adhesives	Coatings for flexible tubes
Sealants	Marine:
Pipes	Primers and protective coatings for ships and marine structures
Maintenance paints	Leisure:
Coil coated steel	Fishing rods
Textile:	Tennis rackets
Equipment parts	Gold club shafts
Glass and carbon fiber sizing agents	Bicycle frames

From the point of view of chemistry, epoxy resins are prepared from monomers containing two or more epoxy groups in its structure. The first system used was based on the well known diglycidyl ether of bisphenol A (DGEBA). Two researchers[3] share the honor of being the inventors of such resin: P. Castan, who at that time was employed by Ciba-Geigy (at present Huntsman), and O. Greenlee who developed the preparation of DGEBA for a small company acquired some years later by Shell. The commercialization of this resin dates back to 1940.[4]

[2] *Market Report: World Epoxy Resin Market*. Acmite Market Intelligence, **2010**.
[3] H. Lee, K. Neville, K. Handbook of Epoxy Resins. McGraw-Hill, New York, **1967**.
[4] P. Castan. Swiss Pat. 211,116, **1940**.

The reaction, still used nowadays, to obtain DGEBA epoxy resins is depicted in **Figure 1.1**. It is prepared by reacting bisphenol A with epichlorohydrin in the presence of a strong basic media such as NaOH. Depending on the ratio between the two reactants the molecular weight of the resulting resin can vary and thus it is possible to find liquid, waxy or solid DGEBA resins.

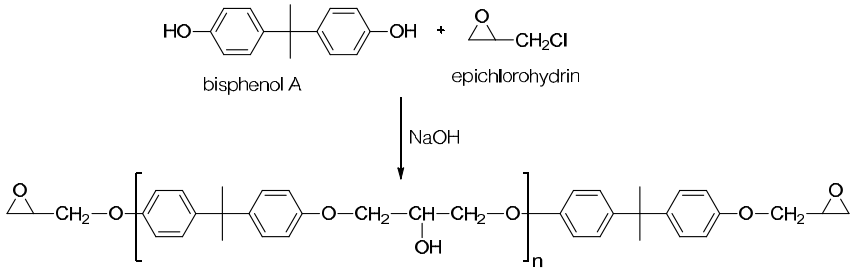

Figure 1.1 Scheme of the synthesis of DGEBA.

Since epoxy resins posses so many different applications that require very different properties, nowadays a great variety of epoxy monomers apart from DGEBA are commercialized. Some of the most important are collected in **Table 1.2**. Depending on the final use of the resin (coatings, sealant, painting, etc) or the way of carrying out the polymerization, a different monomer may be chosen.

Table 1.2 Chemical structure of some of the most common epoxy resins.

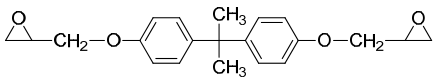 DGEBA	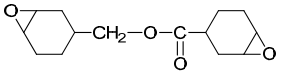 Cycloaliphatic
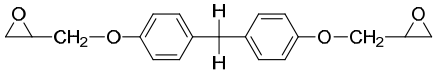 DGEBF	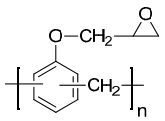 Epoxy Novolac
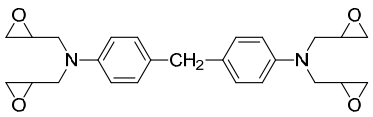 TGMDA	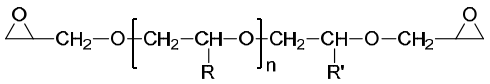 Aliphatic Poly(glycol) Diepoxide

Epoxy resins are capable of reacting with different active compounds known as curing agents (with or without catalyst) or with themselves (via an initiator) to form solid, crosslinked materials. This transformation is generally referred to as curing.[5] Depending on the particular details of the epoxy formulation, curing may be accomplished with the application of external heat (in some cases it works also at room temperature), or with the application of an external source of energy other than heat such as ultraviolet (UV) or electron beam (EB) energy.

The following sections explain into detail the most used epoxy systems divided into thermal and photochemical curing.

[5] C. A. May. *Epoxy Resins. Chemistry and Technology*, 2nd edition. Marcel Dekker, New York, **1988**.

1.1.1 Thermal Curing of Epoxy Resins

The most extended way of promoting the curing reaction is the use of heat. Depending on the curing agent, the temperature required to start the curing can vary from room temperature to more than 200 °C. In general, in what we are calling thermal systems, one can distinguish two types: (a) stochiometric systems, or those that require a certain amount of a second molecule with active functional groups to react with the epoxides of the resin and (b) catalytic systems where homopolymerization takes place initiated either in anionic or cationic conditions.

Stochiometric Systems

The first curing agents that will be discussed are primary and secondary amines. They were the first curing agents used, concretely diethylenetriamine and triethylenetetramine, but nowadays the library of molecules available is huge. The requirement they must fulfill is they must be multinfunctional (more than two) considering that primary amines account for a functionality of two and secondary for a functionality of one.

Aliphatic amines are able to react with epoxides as depicted in **Figure 1.2**. In this case the reaction consists of a polycondensation between the amines and the epoxide groups. Therefore the kinetics of the process is that of a step-growth reaction. Usually when the concentration of epoxy groups is equal to or lower than the concentration of NH groups, side reactions do not take place.

Both primary and secondary react rapidly with epoxy groups at low temperature to form three-dimensional crosslinked structures. However, they can also be cured at elevated temperatures to provide a more densely crosslinked structure with better mechanical properties, elevated-temperature performance and chemical resistance. Other amines, such as aromatic or cycloaliphatic, are less reactive and generally require higher curing temperatures.

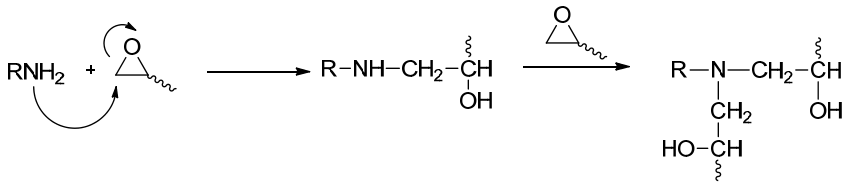

Figure 1.2 Mechanism of reaction between epoxides and primary and secondary amines.

After primary and secondary amines, acid anhydrides are the next most important class of epoxy curing agents. The reaction of anhydrides with epoxy groups is complex, with several competing reactions capable of taking place. The most significant reaction mechanisms are as follows:

1. The opening of the anhydride ring with an alcoholic hydroxyl forms the monoester.
2. Subsequent to the opening of the ring, the nascent carboxylic group reacts with the epoxy to provide an ester linkage.
3. The epoxy groups react with nascent or existing hydroxyl groups, catalyzed by the acid, producing an ether linkage.

At low temperatures, the ether and ester reactions take place up to the same extent while at higher temperatures the ester linkage is predominant. The presence of catalysts such as tertiary amines, metallic salts and imidazoles can change the balance of ester-ether linkages and at the same time accelerate the curing.

Some of the most commonly used anhydrides are depicted in **Figure 1.3**. In general, epoxy resins cured with anhydrides present good overall mechanical properties. However, as occurs often with stochiometric systems, the ratio of epoxy/anhydride is a key factor in order to achieve the best properties.

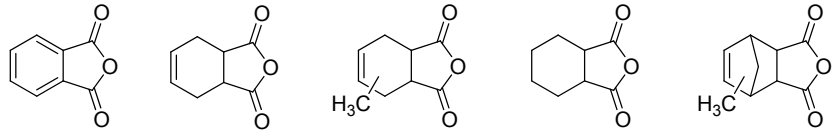

Figure 1.3 Chemical structure of some of the most extended anhydride curing agents: (a) Phtalic anhydride; (b) Tetrahydrophtalic anhydride; (c) Methyl tetrahydrophtalic anhydride; (d) Hexahydrophtalic anhydride; (e) Methyl nadic anhydride.

Other stoichiometric curing agents are for example polyamides and aminoamides, that offer moderately good shear strength, temperature resistance, and environmental resistance; polysulfides and mercaptanes, that although have a main drawback in their disgusting oddor, allow obtaining resins with good properties in terms of flexibility; or even isocyanates.

Catalytic systems

The other big group of curing agents in thermal conditions are initiators. Those are molecules that used in catalytic amounts promote the homopolymerization of epoxides via ring opening polymerization (ROP). This mechanism is similar in terms of kinetics to polyaddition since presents an initiation step, a propagation and finally a termination. In general, one can say that there are three types of ROPs depending on the propagation mechanism: anionic, cationic and ionic-coordinative.[6] This last one is used in the polymerization of epoxides where high molecular weights and stereoselectivity are required but, to the best of our knowledge, they are not used in the field of thermosets.

There are many polymerization initiators to promote the reaction of epoxides in anionic conditions, such as potassium terbutoxide (t-BuOK) or methyl lithium (MeLi),[7] but in the field of epoxy thermosets the most extended anionic initiators are tertiary amines.[5] Tertiary amines such as 1,8-Diazabicyclo[5.4.0]undec-7-ene (DBU), 4-(N,N-dimethylamino) pyridine (DMAP) or 1-methyl imidazole (MI) are some examples of them. The mechanism through which polymerization takes place is depicted in **Figure 1.4**. As can be seen, the first step is the opening of the epoxide by the amine forming an alcoxide. As can be appreciated in the figure, the presence of alcohols that can coordinate with epoxides promotes the initiation step speeding up the reaction. In a following step this alcoxide can propagate the polymerization opening another epoxide and finally forming the crosslinked network.[8]

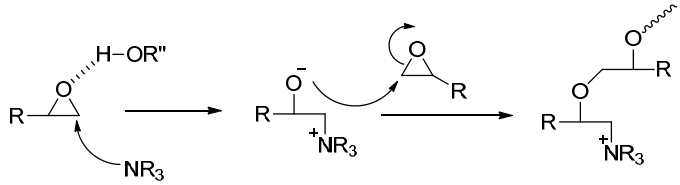

Figure 1.4 Mechanism of polymerization of epoxides catalyzed by amines.

[6] D. J. Brunelle. *Ring-Opening Polymerization: Mechanism, catalysts, structure and utility.* Hanser Publishers, Munich, **1993**.
[7] K. J. Ivin, T. Saegusa. *Ring-Opening Polymerization.* Elsevier Applied Science Publishers, London, **1984**.
[8] B. A. Rozenberg. *Adv. Polym. Sci.* **1986,** *75,* 113.

When the initiation step is catalyzed by Lewis acids, the propagation takes place via a cationic mechanism. $TiCl_4$, $AlCl_3$, $ZnCl_2$, BCl_3, $SiCl_4$, $FeCl_3$, $MgCl_2$, $SbCl_5$ are Lewis acids used as catalysts, but the most extended one is BF_3/amine.[5,9] In recent years also lanthanide triflates have demonstrated to be good cationic initiators.[10-12]

The mechanism of the propagation step for the cationic polymerization of epoxides is shown in **Figure 1.5**. In that case it is more complex than the anionic ROP. As first described by Kubisa and Penczek,[13] there are two propagation mechanisms that coexist: activated chain end (ACE) and active monomer (AM). Both mechanisms start with the coordination of the initiator with the epoxide to promote the ring opening. ACE mechanism consists in the reaction between an activated epoxide and another. On that way the activated epoxide is always linked to the growing chain. On the contrary, AM mechanism requires a hydroxyl group to first open an activated epoxide. Then, there is an intermolecular interchange of protons with an epoxide that becomes now activated. On that way is always the monomer the activated epoxide.

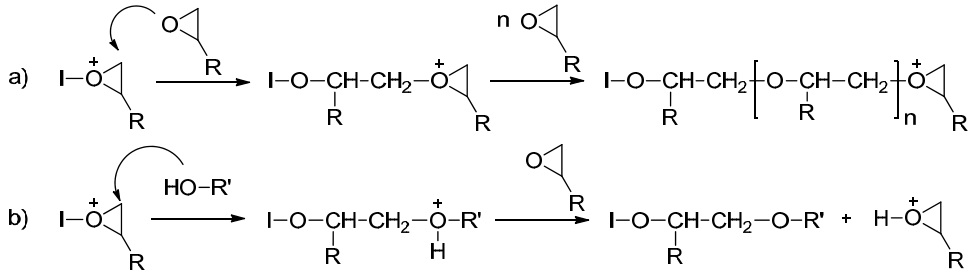

Figure 1.5 Mechanism of the propagation of the cationic ROP of epoxides: a) ACE and b) AM.

1.1.2 UV Curing of Epoxy Resins

Radiation curing technologies are expanding rapidly on an industrial scale. These new technologies use light beams to start photochemical and chemical reactions in organic materials leading to the formation of new polymeric materials whose final uses may be encountered in various industrial areas. They continue to develop and provide a number of economical advantages over the usual thermal operation: rapid curing, low energy requirements, room-temperature treatment, non-polluting and solvent free formulations, and low costs.[14]

On the other hand they also have some drawbacks; being the most important ones the high initial economical investment that is required to work in UV conditions and that at least one substrate must be transparent to the radiant energy. Also the difficulty for the radiation to penetrate in thick films limits its range of application.

The main sources of energy for curing epoxy adhesives by radiation are electron beam (EB) and ultraviolet light (UV). Both provide instantaneous curing of resins that polymerize from a liquid to a solid when irradiated. The UV systems account for approximately 85 percent of the market for radiant cured adhesives, EB systems only account for about 10 percent, and the remainder 5% are visible and infrared light.[1]

---

[9] M. Tackie, G. C. Martin. *J. Appl. Polym. Sci.* **1993,** *48,* 793.
[10] P. Castell, M. Galià, A. Serra, J. M. Salla, X. Ramis. *Polymer* **2000,** *41,* 8465.
[11] K. N. Delfrey. *Rare Earths: Research and Applications*. Nova Science Publishers, New York, **2008**.
[12] S. Kobayashi, M. Sugiura, H. Kitagawa, W. W.-L. Lam. *Chem. Rev.* **2009,** *102,* 2227.
[13] P. Kubisa, S. Penczek. *Prog. Polym. Sci.* **1999,** *24,* 1409.
[14] J.P. Fouassier, J.F. Rabek. *Radiation Curing in Polymer Science and Technology*, Vol. I-IV, Elsevier London, **1993**.

Among UV systems one can distinguish between three types of polymerizations depending on the type of initiation: free-radical, anionic and cationic.

The mechanism of free-radical polymerization is depicted in **Figure 1.6**. First, the light source interacts with the photoinitiator (PI), which is a compound photosensible to UV light that in the case of free-radical polymerization yields a radical. Then this radical initiates the polymerization of the monomer. After that, propagation takes place and also termination occurs randomly. Some of the most common photoinitiators are benzophenone and 2,2-dimethoxy-2-phenylacetophenone.[15]

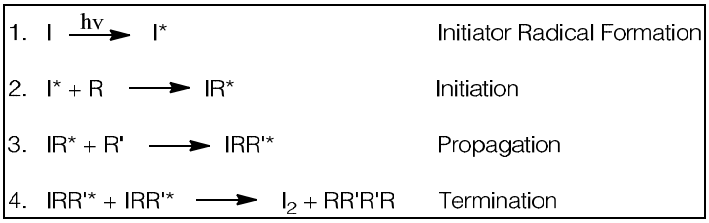

Figure 1.6 Free radical polymerization mechanism.

However, in epoxy thermosets the use of free-radical polymerization is limited to epoxy acrylate monomers. In addition to this limited range of applications, it presents some other problems such as it undergoes inhibition under oxygen atmosphere and the fact that the rate of polymerization experiences a rapid decrease when the light source is removed.[16]

Cationic photopolymerization is the most extended UV curing technique in epoxy thermosets since it exhibits several advantages when compared to free-radical photopolymerization. First of all, cationic photopolymerization is not inhibited by oxygen providing a significant practical advantage for industrial processes since it is not necessary to work in an oxygen free atmosphere to achieve highly crosslinked networks. Moreover, in contrast to the free-radical photopolymerization which experiences a rapid decrease in polymerization rate when the light source is removed (due to radical-radical termination reactions), the cationic polymerizations proceed long after the irradiation has ceased, consuming nearly all of the monomer. This process, called “dark reaction”, is the result of the ability of the acid specie formed by irradiation of the photoinitiator to continue the polymerization.[17]

From the mechanistic point of view, the only difference between thermal and UV cationic curing is the way in which the initiator is formed. In thermal systems the catalyst is present from the very beginning in the mixture and it is activated by thermal treatment. On the contrary, in UV curing, light is used to generate an acid by excitation of the photoinitiator, and then the curing reaction immediately starts.[14] The mechanism of propagation is analogous to the described in the previous section for cationic thermal curing (**Figure 1.5**).

Although there are other types of photoinitiators such as ferrocenium or arylselenium salts, triarylsulfonium and diaryliodonium salts represent the most widely used classes of cationic PI.[18] Properties like thermal stability and inactivity towards monomers at room temperature made these salts very attractive for practical application. The cation is the light-absorbing component and for this reason, its structure controls the UV absorption characteristics and the ultimate

---

[15] J. V. Koleske. *Radiation Curing of Coatings*. ASTM International, Bridgeport, **2002**.
[16] H. E. H Meijer. *Materials Science and Technology*. VCH, Germany, **1997**.
[17] S. P. Pappas. *Radiation Curing Science and Technology*. Plenum Press, New York, **1992**.
[18] J. V. Crivello *J. Polym. Sci. Part A: Polym. Chem.* **1999,** *37,* 4241.

thermal stability of the onium salt. However, the nature of the anion and its stability determines the strength of the acid formed during photolysis and its corresponding initiation efficiency. The nature of the anion also determines the character of the propagating ion pair. This has a direct impact on the kinetics of polymerization and whether termination can occur.[18]

The photosensitivity of diaryliodonium salts were firstly introduced by Ptitsyna *et al.*[19] but it was not until the 1970s when J.V. Crivello decided to apply them as photoinitiators in UV curing.[20,21] The general structure of these salts is depicted in **Figure 1.7**, being the most used counteranions BF_4^-, PF_6^-, AsF_6^- and SbF_6^- in ascending order of acidity. These counteranions are able to generate "superacids" with Hammett acidities (H_0) ranging respectively from -15 to -30.

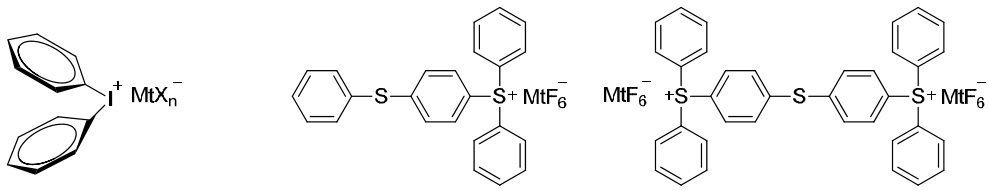

Figure 1.7 Schematic structure of diaryliodonium and triphenylsulphonium salts.

Figure 1.8 shows the mechanism through which the acidic specie is formed in a simplified way. The mechanism involves first the photoexcitation with UV light of the diaryliodonium salt and then the decay of the resulting excited singlet state with both heterolytic and homolytic cleavages of the carbon-iodine bond. Thus, free-radical, cationic, and cation-radical fragments are formed simultaneously. The aryl cations and aryliodine cation radicals generated during photolysis are highly reactive species and react further with solvents, monomers, or impurities to give protonic acids, $HMtX_n$ that can start the cationic polymerization.

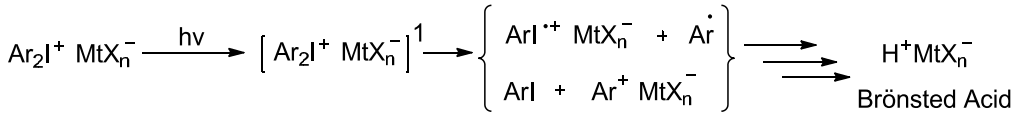

Figure 1.8 Schematic mechanism of formation of Brönsted acids from diaryl sulphonium salts.

Triarylsulphonium salts (**Figure 1.7**) are also able to form strong Brönsted acids through the same mechanism[22] but in their case, the heterolytic cleavage pathway is dominant, rather than the homolytic. On that way these salts are not photosensitized as readily as diaryliodonium. However, they present excellent thermal stability even in the presence of the most nucleophilic and reactive monomers.

Anionic UV curing has been attracting increasing interest from a technological point of view,[23] owing to the following profitable characteristics. This type of polymerization not only do not suffer from the inhibitory effect of atmospheric oxygen but also avoids problems derived from the presence of a photogenerated acid entrapped in cured materials that may bring about

---

[19] (a) O. A. Ptitsyna, M. E. Pudeeva, N. A. Belkevich, O. A. Reutov. *Dokl. Akad. Nauk.* **1965,** *163,* 383; (b) O. A. Ptitsyna, M. E. Pudeeva, N. A. Belkevich, O. A. Reutov. *Dokl. Akad. Nauk.* **1965,** *163,* 671.
[20] J. V. Crivello, J. H. W. Lain. *Journal of Polymer Science,* **1976,** *Symposium No. 56,* 383.
[21] J. V. Crivello, J. H. W. Lain. *Proceedings of Organic Coatings and Plastics Chemistry,* **1978,** *39,* 31.
[22] J. L. Dektar, N. P. Hacker. *J. Chem. Soc. Chem. Commun.* **1987,** 1592.
[23] K. Dietliker, R. Hüsler, J.-L. Birbaum, S. Ilga, S. Villeneuve, K. Studer, T. Jung, J. Benkhoff, H. Kura, A. Matsumoto, H. Oka. *Prog. Org. Coat.* **2007,** *58,* 146.

problems, for instance, the corrosion metal substrates and organic substances. Such a trouble may be eliminated by using a photogenerated base.

The strategy approaching anionic UV curing systems depends on whether the base generated from a photobase generator (PBG) is a primary or secondary amine to react with electrophiles[24,25] or a tertiary amine to accelerate base-catalyzed reactions. In this respect, various types of PBGs have been developed.[26] Representative PBG generating primary or secondary amines includes o-nitrobenzyl derivatives,[27] cobalt amine complexes,[28] acyl oximes[29] and urethane oximes.[30] Aliphatic tertiary amines can be generated by the photolysis of quaternary ammonium salts, such as the DBU derivatives patented by Baudin *et al*.[31]

1.1.3 Physical Transitions during the Curing Process

Regardless of the curing system, there are two main physical transitions that can take place during the curing process of a thermoset: gelation and vitrification. Gelation involves an abrupt change from a liquid-like to a solid-like behavior.[32] **Figure 1.9** illustrates the evolution of (zero-shear) viscosity, elastic modulus and fraction of soluble material (sol fraction) as a function of the conversion, and the gel point is indicated.

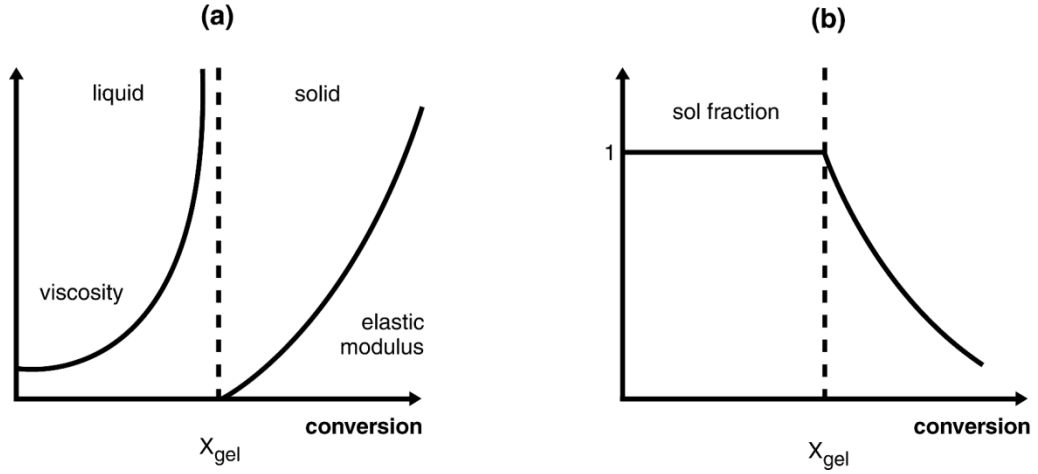

Figure 1.9 Evolution of physical properties of the thermosetting polymer as a function of conversion of reactive groups: (a) zero-shear viscosity and elastic modulus, (b) soluble fraction

Gelation occurs when one of the growing molecules reaches a mass so large that it interconnects every boundary of the system or, in other words, there is only one giant macromolecule present in the system. This means that its contribution to the total number of molecules is absolutely negligible and therefore the giant macromolecule does not contribute to

---

[24] J. F. Cameron, J. M. J. Fréchet. *J. Org. Chem.* **1990,** *55,* 5919.
[25] J. F. Cameron, C. G. Willson, J. M. J. Fréchet. *J. Am. Chem. Soc.* **1996,** *118,* 12925.
[26] M. Tsunooka, K. Suyama, H. Okamura, M. Shirai. *J. Photopolym. Sci. Technol.* **2006,** *19,* 65.
[27] E. J. Urankar, I. Brehm, Q. J. Niu, J. M. J. Fréchet, *Macromolecules* **1997,** *30,* 1304.
[28] C. Kutal, *Coord. Chem. Rev.* **2002,** *211,* 353.
[29] J. Lalevée, X. Allonas, J. P. Fouassier, H. Tachi, A. Izumitani, M. Shirai, M. Tsunooka, *J. Photochem. Photobiol. A: Chem.* **2002,** *151,* 27.
[30] K. Suyama, S. Nakao, M. Shirai, *J. Photopolym. Sci. Technol.* **2005,** *18,* 141.
[31] S. C. Turner, G. Baudin. *Eur. Pat. Appl.* 970085, **1997**.
[32] J-P. Pascault, H. Sauterau, J. Verdu, R. J. J. Williams. *Thermosetting Polymers*. Marcel Dekker, New York, **2002**.

the value of the number average molar mass of the polymer. This is reflected by the fact that $\bar{M}_n$ is unaffected by gelation. The situation is completely different for $\bar{M}_w$. As the mass fraction of the giant species is significant, its contribution to the $\bar{M}_w$ value largely prevails over contributions of the much smaller species. On that way a mathematical definition of gelation states that $\bar{M}_w \rightarrow \infty$ at $x = x_{gel}$. From the applicability point of view the gelation is very important since once a thermosets reaches that point it cannot be processed anymore.[32]

Vitrification is another physical transition that may take place during curing. The theoretical explanation to this transition is the reduction of the system's mobility through the formation of covalent bonds up to a point where the cooperative movements of large portions of the polymer, which are characteristic of rubbery and liquid states, are no longer possible and the curing reaction is stopped. In other words, if the T_g of the growing polymer is equal to the curing temperature the system vitrifies and cannot proceed the curing. On that way, this vitrification process depends on the curing temperature since the possibility of producing cooperative movements of fragments of the thermosetting polymer must increase with temperature. So, the conversion at which vitrification takes place increases with the curing temperature. It is worthy to note that if vitrification takes place at a given temperature, the curing process can be resumed at any time through a post curing at higher temperatures.[32]

1.2 Improvement of Epoxy Thermosets

As it has already put into evidence, epoxy resins present good overall properties. However they also present some drawbacks that limit their range of applications. Some of these, which will be discussed in more detail in the following sections, are their poor toughness which confers them low impact resistance, the shrinkage that undergo during the curing process or the fact that they cannot be removed from a substrate without damaging it. So it is not difficult to understand the need to find new strategies to overcome all of these problems without compromising the other good properties of the resin.

1.2.1 Toughness

In terms of structural applications epoxy resins are in general brittle and notch sensitive. As a result, tremendous effort has been focused on improving the toughness of such materials during past decades and many reviews in this area are available.[33,34] The aim of this section is to give a brief overview of the state of the art in epoxy toughening.

There are many approaches to the improvement of toughness in epoxy resins. The most classical ones, both based on increasing the flexibility of the final network and therefore lowering the T_g, have been the chemical modification of a given rigid epoxy backbone to a more flexible one or lowering the crosslink density by increasing the molecular weight of the epoxy monomers and/or decreasing the functionality of the curing agents.

However, the most successful strategy for improving toughness is the incorporation of a dispersed phase which can be either rigid or soft within the epoxy matrix.[35] Since toughness implies energy absorption, the presence of a second phase allows a better dissipation of energy. Among the second phases used stand out rubbers, thermoplastics and hard inclusions such as silica, glass beads, etc.

---

[33] J. I. Kroschwitz. *High Performance Polymers and Composites*. John Wiley & Sons, New York, **1991**.
[34] C. B. Arends. *Polymer Toughening*, Arends. Marcel Dekker, New York, **1996**.
[35] R. Bagheri, B. T. Marouf, R. A. Pearson. *J. Macromol. Sci. Part C: Polym. Rev.* **2009**, *49*, 201.

The research work on rubber modified epoxy resins was pioneered by McGarry.[36] Probably the rubber system that has attracted the most attention is the family of copolymers of butadiene and acrylonitrile that can be synthesized with carboxylic acid (CTBN) or amine groups (ATBN) both at the chain ends and pendent along the chain (**Figure 1.10**). When a mixture of rubber in epoxy is cured, rubber particles precipitate out as a second phase. However, the main disadvantage of this strategy is that high concentrations of rubber are required to meet the desired toughness improvements.

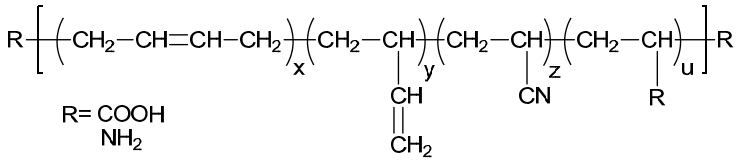

Figure 1.10 Chemical structure of CTBN (R=COOH) and ATBN (R=NH_2).

Other rubber-like particles such as core-shell particles have also been used for the same purpose. In this case, the particles are unreactive modifiers that are dispersed within the epoxy matrix, and can form microphases that help increasing toughness.

Interpenetrating polymer networks (IPNs) with two components, one highly crosslinked (glassy phase) and the other only slightly crosslinked (rubbery phase) is another methodology used in order to improve the toughness. In this case toughening is easily achieved but with a significant diminution of the glass transition temperature and modulus.[37]

In the last years hyperbranched polymers (HBPs) have demonstrated to be very interesting epoxy toughners. In the literature one can find examples of the use of HBPs[38,39] for this purpose. They are able to enhance the flexibility of the network and increase toughness without compromising other properties, such as hardness, modulus or T_g.[40] The improvement in toughness in the case of HBPs is attributed either to the flexibilizing effect induced by the homogeneous incorporation of the HBP or to local inhomogeneities created in the crosslinked network by the formation of phase separated nanoparticles[41] with good interfacial adhesion between phases. The particles hinder the propagation of a certain crack in the material as seen in **Figure 1.11**. Since the interaction between phases plays a key role in this toughness reinforcement mechanism, the structure of the HBP must be carefully selected in order to obtain the best results.

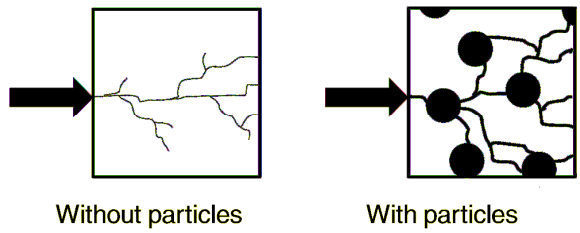

Figure 1.11 Crack expansion in materials with and without particles dispersed.

[36] F. J. McGarry, J. N. Sultan. *J. Polym. Sci.* **1973,** *13,* 29.
[37] X. Ramis, A. Cadenato, J. M. Morancho, J. M. Salla. *Polymer* **2001,** *42*, 9469.
[38] L. Boogh, B. Pettersson, J.-A. E. Månson. *Polymer* **1999,** *40,* 2249.
[39] D. Ratna, R. Varley, G. P. Simon. *J. Applied Polym. Sci.* **2003,** *89,* 2339.
[40] J-F. Fu, L-Y. Shi, S. Yuan, Q-D. Zhong, D-S. Zhang, Y. Chen, J. Wu. *Polym. Adv. Technol.* **2008**, *19*, 1597.
[41] J. Karger-Kocsis, J. Fröhlich, O. Gryshchuk, H. Kautz, H. Frey, R. Mülhaupt. *Polymer* **2004**, *45*, 1185.

Finally, one of the most recent strategies for improving toughness in epoxy resins is the preparation of nanostrucuterd materials. Over the past decades, considerable progress has been made toward understanding the relationship between morphological structures and the resulting properties of multi-component thermosetting blends.[42] It is accepted that the formation of nanostructures in multi-component thermosets can further optimize the interactions between the thermosetting matrix and the modifiers and thus the mechanical properties of materials have been significantly improved. This has been called "toughening by nanostructures".[43] For instance, Mülhaupt *et al.*[44,45] reported the modification of epoxy resin with a branched poly(ε-caprolactone)-*block*-polydimethylsiloxane-*block*-poly(ε-caprolactone) block copolymer. It was found that in the modified thermosets, spherical PDMS particles, about 20 nm in diameter, are uniformly dispersed in the continuous epoxy matrix. The inclusion of a small amount of the copolymer (e.g., 5 wt% or more) led to a significant increase in toughness of the materials.

Other block copolymers containing highly branched structures such as star polymers have been also reported to yield nanotructured materials. Recently, Meng *et al.*[46] have used a star-shaped block copolymer and have obtained phase separation in DGEBA matrix, and even increasing the T_g of the resulting thermosets.

1.2.2 Reworkability

One of the main applications of epoxy resins is in the field of coating microelectronic devices. It is estimated that more than 50 million computers are obsolete every year and with the current technology less than 25% of the printed circuits can be recycled. For that reason it is important to find epoxy technologies that allow the recovery of the coated device in order to be recycled.

The concept of reworkability in thermosets is related to the ability of a material to break-down under controlled conditions in order to be removed from a given substrate (**Figure 1.12**), but it does not mean that the polymeric material can be reused or recycled.

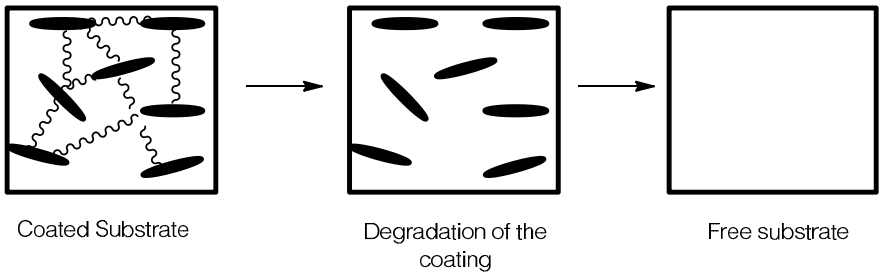

Figure 1.12 Scheme of the process of the elimination of a reworkable coating from a substrate.

In order to obtain reworkable epoxy thermosets the main strategy has been the introduction of thermally labile groups in the structure of the resin. One of the first approaches was the

[42] D.R. Paul and C.B. Bucknall. Chapter 13: Formulation and Characterization of Thermoset - thermoplastic Blends. In *Polymer Blends: Formulation and Perfomance*. John Wiley & Sons, New York, **2000**.
[43] L. Ruiz-Perez, G. J. Royston, J. P. A. Fairclough, A. J. Ryan. *Polymer* **2008,** *49,* 4475.
[44] U. Buchholz, R. Mülhaupt. *Polymer Prepr.* **1992,** *33,* 205.
[45] L. Könczöl, W. Döll, U. Buchholz, R. Mülhaupt. *J. Appl. Polym. Sci.* **1994,** *54,* 815.
[46] Y. Meng, X-H. Zhang,B-Y. Du,B-X. Zhou, X. Zhou, G-R. Qi. *Polymer* **2011,** *52,* 391.

introduction of di-sulphure linkages by Tesoro *et al.*[47,48] which allows the fragmentation of the thermoset with the temperature.

Other authors such as Wong *et al.*[49-51] proposed the use cycloaliphatic epoxy resins with carbonate groups in its structure as the one shown in **Figure 1.13**. Those thermosets were able to be degraded at temperatures below 300 ºC.

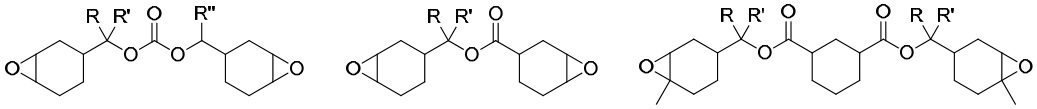

Figure 1.13 Chemical structure of the carbonate proposed by Wang and Wong, and the esters used by Ober *et al.*

Ober and coworkers[52-54] went further in this approach and prepared cycloaliphatic epoxy resins with ester groups highly substituted in β position. On that way the pyrolytic elimination of esters (**Figure 1.14**) is favored and allows the elimination of the coating at temperatures between 200 and 250 ºC.

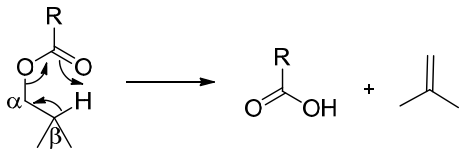

Figure 1.14 Mechanism of pyrolytic β-elimination of esters.

The strategies mentioned up to now present the limitation that in all cases the character of the resin in all cases was cycloaliphatic. To expand the range of application, Okamura *et al.*[55] proposed the use of di and trifunctional monomers with an aromatic ring in the middle (**Figure 1.15**). This ring allows obtaining more rigid networks.

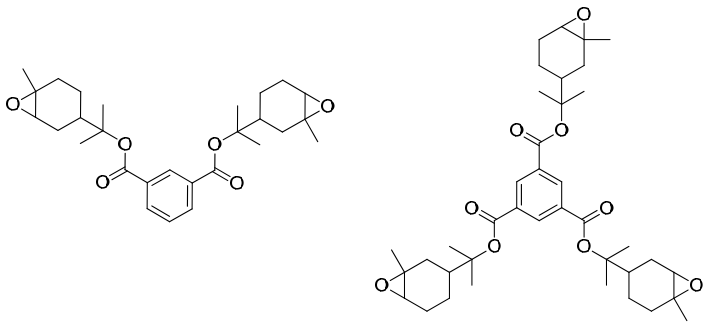

Figure 1.15 Chemical structure of the monomers proposed by Okamaura *et al.*

---

[47] G. C. Tesoro, V. R. Sastri. *J. Appl. Polym. Sci.* **1990,** *39,* 1439.
[48] V. R. Sastri, G. C. Tesoro. *J. Appl. Polym. Sci.* **1990,** *39,* 1425.
[49] L. Wang, H. Li, C. P. Wong. *J. Polym. Sci., Part A: Polym. Chem.* **1999,** *37,* 2991.
[50] L. Wang, H. Li, C. P. Wong. *J. Polym. Sci., Part A: Polym. Chem.* **1999,** *38,* 3771.
[51] H. Li, C. P. Wong. *IEEE Trans. Adv. Packag.* **2004,** *27,* 165.
[52] S. Yang, J. S. Chen, H. Körner, T. Breiner, C. K. Ober. *Chem. Mater.* **1998,** *10,* 1475.
[53] J. S. Chen, C. K. Ober, M. D. Poliks. *Polymer* **2002,** *43,* 131.
[54] J. S. Chen, C. K. Ober, M. D. Poliks, Y, Zhang, U. Wiesner, C. Cohen. *Polymer* **2004,** *45,* 1939.
[55] H. Okamura, K. Shin, M. Tsunooka, M. Shirai. *J. Polym. Sci.: Part A: Polym. Chem,* **2004,** *42,* 3685.

Following the pioneer work, many different thermally labile functional groups have been introduced in the epoxy monomer structure such as sulphones[56] and ureas.[57]

Another strategy that has been developed in recent years is the *in situ* formation of labile groups by cationic ring-opening copolymerization of epoxy resins with cyclic carbonates[58] or with lactones.[59] In these cases, carbonates or esters in the network are formed by polymerization of intermediate species: spiroorthocarbonates or espiroorthoesters respectively.

There are other monomers such as Meldrum's acid derivatives[60,61] that have also been copolymerized with DGEBA in order to introduce highly labile tertiary ester groups in the network.

1.2.3 Shrinkage

Shrinkage is another of the critical points of epoxy resins. The curing process entails shrinkage which is particularly critic in the field of coatings since, together with the difference in the thermal expansion coefficient (TEC) in respect to the substrate leads to the formation of microvoids and microcracks. Those can in turn lead to loosing adhesion with the substrate ruining the coating.[62]

One should distinguish between thermal and chemical shrinkage. During the curing process changes in temperature take place causing thermal shrinkage. This cannot be avoided although changes in the curing schedule help the network to relax better and therefore can be slightly reduced. It should be pointed out that in UV curing, if performed at room temperature this thermal shrinkage does not take place. On the other hand it also exist the so called chemical shrinkage. This shrinkage is caused by the chemical reactions that take place during curing and there are some strategies that will be discussed in this chapter to avoid it or at least reduce it as much as possible.

Chemical shrinkage is strongly linked to the polymerization mechanism (**Figure 1.16**). In poly addition reactions there is a change in molecular distance before and after curing, going from Van der Waals distances to covalent ones. In the case of poly condensation, also the elimination of small molecules contributes to increase the shrinkage, and the higher the size of the eliminated molecule the bigger is such increase.

Ring opening polymerization (ROP) is considered to undergo less shrinkage than the other two mechanisms described. This is due to the fact that per each Van der Waals distance that becomes a covalent bond there is one covalent bond going to a nearly Van der Waals distance. As a rule of thumb, increasing the size of the ring reduces the shrinkage. This effect is depicted in **Figure 1.16**.

Anyhow, all types of curing reactions present shrinkage. There are different strategies to try to overcome this. One of the first approaches was the introduction of inorganic inert charges such as silica, quartz or mica. Also it is possible to use polymeric charges, as for example

---

[56] Y. Shin, A. Kawaue, H. Okamura, M. Shirai. *Reac. Funct. Polym.* **2004,** *61,* 293.
[57] J. Malik, S. J. Clarson. *Polymer* **2002,** *43,* 2561.
[58] R. Cervellera, X. Ramis, J. M. Salla, A. Serra, A. Mantecón. J. Polym. Sci. Part A: Polym. Chem. **2006,** *44,* 4546.
[59] M. Arasa, X. Ramis, J. M. Salla, A. Mantecón, A. Serra. *Polym. Degrad. Stab.* **2007,** *92,* 2214.
[60] L. González, X. Ramis, J. M. Salla, A. Mantecón, A. Serra. *J. Polym. Sci. Part A: Polym. Chem.* **2006,** *44,* 6969.
[61] L. González, X. Ramis, J. M. Salla, A. Mantecón, A. Serra. *Polym Degrad Stab* **2007,** *92,* 596.
[62] R. K. Sadhir, M. R. Luck. *Expanding monomers. Synthesis, characterization and applications.* CRC Press, Boca Raton, **1992**.

polyurethane foams, PVC or polystyrene. However, these approaches significantly worsen other properties of the thermoset: lowers the T_g, reduces the toughness, increases the viscosity of the curing mixtures worsening the processability and in some cases even leads to the loss of transparency.

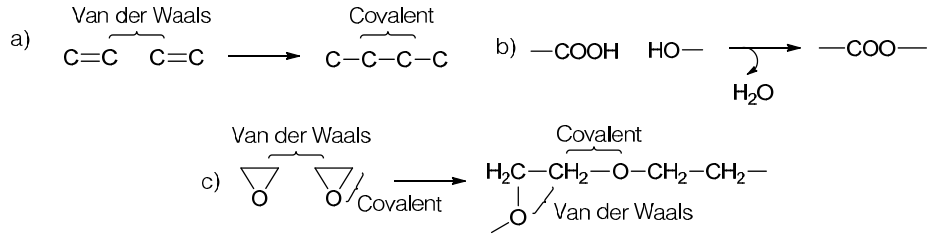

Figure 1.16 Scheme of distances before and after reaction for (a) poly addition; (b) poly condensation; and (c) ring opening polymerization.

It also exists another approach to the shrinkage reduction which is the use of the so called expanding monomers. This term was first coined by William J. Bailey in the 1970s.[63,64] It embraces a series of monomers that during polymerization not only do not undergo shrinkage but present expansion. These monomers are spiranic monomers that must follow the following criteria:

- The rings must be fused.
- There must be at least one heteroatom in each ring.
- The ring opening must be asymmetric.

Examples of monomers that follow these rules are spirocyclic orthoesters (SOE), spirocyclic ortho carbonates (SOC) or bicyclic orthoesters (BOE) (**Figure 1.17**) among others.

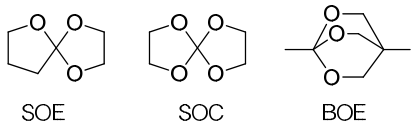

Figure 1.17 Examples of "expanding monomers".

Bailey,[64] by means of dilatometry, studied the volumetric expansion of the homopolymerization of spirocyclic orthoester, 1,4,6-trioxaspiro[4.4]nonane synthesized by Bodenbenner,[65] and observed an expansion of 0.1%.

Endo *et al.* have used expanding monomers to control the shrinkage in cationic[66-68] and anionic[69] epoxy polymerization. Also in anionic systems Brady *et al.*[70] have reported the use of some bi- and tricyclic monomers in the copolymerization with epoxides. However the main

---

[63] W. J. Bailey, J. Elastoplast **1973,** *5,* 142.
[64] W. J. Bailey, R. L.-J. Sun, H. Katsuki, T. Endo, H. Iwama, R. Tushima, K. Saigou, M. M. Bitritto. ACS Symp. Ser. 59, T. Saegusa, E. Goethals, eds. ACS. Washington, **1977**.
[65] K. Bodenbenner. *Ann. Chim*, **1959,** *623,* 183.
[66] T. Takata, T. Endo. *Polym. Prepr. Jpn.* **1988,** *37,* 1559.
[67] H. Nishida, F. Sanda, T. Endo, T. Nakahara, T. Ogata, K. Kusumoto. *Macromol. Chem. Phys.* **1999,** *200,* 745.
[68] T. Hino, T. Endo. *Macromolecules*, **2003,** *36,* 5902.
[69] K. Chung, T. Takata, T. Endo. *Macromolecules* **1995,** *28,* 1711.
[70] R. F. Jr Brady, F. E. Simon. *J. Polym. Sci., Part A: Polym. Chem.* **1987,** *25,* 231.

drawback they all present is the difficulty on synthesizing such complex chemical structures that limit their application in an industrial scale.

Another strategy related to the use of expanding monomers is the use of cyclic carbonates or lactones.[71,72] These monomers can be copolymerized in cationic conditions with DGEBA. In this case, at the first stages of the reaction (before gelation) a spirocyclic orthocarboante or orthoester is formed, yielding a slight increase in shrinkage, but at the end of the curing (after gelation) this *in situ* formed expanding monomers reacts, reducing the shrinkage after gelation, which is the responsible for the internal stresses in thermosets. Unfortunately, the main problem of this strategy is that the T_g of the resulting thermosets falls dramatically down, limiting their range of application.

As an alternative to expanding monomers, hyperbranched polymers have proved their efficacy in reducing the shrinkage. Fernández-Francos *et al.*[73] proposed the use of commercially available HBP Boltorn H30 to reduce the shrinkage, and even obtain expansion. This effect was explained on the basis of the disappearance of inter- and intra-molecular H-bonding of the polymer after being incorporated to the epoxy network leading to an important volumetric expansion. The main advantage of this strategy is that the other properties of the resin are not affected.

1.3 Hyperbranched Polymers and other Highly Branched Topologies

During the past century polymer science and industry have witnessed their blossoming. Researchers such as Staundinger, Flory, Ziegler, Natta, Shirakawa, Sharpless or Grubbs have made great contributions during this time, although their focus has been mainly concentrated in linear chains. However, since the definition of "macromolecules" in 1922 by Staundiger,[74] many different polymeric architectures have been synthesized. **Figure 1.18** shows the broad existing range of structures besides linear polymers.

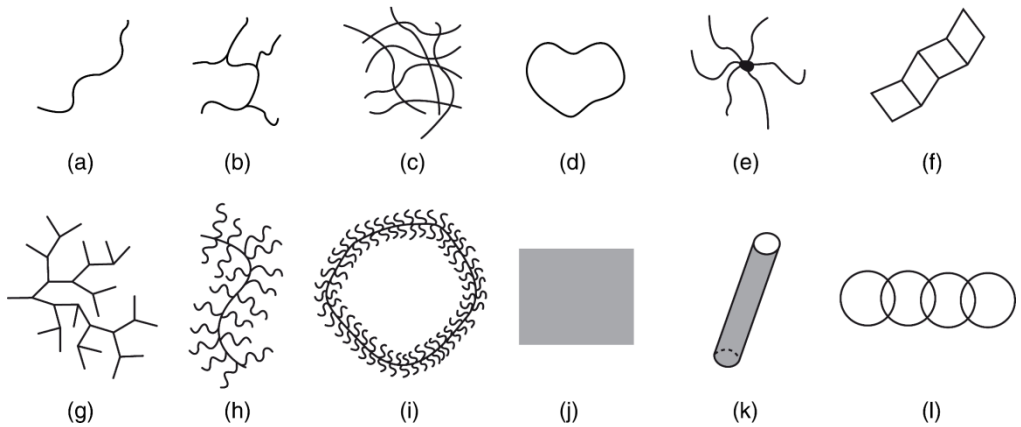

Figure 1.18 Synthesized polymeric topologies: (a) linear, (b) chain-branched, (c) cross-linked, (d) cyclic, (e) star-like, (f) ladder-like, (g) dendritic, (h) linear brush-like, (i) cyclic brush-like, (j)sheet-like, (k) tube-like, and (l) interlocked.

[71] R. Cervellera, X. Ramis, J. M. Salla, A. Mantecón, A. Serra. *J. Appl. Polym. Sci.* **2007,** *103,* 2875.
[72] C. Mas, X. Ramis, J. M. Salla, A. Mantecón, A. Serra. *J. Polym. Sci. Part A: Polym. Chem.* **2003,** *41,* 2794.
[73] X. Fernández-Francos, J. M. Salla, A. Cadenato, J. M. Morancho, A. Serra, A. Mantecón, X. Ramis. *J. Appl. Polym. Sci* ***2009,*** *111,* 2822.
[74] H. Staudinger, J. Fritschi. *Helv. Chim. Acta* **1922,** *5,* 785.

One can see that nearly all of the depicted structures present branching up to some extent, showing its importance in the construction of macromolecules.[75] Among them, the one that concerns us is dendritic polymers. Up to now eight subclasses have been developed. Their schematic structure can be seen in **Figure 1.19**.

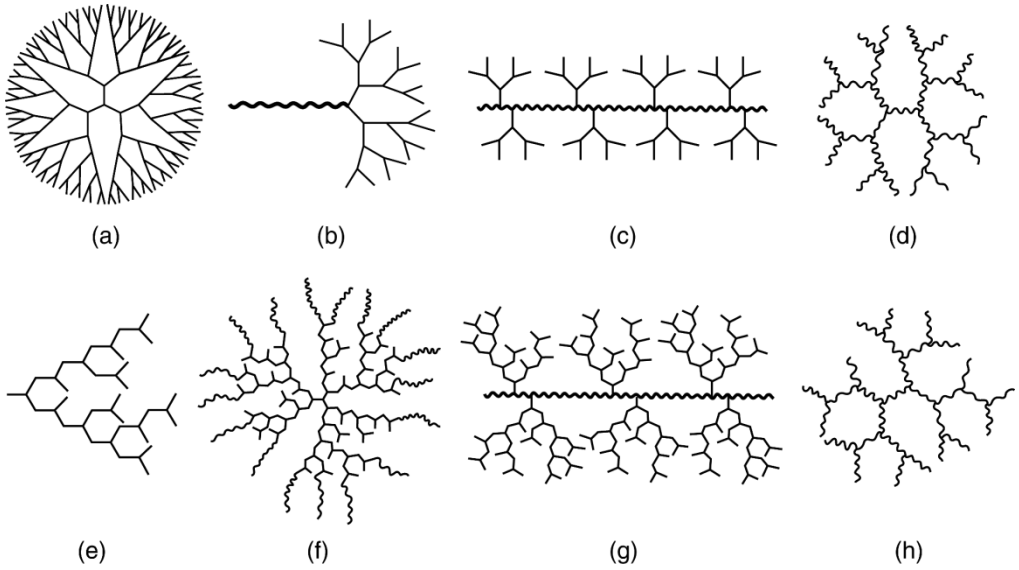

Figure 1.19 Different dendritc structures. (a) Dendrimer, (b) linear-dendritic block copolymer, (c) dendronized polymer, (d) DendriMacro, (e) hyperbranched polymer, (f) multiarm star copolymer or hyperbranched brush, (g) HBP-grafted polymer, and (h) HyperMacro.

1.3.1 History of HBPs

The concept hyperbranched polymer was coined by Kim and Webster,[76-78] late in the 1980s, to define dendritic macromolecules that have a random branch-on-branch topology. However the history of HBPs can be dated to the end of the nineteenth century when Berzelius[79] reported the formation of a resin from tartaric acid (A_2B_2 monomer) and glycerol (B_3 monomer). Later, in 1901, Watson Smith[80] attempted the reaction of phtalic anhydride (latent A_2 monomer) and glycerol (B_3 monomer). Following his report, Callaha, Arsem, Dawson, Howell, and Kiendle *et al.* showed that specific viscosities of the resulting polymer were lower than those of linear analogues.[81-83] In 1909 Baekeland produced the first commercial synthetic plastics and phenolic polymers through the reaction of formaldehyde (latent A_2 monomer) and phenol (latent B_3 monomer).[84,85] The soluble precursor which is formed just before gelation occurs would have the randomly branched topology.

---

[75] D. Yan, C. Gao, H. Frey. *Hyperbranched Polymers: Synthesis, Properties and Applications.* John Wiley & Sons, Singapore, **2011**.
[76] Y. H. Kim. US Patent 4,857,630, **1987**.
[77] Y. H. Kim, O. W. Webster. *J. Am. Chem. Soc.* **1990,** *112,* 4592.
[78] Y. H. Kim, O. W. Webster. *Macromolecules* **1992,** *25,* 5561.
[79] C. Gao, D. Yan. *Prog. Polym. Sci.* **2004,** *29,* 183.
[80] W. Smith. *J.Soc. Chem. Ind.* **1901,** *20,* 1075.
[81] R. H. Kienle, A. G. Hovey. *J. Am. Chem. Soc.* **1929,** *51,* 509.
[82] R. H. Kienle, P. A. van der Meulen, F. E. Petke. *J. Am. Chem. Soc.* **1939,** *61,* 2258.
[83] R. H. Kienle, P. A. van der Meulen, F. E. Petke. *J. Am. Chem. Soc.* **1939,** *61,* 2268.
[84] L. H. Baekeland. *US Patent*, 942699, **1909**.
[85] G. Odian. *Principles of Polymerization,* 3rd edition. John Wiley & Sons, New York, **1991**.

During the 1940s, Flory made a great contribution to the understanding of highly branched structures, defining the concept "degree of braching".[86-90] Moreover, in 1952 he pointed out theoretically that highly branched polymers could be synthesized without risk of gelation by the polycondensation of an AB_x monomer (with $x \geq 2$),[91] settling the principles of the theory of highly branched structures.

It was not before the 1980s when highly branched structures gained popularity. Prior to the above mentioned works of Kim and Webster, Kricheldorf and coworkers[92] prepared highly branched polymers in a one-step copolymerization of AB and AB_2 type monomers. Later, in the 1990s, the amount of work carried out in the field increased exponentially until now.[93] Till date, the number of available HBPs is uncountable, and it is possible to say safely that it is comparable to library of linear polymers. Poly(esters), poly(ethers), poly(ketones), poly(amides), poly(imides), poly(styrenes), poly(acrylates) or poly(olefins) are just an example of them.[94]

1.3.2 Definition and synthesis of HBPs

Hyperbranched polymers (HBPs) are a special type of dendritic polymers and have as a common feature a very high branching density with the potential of branching in each repeating unit. They are usually prepared in a one-pot synthesis, which limits the control on molar mass and branching accuracy and leads to "heterogeneous" products with a distribution in molar mass and branching. This distinguishes hyperbranched polymers from perfectly branched and monodisperse dendrimers.

Due to the statistical character of HBP synthesis, unlike dendrimers, they have molecular weight dispersity, isomerism and a certain degree of branching (DB). As seen in **Figure 1.20** the simplest HBP present four different units: the focal group, linear (L), dendritic (D) and terminal (T) units. Fréchet and coworkers[95] defined the DB as the fraction of terminal and dendritic units from the total.

$$DB = \frac{D+T}{D+T+L} \tag{1.1}$$

However, this expression can be simplified for high molecular weight HBPs were the number of terminal units is very similar to the one of dendritic ones. Therefore, the expression can be rewritten as follows:

$$DB = \frac{1}{1+L/2D} \tag{1.2}$$

Later, Frey, Müller and Yan *et al.*[96,97] have proposed an expression of the DB as a function of conversion, more strict from the theoretical point of view.

$$DB = \frac{2x}{5-x} \tag{1.3}$$

---

[86] P. J. Flory. *J. Am. Chem. Soc.* **1941,** *63,* 3083.
[87] P. J. Flory. *J. Am. Chem. Soc.* **1941,** *63,* 3091.
[88] P. J. Flory. *J. Am. Chem. Soc.* **1941,** *63,* 3096.
[89] P. J. Flory. *J. Am. Chem. Soc.* **1942,** *64,* 132.
[90] P. J. Flory. *J. Am. Chem. Soc.* **1947,** *69,* 30.
[91] P. J. Flory. *J. Am. Chem. Soc.* **1952,** *74,* 2718.
[92] H. R. Kricheldorf, Q. Z. Zang, G. Schwarz. *Polymer* **1982,** *23,* 1821.
[93] M. K. Mishra, S. Kobayashi. *Star and Hyperbranched Polymers.* Marcel Dekker, New York, **1999**.
[94] B. Voit, A. Lederer. *Chem. Rev.* **2009,** *109,* 5924.
[95] C. J. Hawker, R. Lee, J. M. J. Fréchet. *J. Am. Chem. Soc.* **1991,** *113,* 4583.
[96] D. Hölter, A. Burgath, H. Frey. *Acta Polym.* **1997,** *48,* 30.
[97] D. Yan, A. H. E. Müller, K. Matyjaszewski. *Macromolecules* **1997,** *30,* 7024.

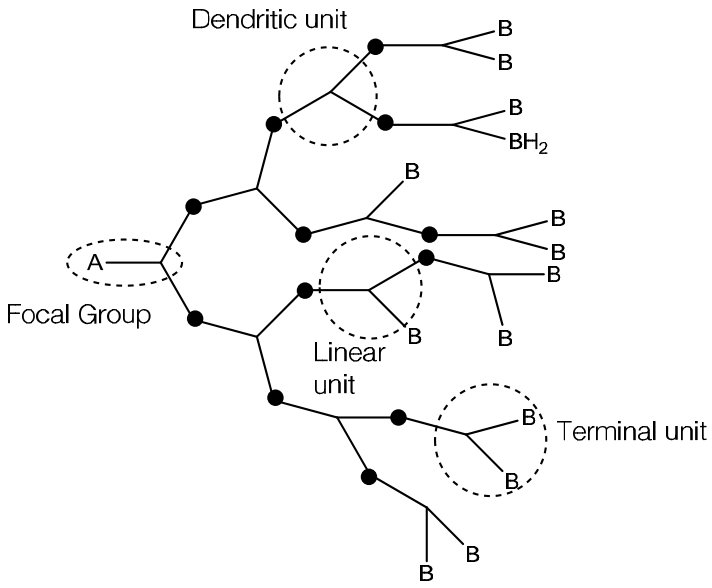

Figure 1.20 Different units present in a HBP obtained from the polymerization of an AB_2 monomer.

Even in HBPs where the DB is high (there are some examples of HBPs with a DB of around 0.7,[98] a much higher value than the predicted by Flory's equations) and present low molecular weight dispersity, their structure is still inhomogeneous. As seen in **Figure 1.21** statistically there are many isomeric forms with the same DB.

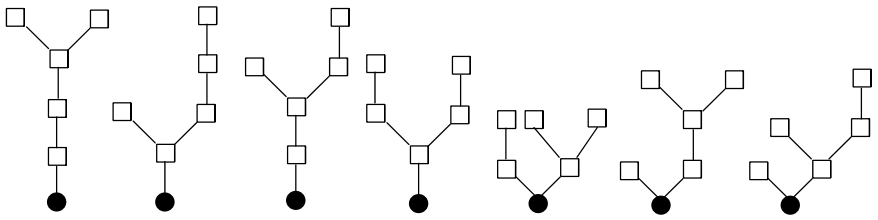

Figure 1.21 Different isomers of the same DB and $\bar{M}_w$.

From the strategy point of view, there are two ways to approach the synthesis of HBPs: bottom-up (polymerizing small molecules, monomers, to achieve the branched macromolecule) and middle-upon (modifying a hyperbranched polymeric precursor).

The bottom-up approach is the most extended way of preparing HBPs. Four methodologies have been developed based on this synthetic strategy: (a) polycondensation of AB_x monomers (for $x \geq 2$); (b) self-condensing chain-growth polymerization of AB* (latent AB_2) monomers; (c) polycondensation of symmetric monomer pairs of A_2 and B_3 monomers under the rule of Flory's equal reactivity; and (d) polymerization of asymmetric monomer pairs (coupling-monomer methodology, CMM) with the principle of non equal reactivity.

Polycondensation of AB_x monomers gave rise to various HBPs without the risk of gelation as described by Flory's equation. An example of this type of polymerization can be found in the early works of Kim and Webster[78] in the synthesis of poly(phenylenes) (**Figure 1.22**). However,

[98] D. S. Thompson, L. J. Markoski, J. S. Moore. *Macromolecules* **1999,** *32*, 4764.

the main problem this methodology presents is the fact that most of AB_x monomers are not commercially available.

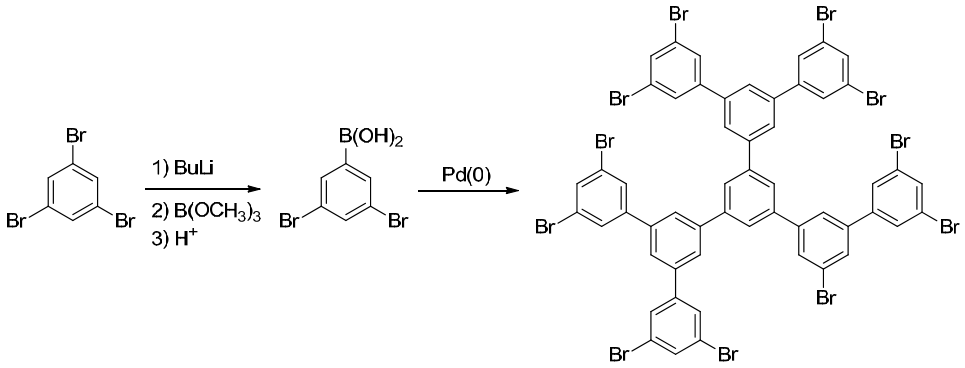

Figure 1.22 Synthesis of poly(phenylenes) from an AB_2 monomer.

Alternatively, polymerization of AB* monomers including vinyl and cyclic molecules can result in HBPs capable of controlling the DB by employing self-condensing vinyl polymerization (SCVP),[99] atom transfer radical polymerization (ATRP),[100] ring-opening polymerization (ROP),[101,102] and proton-transfer polymerization (PTP)[103] techniques. Examples of the synthesis of HBPs through these methodologies are depicted in **Figure 1.23**.

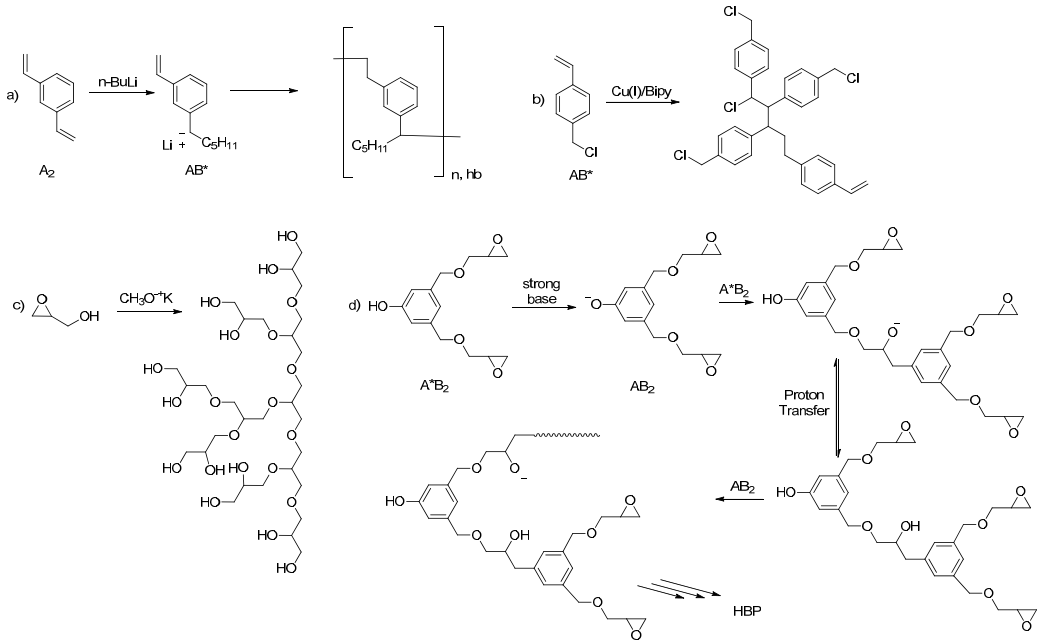

Figure 1.23 Different AB* based hyperbranched synthesis. (a) Self-condensing vinyl polymerization; (b) Atom transfer radical polymerization; (c) Ring opening polymerization; and (d) proton transfer polymerization.

---

[99] J. M. Fréchet, M. Henmi, I. Gitsov, S. Aoshima, M. R. Leduc, R. B. Grubbs. *Science* **1995,** *269* , 1080.
[100] K. Matyjaszewski, S. G. Gaynor, A. Kulfan, M. Podwika. *Macromolecules* **1997,** *30* , 5192.
[101] M. Suzuki, A. Li, T. Saegusa. *Macromolecules* **1992,** *25* , 7071.
[102] A. Sunder, R. Hanselmann, H. Frey, R. Mulhaupt. *Macromolecules* **1999,** *32* , 4240.
[103] H. T. Chang, J. M. J. Fréchet. *J. Am. Chem. Soc.* **1999,** *121* , 2313.

Polycondensation of A_2 and B_3 monomers may achieve soluble HBPs with the advantage of commercial availability of monomers.[104] **Figure 1.24** shows an example of this type of synthesis. It should be noted that high risk of gelation exists during reaction and therefore special skills such as slow addition of A_2 monomers to the diluted solution of B_3 is required. Another possibility is is working in non stoichiometric proportions.

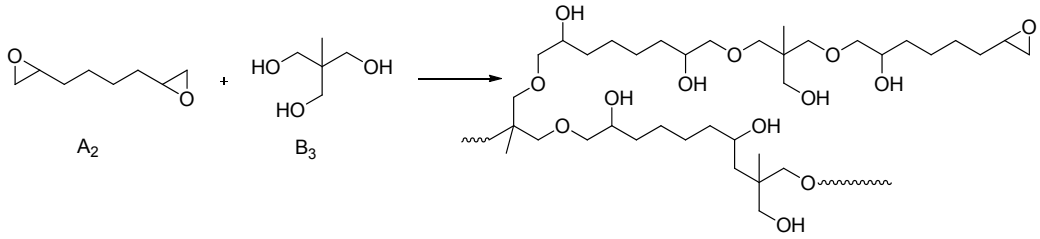

Figure 1.24 Example of an A_2 + B_3 hyperbranched synthesis.

In the CMM approach, based on the rule of non equal reactivity of functional groups in specific monomer pairs such as AA' and B'B_2, an AB_2 intermediate would predominantly form *in situ* in the initial stage of polymerization if the reactivity of A' is faster than that of A or the reactivity of B' is faster than that of B; further reaction would produce hyperbranched macromolecules without gelation.[105] The general mechanism for such polymerization mechsnism is depicted in **Figure 1.25**. It should be commented that this approach have been already used in the synthesis of commercially available poly(ester amides), sold by DSM with the trademark Hybrane®.[106]

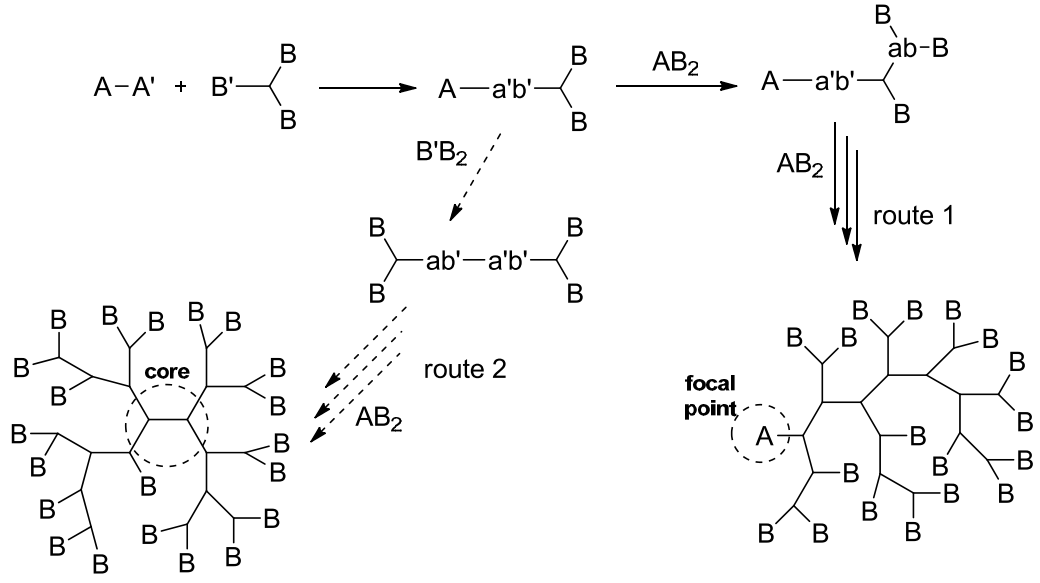

Figure 1.25 General mechanism for the preparation of HBPs through the CMM approach.

Through the middle upon strategy, various new polymers derived from HPs can be obtained by the "attach to", "grafting from", "grafting through" and "building block" approaches (**Figure**

[104] T. Emrick, H. T. Chang, J. M. J. Fréchet. *Macromolecules* **1999,** *32*, 6380.
[105] D. Yan, C. Gao. *Macromolecules* **2000,** *33* , 7693.
[106] P. Froehling, J. Brackman. *Macromol. Symp.* **2000,** *151,* 581.

1.26). The "attach to" approach consist in the modification of the terminal groups of a HBP precursor with another polymer or a small molecule while the "grafting through" uses the terminal groups of the HBP as initiator for the polymerization of a monomer. On the other hand, on the "building block" approach two different polymer precursors are linked together by reaction of terminal groups.

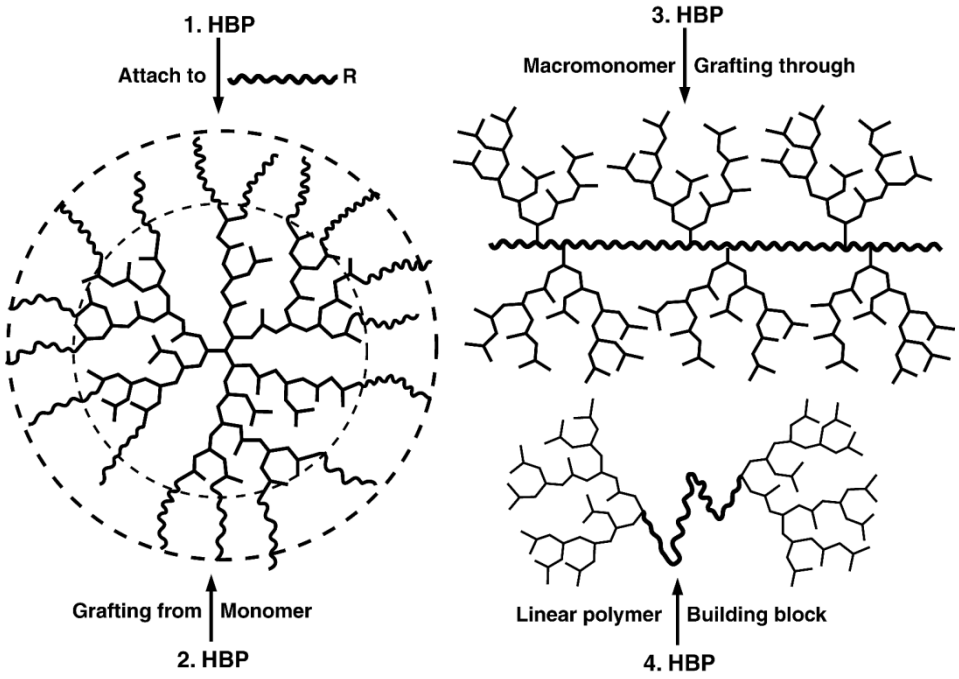

Figure 1.26 Different approaches f the middle-up approach to HBP synthesis.

1.3.3 Applications of HBPs

Nowadays, the field of HBPs can be considered as mature. Looking at the evolution of publications on the topic "hyperbranched polymers" during the last decade (**Figure 1.27**) one can see the interest they arouse. Some of the properties that have made them so popular are their tremendous versatility due to the great number of available monomers, their great number of functional groups per molecule, or their lower viscosity compared to their linear analogues.

Thus, it is not difficult to imagine the great amount of different applications of HBPs nowadays.[79,94,107] One of these applications, as already explained in section 1.2.1, is in the improvement of toughness in the coatings industry. They are used as additive than can phase separate during the curing or introduce flexibility. However, there are many more applications and the aim of this section is to give an overview of some of the most significant.

Also as additive, Dillon *et al.*[108] used a hyperbranched polyester with benzotriazole end groups as UV light stabilizer. Another example is in the rheological modification of polyethylene (LLDPE) such as the alkyl-modified hyperbranched polyester repoted by Hong *et al.*[109]

---

[107] B. Voit. *J. Polym. Sci. Part A: Polym. Chem.* **2005,** *43,* 2679.
[108] M. P. Dillon, J. R. Sounick, R. Vicari, W. W. Wilkinson. International Patent WO 97/12882, **1995**.
[109] Y. Hong, J. J. Cooper-White, M. E. Mackay, C. J. Hawker, E. Malstroem, N. Rehnberg. *J. Rheol.* **1999,** *43,* 781.

Hybrid organic-inorganic nanocomposites have attracted considerable attention in recent years because they combine the advantages of organic polymers (flexibility, lightweight, processability, impact resistance, etc.) and inorganic materials (mechanical strength, chemical resistance, thermal stability, etc.). In this field also HBPs are important. For example, Sangermano *et al.*[110] reported the formation of hybrid coatings using an epoxy functionalyzed hyperbranched aromatic polyester in the presence of TEOS and a coupling agent (GPTS). A UV curing followed by a sol-gel process allowed obtaining the hybrid coatings.

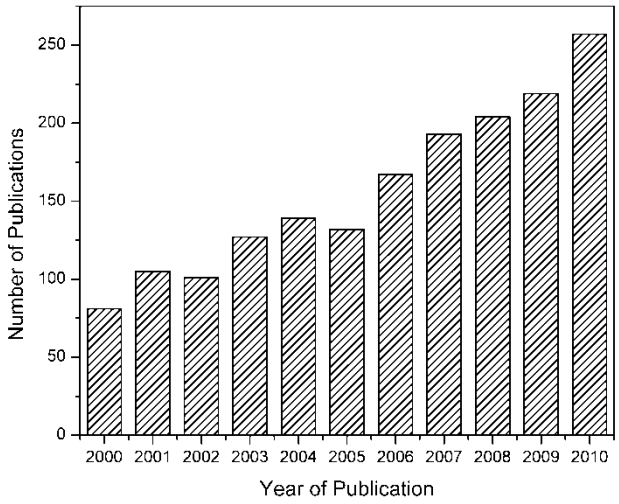

Figure 1.27 Publication numbers with the topic "hyperbranched polymer" searched by ISI Web of Science during the last decade.

Another very active area is the field of biomaterials. Klee *et al.*[111] used a hyperbranched polyester modified with methacrylic end groups to reduce the shrinkage of dental composites. As a surface modifier, Haag *et al.*[112] reported the utilization of hyperbranched polyglycerol with dithiolane end groups to increase the affinity of proteins in a gold surface. But probably the most promising application of HBPs in the field of biomaterials is in drug delivery systems. As cheaper alternatives for dendrimers, the use of commercially available polymers such as Boltorn H32000 ($\bar{M}_n$= 4,600 g/mol) or Hybrane 1690, 1500 and 1200 have been investigated as paracetamol carriers.[113] There are other approaches much more sophisticated, such as the water-soluble, degradable polyesters proposed by Gao *et al.*[114] as promising candidates for drug delivery.

1.3.4 Other Highly Branched Structures

The good properties that have been observed in HBPs have encouraged the scientific world to investigate more complex structures. An example of this is the preparation of multi-arm star polymers. The most successful approach used in their synthesis seems to be the middle-upon, where the end-groups of a hyperbranched polymer are modified with different linear polymeric structures obtaining a molecule with a core-shell structure (**Figure 1.28**). Varying the structure of

---

[110] E. Americo, M. Sangermano, G. Malucelli, A. Priola, G. Rizza. *Macromol. Mater. Eng.* **2006,** *291,* 1287.
[111] J. E. Klee, C. Schneider, D. Hölter, A. Burgath, H. Frey, R. Mülhaupt. *Polym. Adv. Technol.* **2001,** *12,* 346.
[112] C. Siegers, M. Biesalski, R. Haag. *Chem. Eur. J.* **2004,** *10,* 2831.
[113] S. Suttiruengwong, J. Rolker, I. Smirnova, W. Arlt, M. Seiler, L. Lüderitz, Y. Pérez de Diego, P. Janssens. *J. Pharm. Dev. Technol.* **2006,** *11,* 55.
[114] C. Gao, Y. M. Xu, D. Y. Yan, W. Chen. *Biomacromolecules* **2003,** *4,* 704.

the HBP (core) and the modifier (shell) the properties of the resulting multi-arm star polymer change dramatically, allowing researches to tune them for the desired application.[75] Another example are block copolymers containing linear and dendritic blocks that have also been successfully synthesized by many authors.[115,116] They can be synthesized either building the polymers first and then grafting them or preparing one block with a terminal unit that can start the polymerization of the second one. The synthesis of this type of highly branched structures will be discussed into more detail in the introductory section of Chapter 5.

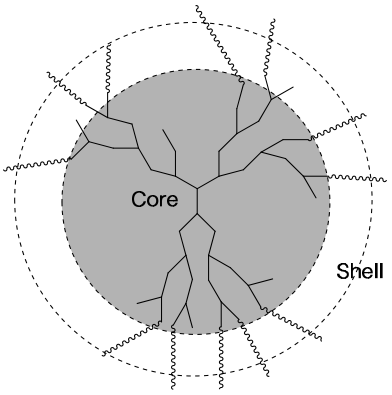

Figure 1.28 Core shell structure of a multi-arm star polymer.

1.4 Scope and Objectives

As explained along this introductory section, epoxy resins are very interesting materials from the industrial point of view. However, they present some drawbacks that limit their range of applications and cause some problems in current materials. The main objective of this thesis is to perform a screening of the use of hyperbranched polymers and other highly branched topologies to improve mechanical properties, reworkability and reducing the shrinkage during curing of epoxy resins.

The specific objectives that this thesis chases can be summarized as follows:

- To study the use of commercially available hyperbranched polymers, either directly or after its chemical functionalization, as chemical modifiers of commercially available epoxy resins.
- To prepare hyperbranched aromatic-aliphatic polyesters and use them as epoxy modifiers to improve the chemical reworkability of the resulting thermosets.
- To synthesize different polymeric amphiphilic structures and use them in the preparation of nanostructured epoxy networks by different polymerization methodologies.
- To explore the utilization of a hyperbranched polyester prepared via thiol-ene click coupling as an agent of latent dual curing of epoxy resins and as toughening additive.
- To determine the improvements achieved by the strategy of using HBPs in the modification of epoxy resins.

---

[115] G. Hizal, U. Tunca, A. Sanyal. *J. Polym. Sci Part A: Polym. Chem.* **2011,** *49,* 4103.
[116] I. Gitsov. *J. Polym. Sci Part A: Polym. Chem.* **2008,** *46,* 5295.

Chapter 2

Materials and Methods

2.1 Materials

2.1.1 Epoxy Resins

Two different epoxy resins have been employed:

- Diglycidyl ether of bisphenol A (DGEBA) with an hydroxylic oligomer content of n=0.028 and an equivalent weight of 182 g/ee, provided by Shell Chemicals with the trade name of Epikote Resin 827.
- 3,4-epoxycyclohexylmethyl-3',4'-epoxycyclohexyl carboxylate with equivalent weight of 126 g/ee provided by Huntsman with the trade name CY 179-1 CH (CE).

2.1.2 Modifiers

Different hyperbranched polymers, both commercially available and synthesized in the laboratory, have been used as modifiers in epoxy formulations. Their chemical structure will be discussed in detail in the corresponding section. Moreover, a sepiolite provided by Tolsa (GLYMO) was also employed.

2.1.3 Curing Agents

Different curing systems have been studied and, as a consequence, diverse curing agents have been employed. For epoxy/anhydride systems, 1,2,3,6-tetrahydrophthalic anhydride (THPA) has been used. In anionic curing systems a tertiary amine has been employed: 1-methyl imidazole (MI). As Lewis acids for the cationic curing two different lanthanide triflates have been

used: $La(OTf)_3$ and $Yb(OTf)_3$. Finally, for the case of photoinitiated curing, a 50% in weight solution of triarylsulfonium hexafluoroantimoniate in propylene carbonate was chosen.

2.2 Characterization Techniques

2.2.1 Differential Scanning Calorimetry (DSC)

A Mettler DSC821e equipped with a robotic arm TSO801RO was used to perform DSC analysis from 30 to 300 °C. To perform tests under room temperature a Mettler DSC822e cooled with liquid nitrogen. Both calorimeters were calibrated using an indium standard (heat flow calibration) and an indium-lead-zinc standard (temperature calibration). Samples of 5 to 10 mg of weight were placed in covered aluminum pans to perform analysis. **Figure 2.1** shows the calorimeters used.

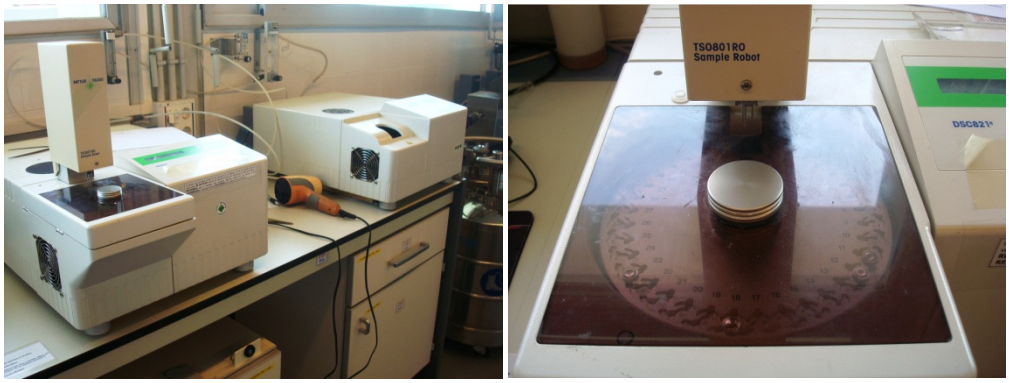

Figure 2.1 Pictures of the calorimeters and the robot used to study thermal curing systems.

Curing Kinetics

The kinetic study using DSC assumes that the heat released during the reaction is proportional to the degree of conversion and that the heat released *dH/dt*. is proportional to the curing rate *dx/dt* .The integration of this signal, in the case that the reaction is complete, yields the total heat released ΔH_{tot}. Mathematically one can express this as follows:

$$\frac{dx}{dt} = \frac{dH/dt}{\Delta H_{tot}} = \frac{dh/dt}{\Delta h_{tot}} \quad (2.1)$$

$$x = \frac{\Delta H_t}{\Delta H_{tot}} = \frac{\Delta h_t}{\Delta h_{tot}} \quad (2.2)$$

where dh/dt and Δh_{tot} are the heat releasing rate and the total heat released normalized in respect to the sample size, ΔH_t is the heat released up to a time t, and Δh_t is the heat released normalized in respect to the sample size. It can be expressed in J/g or in kJ/ee. Finally x is the degree of curing, and can also be expressed as α.

The kinetics of a system can be studied in isothermal or dynamic conditions. In our case we chose to work with dynamic experiments since they present some advantages being the most important the fact that in isothermal conditions it is possible to lose some information of the beginning of the curing and that the curing is not always complete.[1]

[1] A. Turi. *Thermal Characterization of Polymeric Materials, 2nd Edition*. Academic Press, San Diego, **1997**.

Kinetic Analysis

The reaction rate in a condensed phase reaction is usually expressed as $dx/dt = k\, f(x)$ being k the kinetic constant and $f(x)$ a function depending on the conversion. The kinetic constant, k, usually follows the Arrhenius expression:

$$k = Ae^{\frac{-E}{RT}} \tag{2.3}$$

where A is the preexponential factor, E the activation energy, R the gas constant and T the absolute temperature.

In general, a kinetic process is well characterized if one knows E, A and $f(x)$, the so called kinetic triplet. Although strictly speaking this methodology should only be valid for "single-step" processes it can also be applied in systems where more than one chemical (or physical) process coexists. There are two main approaches in the kinetic analysis:

1. *Isoconversional methods (or model-free)*. They study the apparent activation energy without knowing the kinetic model.
2. *Model-fitting methods*. They search an approximation of the experimental data to a kinetic model, and from that the values of the kinetic triplet are obtained.

The isoconversional methodology assumes that the reaction function $f(x)$ is independent of the heating rate β.[2] On that way the kinetics of a process only depends on the degree of conversion at a certain time. It also requires the performance of series of experiments to determine the apparent activation energy. Those experiments can be, for example, dynamic DSC curing at different heating rates.

Depending on the approach used to determine the apparent activation energy, it is possible to classify isoconversional methodologies between lineal and non-lineal. In turn, lineal methodologies can be divided between differential and integral. In this job the integral methodology has been applied. By integrating $dx/dt = k \cdot f(x)$ considering that the temperature is not constant but $T = T_0 + \beta t$ and applying a change of variables $dt = dT/\beta$ one can obtain the following expression:

$$g(x) = \int_0^t Ae^{-E/RT}\, dt = \int_{T_0}^{T} \frac{A}{\beta} e^{-E/RT} dT = \frac{A}{\beta}\int_{T_0}^{T} e^{-E/RT} dT \tag{2.4}$$

where $g(x)$ is an integral function that describes the reaction as $f(x)$.

Eq. (2.4) can be simplified assuming that only at $T_0 = 0$ the reaction is forbidden:

$$g(x) = \frac{A}{\beta}\int_0^T e^{-E/RT} dT \tag{2.5}$$

To resolve this integral, which has no analytical solution, the best strategy is to make an approximation to a simpler expression. To do so, a variable $y = E/RT$ is defined and the change of variables $dy = -E/RT^2$ and $dT = -(R/E)y^2 dT$ is applied:

$$\int_0^T e^{-E/RT} dT = -\frac{E}{R}\int_{\infty}^{y} \frac{e^{-y}}{y^2} dy = \frac{E}{R}\int_{y}^{\infty} \frac{e^{-y}}{y^2} dy = \frac{E}{R} p(y) \tag{2.6}$$

[2] S. Vyazovkin, C. A. Wight. *Thermochim. Acta* **1999,** *340-341*, 53.

Finally to determine $p(y)$ the solution of Murray and White,[3] $p(y) = e^{y}/y^{2}$, which represents the bases of the Kissinger-Akahira-Sunose (KAS)[4,5] methodology, was applied:

$$ln\left(\frac{\beta}{T_{i,x}^2}\right) = ln\left(\frac{A\,R}{g(x)E_x}\right) - \frac{E_x}{RT_{i,x}} \tag{2.7}$$

From that expression the apparent activation energy E_x can be obtained from the slope of the curve $ln(\beta/T_{i,x}^2)$ against $-1/RT_{i,x}$.

Using the model-fitting methodology it is possible to determine a kinetic model. Integrating the expression of the reaction rate depending on the heating rate of the DSC experiment (eq. (2.8)) using the Coats-Redfern[6] approximation the expression eq. (2.9) can be obtained:

$$\frac{dx}{dt} = \beta\frac{dx}{dT} = Ae^{\frac{-E}{RT}}f(x) \tag{2.8}$$

$$ln\left(\frac{g(x)}{T_{i,x}^2}\right) = ln\left(\frac{A\,R}{\beta\,E}\right)\left(1 - \frac{2R\bar{T}}{E}\right) - \frac{E}{RT_{i,x}} \tag{2.9}$$

where $\bar{T}$ is the mean value of temperature of the process and assumes that A and E are constant during the experiment.

Considering $2R\bar{T} \ll 1$ the eq. (2.9) can be simplified as:

$$ln\left(\frac{g(x)}{T_{i,x}^2}\right) = ln\left(\frac{A\,R}{\beta\,E}\right) - \frac{E}{RT_{i,x}} \tag{2.10}$$

For a given kinetic model, the linear representation of $ln[g(x)/T^2]$ versus $1/T$ makes it possible to determine A and E from the slope and the ordinate at the origin. . Different models (**Table 2.1**) are compared with the data obtained and the one that present the best fitting and that has an E value similar to that obtained isoconversionally (considered to be the effective E value) is chosen. Moreover the k has been determined by using eq. (2.3) and A and E values.

Table 2.1 Kinetics models used to determine the kinetic triplet with the model fitting methodology.[7]

Model	*f(x)*	*g(x)*
D_1	$\frac{1}{2x}$	x^2
D_2	$\frac{1}{\ln(1-x)}$	$(1-x)\ln(1-x)+x$
D_3	$\frac{3}{2}\frac{(1-x)^{2/3}}{(1-(1-x)^{1/3})}$	$(1-(1-x)^{1/3})^2$
D_4	$\frac{3}{2}\frac{(1-x)^{1/3}}{(1-(1-x)^{1/3})}$	$1-\frac{2}{3}x-(1-x)^{2/3}$
R_n (R_2, R_3)	$n(1-x)^{1-1/n}$	$1-(1-x)^{1/n}$

[3] P. Murray, J. White. *Trans. Brot. Ceram. Soc.* **1955,** *54,* 204.
[4] T. Akahira, T. Sunose. *Transactional of Joint convention of Four Electrical Institutes* **1969,** 246.
[5] H. E. Kissinger. *Anal. Chem.* **1957,** *29,* 1702.
[6] A. W. Coats, J. P. Redfern. *Nature* **1964,** *201,* 68
[7] P. Budrugeac, E. Segal, L. A. Pérez-Maqueda, J. M. Criado. *Polym. Degrad. Stab.* **2004,** *84,* 311.

n order	$(1-x)^n$	$-\ln(1-x) \quad (n=1)$ $\frac{1-(1-x)^{1-n}}{1-n} \quad (n \neq 1)$
A_n (A_2, A_3)	$n(1-x)(-\ln(1-x))^{1-1/n}$	$(-\ln(1-x))^{1/n}$
n potence	$nx^{1-1/n}$	$x^{1/n}$
Autocatalytic	$x^m(1-x)^n$	$\frac{1}{n-1}\left(\frac{1-x}{x}\right)^{1-n} \quad (n+m=2; n\neq 1)$ $\frac{1}{n-1}\left(\frac{1-x}{x}\right)^{1-n}+\frac{1}{n-2}\left(\frac{1-x}{x}\right)^{2-n}$ $(n+m=3; n\neq 1,2)$

Glass Transition Temperature (T_g)

In order to determine the T_g of the cured materials as well as the T_g of the synthesized hyperbranched polymers DSC experiments were performed in dynamic conditions at 20 °C/min. The evaluation of the glass transition temperature was carried out using the ASTM methodology.

2.2.2 Photo-calorimetry (photo-DSC)

Photo-calorimetric experiments were performed in a Mettler DSC821e modified to irradiate the samples with a UV Hamamatsu LC5 with a double beam Hg-Xe lamp that irradiates both the sample and the reference pans simultaneously (**Figure 2.2**). The furnace of the calorimeter is covered with a silver top with two quartz windows to collimate the light beam. The UV lamp is polychromatic, with maxima at 440, 410, 365, 320 and 300 nm.

Figure 2.2 Photo-calorimeter used to perform photo-DSC experiments.

The shape of the DSC curves obtained with this methodology is depicted in **Figure 2.3**. The reaction starts only after the UV lamp is turned on, and right after a heat released related to the curing reaction is appreciated. In the moment that the UV lamp is turned off a step in the signal is observed. This salt is related to a thermal component, and for that reason it is necessary to perform a second scan to evaluate it. From the difference between curves it is possible to obtain the photo-DSC curve.

The curing conversion can be determined directly from the photo-DSC curve using equation 2.2, or from the remaining heat released in a dynamic postcuring experiment as follows:

$$x = 1 - \frac{\Delta h_{post}}{\Delta h_{theor}} \tag{2.11}$$

where Δh_{post} is the heat released in the postcuring scan and Δh_{theor} is a reference value of the heat released in a complete curing.

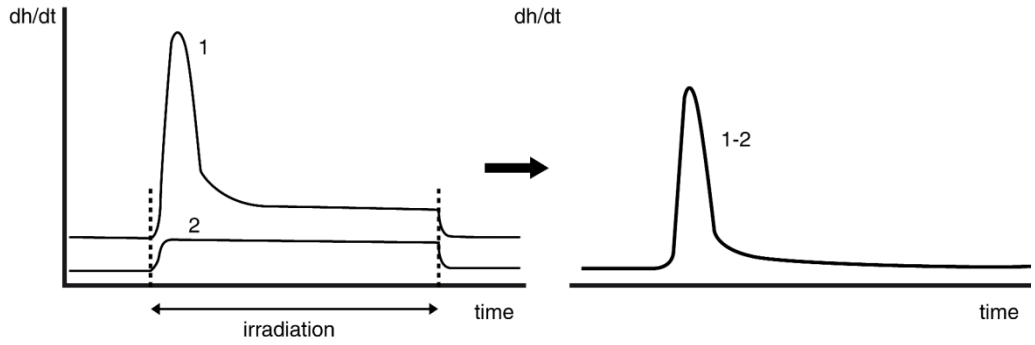

Figure 2.3 Curves obtained in photo-DSC experiments and the substraction curve representing the heat evolved.

To perform experiments samples of approximately 5 mg where placed in aluminum pans and the schedule of experiments was as follows:

1. UV experiment with 4 minutes of thermal preconditioning, 20 minutes of irradiation and 4 minutes without irradiation
2. Second UV experiment with the same parameters as the first one to obtain the blank curve.
3. Thermal postcuring scan at 10 ºC/min up to 300 ºC to determine the remaining heat after the UV curing.

2.2.3 Fourier-Transformed Infrared Spectroscopy (FT-IR)

Two different FT-IR equipments were used. To study thermal curing processes, an FTIR-680PLUS spectrophotometer from JASCO with a resolution of 4 cm^{-1} in the absorbance mode, equipped with an attenuated total reflection accessory (ATR) with thermal control and a diamond crystal (Golden Gate heated single-reflection diamond ATR from Specac-Teknokroma) was used. For UV curing processes a Thermo-Nicolet 5700 FTIR device equipped with a medium pressure mercury lamp Hamamatsu Lightningcure LC5 with an optical guide and a light intensity on the surface of the sample of about 5 $mW \cdot cm^{-2}$ was used. This last device was cooled down with liquid nitrogen. On that way it is possible to record up to 20 spectra per second while with the other FT-IR device 1 spectra per second is recorded. Both equipments can be observed in **Figure 2.4**.

Figure 2.4 IR devices used for photoinitiated (left) and thermal (right) systems.

The principle which allows following the curing reaction using FT-IR measurements is the Lambert-Beer law, which is as follows:

$$A = \varepsilon \times C \times L \tag{2.12}$$

where A is the absorbance of a specie at a certain frequency, ε is the absortivity coefficient, C is the concentration and L is the optical pathway.

If one can identify a band of a functional group that reacts during the curing process, and therefore disappears, it is possible to follow the curing process. In the case of epoxy resins the band followed is the one of the epoxide group, which is at around 915 cm^{-1} for DGEBA and between 760 and 780 cm^{-1} for the cycloaliphatic epoxy resin.

Since the absorbance is proportional to the optical pathway, L, it is necessary to normalize the target band in respect to a reference band that remains unaltered during the curing process. In the case of DGEBA based thermoset the peak at 1508 cm^{-1} corresponding to the phenyl group is chosen whereas in CE based epoxy thermosets the normalization is done in respect to the band of the stretching of ester groups at 1174 cm^{-1}. On that way the conversion x, determined by FT-IR measurements can be written as follows:

$$x = 1 - \frac{\overline{A^t}}{\overline{A^0}} \tag{2.13}$$

where $\bar{A}^t$ is the normalized absorbance at a certain time and $\bar{A}^0$ is the initial absorbance that correspond to the maximum.

In the case of UV cured samples, the formulations are coated onto a silicon wafer (about 50 μm thickness) with a wire-wound applicator. The sample can then be exposed simultaneously to the UV beam, which induces the polymerization, and to the IR beam, which analyzes *in situ* the extent of the reaction.

2.2.4 Dynamic Mechanical Thermal Analysis (DMTA)

Two different equipments were used: a TA DMA 2928 dynamic analyzer operating either in three point bending mode or in single cantilever and a MK III Rheometrics Scientific Instrument operating in tensile or single cantilever mode. In all cases the working frequency was 1 Hz. Both equipments can be seen in **Figure 2.5**.

Figure 2.5 DMTA equipments used to study the viscoelastic properties of the prepared thermosets.

To obtain specimens from thermal curable formulations, they were placed in steel templates and cured with the appropriate curing schedule, depending on each material. On that way, samples of around 25 x 5 x 1.5 mm^3 were obtained. In the case of UV curable formulations, they were coated onto poly(propylene) molds with a wire-wound applicator and exposed to UV radiation with a fusion lamp (H-bulb) in air at a conveyor speed of 5 $m \cdot min^{-1}$, with radiation intensity on the surface of the sample of 280 $mW \cdot cm^{-2}$. The dimensions of the samples obtained are 25 x 15 x 3 mm^3.

DMTA studies the viscoelastic nature of a material by applying an oscilatory stress with a fixed frequency to the sample and monitoring its response at different temperatures. Two parameters can be determined: the complex modulus *(E*)* and the loss factor *(tan δ)*. The modulus contains real and imaginary contributions *(E*=E'+i·E'')*. The real part, *E'*, is a measure of the elastic response of the material, while the imaginary part, *E''*, reflects the viscous response. The maximum of the *tan δ* curve is generally accepted as the T_g of a material although it changes with the frequency used in the experiment.

2.2.5 Thermal Mechanical Analysis (TMA)

The equipment employed for carrying out TMA analysis was a Mettler TMA40. A picture of the device, as well as a magnification of the used clamp can be seen in **Figure 2.6**. This technique was used to evaluate the following characteristics:

- Thermal Expansion Coefficient (TEC) of cured samples.
- Conversion at the gel point.
- Determination of the shrinkage percentage before and after gelation.

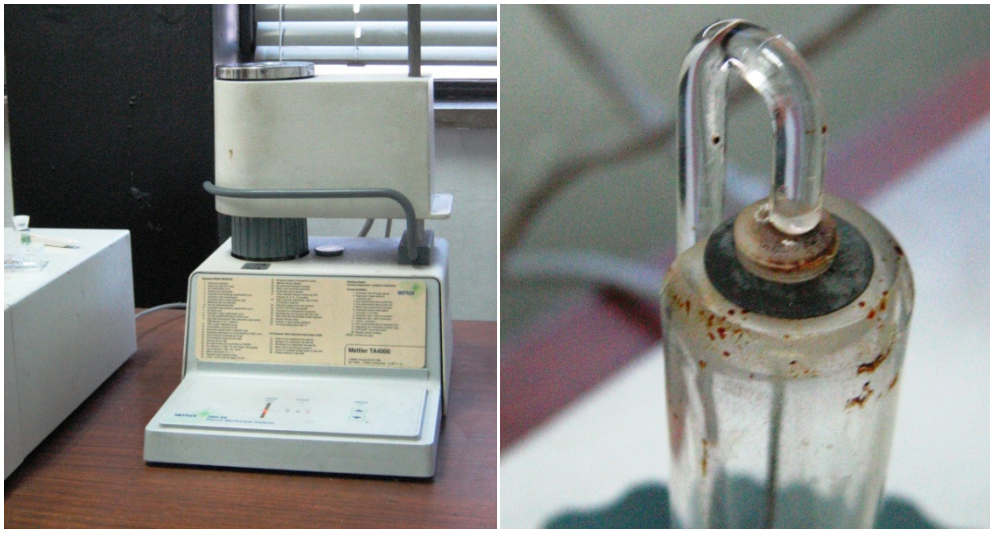

Figure 2.6 TMA apparatus used to perform thermomechanical analysis and magnification of the analyzing probe.

For the TEC determination a disc of the cured sample was placed between two quartz discs and then the system was heated at 10 °C/min and the thickness monitored. A scheme of the curves obtained can be seen in **Figure 2.7**. There are two straight lines: one before the glass transition and another after. The slopes represent the TEC in the glassy state and in the rubbery state, respectively. Additionally, the point at which there is the change in slope can be related to the glass transition of the material.

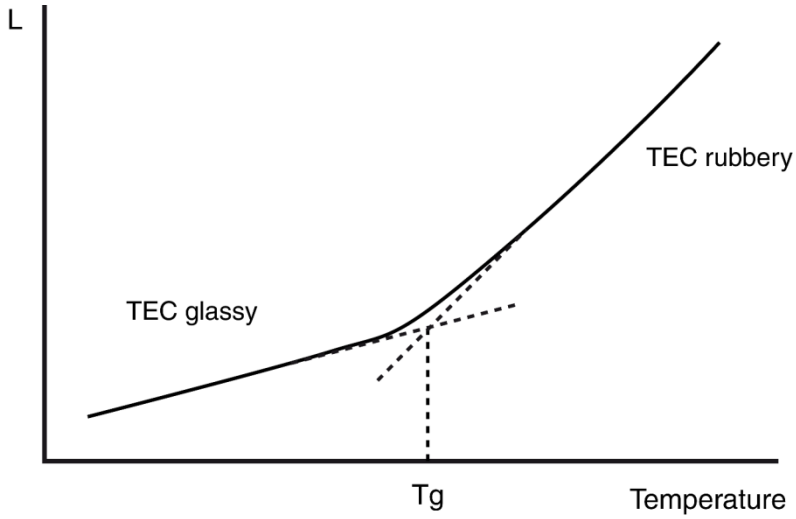

Figure 2.7 Example of the TMA curve for the TEC determination.

The conversion at the gel point was evaluated by means of non-isothermal experiments performed at a heating rate of 5 °C/min applying a periodic force that change (cycle time: 12 s) from 0.0025 to 0.01 N. Samples were supported by two small circular ceramic plates and silanized glass fibers, which were impregnated with the formulation. The gel point was taken in TMA as the temperature at which a sudden decrease in the amplitude of the oscillations was observed (**Figure 2.8**). The gel conversion, α_{gel}, was determined as the DSC conversion at the gelation temperature determined by TMA.

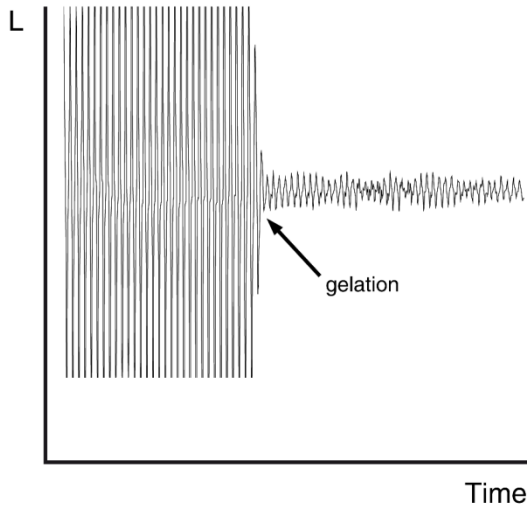

Figure 2.8 Example of the TMA curve for the determination of the gel point.

Finally, to evaluate the shrinkage during curing, isothermal experiments at 120 °C were performed using a force of 0.01 N and the thickness was monitored during the curing process. The degree of shrinkage ($\alpha_{shrinkage}$) can be calculated as follows:

$$\alpha_{shrinkage} = \frac{L_t - L_0}{L_\infty - L_0} \tag{2.14}$$

where L_t, L_0 and L_∞ are, respectively, the thickness at a certain time, at the beginning of the curing and after the reaction is finished. **Figure 2.9** is an example of the curve obtained by TMA.

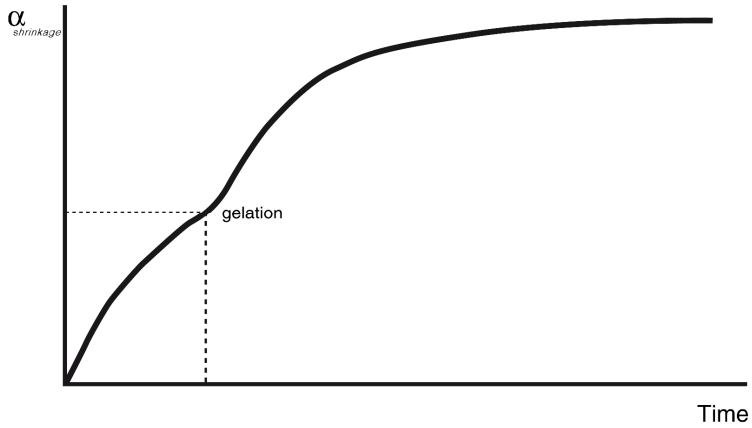

Figure 2.9 Example of the TMA curve for the determination of the shrinkage.

2.2.6 Rheology

Rheological measurements were carried out in the parallel plates (geometry of 25 mm) mode with an ARG2 rheometer (TA Instruments, **Figure 2.10**), equipped with a Peltier system for controlling the temperature. Curable formulations are placed between two aluminum plates with a distance between plates (gap) of approximately 1000 μm. By rheology it is possible to study the gel time, the conversion at the gel point and the evolution of the shrinkage during curing, as well as determining the viscosity of uncured formulations.

Figure 2.10 Rheometer ARG2 used, with a magnification of the geometry used.

Rheological measurements are based on monitoring the tension generated in the sample as a response to the application of an oscillatory shear force. The viscoelasticity of a given polymer reflects in the difference in the applied and measured angle δ. As for the case of DMTA, one can define a complex modulus $G^* = G' + i \cdot G''$.

The complex viscosity (η^*) is determined in multi-frequency experiments at a certain temperature and amplitude. This amplitude must be comprised within the range of linear viscoelasticity.

The gel time is determined in isothermal experiments where the oscillation amplitude changes to adjust to the changes in the material. The point at which $tan\ \delta$ is independent of the

frequency is defined as the gel point (**Figure 2.11**). By stopping the experiment at that point and performing a DSC scan to determine the remaining heat it is possible to determine the conversion at gelation.

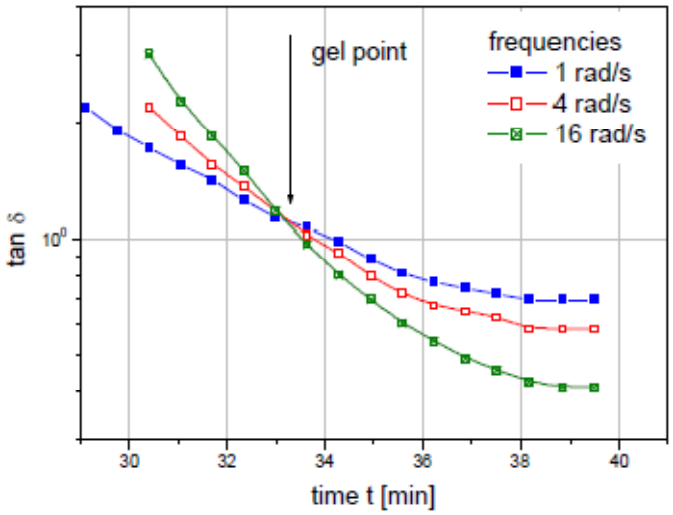

Figure 2.11 Example of gel time determination in a multifrequency experiment.

Finally, to monitor the shrinkage, as for the case of TMA, an isothermal experiment is performed and a force of 0.01 N applied to monitor the gap between plates, when working under gap control conditions.

2.2.7 Thermogravimetry (TGA)

A thermobalance Mettler TGA/SDTA 851e (**Figure 2.12**) was used to analyze the thermal degradation of cured samples and of the synthesized hyperbranched polymers. The degradation was carried out in dynamic conditions, at 10 ºC/min under nitrogen or air, from 30 to 800 ºC. The most important parameters extracted from the analysis of such curves are the initial degradation temperature, the temperature of the maximum degradation rate and the char yield.

Figure 2.12 Thermobalance used for the thermal stability evaluation.

2.2.8 Density and Shrinkage Measurements

The density of both formulations and cured samples were determined in a Micromeritics AccuPyc 1330 Gas Pycnometer (**Figure 2.13**) thermostatized at 30 ºC and using helium as gas. The device works by measuring the amount of displaced gas by the sample. The pressures

observed upon filling the sample chamber and then discharging it into a second empty chamber allow the determination of the sample volume as follows:

$$V_s = V_c + \frac{V_r}{1-\frac{P_1}{P_2}} \tag{2.15}$$

where V_s is the volume of the sample, V_c is the volume of the empty sample chamber, V_r is the volume of reference (obtained from calibration), P_1 is the pressure of the sample chamber and P_2 the combined pressure after expanding the gas to the second chamber.

Figure 2.13 Gas pycnometer employed for the density determination.

From the volume measured and knowing the weight, the density of a certain sample can be easily calculated since $\rho = W/V$.

Alternatively, another methodology was used to determine densities. The density of the uncured formulation was measured with a standard pycnometer in a thermostatically controlled bath at 30 ºC. The density of the cured thermosets was determined indirectly by the flotation method. This consists in finding the optimal concentration of KBr in a water solution that makes the thermoset remain in the middle. Then the density of this solution is measured with the pycnometer.

The evaluation of the shrinkage undergone during curing is obtained by comparison of the shrinkage of the curable formulation and the cured thermosets, using the following expression:

$$Shrinkage\ (\%) = \frac{\rho_{polym} - \rho_{mon}}{\rho_{polym}} \times 100 \tag{2.16}$$

2.2.9 Scanning Electron Microscopy (SEM)

Three different SEM microscopes were used: a Jeol JSM 6400 with 3.5 nm resolution, a FEI Quanta 600 Environmental Scanning Electron Microscope (ESEM) equipped with an X-Ray analyzer and a ZEISS SUPRA™ 40 Field Emission Scanning Electron Microscope (FE-SEM) with a nominal resolution of 1.5 nm. Pictures of two of these equipments can be seen in **Figure 2.14**. For standard SEM analysis, samples were coated with gold while for the FE-SEM analysis with carbon. For ESEM measurements it is not necessary to coat the sample.

SEM is a type of electron microscope that images a sample by scanning it with a high-energy beam of electrons in a raster scan pattern. The electrons interact with the atoms that make up the sample producing signals that contain information about the sample's surface topography, composition, and other properties such as electrical conductivity. FE-SEM uses a

special type of electron gun that allows achieving higher spatial resolutions and minimizes the damaging of the sample. In the case of ESEM the measurements are performed without coating the surface to be observed. This represents an advantage since the same specimens can afterwards be used for other experiments.

Figure 2.14 ESEM (left) and SEM (right) equipments used for obtaining surface images.

2.2.10 Transmission Electron Microscopy (TEM)

The equipment used to perform TEM microcopy, as can be seen in **Figure 2.15**, was a Jeol 1011 microscope. Samples were prepared either cutting thin films with an ultramicrotome at room temperature (cured thermosets) or by deposition of diluted solutions of the samples onto support grids (hyperbranched polymers).

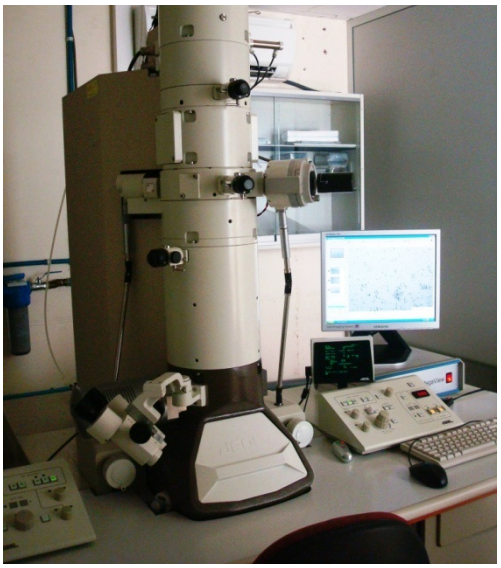

Figure 2.15 TEM equipment used to observe the morphology of the thermosets prepared.

TEM is a microscopy technique whereby a beam of electrons is transmitted through an ultra thin specimen, interacting with the specimen as it passes through. An image is formed from the interaction of the electrons transmitted through the specimen; the image is magnified and

focused onto an imaging device, such as a fluorescent screen, on a layer of photographic film, or to be detected by a sensor such as a CCD camera.

2.2.11 Nuclear Magnetic Resonance (NMR)

Two different equipments were used to confirm the chemical structure of the synthesized hyperbranched polymers: a Bruker DRX 500 NMR spectrometer and a Varian Gemini 400 NMR spectrometer of 400 MHz (**Figure 2.16**). The deuterated solvent to dissolve the sample was chosen in each case being the most common ones $CDCl_3$ and DMSO-d_6. The experimental conditions in the case of ^{1}H-NMR measurements where 500 or 400 MHz of magnetic field, 1 s of delay time (D1) and 14 accumulations to obtain quantitative measurements. For ^{13}C-NMR measurements the magnetic field was 125.75 or 100.6 MHz, a D1 of 0.5 s, 0.2 s of acquisition time and 500 spectra were recorded at least.

Figure 2.16 Picture of the Varian equipment used for the chemical identification of the HBPs.

2.2.12 Size Exclusion Chromatography (SEC)

SEC analysis were carried out with two different equipments:

- An Agilent 1200 series system (**Figure 2.17**) with PLgel 3 μm MIXED-E, PLgel 5 μm MIXED-D and PLgel 20 μm MIXED-A columns in series, and equipped with an Agilent 1100 series refractive-index detector. Calibration curves were based in polystyrene standards having low polydispersities. THF was used as the eluent at a flow rate of 1.0 mL/min, the sample concentrations were 5-10 mg/mL, and injection volumes of 100 μL were used. With this technique it is possible to determine the molecular weight ($\bar{M}_n$, $\bar{M}_w$) of the synthesized HBPs as well as the molecular weight dispersity ($Đ_M$), by comparing the retention time of a diluted solution of the sample with the solution of standards, which are polymers with different molecular weight and narrow distributions.
- A modular build SEC-system coupled with a multi-angle laser light scattering (MALLS) detector DAWN EOS (Wyatt Technologies, USA) and a refractive index (RI) detector (Knauer, Germany) in combination with a PL-GEL 5 μm mixed C column, 300 x 7.5 mm (Polymer Laboratories, UK) using a flow rate of 1 mL/min and THF as eluent. In this case the molecular weight is determined by the light scattering profile of the sample.

Figure 2.17 Agilent chromatograph used for the molecular weight determination of HBPs.

2.2.13 Impact Test

The impact test was performed at 23 ºC by means of an Zwick 5110 impact tester, according to ASTM D 4508-05 (2008) using prismatic rectangular specimens (ca. 20 x 11 x 2.5 mm^3). The pendulum employed had a kinetic energy of 1 J. A picture of the testing machine can be seen in **Figure 2.18**. By means of this technique it is possible to determine the impact energy that a sample can absorb, indicating the toughness of the same. The broken samples were afterwards observed by means of SEM in order to correlate the energy value obtained with the impact surface morphology.

Figure 2.18 Impact testing machine used for the determination of the impact strength of the prepared thermosts.

2.2.14 Microhardness

Microhardness was measured with a Wilson Wolpert (MicroKnoop 401MAV) device (**Figure 2.19**) following the ASTM D1474-98 (2002) standard procedure. For each material 10 determinations were made with a confidence level of 95%. The Knoop microhardness (HKN) was calculated from the following equation:

$$HKN = \frac{L}{A_p} = \frac{L}{l^2 \times C_p} \tag{2.17}$$

where, L is the load applied to the indenter (0.025 Kg), A_p is the projected area of indentation in mm^2, l is the measured length of the long diagonal of indentation in mm, C_p is the indenter constant (7.028 x 10^{-2}) relating l^2 to A_p.

This technique is based on measuring the length of the long diagonal produced by the indentation of a rhomboidal tip. The length is related to the hardness of the material: the shorter the diagonal the hardest the material.

Figure 2.19 Microhardness tester used for the determination of the Knoop hardness of the prepared thermosets.

2.2.15 Pendulum Hardness

The pendulum hardness (Persoz, ASTM D4366) was measured from the damping of the oscillation of the pendulum. Pendulum hardness values are expressed in number of oscillations and are related directly to the softness of the surface of the sample. A sample is placed under a pendulum and the more oscillations, the higher hardness is. A schematic representation of the testing machine can be seen in **Figure 2.17**.

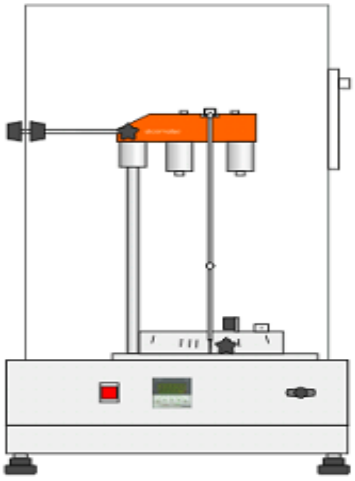

Figure 2.20 Schematic representation of the machine used to determine the pendulum hardness.

2.2.16 Nanoindentation

Nanoindentation studies were performed with a Berkovich tip with its function area calibrated against fused silica standard, at a strain rate of 0.05 s^{-1} in an equipment with continuous stiffness measurement at 45 Hz and 2 nm of amplitude. The hardness and elastic modulus data obtained

are the result of an average of 16 indentation experiments analyzed with the Oliver and Pharr method.[8]

Hardness and elastic modulus were obtained from indentation curves. The load *P* and the indentation depth *h* were continuously measured during the test. **Figure 2.18** shows the load-displacement (indentation depth) curve along with some important parameters used in the Oliver-Pharr analysis.

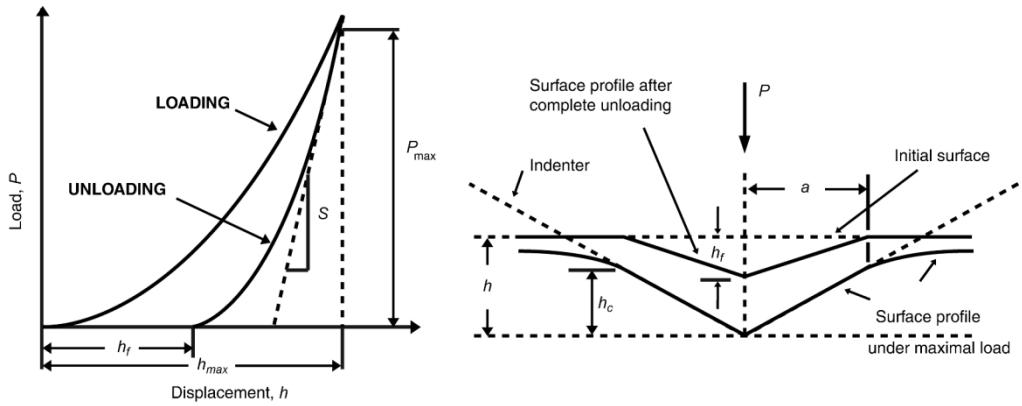

Figure 2.21 A typical load-displacement curve (a) and schematic of a cross-section of an indentation (b).

The most important values are the peak load *(P_{max})*, the maximum depth or total surface deflection max *(h_{max})*, the final or residual depth after complete unloading *(h_f)*, the contact depth *(h_c)* at the maximum load and the slope of the upper portion of the unloading curve *($S = dP/dh$)*. The parameter *S* is known as the elastic contact stiffness and it yields information about the state of contact at a certain point.[9]

An accurate measurement of the elastic contact stiffness *S* and of the projected contact area A_p under load must be performed to calculate the hardness and elastic modulus. The most widely used method for establishing the contact area was developed by Oliver and Pharr. This method uses a power law to fit the unloading curve and takes the tangent at peak load (P_{max}) as the maximum contact stiffness S_{max} or the total system stiffness.[10] The projected contact area, A_p calculated using *S*, should be the actual contact area at the peak load. Extrapolating this line down to $P = 0$ yields a displacement value h_c, the contact depth associated with the peak load.[11]

Using Sneddon's elasticity theory and empirical results of Oliver and Pharr, the contact depth h_c can be calculated as:[12]

$$h_c = h_{max} - \varepsilon \frac{P_{max}}{S} \tag{2.18}$$

where ε is a constant that depends on the geometry of the indenter.

---

[8] W. C. Oliver, G. M. Pharr, *J. Mater. Res.* **1992,** *7*, 1564.
[9] Hay, J. L. and Pharr, G. M. Instrumented indentation testing. In ASM Handbook, Vol. 8: Mechanical Testing and Evaluation, 10th ed. (Kuhn, H. and Medlin, D., eds.). ASM International, 2000, 232–243.
[10] J. L. He, S. Veprek. *Surf. Coat. Tech.* **2003,** *163–164,* 374.
[11] A. R. Franco, G. Pintaude, A. Sinatora, C. E. Pinedo, A. P. Tschiptschin. *J. Mater. Res.* **2004,** *7,* 483.
[12] N. Q. Chinh, J. Gubicza, Z. Kovacs, J. Lendvai. *J. Mater. Res.* **2004,** *19,* 31.

In the Oliver-Pharr method, the data taken from the upper portion of the unloading curve is fitted with the power law relation:

$$P = \alpha(h - h_f)^m \tag{2.19}$$

where m and α are empirical constants, determined after unloading data fitting and h_f is the residual depth.

When the fitting parameters m and α are determined, the residual depth h_f can be evaluated by substitution $h = h_{max}$ = and $P = P_{max}$ in eq. (2.19):

$$h = h_f - \left(\frac{P}{\alpha}\right)^{1/m} \tag{2.20}$$

Now the contact stiffness is obtained from eq. (2.19) differentiating P with respect to h:

$$S = \frac{dP}{dh} = m\alpha(h_{max} - h_f)^{m-1} \tag{2.21}$$

When the contact stiffness S and the projected contact area A_p (A_p=24.5h_c^2 for Vickers and Berkovich indenters[13]) are known, the reduced modulus of indentation E_r can be determined as:

$$E_r = \frac{\sqrt{\pi}}{2\beta}\frac{S}{\sqrt{A_p}} \tag{2.22}$$

where β is a correction factor related to the lack of symmetry of the indenter.

Finally, indentation hardness H is defined as the peak indentation load P_{max} divided by the projected area of contact A_p[14]

$$H = \frac{P_{max}}{A_p} \tag{2.23}$$

[13] A. C. Fischer-Cripps. *Nanoindentation*. Springer, New York, **2004**.
[14] Overview of mechanical testing standards. *Applications Bulletin*, *CSM Instruments*, **2002**, No. 18.

Chapter 3

Use of Commercially Available HBPs in the Modification of Epoxy Resins

3.1 Introduction

One of the most interesting points of HBPs in respect to dendrimers is their lower cost that makes them a real commercial alternative. Nowadays, there are many companies selling HBPs such as, DSM, BASF or Dow Chemical. Among them, the Swedish company Perstorp commercializes a family of HBPs with the trade name Boltorn HX (where X can be 20, 30 or 40) that consists in aliphatic hyperbranched polyesters. **Figure 2.1** shows the idealized chemical structure of such polymers.

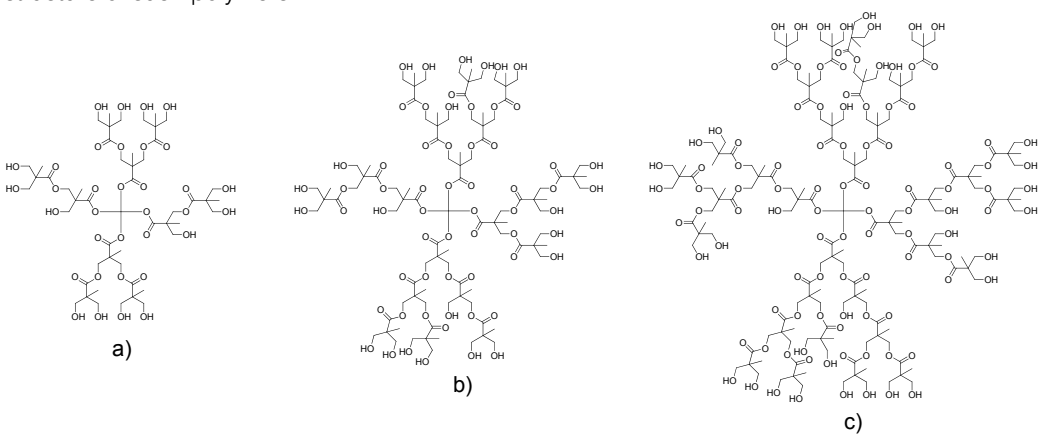

Figure 3.1 Idealized chemical structure of Boltorn (a) H20, (b) H30 and (c) H40.

The synthesis of this type of polymers, as reported by Hult *et al.*,[1] is based on the polycondensation of an AB_2 monomer: 2,2-bis(hydroxymethyl)propionic acid (bis-MPA). A core molecule such as ethoxylated pentaerythritol (PP50) is used in order to control molar mass and molecular weight dispersity. The polymerization is carried out in bulk at around 140 °C using p-toluenesulfonic acid (p-TSA) as catalyst and under vacuum in order to eliminate the water formed (**Figure 3.2**). The addition of the monomer is performed in a pseudo-one step process, which consist on adding the monomer in successive portions corresponding to the stoichiometric amount for each generation.

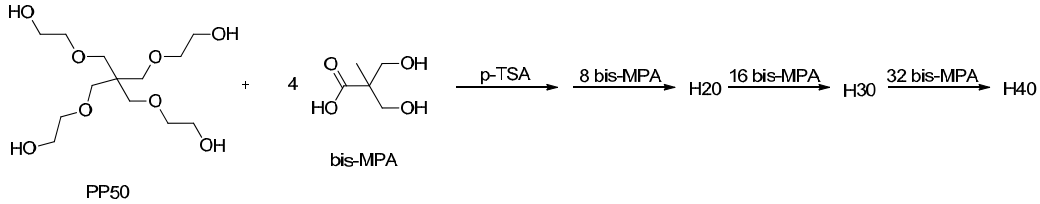

Figure 3.2 Synthesis of Boltorn HX polymers in a pseudo-one pot reaction.

The characterization of these polymers have been extensively studied and particularly interesting has been the work carried out by Zagar *et al.*[2] By means of SEC and NMR they were able to determine among other molecular weight, molecular weight dispersity and degree of branching and the values are shown in **Table 3.1**. The values calculated using the Fréchet definition of DB are close to the theoretical 50% of HBPs. Since molecular weights are small (less than 10 000 g/mol) the simplification of Frey cannot be applied.

Table 3.1 Characterization of Boltorn HX polymers.

HBP	Molar ratio (PP50:bis-MPA)	$\bar{M}_w$ (g/mol)	$\bar{M}_n$ (g/mol)	$Đ_M$	$DB_{Fréchet}$ (%)
H20	1:12	1860	920	2.01	43.5
H30	1:28	3340	1410	2.38	43.0
H40	1:60	6640	2580	2.57	43.0

Other authors such as Fradet *et al.*[3] studied the side reactions that take place during the polycondensation and demonstrated the concurrence of reaction such as cyclizations or isomerations by means of MALDI-TOF mass spectrometry.

Using the middle-up approach many different HBPs based on Boltorn HX polymers can be synthesized. Some of them are commercialized by Perstop as for example Boltorn U3000 or Boltorn W3000. The first one comes from the esterification of the terminal hydroxyl groups of a third generation polyester with different fatty acids whereas the second from the combined esterification with fatty acids and hydrophilic chains, as described in their corresponding datasheets.

Apart from those alternatives provided by the manufacturer, there are many examples in the literature of the modification of Boltorn-like polymers with many different groups in order to make them suitable for different applications. For example, Frey *et al.*[4] modified a polyester precursor

---

[1] E. Malmström, M. Johansson, A. Hult. *Macromolecules* **1995,** *28,* 1698.
[2] E. Zagar, M. Zigon, S. Podzimek. *Polymer* **2006,** *47,* 166.
[3] L. Chikh, M. Tessier, A. Fradet. *Polymer* **2007,** *48,* 1884.
[4] J. E. Klee, C. Schneider, D. Hölter, A. Burgath, H. Frey, R. Mülhaupt, *Polymers for Advanced Technologies* **2001,** *12,* 346.

with methacrylic groups in order to be used as modifier to reduce shrinkage in dental composites. Plummer *et al.*[5] prepared a polyester with trimethyl silyl end groups with different degrees of modification to tune the porosity of poly(methyl silsesquioxane) coatings. Jiang *et al.*[6] introduced benzoyl groups as end groups of Boltorn-like polymers. Their objective was to study the self assembly of these structures induced by the Π-Π stacking of the aromatic rings introduced.

In the field of epoxy thermosets, a modification of Boltorn H30 with long aliphatic chains have been prepared and used as modifier (**Figure 3.3**). The difference in polarity between the core and the shell and the fact that the HBP was not reactive towards epoxides resulted in phase separation of sphere-like particles of the HBP within the epoxy matrix.[7]

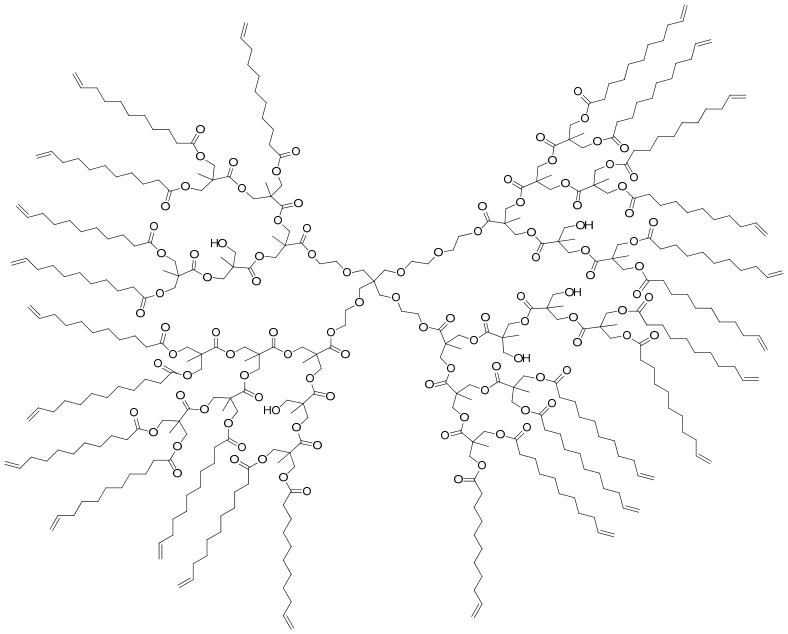

Figure 3.3 Idealized chemical structure of Boltorn H30 esterified with 10-undecenoyl chloride.

In recent years polymer/clay nanocomposites have attracted great interest both in the industrial and academic world. The attractiveness of this type of material lays on the large improvements in the mechanical and thermal properties produced by only small amounts of homogeneously dispersed nanometer-size clays.

The term clay, as defined by Grim,[8] "implies a natural, earthy, fine-grained material which develops plasticity when mixed with a limited amount of water". By plasticity is meant the property of the moistened material to be deformed under the application of pressure, with the deformed shape being retained when the deforming pressure is removed". In the field of polymer/clay nanocomposites the most used clays are montmorillonite and sepiolite.

---

[5] C. J. G. Plummer, L. Garamszegi, T-Q. Nguyen, M. Rodlert, J-A. E. Månson. *J. Mater. Sci.* **2002,** *37,* 4819.
[6] G. Jiang, L. Wang, H. Yu, C. Chen, X. Dong, T. Chen, Q. Yang. *Polymer* **2006,** *47,* 12.
[7] X. Fernández-Francos, D. Foix, A. Serra, J. M. Salla, X. Ramis. *React. Funct. Polym.* **2010,** *70,* 798.
[8] R. E. Grim. Applied Clay Mineralogy. McGraw-Hill, New York, **1962**.

Expandable layered silicate clays, with montmorillonite (MMT) as a typical example,[9] are among the most commonly used nanofillers for polymer nanocomposites. MMT is a naturally abundant, easily accessible soil mineral with a layered structure (**Figure 3.4**).

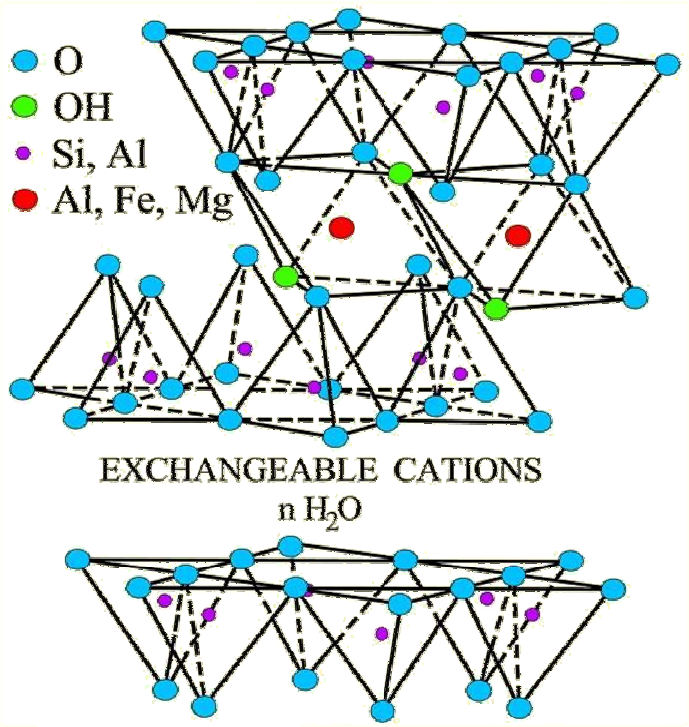

Figure 3.4 Schematic structure of montmorillonite.

The layers consist of two tetrahedral sheets sandwiching an edge-shared octahedral sheet of either aluminum or magnesium hydroxide.[10] When the clay is stacked, each layer is separated by regular van der Waals gaps, called interlayers or galleries. The microstructure of the clay consists of several layers (lamellas of 1 nm) lying parallel forming a primary particle (8-10 nm). These primary particles are, in turn, aggregated into larger irregular particles of size between 0.1 and 10 μm).[11] The layered structure together with the suitable layer charge density enable a rich intercalating chemistry, thus allowing MMT to be intercalated directly with hydrophilic polymers or chemically modified to enhance the compatibility with hydrophobic polymers.[12]

Sepiolite is a fibrous hydrated magnesium silicate whose typical formula is: $Mg_4Si_6O_{15}(OH)_2 \cdot 6H_2O$ (**Figure 3.5**).[13] The name comes from a perceived resemblance of the material to the porous bones of the cuttlefish or sepia. Sepiolite is included in the phyllosilicate group because it contains a continuous two-dimensional tetrahedral sheet of composition SiO.[8] It differs, however, from the other layered silicates because of the lack of continuous octahedral sheets.

---

[9] S. S. Ray, M. Okamoto. *Prog. Polym. Sci.* **2003,** *28,* 1539.
[10] M. Alexandre, P. Dubois. Mater. Sci. Eng. R: Reports **2000,** *28*, 1.
[11] A. Akelah, N. Salahuddin, A. Hiltner, E. Baer, A. Moet. *Nanostructured Materials* **1994,** *4,* 965.
[12] P. C. LeBaron, Z. Wang, T. J. Pinnavaia. *Appl. Clay Sci.* **1999,** *15*, 11.
[13] E. García-Romero, M. Suárez. *Clays and Clay Minerals* **2010,** *58,* 1.

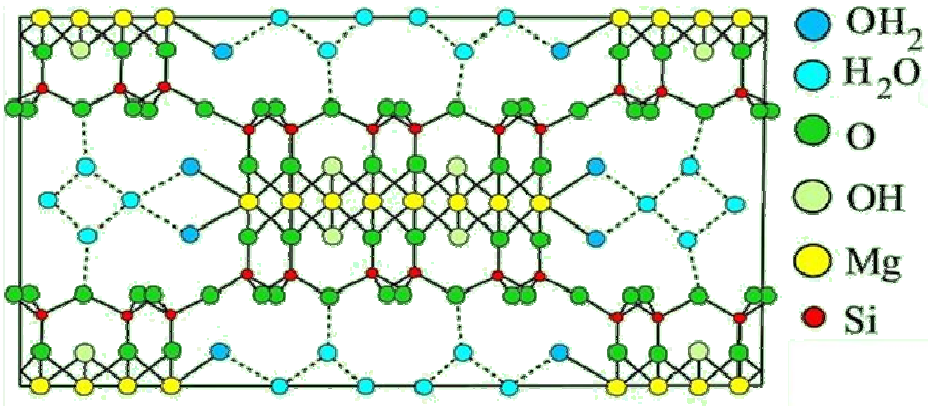

Figure 3.5 Schematic structure of sepiolite.

Sepiolite is composed by elemental particles with needle-like or fibre-like shape. The dimensions of the a single sepiolite fiber may vary between 0.2 to 4 μm in length, 10 to 30 nm in width and 5 to 10 nm in thickness, with open channels of dimensions 3.6 Å x 10.6 Å running along the axis of the particle. These particles are arranged forming loosely packed and porous aggregates with an extensive capillary network which explains their high porosity. Sepiolite has the highest surface area of all the clay minerals, more than 300 m^2/g, and a high sorption capacity.[14]

In the following sections of this chapter the use of Boltorn H30 in the modification of commercially available epoxy systems will be discussed. Particular attention will be paid to the influence of the additive in the curing process as well as in the final properties of the resulting thermosets. The use of Boltorn H30 in the preparation of epoxy/sepiolite clay nanocomposites will be also investigated. Finally, the use of chemically modified Boltorn H30 with different blocking groups (benzoyl and trimethylsilyl) will be studied and we will put into evidence the importance of the end group in the morphology of the final material. This work has yielded the following articles:

3.2 Study on the chemical modification of epoxy/anhydride thermosets using a hydroxyl terminated hyperbranched polymer

3.3 Combined use of sepiolite and a hyperbranched polyester in the modification of epoxy/anhydride thermosets. A study of the curing process and the final properties.

3.4 New thermosets obtained from bisphenol A diglycidyl ether and hydroxyl-ended hyperbranched polymers partially blocked with benzoyl and trimethylsilyl groups.

[14] H. Shariatmadari, A. R. Mermut. *Soil Sci. Soc. Am. J.* **1999,** *63,* 1167

3.2 Study on the chemical modification of epoxy/anhydride thermosets using a hydroxyl terminated hyperbranched polymer

D. Foix[1], Y. Yu[1,2], A. Serra[1], X. Ramis[3], J. M. Salla[3]

[1] Department of Analytical and Organic Chemistry, University Rovira i Virgili, Marcel.li Domingo s/n, 43007 Tarragona, Spain

[2] The Key Laboratory of Molecular Engineering of Polymers, Ministry of Education, Department of Macromolecular Science, Fudan University, Shanghai 200433, China

[3] Laboratory of Thermodynamics, ETSEIB, University Politècnica de Catalunya, Av. Diagonal 647, 08028 Barcelona, Spain

ABSTRACT

Mixtures of diglycidylether of bisphenol A (DGEBA) resin and commercially available hyperbranched polyester (HBP) Boltorn H30 were cured by anhydride to covalently bond the hydroxyl end groups in HBP with the epoxy resin. The curing mixtures were investigated by Differential Scanning Calorimetry (DSC) to study the curing evolution and to evaluate the kinetic parameters. DSC studies suggested that HBP could increase the curing rate of epoxy/anhydride systems at low conversions, but it produced a decelerative effect in the last stages of the curing. The influence of the HBP content and the proportion of anhydride on the curing conversions were discussed in detail. The addition of a tertiary amine was proved to decrease the curing temperatures. By Fourier Transform Infrared Spectroscopy (FTIR) the reaction of hydroxyl groups during the whole process was confirmed. By the determination of the conversion at the gelation, we could prove that it increased on increasing the proportion of HBP in the reactive mixture. By Thermomechanical Analysis (TMA) we could determine a reduction of the shrinkage after gelation.

INTRODUCTION

Hyperbranched polymers (HBP) belong to a group of macromolecules known as dendritic polymers. The main characteristic is their highly branched structure and the large number of functional reactive groups, which increase the solubility and decrease the intrinsic viscosity. However, they present poorer mechanical properties compared to their linear analogues.[1]

Epoxy resins are widely used in coatings, adhesives and polymer composites, but the applications of cured epoxy resins are often restricted by their poor toughness. HBP can be used to improve the toughness of the epoxy materials due to its high density of functional terminal groups, which allows to tune the interaction with the matrix.[2-4] The low viscosity of the HBP improves the processability of the epoxy resins in comparison to that obtained on adding linear polymers or rubbers as toughners.[5,6] Moreover, they not affect the Young's modulus and the glass transition temperature.[2]

Most of the research published until now was focused on epoxy resin/hydroxyl-ended hyperbranched polyester cured with amine.[7,8] In those systems, HBPs were used as a dispersed phase and did not react with epoxy resins. When the molecular weight or the proportion of HBP was high enough, the addition of these modifiers improved the toughness of the epoxy thermosets.[9,10] However, there are a lot of contradictory reports on the modification of epoxy resins with HBP, including miscibility, thermal and mechanical properties of both uncured and cured systems. For example, the use of suitable end groups, such as amines, can be appropriate to enhance the compatibility of HBP and other polymers. Park and Jin[11] synthesized an amine-terminated hyperbranched polyimide by the polycondensation of a commercially

available triamine monomer with a dianhydride, and they observed improvements in the critical stress intensity factor and impact strength of their epoxy blends.

Månson *et al.* modified DGEBA with an epoxy terminated hyperbranched polyester produced by Perstorp using isophoronediamine as curing agent. They demonstrated that epoxy terminated HBPs take part into the reaction of amine cured epoxy resins. This has been shown to affect thermodynamic behavior,[12,13] the gelling and network build-up[14] as well as the final morphologies.[15] Their work evidenced the ability of HBP to toughen brittle epoxy matrix. In contrast, Wu *et al.*[10] showed that no particular advantages were achieved by the use of hyperbranched polyesters in comparison to the analogous linear polymers. However, the polymers they investigated had hydroxyl or acetyl as terminal groups, while the polymers used by Månson *et al.* were always epoxy ended.[2] Thus, the difference in the terminal groups seems to have a profound effect on the properties of the materials. In fact, epoxy groups are reactive in amine curing systems while hydroxyl groups are not at the conventional curing temperatures.

Epoxy anhydride systems are particularly important in electronic materials. They are usually modified to improve their processing, thermal and mechanical properties.[16,17] The addition of a hydroxyl terminated HBP to these systems would provide ester linkages by reaction of anhydride not only with epoxides but also with hydroxyl groups. In this way, the chemical incorporation of the HBP should produce a profound effect on the properties of the final epoxy thermosets and also in their curing behavior.

Until now, there are few reports[18,19] regarding the influence of hydroxylic HBP on the toughness and thermal properties of epoxy resins cured with anhydride but these works show an increase in the toughness of the cured materials. However, the chemical processes and the structure of the cured material have not been fully clarified because in a recently published study of Yang *et al.*[19] the effect of the hydroxyl groups in the final properties was attributed to hydrogen instead covalent bonding. They assumed that hydroxylic groups did not react with anhydrides in the formulation studied.

In thermosetting coatings the loss of adhesion arises from the shrinkage that takes place on curing. This shrinkage also leads to the appearance of imperfections, which reduce their protective capability.[20] In a previous work of our research group,[21] we could demonstrate that the addition of a hydroxyl terminated HBP to the DGEBA induces an expansion during curing, which increases with the proportion of modifier. The cationic mechanism through which the curing took place led to the formation of covalent bonds between the HBP and the epoxy matrix.

In the present article, we report the effect of the addition of a commercial hydroxyl terminated HBP polyester, Boltorn H30, on the curing process of epoxy/anhydride/amine systems. The role of the hydroxylic groups of HBP is investigated in detail.

EXPERIMENTAL

Materials

Diglycidylether of bisphenol A (DGEBA) Epitoke Resin 827 was provided by Shell Chemicals with epoxy equivalent of 182 g/eq. 1,2,3,6-Tetrahydrophthalic anhydride (THPA), N,N-dimethylbenzylamine (BDMA) from Aldrich were used without further purification.

A hydroxyl terminated hyperbranched aliphatic polyester produced by Perstorp with the trademark Boltorn H30 was used as modifier. Its chemical structure is shown in **Scheme 1**. The molecular weight of H30, as reported on data sheet, is about 3600 g/mol and the theoretical number of OH groups is 32/molecule.

Sample preparation

The compositions of the formulations studied containing amine are collected in **Tables 1** and **2**. In **Table 1** the formulations containing a 10 wt% of Boltorn H30, with different epoxy/anhydride ratio are collected. The amine/anhydride molar ratio was kept unchanged. In **Table 2** the formulations with several ratios DGEBA/Boltorn H30/anhydride are specified. The formulation of the simple DGEBA/THPA was 1:1 in molar ratio and for the 10% H30/DGEBA/THPA was the same and adding a 10% in weight of the HBP.

The mixtures were prepared by adding THPA to the DGEBA resin at 100 °C and mixing until the solution became clear (around 3 min). The selected amounts of Boltorn H30 were added to the previously prepared mixture and then they were stirred at 100 °C until a transparent mixture was obtained. After that, BDMA was added, stirred, cooled down to -10 °C and maintained at this temperature until used.

Table 1 Composition of the samples studied (epoxide, anhydride, amine and hydroxylic groups) of the formulations with a 10 wt% of Boltorn H30.

Sample		DGEBA	THPA	BDMA	H30
DGEBA/THPA/BDMA	wt [a]	54.5	45.5	0.55	--
	mol [b]	1	1	0.0136	--
10% (1:0)[c] H30	wt	49	41	0.49	10
	mol	1	1	0.0136	0.33
10% (1:0.25) H30	wt	47.2	42.8	0.51	10
	mol	0.92	1	0.0136	0.32
10% (1:0.50) H30	wt	45.5	44.5	0.53	10
	mol	0.85	1	0.0136	0.30
10% (1:1) H30	wt	41.7	48.3	0.58	10
	mol	0.72	1	0.0136	0.28

a. wt% of DGEBA, THPA, BDMA and H30.

b. Molar ratio of epoxide, anhydride, amine and hydroxyl groups.

c. Notation means: mol anhydride/mol hydroxyl which could react.

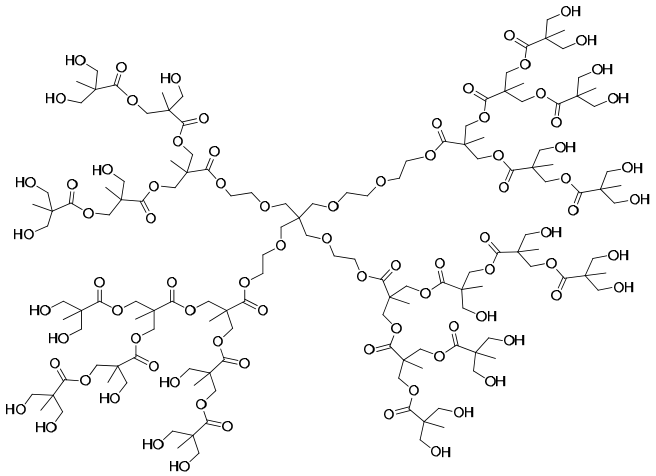

Scheme 1 Idealized chemical structure of the commercial hyperbranched polymer Boltorn H30.

Characterization techniques

Calorimetric studies were carried out on a Mettler DSC-821e thermal analyzer in covered Al pans under N_2. The calorimeter was calibrated using an indium standard (heat flow calibration) and an indium-lead-zinc standard (temperature calibration). The samples weighed approximately 5-10 mg. In the dynamic curing process the degree of conversion by DSC (x_{DSC}) was calculated as follows:

$$x_{DSC} = \frac{\Delta h_T}{\Delta h_{tot}} \quad (1)$$

where Δh_T is the heat released up to a temperature T, obtained by integration of the calorimetric signal up to this temperature, and Δh_{tot} is the total reaction heat associated with the complete conversion of all reactive groups.

The kinetic studies were performed at heating rates of 2, 5, 10 and 15 ºC/min in N_2 atmosphere. The precision of the given enthalpies is ± 3%.

The glass transition temperature for each material (T_g) was calculated after complete curing, by means of a second scan, as the temperature of the half-way point of the jump in the heat capacity when the material changed from the glassy to the rubbery state. The precision of the determined temperatures is estimated to be ±1 ºC.

Table 2 Composition in wt % of the mixture and molar ratio between epoxy, anhydride and hydroxyl groups of the formulations with different weight percent of H30.

Sample		DGEBA	THPA	BDMA	H30
5% H30	wt [a]	50	45	0.54	5
	mol [b]	0.928	1	0.0136	0.15
10% H30	wt	45.5	44.5	0.53	10
	mol	0.85	1	0.0136	0.30
15% H30	wt	40.8	44.2	0.53	15
	mol	0.77	1	0.0136	0.458
20% H30	wt	36.2	43.8	0.52	20
	mol	0.69	1	0.0136	0.62

a. wt% of DGEBA, THPA, BDMA and H30.

b. Molar ratio of epoxide, anhydride, amine and hydroxyl groups.

The FTIR spectra of the samples during curing were recorded in a FTIR-680PLUS spectrophotometer from JASCO with a resolution of 4 cm^{-1} in the absorbance mode, equipped with an attenuated total reflection accessory (ATR) with thermal control and a diamond crystal (Golden Gate heated single-reflection diamond ATR from Specac-Teknokroma).

The disappearance of the absorbance peak at 915 cm^{-1} (epoxy bending) was used to monitor the epoxy conversion. The consumption of the reactive carbonyl group in the anhydride was evaluated by measuring the changes in absorbance at 1862 cm^{-1} (carbonyl C=O symmetric stretching of anhydrides) and 1778 cm^{-1} (carbonyl C=O asymmetric stretching of anhydrides). The peak at 1609 cm^{-1} (phenyl group) was chosen as an internal standard. Conversions of the different reactive groups, epoxide and anhydride, were determined by the Lambert-Beer law from the normalized changes of absorbance at 915 and 1778 cm^{-1}. From the conversions and taken into account the molar formulation of the mixtures, the molar evolution of the reactive groups, which participates in the curing were represented.

$$\alpha_{anhydride} = 1 - \left(\frac{\bar{A}^t_{1778}}{\bar{A}^o_{1778}}\right) \quad \alpha_{epoxy} = 1 - \left(\frac{\bar{A}^t_{915}}{\bar{A}^o_{915}}\right) \tag{2}$$

where $\bar{A}^o$ and $\bar{A}^t$ are, respectively, the normalized absorbance of the reactive group before curing and after a reaction time t.

Optical microscopy with polarized light (Axiolab Zeiss equipped with a Linkam TP92 hot stage) was used to study the morphology of some samples.

The gelation point was determined by solubility tests. Before gelation the material is completely soluble in dichloromethane and once past the gel point the solubility falls steeply. The conversion at the gelation was determined by the residual enthalpy in the DSC of the gelled sample after quenching it in liquid nitrogen.

TMA (Mettler TMA40) was used to determine the conversion at the gel point and the shrinkage undergone during curing. The samples were supported by two small circular ceramic plates and silanized glass fibers, which were impregnated with the samples. For the former determination, non-isothermal experiments were performed between 40 and 225 °C at a heating rate of 5 °C/min applying a periodic force that change (cycle time = 12 s) from 0.0025 to 0.01 N. When the material reaches sufficient mechanical stability (gelation) the TMA measuring probe deforms less the sample and the amplitude of the oscillations is reduced. The gel point was taken in TMA as the temperature at which sudden decrease in the amplitude of the oscillations was observed. The gel conversion, α_{gel}, was determined as the DSC conversion at the temperature gelled in TMA in a non-isothermal experiment. Isothermal experiments at 120 °C were performed by application of a force of a 0.01 N in order to monitor contraction during the curing process and to determinate the shrinkage after curing.[22,23]

The shrinkage was calculated from the densities of the materials before and after curing, which were determined using a Micromeritics AccuPyc 1330 Gas Pycnometer thermostatized at 30 °C. The densities were measured with a precision of ± 0.001. The precision of the shrinkage calculated values is 0.2%.

Kinetic analysis

Integral non-isothermal kinetic analysis was used to determine the kinetic triplet (*A* is the pre-exponential factor, *E* is the activation energy and *g(x)* is the integral function of degree of conversion).

If we accept that the dependence of the rate constant on the temperature follows the Arrhenius equation, non-isothermal kinetic analysis may start with the kinetic equation:

$$\frac{dx}{dt} = \beta \frac{dx}{dT} = Ae^{-\frac{E}{RT}} f(x) \tag{3}$$

where β is the heating rate, dx/dt is the rate of conversion, R is the universal gas constant, T is the temperature and $f(x)$ is the differential conversion function.

By integrating Eq. (3) and using the Coats-Redfern[24] approximation to resolve the so-called temperature integral and considering that $2RT/E << 1$ the Kissinger-Akahira-Sunose equation (KAS) may be written as:

$$ln\frac{\beta}{T^2} = \ln\left[\frac{AR}{g(x)E}\right] - \frac{E}{RT} \tag{4}$$

For each conversion degree, the linear representation of $ln[\beta/T^2]$ versus T^{-1} enables E and $ln[AR/g(x)E]$ to be determined from the slope and the ordinate in the origin. If the reaction

model, *g(x)*, is known, for each conversion the corresponding pre-exponential factor can be calculated for every activation energy.

In this study, we used the reduced master curves procedure of Criado[25] and the Coats-Redfern method to assign a reaction model to the systems studied.[26] By the Coats-Redfern method we selected the model which presented the best adjustment and had an activation energy similar to that obtained isoconversionally (considered to be the true). Different kinetic models have been studied: diffusion (D_1, D_2, D_3 and D_4), Avrami-Erofeev (A_2, A_3 and A_4), power law, phase-boundary-controlled reaction (R_2 and R_3), autocatalytic (n + m = 2 and 3) and order n (n = 1, 1.5, 2 and 3). The rate constant, *k*, was calculated with E and A determined at conversion of 0.2, using the Arrhenius equation.

RESULTS AND DISCUSSION

The aliphatic polyester Boltorn series have been used in the modification of epoxy resins.[27,28] In most cases, H30 was either dissolved into acetone or directly mixed with DGEBA at a temperature around 80 ºC and then hardeners were added to get a homogeneous solution. In our case, when H30 and DGEBA were dissolved in acetone a transparent solution was formed but, when acetone was evaporated, the HBP separated from the DGEBA to form a viscous white mixture with small particles (as shown in **Figure 1**) indicating the poor compatibility of both reactants. However, the addition of hardeners can change the miscibility of H30 in epoxy matrices by changing the polarity of the mixture or by forming hydrogen bonds.

The curing process of epoxides by anhydrides has been extensively studied for more than 50 years.[29,30] We chose an epoxy/anhydride/HBP system on the basis of the following three assumptions: (1) the anhydride would enhance the miscibility of HBP in the epoxy matrix; (2) the primary alcohols of the HBP would increase the epoxy/anhydride curing rate as reported in the literature;[31,32] (3) the anhydride group would react with the hydroxyl groups of HBP leading to more homogeneous materials. The limitation of the use of anhydrides as curing agents is the long curing time and the high temperature needed to obtain optimal properties. Thus, the use of catalysts is usually needed to overcome this drawback. Among these catalysts, tertiary amines are the most used.

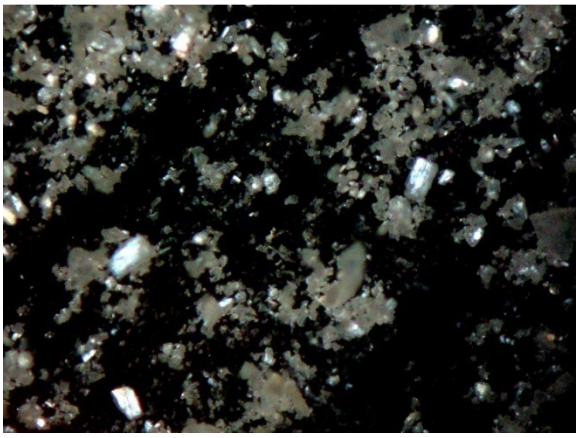

Figure 1 Polarized optical microscopy image of neat H30 at room temperature at a magnification of 200x.

Scheme 2 shows the main reactions that take place on curing epoxide/anhydride mixtures without amine.[33] The first reaction (a) is the opening of the anhydride by a hydroxyl group, yielding a monocarboxylic ester. In our reactive mixture, hydroxyl groups are present in very

little proportions in the DGEBA but there are many of them in the H30, and therefore this process can be of a great importance. The monocarboxylester can react with an epoxide to form a hydroxydiester (b) or protonate an epoxide, which can homopolymerize by a ring-opening mechanism (c). The hydroxyl groups present can further react with the anhydride to form ester linkages (d) or initiate a polyetherification (e).

The addition of amine to the epoxy/anhydride curing system changes the reaction mechanism.[29] In **Scheme 3** the reactions implied are collected. First of all, the amine as a nucleophile attacks the anhydride to form a carboxylate (a), which can open the oxirane ring (b). The alkoxide intermediate formed can either react with anhydride (c) forming a polyester or with epoxide (d) leading to a polyether.

When no amine is present in the curing system, the reaction takes place in an acidic medium, whereas on adding amine it becomes basic. It has been described that acid catalyzed systems favor polyetherification whereas basic catalyzed systems favor polyesterification.[16,29] Polyetherification is undesirable since it results in unreacted anhydrides and/or acid monoesters in the thermoset.

Because of the complex reaction mechanism, in both catalyzed and uncatalyzed systems, stoichiometric proportions are not always suitable. Therefore, it is necessary to find the optimal amounts of anhydride. This task is even more necessary when a hydroxylic modifier is added, because it can promote the mechanism depicted in **Scheme 2**, even in amine catalyzed curings.

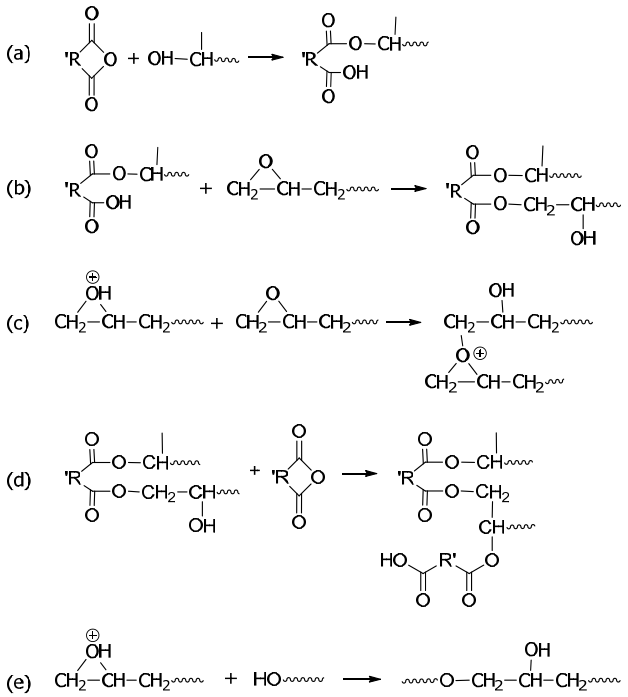

Scheme 2 Reaction mechanism of the curing of epoxides with anhydrides.

Calorimetric Studies

Epoxy/anhydride/H30 Curing Process

We used the DSC to investigate the role of hydroxyl groups in the evolution of the curing process. We investigated a 1:1 (mol/mol) stoichiometric mixture of DGEBA/THPA and compared

it to another mixture with a 10 wt% of H30 (named as 10% H30/DGEBA/THPA). **Figure 2a** shows the calorimetric curves from 30 to 300 ºC of these mixtures. As one can see, the addition of H30 clearly changes the shape of the exotherm. Neat DGEBA/THPA system, with a very low proportion of hydroxyl groups, shows two exothermic peaks with two maxima at 193 and 275 ºC. The first one could correspond to esterification of hydroxyl groups (**Scheme 2**, reactions a and d), and the second to the reaction in which epoxide groups open (**Scheme 2**, reactions b, c and e). The high temperature at which this exotherm appears can lead to the overlapping with a degradation process. In the sample that contains H30 the peaks are partially overlapped and shifted to 186 and 231 ºC. From this result we can state that the presence of the H30 allows curing at lower temperature.

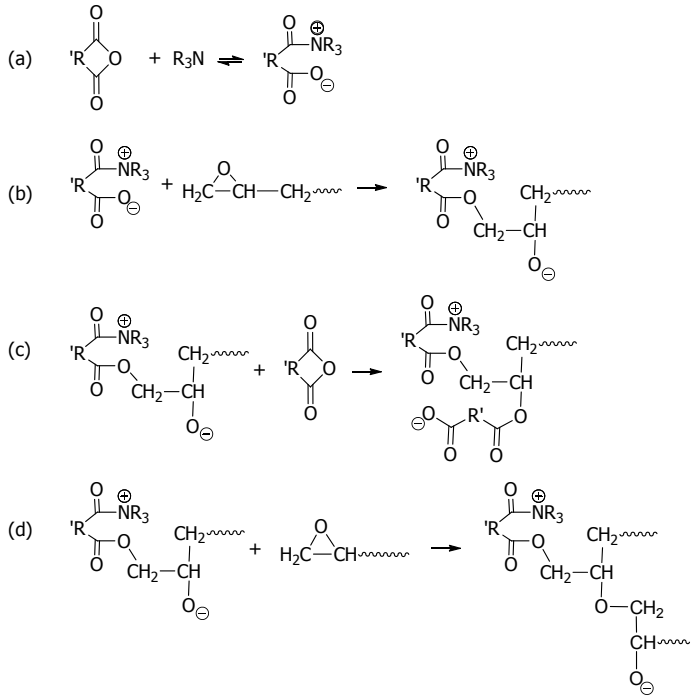

Scheme 3 Reaction mechanism of the curing of epoxides with anhydrides catalyzed by a tertiary amine.

After the dynamic curing until 300 ºC we determined the glass transition temperatures of both materials (**Figure 2b**). The values obtained demonstrate that neat DGEBA/THPA cannot be fully cured in this schedule and a T_g of only 94 ºC can be observed. In contrast, on adding a 10wt% of H30 to the mixture, the cured material shows a higher value of 111 ºC. This material was transparent and homogeneous by optical microscopy, which accounts for a covalent incorporation of the H30 to the network.

Epoxy/anhydride/H30/amine Curing Process

In an analogous way, we studied the effect of adding a tertiary amine as catalyst and which was the best epoxy/anhydride/H30 proportions. The proportion of tertiary amine (BDMA) was fixed as 0.0136 mol by mol of anhydride added to the mixture (approx. 0.5% in weight), according to the literature.[34] The formulations studied are detailed in **Table 1** and were prepared taking a fixed proportion of 10wt% of H30, to begin the study. In the formulations, the epoxy/anhydride ratio was decreased to allow the anhydride to react with increasing proportions

of hydroxyl groups. Because of one mol of anhydride can react with one mol of epoxide or with two mols of hydroxyl groups, the stoichiometric proportion is the 1:0.50, which corresponds to an epoxy/anhydride/hydroxy molar ratio (1:1:2).[16] The total heat evolved in the curing of neat epoxy resin was found to be 289 J/g, which corresponds to a value of 96.5 kJ by epoxy equivalent, similar to the reported by other authors.[35]

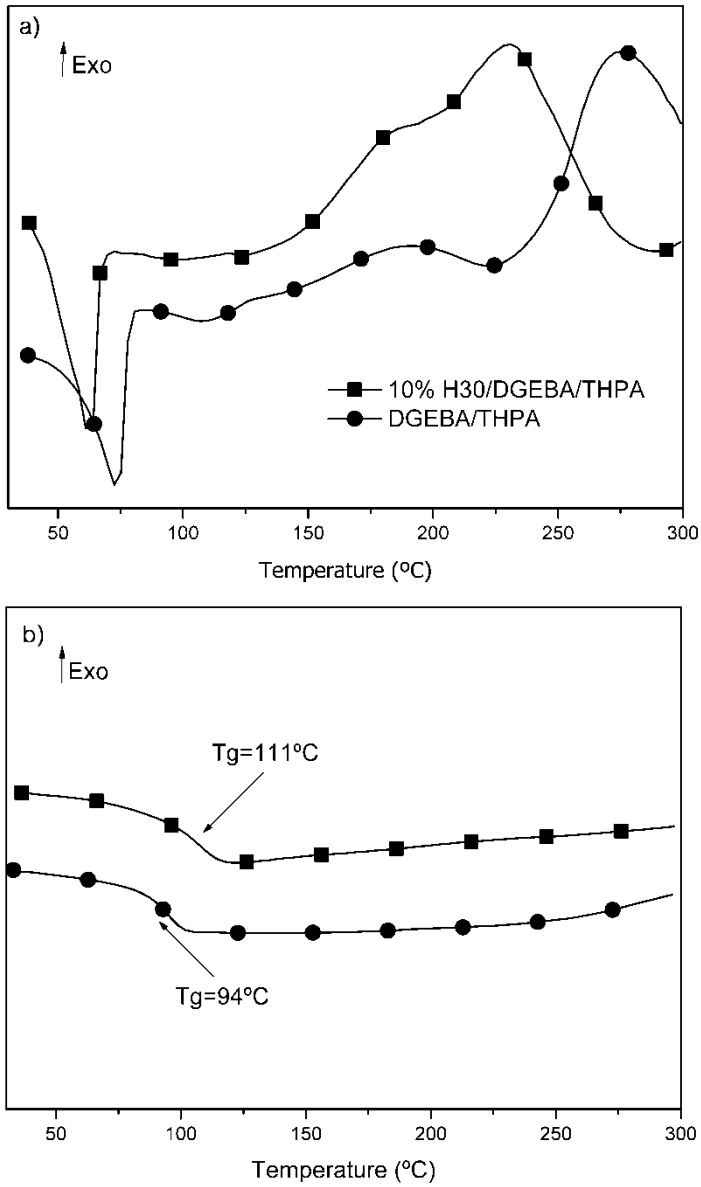

Figure 2 Calorimetric curves of DGEBA/THPA 1:1 (mol/mol) with and without H30 recorded at a heating rate of 10 °C/min (a); glass transition temperatures of the two materials after dynamic scanning (b).

Figure 3 shows the calorimetric curves of the formulations described in **Table 1**. Although in the curves only one exotherm can be clearly appreciated, which corresponds to the reaction of epoxide with anhydride, in formulations containing H30 a second small broad exotherm above

180 °C can be detected. Montserrat *et al.*[28] attributed this broad exotherm to the uncatalyzed curing of the remaining epoxy/anhydride and it strongly depends on the proportion of the amine added. In our case, the addition of the HBP changes the overall proportion of amine, which can explain the appearance of this little exotherm that cannot be appreciated in the image size used in the figure.

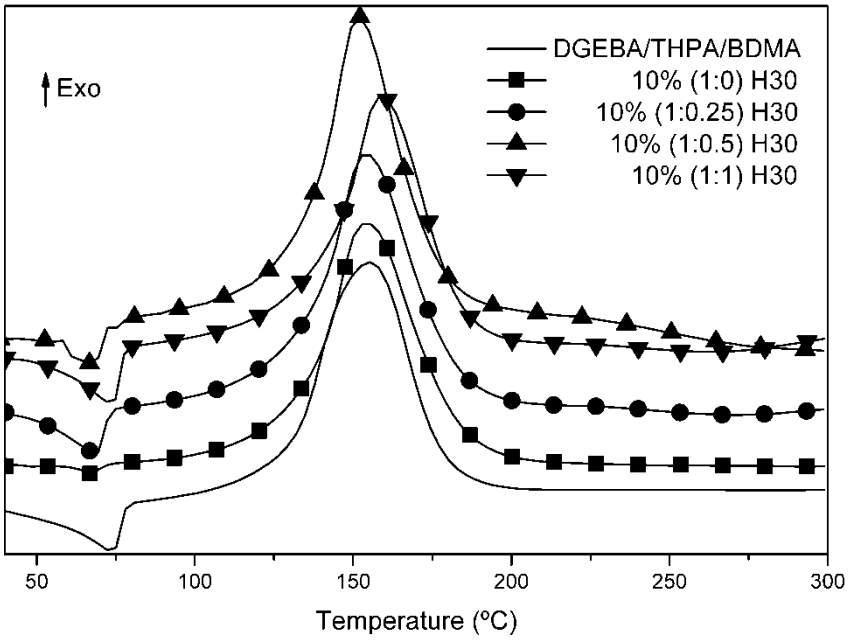

Figure 3 Calorimetric curves for the curing of 10 wt% H30 modified systems with different epoxy/anhydride molar ratio at a heating rate of 10 °C/min.

The calorimetric data of the curing processes and the T_g*s* of the materials are listed in **Table 3**. On changing the formulation, one can observe no significant differences, neither in the onset temperature nor in the maximum of the peak or in the enthalpy released on curing. Although the T_g*s* after a dynamic curing do not show significant differences, after an isothermal curing schedule the highest observed T_g is for the 10% (1:0.50) H30 formulation, which makes it the best one for further studies. In this formulation all the epoxy and hydroxyl groups can react with anhydride, which explains the highest T_g achieved. This result confirms that all hydroxyl groups in the HBP react with anhydride. However, to reach a high T_g value, the isothermal curing schedule should include a post-cure at higher temperature (about 200 °C) to allow the complete polymerization of all reactive groups.

In the 10% (1:0) and (1:0.25) H30 formulations (with an excess of hydroxyl groups) the T_g*s* after dynamic curing are higher than after isothermal curing. Thus, isothermal postcuring at 200 °C seems to be not enough for the complete reaction of these samples. In the 10% (1:1) H30 sample there is an excess of anhydride and therefore some carboxylic groups remains unreacted and neither dynamic nor isothermal curing can reach a high T_g value.

Epoxy/anhydride/amine Systems with Several H30 Proportions

Knowing that the maximum curing is reached when one anhydride reacts either with an epoxide or with two hydroxyl groups of the H30, we studied the influence of adding different amounts of the HBP to the curing mixture. The formulations studied are given in **Table 2**.

The calorimetric curves are summarized in **Figure 4** and the data are listed in **Table 4**. As we can see in the figure, there is no much influence in the shape and temperatures of the exotherm on changing the proportion of H30. On increasing this proportion, the total heat evolved shows a decline due to the lower proportion of epoxide in the mixture. T_g values obtained from the materials after the dynamic curing are similar, but the maximum value is reached with a 10% of H30. An isothermal schedule allows, generally, obtaining completely cured materials with higher T_gs. The materials containing H30 show higher T_gs than the neat system, with the exception of the 20% H30 sample. This can be explained by a plasticizing effect of the high proportion of HBP in the thermoset.

Table 3 Thermal data of the curing and glass transition temperatures for the DGEBA / THPA / BDMA mixtures with different excess of anhydride.

Sample	T_{onset} [a] (ºC)	T_{max} [b] (ºC)	Δh (J/g)	T_g [c] (ºC)	T_g [d] (ºC)
DGEBA/THPA/BDMA	130	155	289	109	110
10% (1:0) H30	134	154	263	108	98
10% (1:0.25) H30	134	154	273	109	103
10% (1:0.5) H30	134	152	276	108	115
10% (1:1) H30	140	159	270	95	102

a. Onset temperature of the curing exotherm registered at 10 ºC/min.
b. Temperature of the maximum of the curing exotherm registered at 10 ºC/min.
c. T_g determined after curing in a dynamic scan registered at 20 ºC/min.
d. T_g determined after isothermal curing at 150 ºC for 5 hours and 200 ºC for 2 hours in a dynamic scan registered at 20 ºC/min.

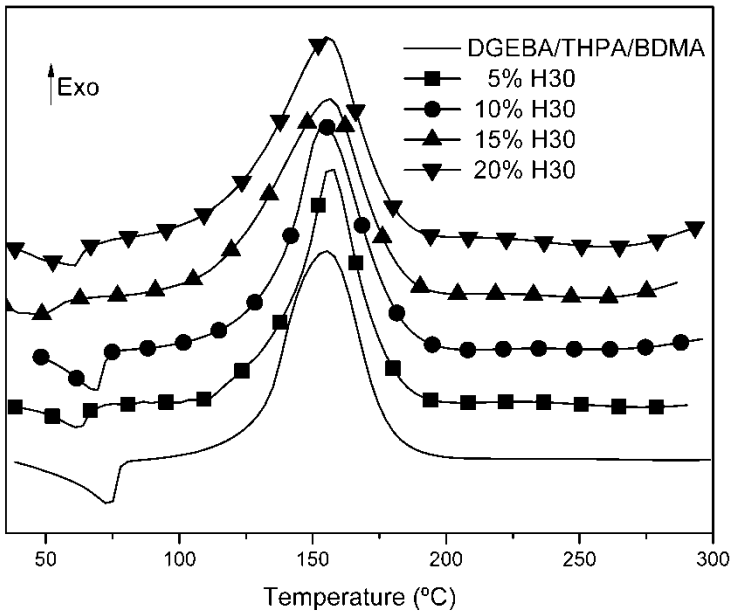

Figure 4 Calorimetric curves for the curing of DGEBA/THPA mixtures containing different amounts of H30 at a heating rate of 10 ºC/min.

By the isoconversional methodology we obtained the evolution of the activation energies during the curing process. From the calorimetric curves and applying the *Eq. (4)*, we obtained

the activation energy for each degree of conversion in all the formulations studied. **Figure 5** shows the plot of the apparent activation energy against the degree of conversion for the curing of the samples containing different proportions of H30. It can be seen, that the activation energies are practically constant during the curing process and the values calculated at 50% of conversion are collected in **Table 4**. Not many differences among the activation energies of the mixtures studied can be appreciated.

Table 4 Calorimetric data of DGEBA/THPA/BDMA mixtures with different amounts of H30.

Sample	Δh (J/g)	T_g [a] (°C)	T_g [b] (°C)	E_a [c] (kJ/mol)	lnA [d] (s^{-1})	$k_{140°C} \times 10^3$ [e] (s^{-1})
0% H30	289	109	110	73	16.59	8.68
5% H30	284	114	118	74	16.65	8.29
10% H30	276	108	115	74	16.88	9.11
15% H30	251	111	117	73	16.46	9.47
20% H30	232	112	103	72	16.48	11.82

a. After dynamic scanning at 10 °C/min, registered at 20 °C/min.
b. After isothermal curing at 150 °C for 5 hours and post-cured at 200 °C for 2 hours, registered at 20 °C/min.
c. Values of activation energy at 50% of conversion, evaluated by the isoconversional non-isothermal procedure.
d. Pre-exponential factor for the n = 1.5; m = 0.5 kinetic model with $g(\alpha) = [1-(1-\alpha)^{1/3}]$.
e. Values of rate constant at 140 °C using the Arrhenius equation at a conversion of 20%.

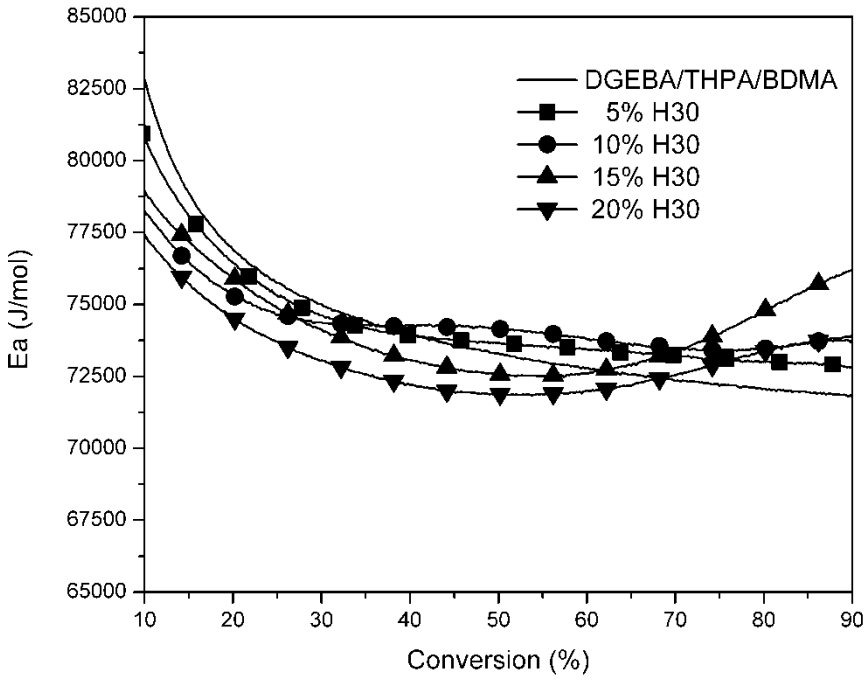

Figure 5 Apparent activation energy (*Ea*) of the systems with different amounts of H30 in % w/w.

Figure 6 shows the plot of the degree of conversion against temperature. From this figure we can observe the acceleration promoted by the hydroxylic groups at the beginning of the curing (20-30% of conversion). This observation is confirmed by the rate constants calculated at a 20% of conversion collected in **Table 4**. The rate constants were calculated as explained in the experimental part, using the kinetic model n = 1.5, m = 0.5, which fits better with the experimental curve and the activation energy value. On increasing the proportion of the HBP in the formulation the rate constant increases. However, in the 5% sample the amount of hydroxylic groups is so little that no effect is observed. On increasing the conversion, the tendency changes: at around 50% the rates are similar for all the formulations and over 80% H30 has a retardant effect. Thus, it seems that the reaction of hydroxyl groups with anhydrides begins from the very beginning following the mechanism depicted in **Scheme 2**, but their complete reaction is only achieved at the end of the curing at high temperatures. This is in agreement with the previous observation that a post-cure at high temperatures is needed to reach the complete curing.

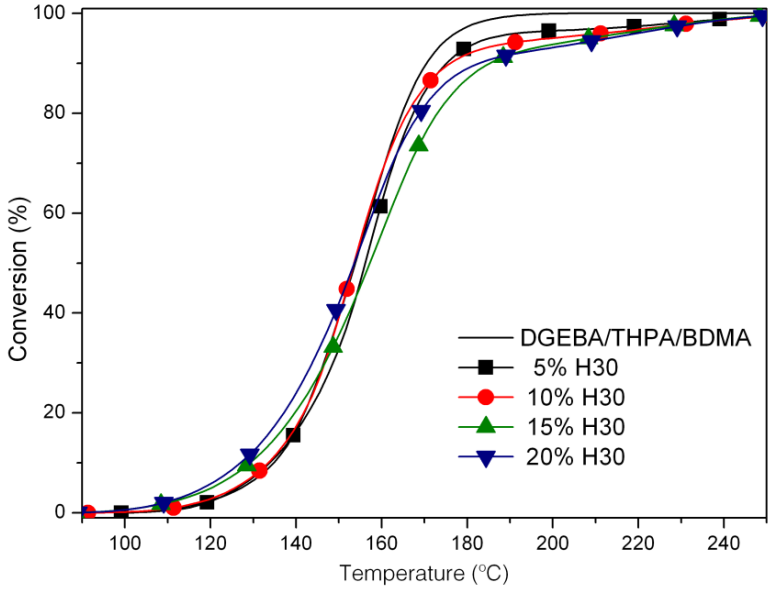

Figure 6 Degree of conversion against time of DGEBA/THPA/BDMA samples with different amounts of H30.

FTIR Studies

We followed the evolution of the reactive groups, which participate in the curing reaction by FTIR/ATR to see if the hydroxyl groups incorporate covalently during the first stages of the curing, which implies that the uncatalyzed mechanism depicted in **Scheme 2** occurs. The sample 10% H30 was placed in the FTIR/ATR at 150 °C and spectra were recorded every 10 s. **Figure 7** shows some of the spectra obtained at different reaction times. The most significant bands in the initial spectrum are the one at 915 cm^{-1} (epoxide), the 1862 and 1778 cm^{-1} of anhydride and the ester band of the HBP at 1731 cm^{-1}. As the reaction goes on, the bands corresponding to the anhydride and to the epoxide diminish, whereas the ester band grows up. In the final spectrum, the anhydride bands have completely disappeared and no carboxylic acid absorptions appear which indicates that the complete reaction has taken place. Plotting the evolution of the mols of anhydride and epoxide against time we can see that the anhydride disappears faster than the epoxide (**Figure 8**). In the same figure we have also represented the

difference between the mols of both reactants against time. This representation shows that the difference becomes smaller during the curing. This fact can be rationalized in the basis of the reaction of anhydride with hydroxyl groups of the HBP, which takes place since the beginning of the curing but it is not until the end that this reaction is completed. Anyhow, it is quite clear that HBP is covalently incorporated to the network structure. This observation is in contradiction with the statement made by Yang *et al.*[19] who suggested that hydroxylic groups do not react in similar formulations, but form hydrogen bonds with the oxygens in the matrix. The covalent incorporation of the HBP in the polymer matrix is of a great importance in the properties of the thermoset.

We can see in **Figure 8** that the anhydride disappears faster than the epoxide. This result can justify the increase in the reaction rate at low conversions when the concentration of HBP increases.

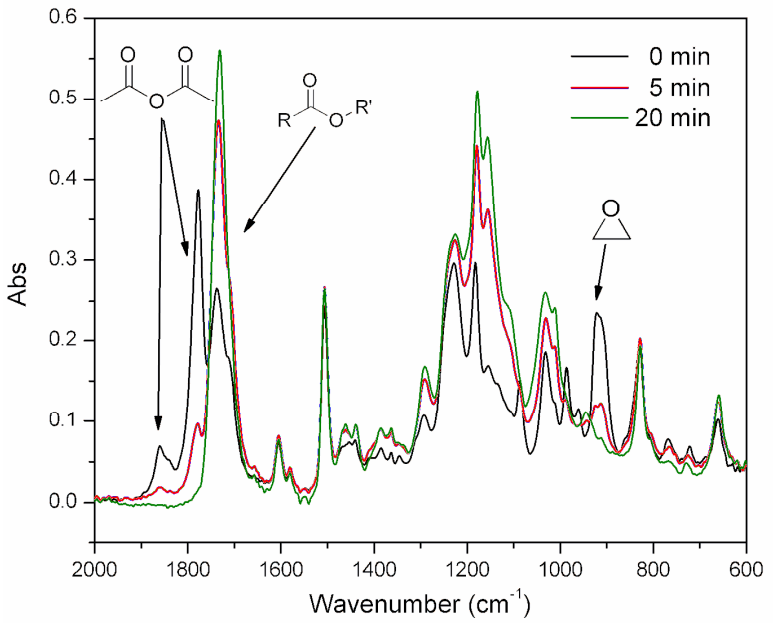

Figure 7 FTIR-ATR spectra of the mixture of the curing process of a 10% H30 mixture at 150 ºC at different curing times.

Gel Point

In the curing process of a given thermoset stresses within the material are generated due to bond formation. Before gelation, the material has enough mobility to disperse these stresses. However, once the material reaches its gel point this stress may originate microcracks that reduce, for example, its performance as coating. Thus, increasing the conversion before the gelation is very interesting from the point of view of the application of the material.

In **Table 5** the values for the conversion at gelation of blends of DGEBA and THPA with different amounts of H30 are collected. We determined the conversion at the gel point by two different methodologies: the first one is the solubility method *(α_{sol})* and the second one is by using TMA *(α_{gel})* as explained in the experimental part. **Figure 9** shows the α_{gel} determination method for the 20% H30 formulation at 5 ºC/min as an example. From the values of the table, we can see that the conversions are higher for the TMA method than for the solubility test, but in any case it is quite clear that the addition of HBP increases the conversion before the gel point in all

the blends. However, there is a drop in the conversion for the sample with a 20% of H30, which can be attributed to the fact that not all the hydroxyl groups of HBP can react due to topological reasons, similarly to what Manson *et al.* reported.[36] The gelation times do not change significantly on adding H30.

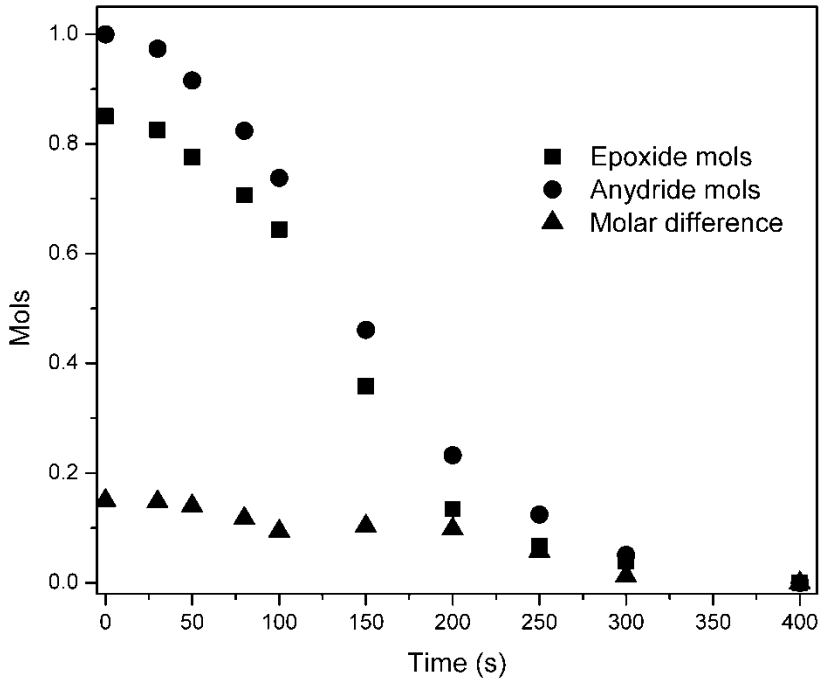

Figure 8 Evolution of the anhydride and the epoxide mols during an isothermal curing at 150 °C of a 10% H30 sample followed by FTIR/ATR.

Table 5 Conversion at the gelation, gel times, shrinkage before gelation, densities before and after curing and global shrinkage of the formulation studied containing different proportions of H30.

Sample	α_{gel} [a]	α_{sol} [b]	t_{gel} [c] (min)	α_{shr} [d]	ρ_{mon} (g/ml)	ρ_{polym} (g/ml)	Shrinkage [e] (%)
0% H30	0.63	0.58	19.8	0.48	1.199	1.253	4.3
5% H30	-	0.64	19.7	-	1.199	1.256	4.5
10% H30	0.7	0.67	20.2	0.57	1.201	1.264	5.0
15% H30	-	0.68	18.2	-	1.203	1.279	5.9
20% H30	0.77	0.65	19.5	0.58	1.206	1.271	5.1

a. Conversion at the gel point determined as the conversion reached by non-isothermal TMA and DSC tests at 10 °C/min (as represented in **Figure 9**).
b. Conversions at the gel point determined by solubility tests and non-isothermal DSC.
c. Gelation time determined by solubility tests at 120 °C.
d. Degree of shrinkage before gelation determined by TMA at 120 °C.
e. Global shrinkage obtained from the densities as: $((\rho_{polym} - \rho_{mon})/\rho_{polym}) \times 100$.

Shrinkage

It has been reported that the use of anhydrides in the curing of epoxy resins is very interesting from the point of view of the low shrinkage during the process, because of the ring-opening mechanism followed implies a reduced contraction.[16,20] However, the reaction of hydroxyl groups with anhydride follows a polycondensation mechanism, with a more pronounced shrinkage. For this reason, it is interesting to determine the influence of the addition of hydroxylic HBP in the DGEBA/anhydride curing. The global shrinkage during curing can be calculated from the density values of the material before and after curing. We determined these densities with an automatic gas pycnometer and the results are collected in **Table 5**. As we can see, the global shrinkage of the unmodified material is low and it does not increase much on adding a little proportion of HBP. However, a higher proportion of HBP increases the shrinkage but in any case it reaches a 6%. Klaus *et al.*[37] reported a 5.4% of shrinkage for DGEBA/THPA curing, which is higher than the one obtained by us. The results obtained are different from those obtained in a previous study on the cationic curing of DGEBA and H30[21] in which an expansion of the material was observed. However, the mechanism of polymerization was in that case a ring-opening mechanism without polycondensation.

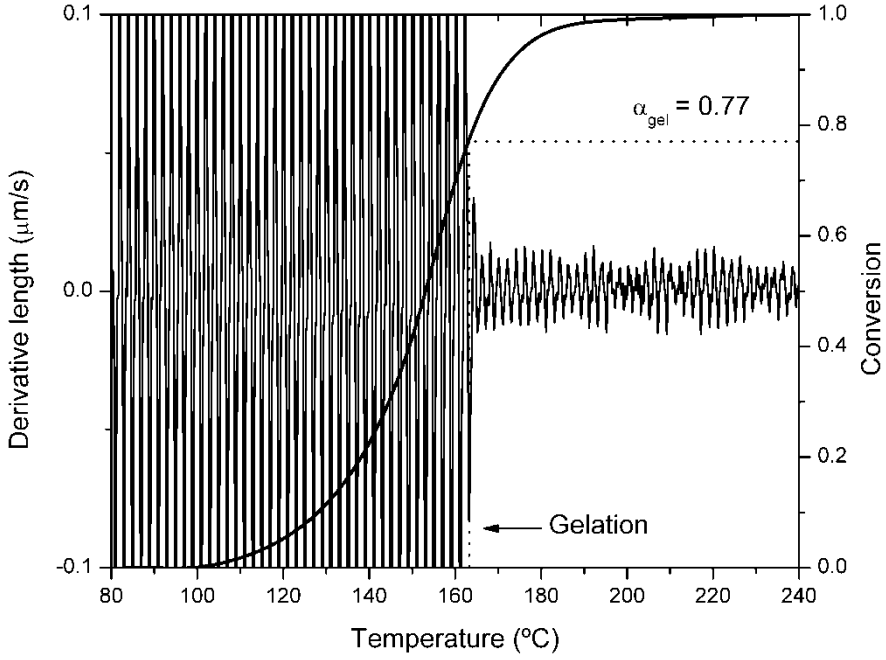

Figure 9 Gel point determination using combined TMA and DSC for the 20% of H30 sample.

By TMA we determined the evolution of the shrinkage before and after gelation. In the values collected in **Table 5** we can see that on adding HBP to the reactive mixture the shrinkage before gelation increases. This result is interesting from the point of view of the reduction of internal stress, which is originated by the shrinkage after gelation because of the loss of mobility in the material. The reduction of the shrinkage after gelation takes more importance when comparing our system (with hydroxyl groups added) to other systems that cure via polycondensation mechanism. The reduction of the shrinkage after gelation was also observed in the cationic curing of DGEBA and H30.[21]

Thermal and mechanical properties of the modified materials obtained for these systems will be published in a forthcoming paper.

CONCLUSIONS

The curing of DGEBA/THPA catalyzed by BDMA with different proportions of hydroxylic HBP (H30) was studied by DSC and the best proportion of anhydride was found to be the stoichiometric one, in which one anhydride reacts either with an epoxide or with two hydroxyl groups.

The presence of hydroxyl groups increased the reaction rate at the beginning of the curing but slowed it down at the end.

On adding HBP to the DGEBA/THPA mixture the T_gs of the materials increased. However, when the proportion was 20% this value dropped down.

Hydroxylic HBP incorporated covalently to the network from the beginning of the curing, but high temperature was required to complete the reaction.

The conversion at the gelation was increased on increasing the proportion of HBP in the reactive mixture.

The addition of the H30 to the DGEBA/THPA system slightly increased the global shrinkage. However, the shrinkage after gelation was reduced.

ACKNOWLEDGEMENTS

Authors from the Rovira i Virgili University would like to thank the CICYT (Comisión Interministerial de Ciencia y Tecnología) and FEDER (Fondo Europeo de Desarrollo Regional) (MAT2008-06284-C03-01) and the authors from the Universitat Politècnica de Catalunya to CICYT and FEDER (MAT2008-06284-C03-02) for their financial support. Y.Y. acknowledges the Juan de la Cierva Program, Ministry of Science and Innovation of Spain. D.F. acknowledges the Grant FI-2007 from the Catalonian Government.

REFERENCES

1. B. Voit. *J. Polym. Sci. Part A: Polym. Chem.* **2005,** *43,* 2679.
2. L. Boogh L, B. Pettersson, J. A. E. Månson. *Polymer* **1999,** *40,* 2249.
3. R. Mezzenga, J. A. E. Månson. *J. Mater. Sci.* **2001,** *36,* 4883.
4. J. Fröhlich, H. Kautz, R. Thomann, H. Frey, R. Mülhaupt. *Polymer* **2004,** *45,* 2155.
5. D. Ratna, R. Varley, G. P. Simon. *J. Appl. Polym. Sci.* **2004,** *92,* 1604.
6. C. Gao, D. Yan. *Prog Polym Sci* **2004,** *29,* 183.
7. M. Frigione, E. Calò. *J. Appl. Polym. Sci.* **2008,** *107,* 1744.
8. Q. Guo, A. Habrard, Y. Park, P. J. Halley, G. P. Simon. *J. Polym. Sci. Part B: Polym. Phys.* **2006,** *44,* 889.
9. D. Ratna, G. P. Simon. *Polymer* **2001,** *42,* 8833.
10. H. Wu, J. Xu, Y. Liu, P. Heiden. *J. Appl. Polym. Sci.* **1999,** *72,* 151.
11. F. L. Jin, S. J. Park. *J. Polym. Sci. Part B: Polym. Phys.* **2006,** *44,* 3348.
12. R. Mezzenga, L. Boogh, J. A. E. Månson. *J. Polym. Sci. Part B: Polym. Phys.* **2000,** *38,* 1883.
13. R. Mezzenga, L. Boogh, J. A. E. Månson. *J. Polym. Sci. Part B: Polym. Phys.* **2000,** *38,* 1893.
14. C. J. G. Plummer, R. Mezzenga, L. Boogh, J. A. E. Månson. *Polym. Eng. Sci.* **2001,** *41,* 43.
15. R. Mezzenga, C. J. G. Plummer, L. Boogh, J. A. E. Månson. *Polymer* **2001,** *42,* 305.
16. C. A. May. *Epoxy Resins. Chemistry and Technology*, 2nd edition. Marcel Dekker, New York, **1988**.
17. R. J. Varley, W. Tian. *Polym. Int.* **2004,** *53,* 69.
18. X. X. Wang, Z. G. Jiang, Y. F. Zhang. *Chin. Chem. Lett.* **2006,** *17,* 125.
19. J. P. Yang, Z. K. Chen, G. Yang, A. Y. Fu, L. Ye. *Polymer* **2008,** *49,* 3168.

20. R. K. Sadhir, M. R. Luck. *Expanding monomers. Synthesis, characterization and applications.* CRC Press, Boca Raton, **1992**.
21. X. Fernández-Francos, J. M. Salla, A. Cadenato, J. M. Morancho, A. Serra, A. Mantecón, X. Ramis. *J. Appl. Polym. Sci.* **2009,** *111,* 2822.
22. R. Giménez, X. Fernández-Francos, J. M. Salla, A. Serra, A. Mantecón, X. Ramis. *Polymer* **2005,** *46,* 10637.
23. S. González, X. Fernández-Francos, J. M. Salla, A. Cadenato, A. Serra, A. Mantecón, X. Ramis. *J. Appl. Polym. Sci.* **2007,** *104,* 3406.
24. A. W. Coats, J. P. Redfern *Nature* **1964,** *201,* 68.
25. J. M. Criado. *Thermochim. Acta* **1978,** *24,* 186.
26. X. Ramis, J. M. Salla, A. Cadenato, J. M. Morancho. *J. Therm. Anal. Calorim.* **2003,** *72,* 707.
27. G. Cicala, A. Recca, C. Restuccia. *Polym. Eng. Sci.* **2005,** *45,* 225.
28. D. Ratna, G. P. Simon. *Polym. Eng. Sci.* **2001,** *41,* 1815.
29. W. Fisch, W. Hofman, J. Koskikallio. *J. Appl. Chem.* **1956,** *6,* 429.
30. L. A. O'Neill, C. P. Cole. *J. Appl. Chem.* **1956,** *6,* 356.
31. E. M. Woo, J. C. Seferis. *J. Appl. Polym. Sci.* **1990,** *40,* 1237.
32. S. Montserrat, C. Flaqué, M. Calafell, G. Andreu, J. Malek. *Thermochim. Acta* **1995,** *269,* 213.
33. W. G. Potter. *Epoxide resins.* Plastics Institute, Bristol, **1970**.
34. E. M. Petrie. *Epoxy adhesive formulations.* McGraw-Hill, New York, **2006**.
35. C. H. Klute, W. Viehmann. *J. Appl. Polym. Sci.* **1961,** *5,* 86.
36. R. Mezzenga, L. Boogh, J. A. E. Månson. *Macromolecules* **2000,** *33,* 4373.
37. I. S. Klaus, W. S. Knowles. *J. Appl. Polym. Sci.* **1966,** *10,* 887.

3.3 Combined use of sepiolite and a hyperbranched polyester in the modification of epoxy/anhydride thermosets. A study of the curing process and the final properties

D. Foix[1], M. T. Rodríguez-Blasco [2], F. Ferrando[3], X. Ramis[4], A. Serra[1]

[1] Department of Analytical and Organic Chemistry, University Rovira i Virgili, Marcel.li Domingo s/n, 43007 Tarragona, Spain
[2] Institute of Optics, Color and Image. Department of Color, AIDO, Technological Park, Nicolás Copérnico 7-13, 46980 Paterna, Spain.
[3] Mechanical Engineering, University Rovira i Virgili, Països Catalans 26, 43007 Tarragona, Spain
[4] Laboratory of Thermodynamics, ETSEIB, University Politècnica de Catalunya, Av. Diagonal 647, 08028 Barcelona, Spain

ABSTRACT

The curing reaction of formulations of diglycidyl ether of bisphenol A (DGEBA) and tetrahydrophtalic anhydride (THPA) catalyzed with a tertiary amine and containing sepiolite and/or hyperbranched poly(ester) has been studied by means of DSC, and the effect of each additive has been evaluated. The resulting thermosets have been characterized by DMTA, TGA and also the shrinkage during the curing process has been determined. The influence of the additives in the toughness of the resulting thermosets has been determined by performing standardized impact tests and observing the fracture surfaces by SEM. The values of impact strength have been correlated to the morphology of the samples by means of TEM. Also microhardness of the cured materials has been measured.

INTRODUCTION

Epoxy resins are among the most commercially successful thermosetting materials, especially as adhesives, coatings, encapsulation of electronic components and matrices of composite materials, etc.[1,2] The explanation to the extended usage of such materials can be found in the excellent properties they present in terms of chemical and thermal stability, heat distortion, high stiffness and versatility among others.[3] However, they present also some drawbacks that limit their range of applications. One of the most significant is their poor impact resistance, since due to their high crosslinking density epoxy resins are inherently brittle thermosets.

Hyperbranched polymers (HBPs) belong to a group of macromolecules known as dendritic polymers. Their main characteristics are their highly branched structure and the large number of functional reactive groups present in the shell of the structure, which can increase the solubility and decrease the intrinsic viscosity.[4] In recent years HBPs have aroused as very interesting additives for toughness improvement in epoxy resins, although most of the literature is focused either in amine cured epoxy resins[5-7] or in catalyzed epoxy homopolymerization in thermal or photochemical conditions.[8] Few authors have dealt with epoxy/anhydride systems modified with HBPs.[9,10] However, in most cases they have proved to yield significant improvements in toughness at relatively low concentrations (around 10%). Depending if there is phase separation of the HBP within the epoxy matrix during the curing process, the reinforcement mechanism is based on the flexibility added to the network by the introduction of the polymeric additive (homogeneous systems) or because the dispersed soft particles of the HBP help to hinder the propagation of the cracks (phase separated systems).[11]

The use of nanofillers have attracted even more interest, both in academic and industrial fields, because they often exhibit dramatic improvements in thermal and mechanical properties of polymer matrix even at very low loadings.[12] In fact, the exfoliation of laminar nanofillers with high surface area frequently improves, at loadings about 5%, the physical and mechanical properties of polymers.[13,14] Most of the literature regarding nanocomposites is devoted to lamellar-layered silicates,[15,16] preferentially montmorillonite. Due to its highest cation exchange capacity, can be easily transformed into organophilic, which helps to compatibilize the clay with the epoxy matrix. Owing to the nanometer-sized particles obtained by dispersion, these nanocomposites exhibit markedly improved mechanical, thermal, optical, and physico-chemical properties when compared with the pure polymer or conventional (microscale) composites as firstly demonstrated by Kojima *et al.*[17] Apart from montmorillonite, there are other silicates that due to their structure are good candidates to be dispersed as inorganic nanofillers in polymers. Among them, sepiolite is one the most interesting.

Sepiolite is a microcrystalline hydrated magnesium silicate, with formula $Si_{12}O_{30}Mg_8(OH,F)_4(H_2O)_4 \cdot 8H_2O$, that exhibits needlelike morphology, very high surface area (BET 374 m^2/g) and a very high density of silanol groups (2.2 groups per 100 $Å^2$).[18] Due to these silanol groups, sepiolite can be modified to introduce in its cavities organic moieties that can improve its interaction with epoxy resins. Actually, in recent years one can find some examples in the improvement of toughness of epoxy resins with sepiolite in UV cured systems[19] or amine cured epoxides,[20-22] but no attention has been paid to epoxy/anhydride systems.

In the current paper, we present a study on the effect of the combined addition of sepiolite and Boltorn H30 hyperbranched polyester to an epoxy/anhydride system. In a previous study,[23] we investigated the curing process of Boltorn H30/DGEBA/tetrahydrophthalic anhydride systems. The present work completes that study, by investigating their thermal and mechanical properties and expands the scope to sepiolite modified formulations.

EXPERIMENTAL PART

Materials

Diglycidylether of bisphenol A (DGEBA) Epitoke Resin 827 was provided by Shell Chemicals with an epoxy equivalent of 182 g/eq. 1,2,3,6-Tetrahydrophthalic anhydride (THPA), N,N-dimethylbenzylamine (BDMA) from Aldrich were used without further purification.

A hydroxyl terminated hyperbranched aliphatic polyester produced by Perstorp with the trademark Boltorn H30 was used as a modifier. Its chemical structure is shown in **Scheme 1**. The molecular weight of Boltorn H30, as reported on data sheet, is about 3,600 g/mol and the theoretical number of OH groups is 32/molecule.

The inorganic filler was a sepiolite modified with glycidylsilane to improve the compatibility with epoxy systems (provided by Tolsa S.A. Spain). It is a complex magnesium silicate characterized by a needle-like morphology and very high surface area (BET 374 m^2/g).

Sample Preparation

The composition of all the studied mixtures is collected in **Table 1**. The samples are noted as X%SepY%H30, where X and Y are the weight percentage of sepiolite and Boltorn H30, respectively.

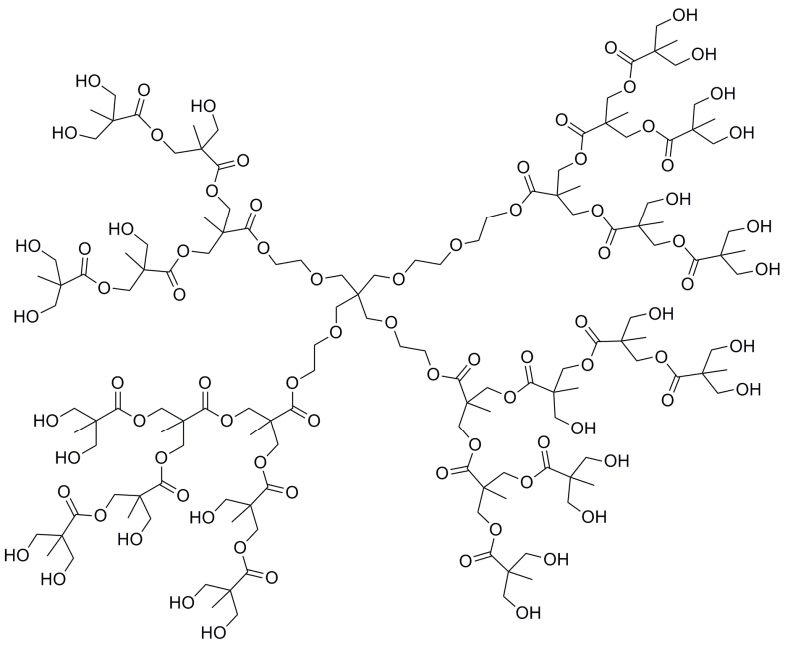

Scheme 1 Idealized chemical structure of Boltorn H30.

Table 1 Composition of all the studied formulations.

Sample	DGEBA (%)	THPA (%)	H30 (%)	BDMA [a] (phr)	Sepiolite [b] (phr)
0%Sep0%H30	54.5	45.5	0	0.55	0
0%Sep5%H30	50	45	5	0.54	0
0%Sep10%H30	45.5	44.5	10	0.53	0
1%Sep0%H30	54.5	45.5	0	0.55	1
1%Sep5%H30	50	45	5	0.54	1
1%Sep10%H30	45.5	44.5	10	0.53	1
3%Sep0%H30	54.5	45.5	0	0.55	3
3%Sep5%H30	50	45	5	0.54	3
3%Sep10%H30	45.5	44.5	10	0.53	3
5%Sep0%H30	54.5	45.5	0	0.55	5
5%Sep5%H30	50	45	5	0.54	5
5%Sep10%H30	45.5	44.5	10	0.53	5

a. Added with respect to the anhydride.
b. Added with respect to the mixture.

First of all mixtures of DGEBA containing the appropriate amount of sepiolite (1, 3 or 5%) were sonicated with a Branson Digital Sonifier for 1 hour using an amplitude of 12 %. Then THPA and H30 were added in the corresponding proportion and the mixture heated at 100 °C to obtain a transparent solution (not totally transparent for samples containing 5% of sepiolite). To perform DSC studies, BDMA was added and the mixture was quenched with liquid nitrogen to avoid the beginning of the curing, and then analyzed.

To prepare specimens for DMTA, TGA, density and mechanical properties measurements the preparation procedure was the same but after adding BDMA, mixtures were immediately

placed in steel templates treated with silicone to avoid the stacking of the final thermosets. The curing schedule was 150 ºC for 5 hours and 2 hours at 200 ºC as post-curing.

Characterization Techniques

Calorimetric studies were carried out on a Mettler DSC-821e thermal analyzer in covered Al pans under N_2. The calorimeter was calibrated using an indium standard (heat flow calibration) and an indium-lead-zinc standard (temperature calibration). The samples weighed approximately 7 mg. In the dynamic curing process the degree of conversion by DSC (x_{DSC}) was calculated as follows:

$$x_{DSC} = \frac{\Delta h_T}{\Delta h_{tot}} \quad (1)$$

where Δh_T is the heat released up to a temperature T, obtained by integration of the calorimetric signal up to this temperature, and Δh_{tot} is the total reaction heat associated with the complete conversion of all reactive groups. The kinetic studies were performed at heating rates of 2, 5, 10 and 15 ºC/min in N_2 atmosphere. The precision of the given enthalpies is ± 3%. Different models where evaluated following a procedure described elsewhere:[24,25] diffusion (D_1, D_2, D_3 and D_4), Avrami-Erofeev (A_2, A_3 and A_4), power law, phase-boundary-controlled reaction (R_2 and R_3), autocatalytic (n+m = 2 and 3) and order n (n = 1, 1.5, 2 and 3). The rate constant, k, was calculated at conversion of 0.5, using the Arrhenius equation.

The glass transition temperature for each material (T_g) was calculated after complete curing, by means of a second scan, as the temperature of the half-way point of the jump in the heat capacity when the material changed from the glassy to the rubbery state. The precision of the determined temperatures is estimated to be ±1 ºC.

Dynamic mechanical thermal analysis (DMTA) was performed in a TA DMA 2928 dynamic analyzer operating in three point bending mode at 1Hz. The storage modulus *(E')* and *tan* δ were measured from 30 to 220 ºC at 3 ºC/min on prismatic rectangular specimens (ca. 10 x 5 x 1.5 mm^3).

The fracture area of the specimens was observed by scanning electron microscopy (SEM). The samples were metalized with gold and observed with a Jeol JSM 6400 with 3.5 nm resolution.

Transmission electron microscopy (TEM) was performed with a Jeol 1011 microscope and the samples were prepared by cutting each thermoset with a microtome at room temperature.

Thermogravimetric analyses (TGAs) were carried out in a Mettler TGA/SDTA 851e thermobalance. Cured samples prepared as for DMTA analysis with an approximate mass of 8 mg were degraded between 30 and 800 ºC at a heating rate of 10 ºC/min in N_2 (100 cm^3/min measured in normal conditions).

The shrinkage was calculated from the densities of the materials before and after curing, which were determined using a Micromeritics AccuPyc 1330 Gas Pycnometer thermostatized at 30 ºC. The densities were measured with a precision of ±0.001. The precision of the shrinkage calculated values is 0.2%.

Impact test were performed at 23 ºC by means of an Zwick 5110 impact tester, according to ASTM D 4508-05 (2008) using prismatic rectangular specimens (ca. 20 x 11 x 2.5 mm^3). The pendulum employed had a kinetic energy of 1 J.

Microhardness was measured with a Wilson Wolpert (MicroKnoop 401MAV) device following the ASTM D1474-98 (2002) standard procedure. For each material 10 determinations were

made with a confidence level of 95%. The Knoop microhardness (HKN) was calculated from the following equation:

$$HKN = \frac{L}{A_p} = \frac{L}{l^2 \times C_p} \quad (2)$$

where, L is the load applied to the indenter (0.025 Kg), A_p is the projected area of indentation in mm^2, l is the measured length of the long diagonal of indentation in mm, C_p is the indenter constant (7.028×10^{-2}) relating l^2 to A_p.

RESULTS AND DISCUSSION

Calorimetric Studies

By means of differential scanning calorimetry (DSC) we have studied the curing process of all the formulations prepared. **Figure 1** shows some of the calorimetric curves. In this figure one can appreciate that at low temperatures an endotherm appears, which can be attributed to the melting of THPA followed by the exotherm corresponding to the curing process. As we can see, the exotherm has a relatively unimodal shape indicating that all the processes involved occur quasi simultaneously, although the changes in the shape when H30 was added suggest the chemically incorporation of H30 into the matrix. It should be commented, that the chemical reactions taking part in the curing process includes the alternate copolymerization reaction of epoxy and anhydride catalyzed by amine and the reaction of hydroxyl with anhydride (**Scheme 2**) as we have demonstrated in a previous study.[23]

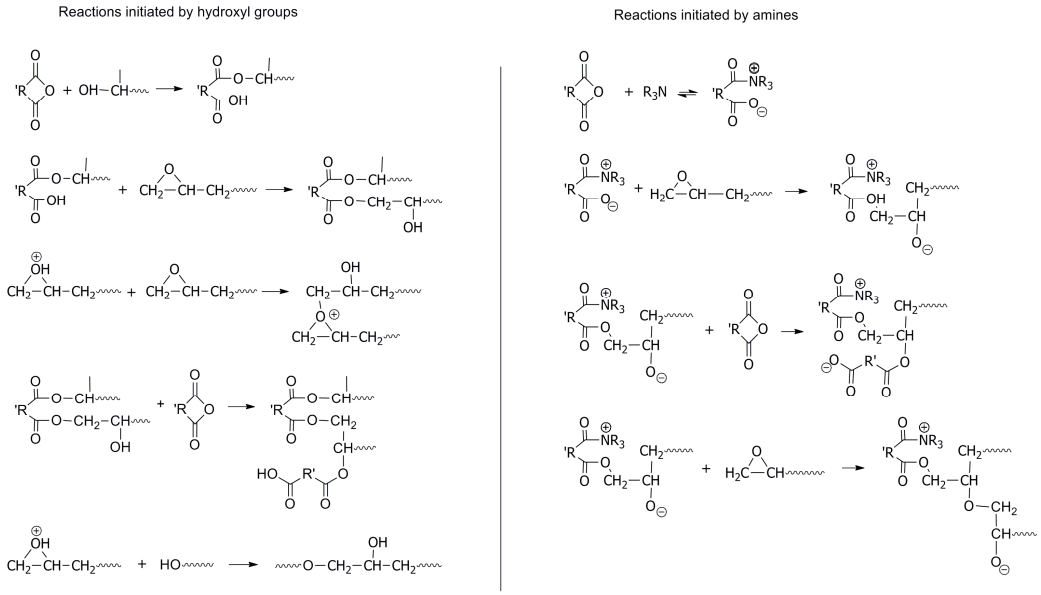

Scheme 2 Reaction involved in the curing process of epoxides with anhydrides catalyzed by amines in the presence of hydroxyl groups.

Table 2 shows the temperature of the maximum of the peak and the values of the enthalpy released per gram of mixture for all the studied formulations. Regarding the addition of the HBP one can see that the enthalpy released decreases proportionally to the amount added. This is due to the fact that on adding HBP the proportion of epoxy groups decreases and therefore the enthalpy must be lower. In all cases conversions are quantitative as confirmed by calculations and FTIR experiments. On the other hand, on adding sepiolite there is no appreciable decrease

of the heat evolved up to a proportion of 5 %. This can be better appreciated in the enthalpy released per epoxy equivalent. As one can see, in all cases the values obtained are around 100 kJ/ee, the value considered to represent the complete curing.[26]

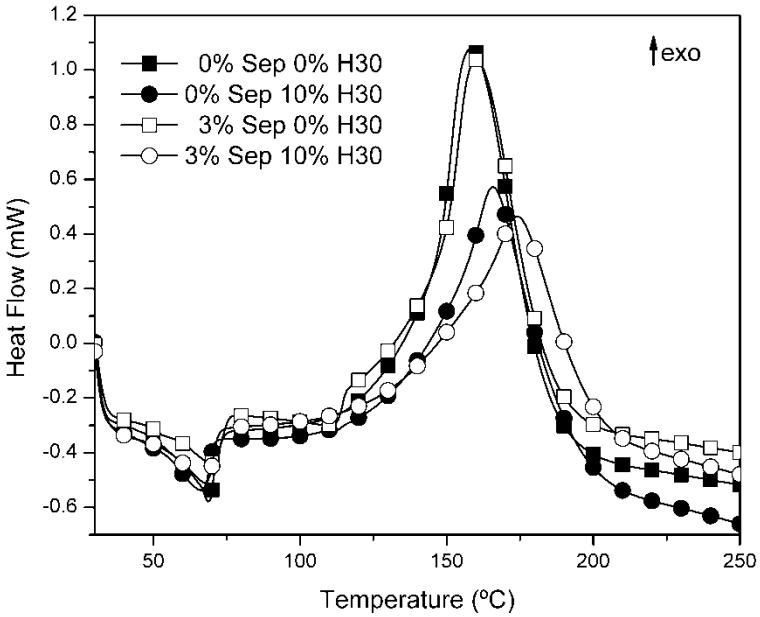

Figure 1 Curing exotherm curves for some of the formulations studied obtained in DSC scan at 10 ºC/min under N_2.

Table 2 Maximum of the exotherm, enthalpy released, kinetic parameters and glass transition temperature of all the studied formulations.

Sample	Tp [a] (ºC)	Δh (J/g)	Δh (kJ/ee)	Ea [b] (kJ/mol)	ln$A$ [c] (s^{-1})	$k_{150ºC}$ x 10^3 [d] (s^{-1})	T_g [e] (ºC)
0%Sep0%H30	158	300	101	74	15.4	11.07	107
0%Sep5%H30	166	285	103	76	15.2	8.90	110
0%Sep10%H30	166	278	110	73	15.1	8.17	111
1%Sep0%H30	161	298	101	69	15.4	10.95	106
1%Sep5%H30	170	275	101	77	15.1	7.91	111
1%Sep10%H30	170	269	107	76	15.0	7.29	113
3%Sep0%H30	160	305	105	75	15.4	10.58	103
3%Sep5%H30	165	276	104	78	15.1	7.82	107
3%Sep10%H30	170	269	109	82	15.0	7.22	105
5%Sep0%H30	159	280	98	70	15.3	10.19	105
5%Sep5%H30	165	250	96	74	15.1	8.07	111
5%Sep10%H30	166	240	100	74	15.0	7.32	109

a. Temperature of the maximum of the curing exotherm registered at 10 ºC/min.
b. Values of activation energy at 50% of conversion, evaluated by the isoconversional non-isothermal procedure with a precision of ± 2 kJ/mol.
c. Pre-exponential factor for the n=1.5; m=0.5 kinetic model with $g(x)=[(1-x)\,x^{-1}]^{-0.5}(0.5)^{-1}$.
d. Values of rate constant at 150 ºC using the Arrhenius equation at a conversion of 50%.
e. T_g determined after curing in a dynamic scan registered at 20 ºC/min.

The kinetic parameters of the curing processes were evaluated by the non-isothermal kinetic analysis methodology.[24] In that way, it is possible to estimate the activation energy *(E_a)*, the pre-exponential factor *(lnA)* and the rate constant *(k)*, which are collected in **Table 2**. Both, the addition of sepiolite and of Boltorn H30, have no significant influence on the E_a, indicating that all the systems follow a similar curing profile. **Figure 2** shows the plot of E_a versus conversion for some of the formulations studied and, as it can be seen, the value remains practically constant during the curing process indicating that the reactivity does not change significantly along the curing.

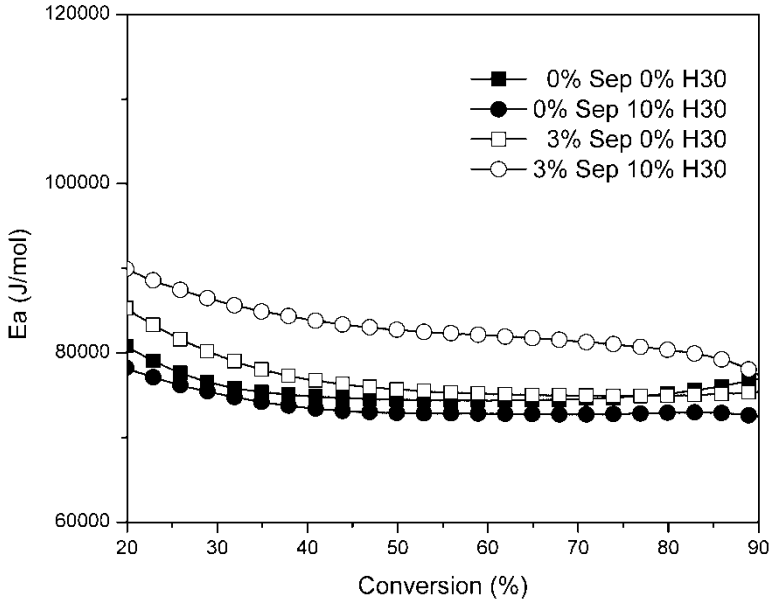

Figure 2 Activation energy against conversion for some of the studied formulations.

The parameter that better shows the curing rate is the kinetic constant *k*. From the values collected in **Table 2** it is possible to observe that, as we have already demonstrated in a previous article,[23] at concentrations up to a 10%, Boltorn H30 decelerates the curing process. Moreover, the addition of sepiolite also produces a decelerative effect. This can be rationalized on the basis of the increase in viscosity produced on adding the clay.

The T_g*s* of the final thermosets were also determined by means of DSC, and the values obtained are collected in the same table. The addition of sepiolite does not affect significantly the T_g*s* of the materials, which can be related to a good dispersion of the filler. Also the addition of Boltorn H30 scarcely affects this parameter, but slightly increases it. This corresponds to a characteristic of HBP polymers, which can modify the properties of epoxy resins without compromising the T_g.[10]

Dynamic Mechanical Thermal Studies (DMTAs)

Dynamic mechanical thermal analysis provides essential information about the viscoelastic behavior of a given material, being the maximum in *tan* δ often related to its T_g. **Figure 3** shows, as an example, the *tan* δ plots for some of the prepared materials. The first noticeable fact is the presence of a main peak, related to the T_g and a smaller second peak at higher temperatures in all formulations. This can be related to two zones of different crosslinking degree inside the material. One can rationalize that the complexity of the system with so many different reactions

taking place could be the responsible of this splitting. It is worth to note that the smaller peak is only shifted at lower temperature in formulations containing a 5% of sepiolite.

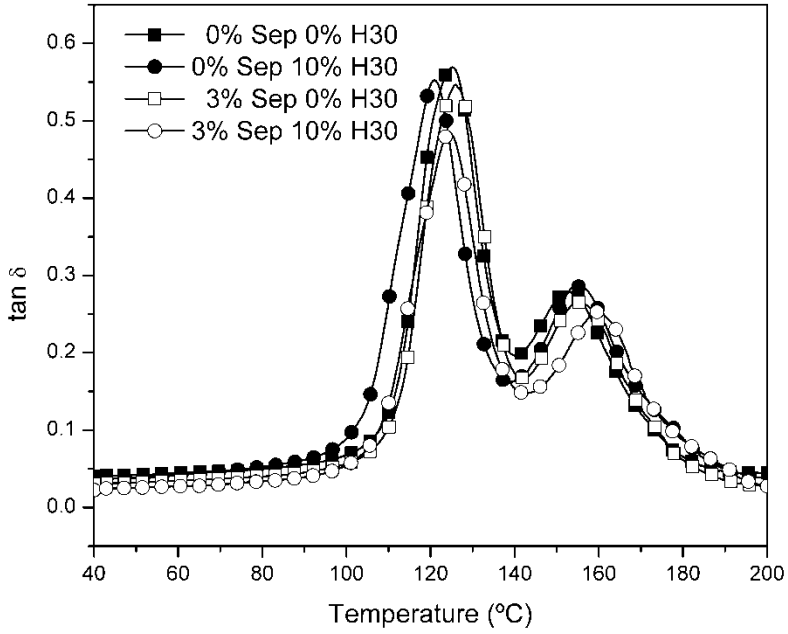

Figure 3 Tan δ versus temperature curves for some of the studied thermosets obtained.

With regards to the maximum of *tan δ* of the materials, **Table 3** collects the values for all the prepared thermosets. One can see how on adding HBP to the samples there are only little variations (less than 10 ºC for 10% of Boltorn H30) due to the flexibilization introduced by its polymeric structure. Similarly, the addition of the clay does not produce any drop down of the maxima and even in some cases a slight increase can be appreciated. This could indicate a good dispersion of the nanofillers since agglomeration can lead to decreases of the T_g.[22]

Another interesting value obtained from DMTA analysis is the modulus at the rubbery state. This can be related to the flexibility of the network. All the values of modulus are collected in **Table 3**. As expected, the addition of sepiolite increases the modulus in the rubbery state proportionally to the amount added. This can be explained from the rigidity of the rod-like structure of the clay. Moreover, also the addition of HBP yields an increasing of *E'*. On that case, the explanation is based in the fact that hydroxyls may lead to a more crosslinked network. Even more interesting is the cooperative effect shown by the two additives. Taking as an example samples with a 5% of sepiolite, one can see that the addition of Boltorn H30 is able to increase *E'* up to a higher extent.

Thermogravimetric Analysis

Nowadays a lot of concern is put in the reduction of the amount of residues generated by the industry. In the field of coatings, epoxy resins are well-known for lacking in reworkability, this is they cannot be removed from coated substrates due to their high thermal stability once their service life is over. Although epoxy/anhydride systems already have lower thermal stability since esters degrade via β-elimination at temperatures around 200 ºC,[27] the further reduction of the onset temperature of degradation of these thermosets is interesting from the technological and environmental point of view. **Table 3** collects the degradation data of all the prepared

thermosets (temperature of initial degradation, temperature of maximum rate of degradation and char yield), and **Figure 4** shows the thermograms of some of the studied materials as an example. First, it is appreciated that the addition of a 10% of Boltorn H30 can reduce the initial degradation temperature around 20 ºC obtaining thermosets that begin to degrade at around 250 ºC, the temperature at which a thermoset can be considered as reworkable. On the other hand, the addition of sepiolite does not affect this initial degradation temperature. As seen in **Table 3**, all the formulations containing the same amount of HBP present similar values of $T_{2\%}$ regardless of the amount of sepiolite. However, as expected, the addition of the inorganic filler yields an increase of the char yield, proportional to the amount added.

Table 3 Dynamic mechanical, thermal stability, density and shrinkage data for all the studied formulations.

Sample	*Tan δ* (ºC)	*E'* [a] (MPa)	$T_{2\%}$ [b] (ºC)	T_{max} [c] (ºC)	Char [d] (%)	ρ_{mon} (g/ml)	ρ_{pol} (g/ml)	Shrinkage [e] (%)
0%Sep0%H30	125	16.8	285	415	8.5	1.191	1.239	4.0
0%Sep5%H30	123	21.0	264	410	9.0	1.194	1.246	4.4
0%Sep10%H30	121	20.8	259	406	8.5	1.190	1.245	4.6
1%Sep0%H30	126	19.7	278	414	9.6	1.191	1.235	3.7
1%Sep5%H30	126	23.0	268	409	10.8	1.199	1.247	4.0
1%Sep10%H30	122	21.2	263	406	10.2	1.201	1.250	4.1
3%Sep0%H30	126	23.1	279	414	12.6	1.207	1.252	3.7
3%Sep5%H30	124	27.7	258	409	12.7	1.205	1.253	4.0
3%Sep10%H30	125	25.8	252	408	13.0	1.210	1.261	4.2
5%Sep0%H30	126	27.1	281	416	14.0	1.219	1.267	3.9
5%Sep5%H30	126	28.8	269	408	13.8	1.221	1.275	4.4
5%Sep10%H30	120	29.1	251	405	13.8	1.219	1.275	4.6

a. Measured at the maximum of *tan δ* + 75 ºC.
b. Temperature of the onset of degradation.
c. Temperature of the maximum rate of degradation.
d. Char yield at 800 ºC under N_2.
e. Shrinkage calculated as: $[(\rho_{mon} - \rho_{pol}) / \rho_{mon}] \times 100$.

Mechanical Properties and Electron Microscopy

Toughness is one the weakest properties of epoxy resins and for that reason a lot of efforts have been made to improve it. In our case, standard impact test was used to investigate the toughness of all the prepared thermosets. As seen in **Table 4**, the addition of sepiolite can improve the toughness of the resulting thermoset up to a concentration of 5% as demonstrated in samples 0%Sep0%H30 to 3%Sep0%H30. Toughness reaches a maximum for samples with a 3% of sepiolite but at a concentration of 5% percolation takes place and the properties drop down. This was assessed by transmission electron microscopy (TEM). As seen in **Figure 5**, whereas in samples with 1 and 3% of sepiolite few aggregates are present, samples containing 5% present big aggregates that result in the observed decrease in the impact resistance. However the addition of Boltorn H30 changes the polarity of the matrix and the micrograph of 5%Sep10%H30 shows a slightly better dispersion of the sepiolite.

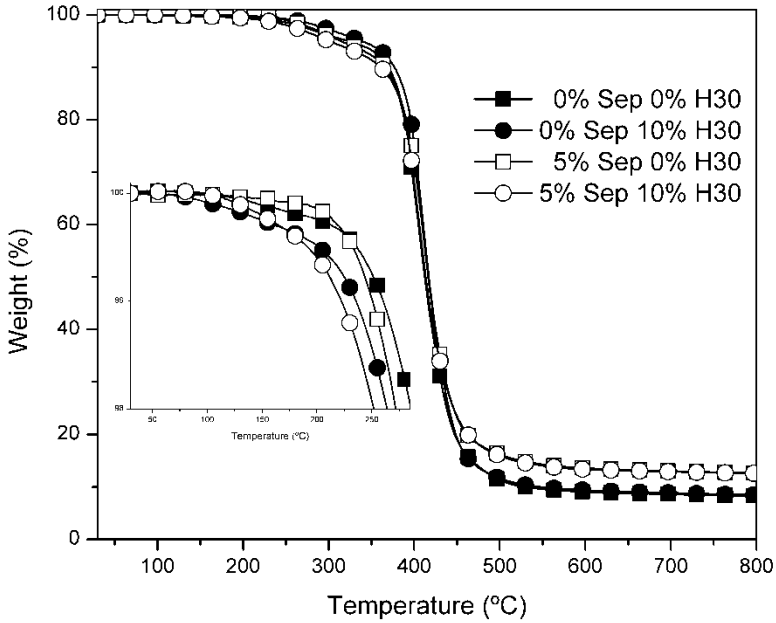

Figure 4 Weight loss curves for some of the studied thermosets obtained in a TGA scan at 10 ºC/min under N_2.

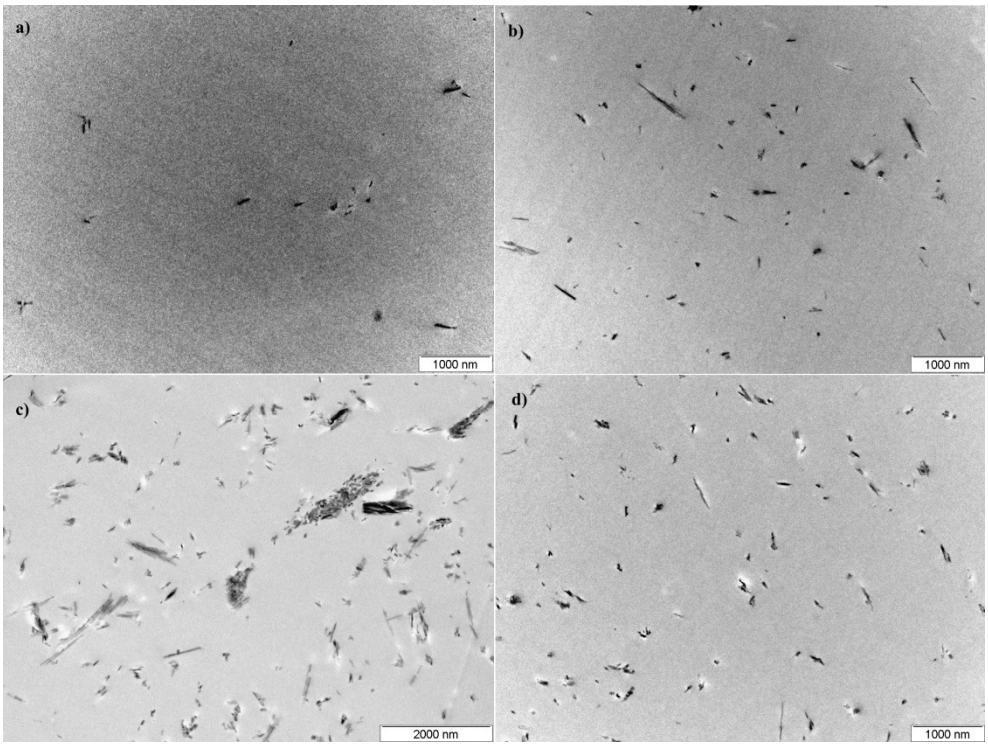

Figure 5 TEM micrographs of a) 1%Sep0%H30, b) 3%Sep0%H30, c) 5%Sep0%H30 and d) 5%Sep10%H30 at 20000 magnifications.

Table 4 Impact strength and microhardness values together with its uncertainty for all the studied formulations.

Sample	Impact Strength (kJ/m²)	Microhardness (HKN)
0%Sep0%H30	2.1 ± 0.2	22.7 ± 0.3
0%Sep5%H30	2.7 ± 0.3	25.6 ± 0.2
0%Sep10%H30	3.5 ± 0.2	27.7 ± 0.4
1%Sep0%H30	2.3 ± 0.3	20.6 ± 0.5
1%Sep5%H30	3.1 ± 0.3	21.9 ± 0.4
1%Sep10%H30	3.7 ± 0.2	24.1 ± 0.4
3%Sep0%H30	3.0 ± 0.2	18.1 ± 0.5
3%Sep5%H30	3.2 ± 0.3	18.2 ± 0.6
3%Sep10%H30	3.6 ± 0.4	19.8 ± 0.3
5%Sep0%H30	2.4 ± 0.2	9.5 ± 0.5
5%Sep5%H30	2.7 ± 0.2	10.1 ± 0.5
5%Sep10%H30	2.8 ± 0.3	13.0 ± 0.4

The addition of Boltorn H30, as observed by other authors,[9,28] also leads to improvement in toughness (samples 0%Sep0%H30 to 0%Sep10%H30). Moreover, the addition of HBP to samples containing sepiolite can further increase the toughness by combining two mechanisms of reinforcement: hindering of the propagation of the crack by sepiolite and flexibilizing the matrix by H30. Also the fact that a better dispersion of sepiolite can be achieved by the presence of the HBP (as seen by TEM) helps to explain the observed improvements.

The values of impact strength were correlated with the fracture surface of all the samples by scanning electron microscopy (SEM). Figure 6 shows the fracture surface at 60 magnifications of the samples 0%Sep0%H30 (a), 0%Sep10%H30 (b), 3%Sep0%H30 (c) and 3%Sep0%H30 (d). On comparing micrographs **6a** and **6c** one can notice the high improvement achieved by the addition of sepiolite moving from a glassy to a very rough surface, indicating the improvement in toughness. Also the improvement caused by the addition of Boltorn H30 was visually assessed. In samples containing HBP in its formulation (**6b**) the cracks are thicker than in the neat material (**6a**) indicating a more difficult propagation of the crack.[29] Finally, the sample with sepiolite and HBP (**6d**) shows the combined effect of both: a rough surface, indicating a plastic deformation and thicker cracks.

Another property studied for our materials was microhardness. These measurements are very useful in rating coatings on rigid substrates for their resistance to mechanical abuse, such as that produced by blows, gouging and scratching. This technique is used in the industry to characterize the mechanical properties related to resistance and hardness of materials and it measures their capability to resist static loads or applied at low rates. In our case, the addition of the sepiolite causes a decrease in the hardness of the material. Anyhow, samples containing up to 3% of sepiolite present HKN over 18 and the material can still be considered hard enough for potential applications. As observed in the impact resistance, a concentration of 5% of sepiolite produces a more pronounced decrease in the properties, probably due to percolation effects.

Contrary to the effect of sepiolite, the addition of H30 produces an increase in the hardness of the thermoset. The higher crosslinking density produced by the addition of the HBP can compensate the addition of sepiolite and for example the sample 3%Sep10%H30 has an HKN of nearly 20, similar to neat thermosets. There are other examples in the literature where the addition of a HBP can lead to the improvement of hardness in epoxy/anhydride systems.[10] On

that case the polymer used was Hybrane S1200, commercialized by DSM. Both polymers present hydroxyl end groups that lead to an increase in the crosslinking density and therefore in the hardness of the material.

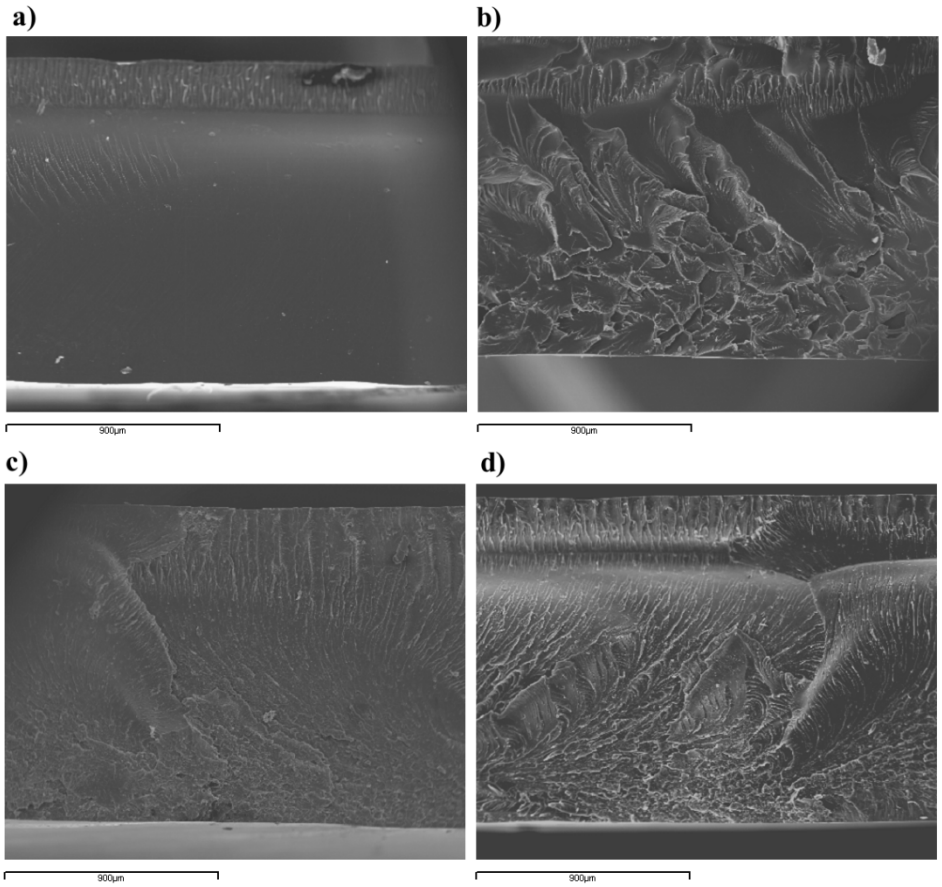

Figure 6 SEM micrographs for samples a) 0%Sep0%H30, b) 0%Sep10%H30, c) 3%Sep0%H30 and d) 3%Sep0%H30 at 60 magnifications.

Shrinkage

Shrinkage is one of the milestones in coatings industry. During the curing process the volume of the material is reduced, producing stresses, microvoids and microcracks that worsen the quality of the coating. To overcome this, one strategy has been the addition of Boltorn H30 to epoxy formulations in the cationic curing of DGEBA and in that case even expansion was reported.[30] However, in epoxy/anhydride systems we proved that this modifier not only does not produce expansion, but even increases the shrinkage at high concentrations.[23] This has been explained on the basis of the different mechanisms involved in the incorporation of hydroxyls into the network. While in cationic systems they are incorporated by the AM mechanism of propagation of ring-opening polymerization,[31] in epoxy anhydride systems the incorporation takes place by a condensation reaction. In the present work we have investigated if the presence of sepiolite affects the shrinkage. **Table 3** collects all the data of the densities before and after curing for all the studied formulations as well as the shrinkage calculated. As stated

previously, the addition of HBP to the formulation causes a slight increase in the shrinkage on curing (as seen in samples 0%SepY%H30).

The addition of sepiolite increases the density of the starting mixture due to the dispersion of a solid, but also the resulting polymer has a higher density compared with the neat material. On that way, the value of shrinkage is not affected by the addition of sepiolite. Observing the values, one can see that the only important factor is the Boltorn H30 content, and samples containing the same amount of HBP presented a similar value of shrinkage regardless of the proportion of sepiolite added.

CONCLUSIONS

New nanocomposites have been obtained by dispersing different amounts of sepiolite and Boltorn H30 in DGEBA/THPA mixtures and curing them with BDMA as the catalyst.

Due to an increase of viscosity, the addition of sepiolite produces a decrease on the curing rate. The same effect is observed for the addition of Boltorn H30 up to a concentration of 10%.

The T_g of the resulting thermoset remains practically unaffected for all the formulations studied regardless of the amount and of modifiers added.

By means of DMTA we could observe that all the materials were inhomogeneous, due to the complexity of the reactions that can take place during the curing. The maximum of $tan\,\delta$ for all samples was the same, indicating a good dispersion of the additives. The E' at the rubbery state showed that both sepiolite and HBP were able to increase the crosslinking density and this effect can be cooperative.

Standardized impact tests demonstrated that the addition of sepiolite up to a concentration of 3% slightly increases the toughness of the system. Higher concentrations lead to agglomerates of sepiolite in the matrix (as demonstrated by TEM microscopy) that worsen the impact resistance. The combined addition of Boltorn H30 and sepiolite lead to the toughest materials.

From the SEM observation of the fracture area of impacted specimens we could detect an increase of the plasticity of the fracture with the addition of sepiolite, whereas thermosets containing HBP presented thicker cracks that also denote improvement of the impact resistance. The combined effect of these modifiers was confirmed by this technique.

Microhardness could be improved by the addition of HBP to the mixtures due to the increase in the crosslinking density. On the contrary, the addition of sepiolite led to worsen the microhardness, especially in the case of adding a 5%.

The thermal stability of the thermosets remained unaffected by the addition of sepiolite and the only difference observed was the expected increase in the char yield. On the contrary, Boltorn H30 slightly reduced the thermal stability and thus allowed obtaining thermosets with improved reworkability.

ACKNOWLEDGEMENTS

The authors from the University Rovira i Virgili and from University Politècnica de Catalunya would like to thank MICINN (Ministerio de Ciencia e Innovación) and FEDER (Fondo Europeo de Desarrollo Regional) (MAT2011- 27039-C03-01 and MAT2011-27039-C03-02) for their financial support. D.F. acknowledges the grant FPU-2008 from the Spanish Government. We would like to thank TOLSA and Perstorp for kindly supplying sepiolite and Boltorn H30, respectively.

REFERENCES

1. J-P. Pascault, H. Sauterau, J. Verdu, R. J. J. Williams. *Thermosetting Polymers*. Marcel Dekker, New York, **2002**.
2. E. M. Petrie. *Epoxy adhesive formulations.* McGraw-Hill, New York, **2006**.
3. C. A. May. *Epoxy Resins. Chemistry and Technology*, 2nd edition. Marcel Dekker, New York, **1988**.
4. B. Voit, A. Lederer. *Chem. Rev.* **2009,** *109,* 5924.
5. D. Ratna, R. Varley, R. K. Singh Raman, G. P. Simon. *J. Mat. Sci.* **2003,** *38,* 147.
6. R. Mezzenga, C. J. G. Plummer, L. Boogh, J. A. E. Månson. *Polymer* **2001,** *42,* 305.
7. R. Mezzenga, J. A. E. Månson. *J. Mat. Sci.* **2001,** *36,* 4883.
8. M. Sangermano, M. Messori, M. Martin-Galleco, G. Rizza, B. Voit. *Polymer* **2009,** *50,* 5647.
9. J-P. Yang, Z-K. Chen, Y. Guo, Sh-Y. Fu, L. Ye. *Polymer* **2008,** *49,* 3168.
10. M. Morell, X. Ramis, F. Ferrando, Y. Yu, A. Serra. *Polymer* **2009,** *50,* 5374.
11. R. Bagheri, B. T. Marouf, R. A. Pearson. *J. Macromol. Sci. Part C: Polym. Rev.* **2009,** *49,* 201.
12. P. M. Ajayan, L. S. Schadler, P. V. Braun. *Nanocomposite Science and Technology.* Wiley, New York, **2004**.
13. E. P. Giannelis. *Adv. Mater.* **1996,** *8,* 29.
14. S. S. Ray, M. Okamoto. *Prog. Polym. Sci.* **2003,** *28,* 1539.
15. R. A. Vaia, G. Price, P. N. Ruth, H. T. Nguyen, J. Lichtenhan. *Appl. Clay Sci.* **1999,** *15,* 67.
16. G. Kickelbick. *Prog. Polym. Sci. 2003, 28,* 83.
17. Y. Kojima, A. Usuki, M. Kawasumi, A. Okada, Y. Fukushima, T. Karauchi, O. Kamigaito. *J. Mater. Res.* **1993,** *8,* 1185.
18. H. Shariatmadari, A. R. Mermut. *Soil Sci. Soc. Am. J.* **1999,** *63,* 1167.
19. M. Sangermano, E. Pallaro, I. Roppolo, G. Rizza. *J. Mater. Sci.* **2009,** *44,* 3165.
20. A. Nohales, L. Solar, I. Porcar, C. I. Vallo, C. M. Gómez. *Eur. Polym. J.* **2006,** *42,* 3093.
21. E. Franchini, J. Galy, J-F. Gerard. *J. Colloid Interf. Sci.* **2009,** *329,* 38.
22. A. Nohales, R. Muñoz-Espí, P. Félix, C. M. Gómez. *J. Appl. Polym. Sci.* **2011,** *119,* 539.
23. D. Foix, Y. Yu, A. Serra, X. Ramis, J. M. Salla. *Eur. Polym. J.* **2009,** *45,* 1454.
24. X. Ramis, J. M. Salla, C. Mas, A. Mantecón, A. Serra. *J. Appl. Polym. Sci.* **2004,** *92,* 381.
25. X. Ramis, J. M. Salla, A. Cadenato, J. M. Morancho. *J. Thermal. Anal. Calorim.* **2003,** *72,* 707.
26. J. Brandrup, E. H. Immergut, E. A. Grulke. *Polymer Handbook*, 4th ed. Wiley-Interscience, New York, **1999**.
27. P. Sivasamy, M. Palaniandavar, C. T. Vijayakumar, K. Ledered. *Polym. Degrad. Stab.* **1992,** *38,* 15.
28. L. Boogh, B. Pettersson, J. A. E. Månson. *Polymer* **1999,** *40,* 2249.
29. D. Hull, *Fractography, observing measuring and interpreting fracture surface topography.* Cambridge University Press, Cambridge, **1999**.
30. X. Fernández-Francos, J. M. Salla, A. Cadenato, J. M. Morancho, A. Serra, A. Mantecón, X. Ramis. *J. Appl Polym Sci,* **2009,** *111,* 2822.
31. P. Kubisa, S. Penczek. *Prog. Polym. Sci.* **1999,** *24,* 1409

3.4 New thermosets obtained from bisphenol A diglycidyl ether and hydroxyl-ended hyperbranched polymers partially blocked with benzoyl and trimethylsilyl groups

D. Foix[1], X. Fernández-Francos[2], J. M. Salla[2], A. Serra[1], J. M. Morancho[2], X. Ramis[2]

[1] Department of Analytical and Organic Chemistry, University Rovira i Virgili, Marcel.li Domingo s/n, 43007 Tarragona, Spain
[2] Laboratory of Thermodynamics, ETSEIB, University Politècnica de Catalunya, Av. Diagonal 647, 08028 Barcelona, Spain

ABSTRACT

New epoxy thermosets with improved flexibility were prepared by chemical modification of bisphenol A diglycidyl ether (DGEBA) with hyperbranched polymers (HBPs). Hydroxyl-ended hyperbranched polyesters were modified by blocking part of the hydroxyl groups with trimethylsilyl or benzoyl groups. The curing of mixtures of DGEBA with various proportions of two modified HBPs using ytterbium triflate as cationic initiator was investigated using differential scanning calorimetry and thermomechanical analysis. The characterization of these materials was performed using several thermal analysis techniques and their morphology was investigated using electron microscopy. High proportions of HBPs reduced the glass transition temperature and the relaxed storage modulus but barely affected gelation. The overall curing shrinkage was controlled by the content of hydroxyl groups and by the changes of HBP molecular interactions during curing. The results indicated that the relative proportion and type of terminal groups play a role in the evolution of the curing and the properties of the thermosets. Hydroxyl groups promoted the covalent incorporation of the HBP to the network via hydroxyl-induced chain-transfer reactions, whereas benzoyl groups promoted phase separation. Formulations containing HBP blocked with benzoyl groups showed two phases connected through covalent linkages between the HBP-rich phase and the epoxy matrix.

INTRODUCTION

Epoxy thermosets are rigid and brittle polymeric materials. While rigidity and strength are desired for many engineering applications, brittleness reduces their applicability. Therefore, toughening is necessary to broaden their technological use. The addition of a second phase, either rigid or soft, can be a solution to this problem.[1] There are two classic methods for the modification of epoxies with a soft second phase: the use of reactive oligomers; and the rubber modification technique. The use of block copolymers able to induce micro- or nanostructuring has also been reported.[2] Other authors[3,4] reported an improvement in mechanical properties by reducing the crosslinking density, which is related to the ductility of the matrix.

In recent years, the use of hyperbranched polymers (HBPs) as toughness modifiers in epoxy thermosets has been proposed.[5-9] These polymers present some advantages such as their structural versatility, the presence of a great number of terminal reactive groups and their low viscosity compared to analogous linear polymers. Several authors reported an increase in toughness without compromising Young's modulus and thermomechanical properties.[5,10] In addition, this type of modifier has been applied for the reduction in internal stresses in epoxy thermosets and their composites.[11] The occurrence of internal stresses, which form voids and cracks and lead to the loss of adhesion, can be caused by shrinkage during curing. Reduction in shrinkage has also been accomplished by the use of HBPs as reactive modifiers. In previous papers,[10,12] we reported a reduction in shrinkage, and even an expansion, when a hydroxyl-

ended HBP was chemically incorporated into an epoxy matrix. However, other authors[13] reported the opposite effect, a density increase of materials, and therefore this point should be further investigated.

The commercial availability of Boltorn® HBPs of various molecular weights, aliphatic polyesters with hydroxyl end groups, has made them some of the most studied hyperbranched modifiers for epoxy thermosets.[9,12,14,15] Depending on the curing agent selected and the compatibility between the HBP and the matrix, either by physical miscibility or covalent bonding between the HBP end groups and the epoxy matrix, the crosslinked materials can be homogeneous or show phase separation.

The aim of the work reported here was to investigate the effect of the partial blocking of hydroxyl groups of Boltorn H30 with benzoyl and trimethylsilyl groups on the cationic curing of formulations of epoxy resin based on bisphenol A diglycidyl ether (DGEBA) with added HBP: kinetics of the curing process, gelation, shrinkage, thermomechanical properties and morphology of the resulting materials. Ytterbium triflate was selected as curing agent, since we previously demonstrated that this cationic initiator is able to covalently incorporate Boltorn H30 into DGEBA epoxy matrix by hydroxyl-induced chain-transfer reactions, the so-called activated monomer (AM) mechanism.[12,16] The presence of some remaining hydroxyl groups in the modified HBPs helps in the linkage of the modifier to the epoxy matrix and thus can affect gelation, shrinkage and thermomechanical characteristics. Trimethylsilyl and benzoyl groups were selected as blocking groups because of their different characteristics and affinity for the matrix and the easy modification of H30 by direct reaction with trimethylsilyl or benzoyl chlorides. **Scheme 1** depicts the structures of the HBPs used as modifiers (H30-Bz and H30-Si, with terminal benzoyl and trimethylsilyl groups respectively).

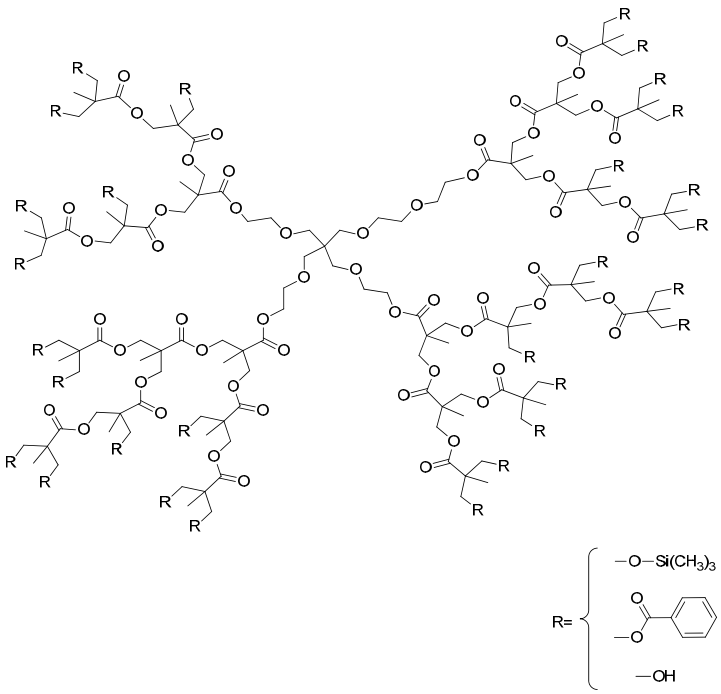

Scheme 1 Idealized chemical structures of the three HBPs studied: H30, H30-Bz and H30-Si.

EXPERIMENTAL PART

Materials

Boltorn H30 (weight-average molecular weight Mw = 3600 g mol^{-1}, hydroxyl number = 480-510 g/(g_{KOH}), according to its datasheet) was supplied by Perstorp and used as received. Diglycidyl ether of Bisphenol A (DGEBA) Epitoke Resin 827 was provided by Shell Chemicals with an epoxy equivalent of 182 g/ee and was dried before use. Benzoyl chloride, triethylamine and trimethylsilyl chloride were purchased from Aldrich and used without further purification. Ytterbium triflate from Aldrich was used as received. Tetrahydrofuran (THF) was dried over sodium and then distilled. Hexane was distilled over calcium chloride.

Synthesis of H30-Bz

In a 500 mL three-necked round-bottomed flask, 10 g (0.09 mol hydroxyl groups) of Boltorn H30 was dissolved in 300 mL of THF and 25 mL (0.18 mol) of triethylamine was added. Under gentle magnetic stirring, 12 mL (0.10 mol) of benzoyl chloride was slowly added to the flask using a dropping funnel. The reaction was kept at room temperature for 24 h under argon atmosphere. Then, the precipitate was filtered off and THF eliminated under reduced pressure. The residue was washed several times with cold hexane and the resulting product dried in a vacuum oven at 50 ºC overnight. A pale yellow viscous liquid was obtained in 85% yield.

^{1}H NMR (400 MHz, $CDCl_3$; δ, ppm): 8.05-7.80 (45H, aromatics), 7.55-7.40 and 7.40-7.25 (70H, aromatics), 4.55-3.95 (104H, COO-CH_2-), 3.80–3.20 (66H, CH_2-OH,-O-CH_2 (core)), 1.3-1.0 (97H,-CH_3).

^{1}H NMR analysis indicated a degree of modification of 40%, and the glass transition temperature (T_g) was found to be 40 ºC.

Synthesis of H30-Si

In a 500 mL three-necked round-bottomed flask, 10 g (0.09 mol hydroxyl groups) of Boltorn H30 was dissolved in 200 mL of THF. The mixture was then heated to 65 ºC and 13.9 mL (0.01 mol) of triethylamine was added. Finally, 11.4 mL (0.09 mol) of trimethylsilyl chloride was added dropwise. The reaction mixture was stirred for a further 30 min at the same temperature and the heating bath then removed. After 10 min, the white precipitate was filtered off and the THF eliminated under reduced pressure. The remaining viscous oil was re-dissolved in hexane, filtered and the solvent was eliminated in a rotary evaporator. The product was dried in a vacuum oven at 50 ºC for 24 h to obtain a white viscous liquid in 70% yield.

^{1}H NMR (400 MHz, $CDCl_3$; δ, ppm): 4.40-4.10 (48H, COO-CH_2-), 3.80-3.50 (80H, SiO-CH_2-, HO-CH_2 and -O-CH_2 (core), m), 1.30-1.00 (85H,-CH_3), 0.15-0.05 (203H, OSi-CH_3).

^{1}H NMR analysis indicated a degree of modification of 70% and the T_g was found to be -30 ◦C.

Preparation of the curing mixtures

Mixtures were prepared by first heating and mixing the corresponding amounts of DGEBA and HBP until a clear solution was obtained. Then, 1 phr (parts per hundred parts of mixture) of ytterbium triflate was added and mixed thoroughly. Samples were kept at -20 ºC before use to prevent polymerization. **Table 1** gives the notation and composition of the various formulations studied.

Measurements

^{1}H NMR spectra (400 MHz) were obtained with a Varian Gemini 400 spectrometer. Spectra were acquired in 1 min and 16 scans with a 1.0 s time between pulses (D1). $CDCl_3$ was used as a solvent and internal standard.

Calorimetric analyses were carried out using a Mettler DSC-822e calorimeter with a TSO801RO robotic arm. Samples of approximately 10 mg were cured in aluminum pans in a nitrogen atmosphere. Non-isothermal experiments were performed from 0 to 225 ºC at heating rates of 2, 5, 10 and 15 ºC/min to determine the reaction heat and the kinetic parameters. In the non-isothermal curing process, the degree of conversion at a given temperature T was calculated as the quotient between the heat released up to T and the total reaction heat associated with the complete conversion of all reactive groups. T_g of the cured materials was determined with a second scan at 10 ºC/min after dynamic curing using the mid-point method, with the error estimated to be approximately ±1 ºC. T_g of the HBPs was determined using a similar procedure.

Thermomechanical analysis was carried out in a nitrogen atmosphere using a Mettler TMA40 thermomechanical analyzer. A 0.8 mm thickness of silanized glass fibre mesh was impregnated with the reacting liquid mixture and this was placed between two 6 mm diameter ceramic plates. Isothermal experiments at 130 ºC were performed by applying a periodic force of between 0.0025 and 0.01 N to monitor contraction during the curing process.[12] The gel conversion, α_{gel}, was determined as the DSC conversion at the temperature of the material gelled in TMA in a non-isothermal experiment according to a methodology described previously.[17]

Table 1 Composition and notation of the studied systems using 1 phr of ytterbium triflate as initiator.

HBP (%) [a]	eq_{ini}/eq_{epoxy} [b]	H30[c]			H30-Bz[c]		
		Sample	eq_{OH}/eq_{epoy} [d]	n_{HBP}/n_{DGEBA} [e]	Sample	eq_{OH}/eq_{epoy} [d]	n_{HBP}/n_{DGEBA} [e]
0	0.00294	DGEBA	0.0000	0.0000	DGEBA	0.0000	0.0000
5	0.00312	5% H30	0.0874	0.0116	5% H30-Bz	0.0444	0.0040
10	0.00329	10% H30	0.1849	0.0184	10% H30-Bz	0.0940	0.0084
15	0.00349	15% H30	0.2937	0.0260	15% H30-Bz	0.1493	0.0133

HBP (%)[a]	eq_{init}/eq_{epoxy} [b]	H30-Si[c]		
		Sample	eq_{OH}/eq_{epoy} [d]	n_{HBP}/n_{DGEBA} [e]
0	0.00294	DGEBA	0.0000	0.0000
5	0.00312	5% H30-Si	0.0282	0.0035
10	0.00329	10% H30-Si	0.0596	0.0075
15	0.00349	15% H30-Si	0.0947	0.0118

a. Percentage by weight of hyperbranched polymer.
b. Ratio of equivalents (initiator/epoxy).
c. H30, H30-Bz and H30-Si indicate the hyperbranched polymer studied: H30 (32 OH, 3,600 g/mol), H30-Bz (19.2 OH, 12.8 benzoyl, 4,822 g/mol) and H30-Si (9.6 OH, 22.4 trimethylsiloxy, 5,430 g/mol).
d. Ratio of equivalents (hydroxyl/epoxy).
e. Molar ratio (hyperbranched/DGEBA).

Dynamic mechanical thermal analysis (DMTA) was carried out with a TA Instruments DMTA 2980 analyzer. The samples were cured isothermally in a mould at 150 ºC for 3 h and were then

subjected to a post-curing for 1 h at 180 ºC. Before the samples were prepared, they were degassed in a vacuum oven at 80 ºC for 1 h. Three-point bending of 10 mm was performed on prismatic rectangular samples (1.5 × 9 × 5 mm^3). The apparatus operated dynamically at 3 ºC/min from 35 to 200 ºC or -80 to 200 ºC at a frequency of 1 Hz.

TGA was carried out with a Mettler TGA-50 thermobalance. Cured samples with an approximate mass of 5 mg were heated from 30 to 700 ºC at a heating rate of 10 ºC/min in a nitrogen atmosphere.

The density of the samples was measured before curing by the standard procedure of filling a pycnometer with the viscous mixture in a thermostatically controlled bath at 30 ºC. The density of the cured samples was determined indirectly by the flotation method, starting from solutions of KBr with densities that were lower and higher than that of the sample. The shrinkage was calculated from the density measurements of the cured and uncured materials.

The gel content of the cured materials was determined by measuring the weight loss after extracting with chloroform for 24 h at boiling temperature.

The fracture surface of the specimens was observed with an environmental scanning electron microscopy (ESEM) instrument (model FEI Quanta 600) and the distribution of the silicon in the sample was observed using elemental mapping.

Transmission electron microscopy (TEM) was performed with a Jeol 1011 microscope. The samples were prepared using an ultramicrotome at room temperature.

The kinetic triplet (pre-exponential factor, activation energy and kinetic model) of the curing was determined using integral isoconversional non-isothermal kinetic analysis, the Kissinger-Akahira-Sunose equation, combined with the Coats-Redfern procedure. Due to the compensation effect between pre-exponential factor and activation energy, we only discuss data for rate constants calculated using the Arrhenius equation from the aforementioned kinetic parameters. Details of the kinetic methodology are given in a previous study.[18]

RESULTS AND DISCUSSION

The modification of Boltorn H30 polymers with benzoyl or methylsilyl groups was performed as described above using conventional procedures. The silylation of the HBP and its structural characterization were previously described by Plummer *et al.*[19] They calculated the degree of silylation using ^{1}H NMR spectroscopy.

The benzoylated HBP with various degrees of modification was first described by Jiang *et al.*[20] and its self-assembling was also investigated. Those authors attached benzoyl groups by reaction of terminal hydroxyl with benzoyl chloride in dimethylformamide in the presence of triethylamine as an acceptor of HCl. Instead of dimethylformamide we used THF as solvent at room temperature and this enabled a high degree of benzoylation of the hydroxyl groups. The characterization of H30-Si and H30-Bz was performed using ^{1}H NMR spectroscopy and the results obtained agree well with those published before. While H30-Bz has T_g of 40 ºC, the value for H30-Si is about -30 ºC, according to the longer length and higher flexibility of O-Si and C-Si bonds.

The cationic curing of DGEBA with various amounts of H30-Bz andH30-Si using ytterbium triflate as initiator was studied to obtain new thermosets with higher flexibility. The results obtained are compared with those previously obtained using Boltorn H30[12] and with new results using H30. **Tables 2** and **3** summarize the thermal data obtained for H30-Bz and H30-Si, respectively. The similarity between enthalpies per epoxy equivalent and those reported for

other epoxy systems indicates that epoxides have reacted almost completely.[21] Fourier transform infrared (FTIR) spectra of cured samples show that the absorbance band at 915 cm^{-1}, due to the oxirane group, disappears completely. Although it is expected that hydroxyl groups participate in the cationic curing of epoxides via the AM mechanism (see *Scheme 1* in Fernández-Francos *et al.*[12]), it is not possible to prove it with FTIR because for every hydroxyl group that participates in the process, another one is formed. The almost completely insoluble material (see gel content in **Tables 2** and **3**) suggests that the HBPs become covalently linked to the network and that at least part of hydroxyls react via the AM mechanism. As the AM mechanism is more likely with a higher content of hydroxyl groups, it is expected that the degree of chemical incorporation increases with the presence of hydroxyl groups (H30 > H30-Bz > H30-Si).

Table 2 Gel content and calorimetric, DMTA and TGA data of DGEBA/HBP mixtures with various amounts of H30-Bz.

H30-Bz (%)	Gel content (%)	DSC				DMTA		TGA	
		Δh[a] (J/g)	Δh[b] (kJ/ee)	T_g (ºC)	ΔC_p[c] (J·g/K)	Tan δ[d] (ºC)	E'[e] (MPa)	T_{onset}[f] (ºC)	T_{max}[g] (ºC)
0	100	526	95.8	130	0.201	161	56.4	258	344
5	99	497	95.2	123	0.222	154	47.8	263	341
10	98	470	95.0	116	0.240	140	32.8	273	344
15	97	448	96.1	110	0.276	129	19.9	265	347

a. Enthalpies per gram of mixture.
b. Enthalpies per equivalent of epoxy group.
c. Difference in heat capacity when the material changes from glassy to rubbery state.
d. Temperature of maximum of *tan* δ at 1 Hz.
e. Relaxed modulus determined at maximum of *tan* δ + 50 ºC.
f. Temperature of the onset of decomposition for the TGA data at 10 ºC/min calculated for a 2% weight loss.
g. Temperature of the maximum decomposition rate based on the on the TGA data at 10 ºC/min.

Table 3 Gel content and calorimetric, DMTA and TGA data of DGEBA/HBP mixtures with various amounts of H30-Si.

H30-Si (%)	Gel content (%)	DSC				DMTA		TGA	
		Δh[a] (J/g)	Δh[b] (kJ/ee)	T_g (ºC)	ΔC_p[c] (J·g/K)	Tan δ[d] (ºC)	E'[e] (MPa)	T_{onset}[f] (ºC)	T_{max}[g] (ºC)
0	100	526	95.8	130	0.201	161	56.4	258	344
5	99	500	95.8	123	0.245	149	43.2	230	344
10	97	475	96.1	119	0.254	129	22.9	228	349
15	97	450	96.4	109	0.271	-	-	237	353

a. Enthalpies per gram of mixture.
b. Enthalpies per equivalent of epoxy group.
c. Difference in heat capacity when the material changes from glassy to rubbery state.
d. Temperature of maximum of *tan* δ at 1 Hz.
e. Relaxed modulus determined at maximum of *tan* δ + 50 ºC.
f. Temperature of the onset of decomposition for the TGA data at 10 ºC/min calculated for a 2% weight loss.
g. Temperature of the maximum decomposition rate based on the on the TGA data at 10 ºC/min.

T_g of the cured systems with H30-Bz and H30-Si was determined using DSC and DMTA (**Tables 2** and **3**). The presence of H30-Bz and H30-Si in the materials leads to a progressive decrease in T_g with increasing modifier content. Various factors can contribute to this behaviour: (1) chain-transfer reactions between the HBP hydroxyl and DGEBA epoxy groups (AM mechanism) prevent chain growth and the subsequent generation of a new growing chain reduces the crosslinking density of the epoxy network; (2) the large free volume originating from the incorporation of the HBP in the three-dimensional epoxy network tends to increase the molecular mobility, especially when large groups, like H30-Bz and H30-Si, are added to epoxy systems;[9] (3) the plasticizing effect of dangling HBP linked to the epoxy matrix; and (4) a lower crosslinking density obtained when blocked HBP is chemically incorporated into the network.[22,23] Formulations with H30-Bz and H30-Si show similar T_g, determined after dynamic curing using DSC, whereas T_g of H30-Si, obtained from DMTA after isothermal curing, is slightly lower than T_g of H30-Bz. Differences can be caused by both a difference in curing schedule of DSC samples (dynamic curing) and DMTA samples (isothermal curing) and the different accuracy in the determination of the glass transition using these two techniques. It is accepted that DMTA allows more unambiguous determination of T_g.[24] The lower density (**Table 4**) of DGEBA/H30-Si formulations, caused by the presence of C-Si and O-Si bonds, which are longer than C-C and C-O bonds and favour mobility, can lead to networks with lower T_g. The increase in C_p on increasing the proportion of HBP can be related to a reduction of the crosslinking density.[25] The lower values of C_p for DGEBA/H30-Bz in comparison to DGEBA/H30-Si formulations can also be rationalized on the same basis.

Table 4 Gel conversion, densities and shrinkage of the studied systems.

HBP (%)	H30				H30-Bz			
	α_{gel} (%)	ρ_{mon} (g/cm^3)	ρ_{pol} (g/cm^3)	Shrinkage [a] (%)	α_{gel} (%)	ρ_{mon} (g/cm^3)	ρ_{pol} (g/cm^3)	Shrinkage [a] (%)
0	23	1.167	1.193	2.20	23	1.167	1.193	2.20
5	26	1.169	1.174	0.43	19	1.166	1.197	2.64
10	31	1.168	1.122	-4.10	23	1.169	1.198	2.46
15	34	1.171	1.102	-6.26	25	1.170	1.201	2.67

HBP (%)	H30-Si			
	α_{gel} (%)	ρ_{mon} (g/cm^3)	ρ_{pol} (g/cm^3)	Shrinkage [a] (%)
0	23	1.167	1.193	2.20
5	21	1.154	1.188	2.95
10	24	1.149	1.188	3.37
15	19	1.147	1.190	3.75

a. Shrinkage determined as $[(\rho_{pol} - \rho_{mon})/\rho_{pol}] \times 100$.

Figure 1 shows the DSC traces at 10 °C/min for various DGEBA/H30-Si formulations. The reaction rate decreases as the H30-Si proportion increases, as reflected by the calculated rate constants shown in **Figure 2**. Formulations containing H30-Bz present a similar behaviour, although the decrease in the curing rate on increasing the H30-Bz content is much less. In order to better understand the effect of hydroxyl end group content on the reaction rate, **Figure 3** shows the calorimetric curves at 10 °C/min for neat DGEBA and formulations with 15% of H30, H30-Si and H30-Bz. The calculated rate constants are plotted in **Figure 4**.

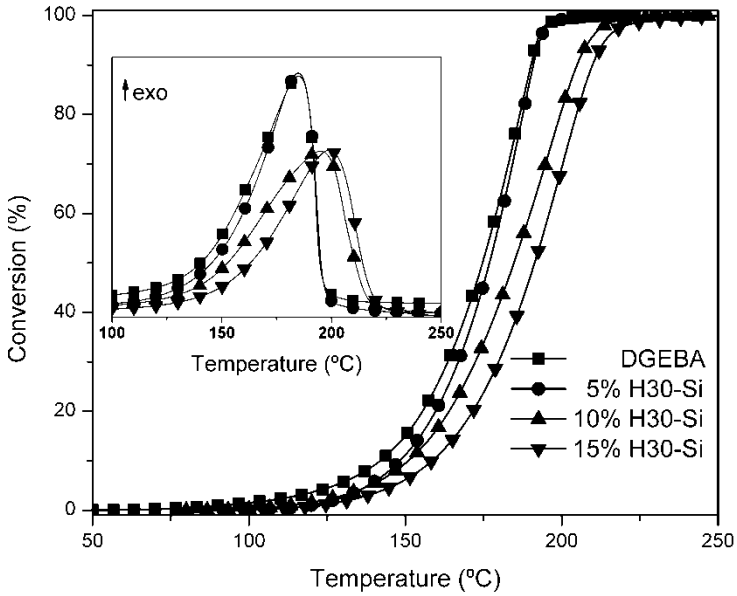

Figure 1 Calorimetric curves (inset) and conversion degree against temperature of curing of DGEBA/H30-Si mixtures containing different percentage of H30-Si at a heating rate of 10 ºC/min.

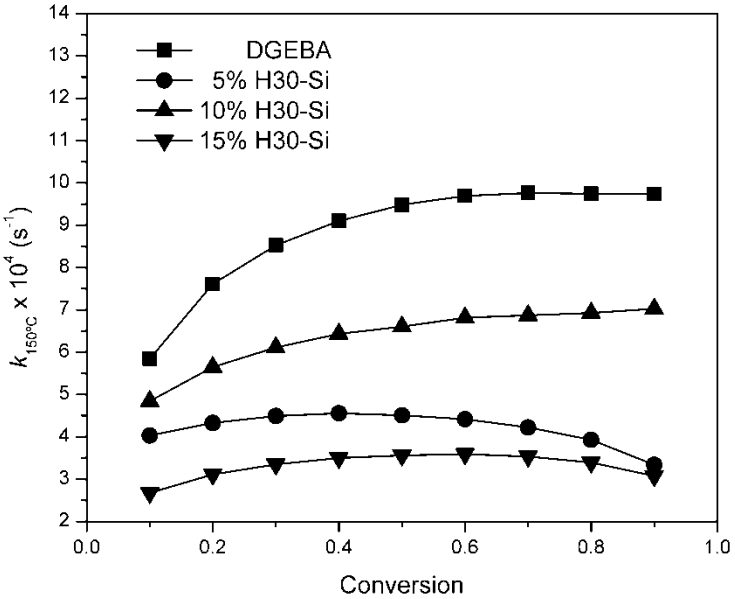

Figure 2 Rate constant at 150 ºC against degree of conversion of the curing with various amounts of H30-Si.

The values of rate constants (**Figures 2** and **4**) demonstrate how the amount and type of HBP modify the kinetics of reaction although the values remain almost invariant during curing. The curing is decelerated by H30-Si and to a lesser extent by H-30-Bz, whereas H30 accelerates the curing. In a previous paper[12] we showed how H30 increased the reaction rate only when it was added in amounts above 10%. The low proportion of hydroxyl groups in the formulations containing modified HBPs agrees with this previous result.

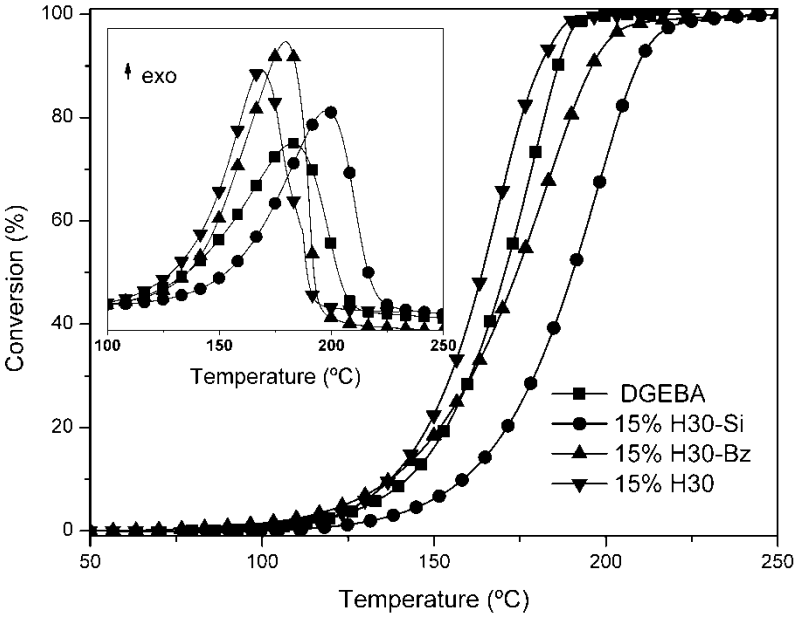

Figure 3 Calorimetric curves (inset) and degree of conversion against curing temperature of DGEBA and DGEBA with 15% of H30, H30-Bz and H30-Si mixtures at a heating rate of 10 °C/min.

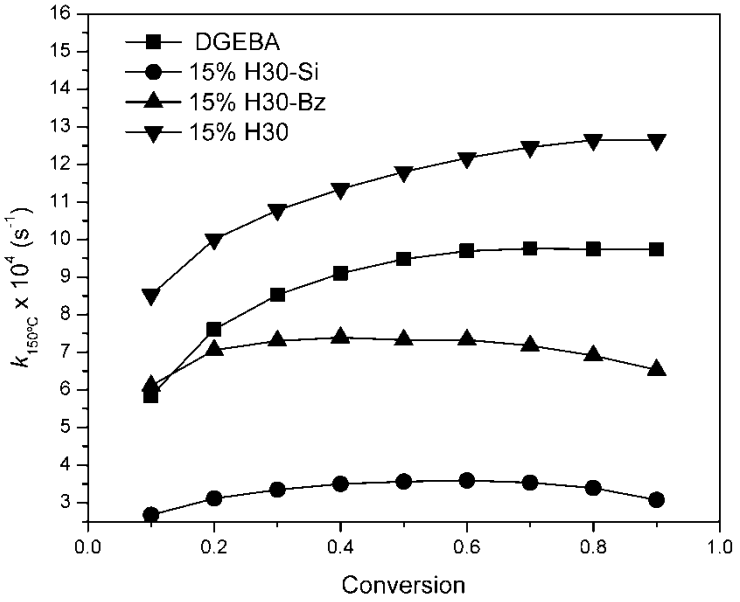

Figure 4 Rate constant at 150 °C against degree of conversion of the curing with 15% of H30-Bz, 15% of H30-Si and 15% of H30 and without HBP.

It is accepted that two different mechanisms operate in cationic ring-opening polymerization of epoxides, the activated chain-end (ACE) and the activated monomer (AM) mechanisms.[16] The AM mechanism is preferred in the presence of a relatively high content of initiator and hydroxyl groups.[26] However, the overall effect of HBPs on kinetics and rate constants is more complex and depends on the relative contribution of the following factors: (1) competition between

propagation mechanisms (AM and ACE) as mentioned above; (2) dilution of DGEBA epoxy groups in the reaction mixture as the modifier content is increased; (3) increase in viscosity;[27] (4) modification of the crosslinking density; and all these conditioned by (5) the presence and amount of hydroxyl groups,[28] initiator and active species. In general, the higher viscosity of the reaction medium when HBP is added tends to decrease the reaction rate (especially for H30-Bz and H30-Si) and only when the amount of hydroxyl groups is very high (>10%H30) is the reaction accelerated. The higher content of hydroxyl groups in DGEBA/H30-Bz formulations compared to DGEBA/H30-Si can account for the observed higher reaction rate (**Table 1**).

The results of TGA in nitrogen atmosphere are summarized in **Tables 2** and **3**. The addition of HBP barely modifies the thermal stability of the network (T_{max}), but some minor differences can be observed for onset temperature. The presence of H30-Bz in the thermoset slightly increases the onset temperature, which can be related to the presence of thermally stable benzoyl groups. The lower onset temperature values of the materials containing H30-Si can be attributed to the presence of ester and trimethylsilyloxy labile groups in the network.

Table 4 shows the effect of adding HBP on shrinkage and gelation. In previous work[12] we proved that the addition of H30 to a DGEBA reduced the shrinkage during cationic curing and even expansion was obtained. This behaviour can be attributed to a reduction in intramolecular H30 hydrogen bond interactions and an increase in free volume when H30 is chemically incorporated into the network. Lederer *et al.*[29] demonstrated the more compact structure of hydroxylic HBPs in comparison to phenyl group ended HBPs. The addition of H30-Bz and H30-Si does not reduce the shrinkage like H30 and even a slightly increase in shrinkage is observed when H30-Si is used. The structure of H30-Si in liquid DGEBA, before curing, is already expanded (low density; **Table 4**) due to the fewer hydrogen bond interactions. When H30-Si reacts with the epoxy groups of DGEBA, for every bond formed a van der Waals distance changes to a covalent distance producing same degree of contraction. Although H30-Bz shows a compact structure before curing, it barely modifies the shrinkage because the Π-Π stacking interactions between benzoyl groups prevent the expansion of H30-Bz when it is chemically incorporated into epoxy matrix.

In addition to the global shrinkage during curing, it is important to know if shrinkage takes place before or after gelation, because stresses only originate after gelation due to the restricted mobility of the polymeric chains. **Figure 5** shows the dimensional changes and the deformability of the materials during curing in TMA for the formulations containing 10% of H30 and H30-Bz. The curve corresponding to the DGEBA/H30-Bz formulation shows a continuous shrinkage during the whole curing process, whereas DGEBA/H-30 system experiences a large expansion followed by a slight contraction. Again, the differences observed can be related to the different content of hydroxyl groups and to a reduction in intramolecular H30 hydrogen bond interactions due to the reaction between hydroxyl and epoxy groups.[9] DGEBA/H30-Si formulations present similar trends to H30-Bz mixtures but with a more pronounced shrinkage.

In **Table 4** the values for the conversion at gelation (α_{gel}) with various proportions and types of HBP are collected. We can observe that there isnosignificant variation in α_{gel} whenH30-Bz orH30-Si is used, whereas H30 leads to a steady increase in α_{gel}. Solubility tests confirm that α_{gel} is constant for all formulations using H30-Bz or H30-Si, but strongly increases when H30 content is increased. In previous works,[12,30] we demonstrated that α_{gel} increased on increasing the H30 content and, accordingly, the amount of hydroxyl groups. These results suggest a scarce chemical incorporation of the modified HBPs into the network because of the low available number of hydroxyl groups.

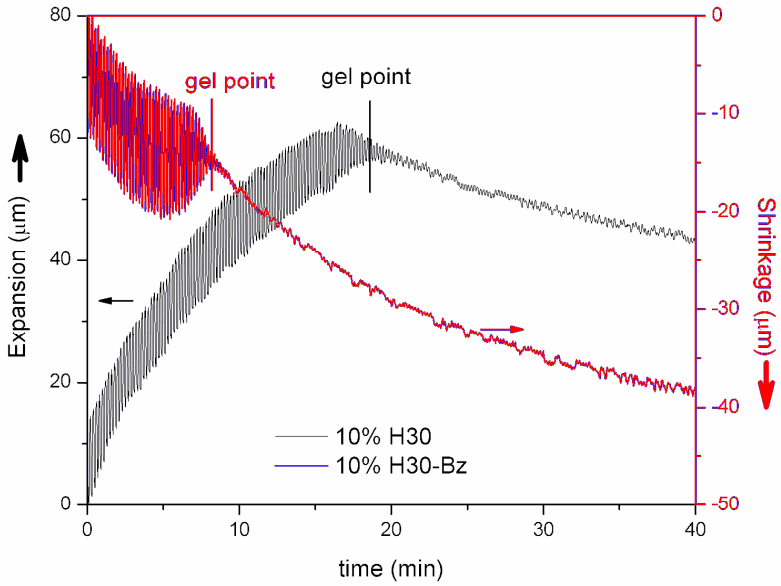

Figure 5 TMA thermograms of isothermal curing at 130 °C with 10% H30 and 10% H30-Bz. Gel points are also indicated.

Figures 6 and **7** show the mechanical relaxation spectra at 1 Hz for the DGEBA/H30-Bz thermosets. It can be seen that on increasing the H30-Bz proportion in the formulation, the modulus-temperature and *tan δ*- temperature curves shift to lower temperatures, indicating that T_g decreases as the proportion of HBP increases, as seen above.

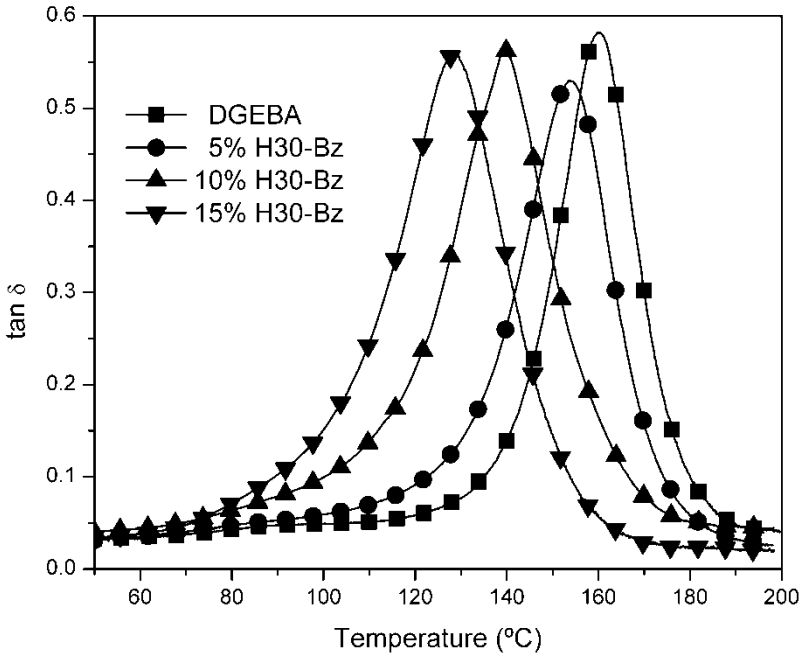

Figure 6 *Tan δ* vs temperature at 1 Hz for several DGEBA/H30-Bz formulations.

When H30-Si modifier is added, similar results are obtained (data not shown) but the values of the maximum of tan δ are slightly lower (**Tables 2** and **3**). According to the rubber elasticity theory,[31] the relaxation modulus in the rubbery state is inversely proportional to the molecular weight between crosslinking nodes and therefore directly proportional to the crosslinking density. It can be observed that on increasing the HBP content, the relaxation modulus decreases because of the formation of more flexible structures in the cured material. The presence of blocked terminal groups in the HBPs reduces the crosslinking density and, in this way, the HBP can act as an internal plasticizer. This effect is more evident in H30-Si than in H30-Bz formulations, since H30-Si contains a greater proportion of blocking units, which are much more flexible than benzoyl groups. In addition, the higher T_g of neat H30-Bz (40 ºC) than neat H30-Si (-30 ºC) can contribute to the differences observed when both HBPs are used as modifiers.

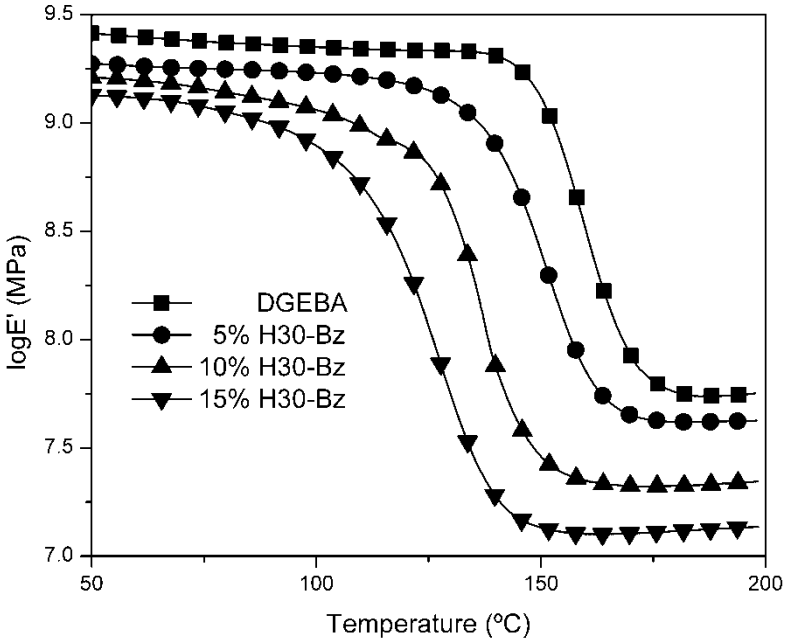

Figure 7 Logarithm of the storage modulus vs temperature at 1 Hz for several DGEBA/H30-Bz formulations.

Although the *tan δ* curves apparently show a single and unimodal α relaxation, which is typical of single-phase materials, the loss modulus-temperature curves (**Figure 8**) show the occurrence of a second relaxation between α and β relaxation when H30-Bz is present in the formulation. This relaxation, although low in magnitude, can be attributed to an HB30-Bz-rich phase with T_g of ca 40 ºC. Therefore, it seems that H30-Bz/DGEBA thermosets present a certain degree of phase separation. For DGEBA/H30-Si systems it is not possible to detect any relaxation associated with an H30-Si-rich phase, but it must be noted that if there was such relaxation it would appear close to -30 ºC and overlap the β-relaxation (attributed to glyceryl or diphenylpropane groups). In previous work,[12] we could see that DGEBA/H30 thermosets showed a single phase due to the complete chemical incorporation of H30 into the network.

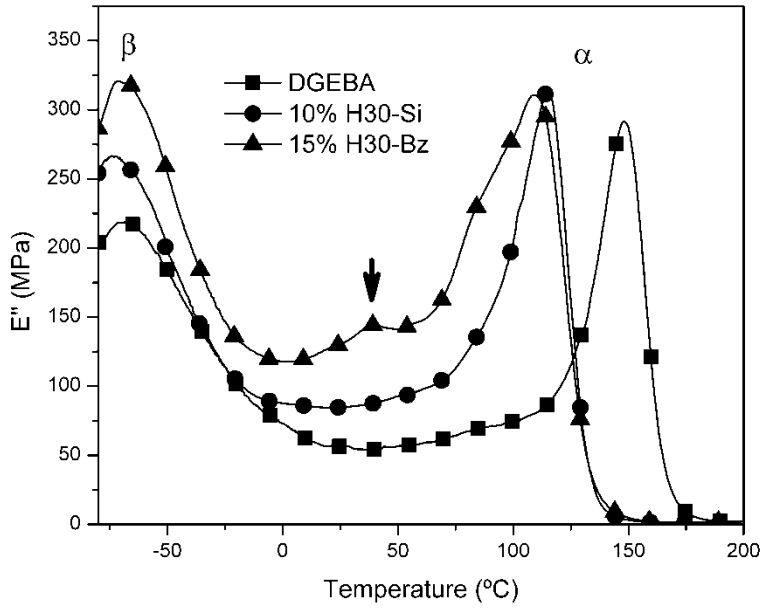

Figure 8 Loss modulus vs temperature at1 Hz for several formulations.

To confirm the phase separation in H30-Bz-modified materials, we studied isothermally cured samples using electron transmission microscopy. **Figure 9** shows TEM micrographs of cured DGEBA with and without H30-Bz. The TEM micrograph of the10%H30-Bz formulation reveals the existence of dispersed HBP-rich particles, with a size between 50 and 350 nm. The non-spherical form of the particles can be explained by the chemical interaction between the HBP-rich particles and the epoxy matrix via hydroxyl-induced chain-transfer reactions. From the TEM images it is estimated that a maximum of 4% of H30-Bz is segregated into particles, whereas the other 6% is dispersed homogeneously within the epoxy matrix. The 5 and 15% H30-Bz formulations show similar morphology with ca 1.5 and 4.5% of dispersed HBP-rich particles, respectively. In contrast, TEM micrographs of cured DGEBA/H30-Si formulations do not show any phase separation. **Figure 10** shows an ESEM micrograph of the fracture surface of the material containing 10% of H30-Si in which the elemental mapping of silicon is highlighted as dots. All the micrographs present a homogeneous appearance without any phase separation. This homogeneity can be attributed to the covalent linkages of the remaining hydroxyl groups of H30-Si to the epoxy matrix, which compatibilizes both components.

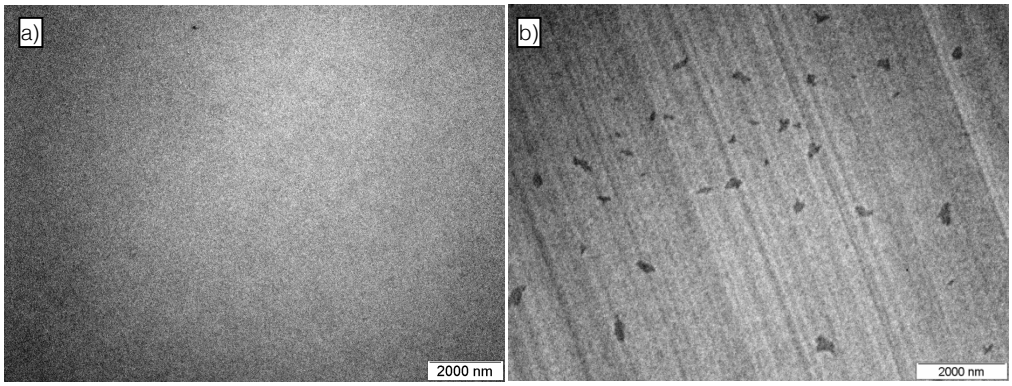

Figure 9 TEM micrographs: (a) neat DGEBA; (b) DGEBA with 10% H30-Bz.

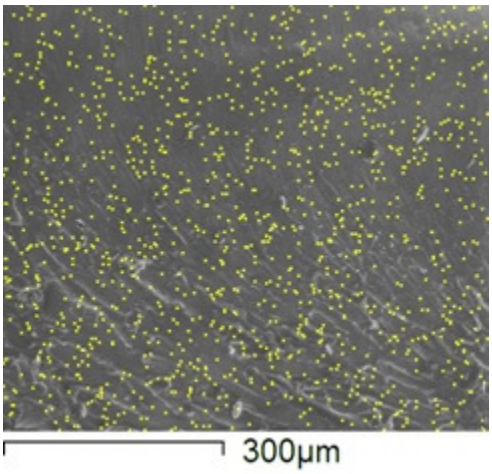

Figure 10 ESEM micrograph of a mixture DGEBA with 10% H30-Si. Siliceous distribution is shown as dots.

Jiang *et al.*[20,32,33] reported that benzoyl-terminated HBP presents a spontaneous molecular self-assembly process with differently shaped structures, depending on the content of hydroxyl and benzoyl groups, which was attributed to the different hydrophilic character of HBP core and benzoyl groups. They observed that no self-assembled structures were formed using a HBP with hydroxyl terminal groups in all arms. Hydrogen bonding between hydroxyl and ether or carbonyl groups, along with the Π-Π stacking interaction between phenyl groups, drive the molecular self-assembly process and consequently the phase separation. This is probably the reason why H30-Bz presents phase separation whereas H30 and H30-Si do not. Taking into account that the content of hydroxyl groups decreases in the order H30 > H30-Bz > H30-Si, it can be concluded that the amount of hydroxyl groups playing a part is not the unique factor driving the phase-separation process. The different hydrophilicity of the HBP cores and the branch end groups, as well as the physical interaction between groups in addition to the possibility of chemical bonding between the HBP and the matrix, are other factors that can contribute to the resulting morphology.

CONCLUSIONS

A commercial hyperbranched polyester with hydroxyl terminal groups was partially blocked with trimethylsilyl or benzoyl units to explore the application of these HBPs as flexibilizing modifiers of epoxy systems.

Ytterbium triflate was demonstrated to be an effective initiator in the cationic curing of DGEBA/hydroxyl-terminated HBPs. There was a chemical incorporation of the HBP into the network through the reaction between hydroxyl and epoxy groups via an AM mechanism, which affected the curing. H30-Bz and H30-Si with low content of hydroxyl groups hardly affected gelation whereas unmodified H30 strongly reduced the shrinkage and increased conversion at the gel point. The degree of compactness of HBP before curing, the benzoyl interactions, the hydrogen bonding interactions and their changes during curing are the factors that control the shrinkage.

Thermosetting materials with improved flexibility were obtained by increasing the proportion of modified HBPs and a progressive decrease of T_g and relaxed storage modulus was observed. The content and type of terminal groups play an important role in the curing and in

the final properties of the cured materials. High hydroxyl content increases the reaction rate and the covalent incorporation of the HBP via hydroxyl-induced chain-transfer reactions, whereas terminal groups like benzoyl facilitate phase separation due to the different hydrophilic character of the HBP core and the benzoyl groups and to the molecular interactions.

ACKNOWLEDGEMENTS

The authors thank MICINN (Ministerio de Ciencia e Innovación) and FEDER (Fondo Europeo de Desarrollo Regional) for their financial support (grants MAT2008-06284-C03-01 and MAT2008-06284-C03-02) and the Generalitat de Catalunya for her financial help (2009-SGR-1512). DF acknowledges grant FPU-2008 from the Spanish Government. The authors acknowledge David Serrano from his support in the accomplishment of experiments.

REFERENCES

1. R. Bagheri, B. T. Marouf, R. A. Pearson. *J. Macromol. Sci. C* **2009,** *49,* 201.
2. S. Ritzenthaler, F. Court, L. David, E. Girard-Reydet, L. Leibler, J. P. Pascault. *Macromolecules* **2002,** *35,* 6245.
3. M. Franco, I. Mondragon, C. B. Bucknall. *J. Appl. Polym. Sci.* **1999,** *72,* 427.
4. R. A. Pearson, A. F. Yee. *J. Mater. Sci.* **1989,** *24,* 2571.
5. L. Boogh, B. Petterson, J. A. E. Månson. *Polymer* **1999,** *40,* 2249.
6. R. J. Varley, W. Tian. *Polym. Int.* **2004,** *53,* 69.
7. D. Zhang, D. Jia. *J. Appl. Polym. Sci.* **2006,** *101,* 2504.
8. G. Xu, W. Shi, M. Gong, F. Yu, J. Feng. *Polym. Adv. Technol.* **2004,** *15,* 639.
9. J-P. Yang, Z-K. Chen, G. Yang, S-Y. Fu, L. Ye. *Polymer* **2008,** *49,* 3168.
10. M. Morell, X. Ramis, F. Ferrando, Y. Yu, A. Serra. *Polymer* **2009,** *50,* 5374.
11. Y Eom, L Boogh, V Michaud, J. A. E. Månson. *Polym. Compos.* **2002,** *23,* 1044.
12. X. Fernández-Francos, J. M. Salla, A. Cadenato, J. M. Morancho, A. Serra, A. Mantecón, X. Ramis. *J. Appl. Polym. Sci.* **2009,** *111,* 2822.
13. M. Sangermano, A. Priola, G. Malucelli, R. Bongiovanni, A. Quaglia, E. Amerio, B. Voit, A. Ziemer. *Macromol. Mater. Eng.* **2004,** *289,* 442.
14. R. Mezzenga, C. J. G. Plummer, L. Boogh, J. A. E. Månson. *Polymer* **2001,** *42,* 305.
15. G. Cicala, A. Recca, C Restuccia. *Polym. Eng. Sci.* **2005,** *45,* 225.
16. L. Matejka, P. Chabanne, L. Tighzert, J. P. Pascault. *J. Polym. Sci. A: Polym. Chem.* **1994,** *32,* 1447.
17. S. González, X. Fernández-Francos, J. M. Salla, A. Serra, A. Mantecón, X. Ramis. *J. Appl. Polym. Sci.* **2007,** *104,* 3406.
18. X. Ramis, J. M. Salla, C. Mas, A. Mantecón, A Serra. *J. Appl. Polym. Sci.* **2004,** *92,* 381.
19. C. J. G. Plummer, L. Garamszegi, T-Q. Nguyen, M. Rodlert, J. A. E. Månson. *J. Mater. Sci.* **2002,** *37,* 4819.
20. G. Jiang, L. Wang, H. Yu, Ch. Chen, X. Dong, T. Chen, Q. Yang. *Polymer* **2006,** *47,* 12.
21. J. Brandrup, E. H. Immergut. *Polymer Handbook*. Wiley, New York, **1975**.
22. D. Zhang, D. Jia. *J. Appl. Polym. Sci.* **2006,** *101,* 2504.
23. M. Sangermano, G. Malucelli, R. Bongiovanni, A. Priola, A. Harden. *Polym. Int.* **2005,** *54,* 917.
24. J. P. Pascault, H. Sautereau, J. Verdu, R. J. J. Williams. *Thermosetting Polymers*. Marcel Dekker, New York **2002**.
25. S. Montserrat. *Polymer* **1995,** *36,* 435.
26. J. M. Salla, X. Fernández-Francos, X. Ramis, A. Mantecón, A. Serra. *J. Thermal. Anal. Calorim.* **2008,** *91,* 385.

27. D. Ratna, R. Varley, G. P. Simon. *J. Appl. Polym. Sci.* **2003,** *89,* 2339.
28. M. Sangermano, G. Malucelli, R. Bongiovanni, A. Priola, A. Harden, N. Rehnberg. *Polym. Eng. Sci.* **2003,** *43,* 1460.
29. A. Lederer, M. A. Elrehim, F. Schallausky, D. Voigt, B. Voit. *e-Polymers* **2006,** 039.
30. D. Foix, Y. Yu, A. Serra, X. Ramis, J. M. Salla. *Eur. Polym. J.* **2009,** *45,* 1454.
31. L. E. Nielsen. *J. Macromol. Sci. Rev. Macromol. Chem.* **1969,** *C3,* 69.
32. G. Jiang, L. Wang, T. Chen, X. Dong, H. Yu, J. Wang, C. Chen. *J. Polym. Sci. A: Polym. Chem.* **2005,** *43,* 5554.
33. G Jiang, L Wang, T Chen, X Dong, H Yu, J Wang, C. Chen. *Polymer* **2005,** *46,* 5351.

Chapter 4

Improvement of the Chemical Reworkability of Epoxy Resins with HBPs

4.1 Introduction

The polymerization of AB_2 monomers is a very efficient way of preparing hyperbranched polymers since no gelation can take place and therefore high molecular weights can be achieved without risk. Among them, polyesters are a dominating class of materials due to their relatively easy synthesis and the availability of suitable monomers. In addition, polyesters have in general a high level of commercial importance, and a variety of well-known processing technologies are available.

Among HB polyesters one can find aliphatic structures as the commercial available Boltorn type polymers, aliphatic-aromatic[1] and purely aromatic[2-4] ones, all based on AB_2 acid/alcohol monomers. **Figure 4.1** shows the chemical structure of some of these monomers. In the case of full aromatic polyesters the previous activation of the phenolic groups is required in order to achieve high molecular weights. The most used strategies for such activation are acetylation and trimethylsililation.[5]

[1] P. Kambouris, C. J. Hawker. *J. Chem. Soc., Perkin Trans.* **1993**, *1*, 2717.
[2] C. J. Hawker, R. Lee, J. M. J. Fréchet. *J. Am. Chem. Soc.* **1991**, *113*, 4583.
[3] S. R. Turner, B. Voit, T. H. Mourey. *Macromolecules* **1993**, *26*, 4617.
[4] H. R. Kricheldorf, O. Stöber. *Macromol. Rapid Commun.* **1994**, *15*, 87.
[5] M. G. McKee, S. Unal, G. L. Wilkes, T. E. Long. *Prog. Polym.Sci.* **2005**, *30*, 507.

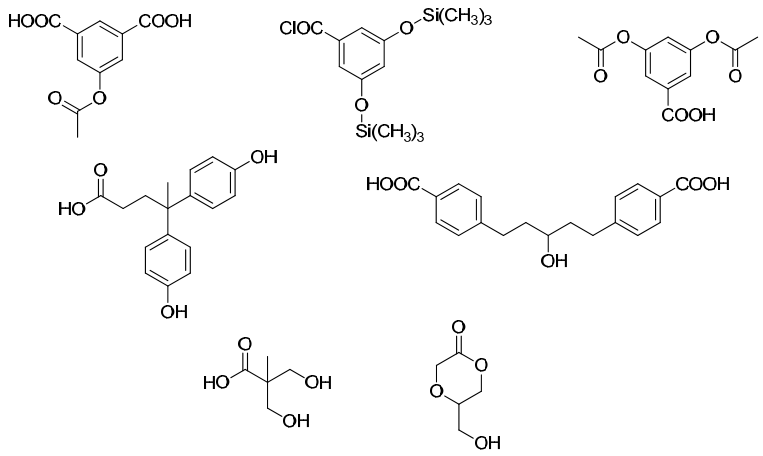

Figure 4.1 Available AB_2 monomers for the synthesis of hyperbranched polyesters.

Bis(4-hydroxyphenyl)pentanoic acid is an AB_2 monomer that can be used without any further modification to obtain aliphatic-aromatic HB polyesters, either directly in melt,[1,6] or in solution polycondensation. In the case of melt polycondensation, dibutyltindiacetate is used as catalyst and the reaction performed at 185 ºC under vacuum for 24 hours. However, in order to obtain higher molecular weights and more narrow distributions the methodology of the solution polycondensation should be employed. The polymerization reaction is depicted in **Figure 4.2**. The methodology is based on the use of a coupling agent such as N, N'-dicyclohexylcarbodiimide (DCC) and a catalyst, for example dimethyaminopyridinium p-toluenesulfonate (DPTS), and the reaction is performed in DMF. On that way, molecular weights as high as 40,000 g/mol can be achieved.[7] Another advantage of this methodology is the fact that it can be carried out at room temperature.

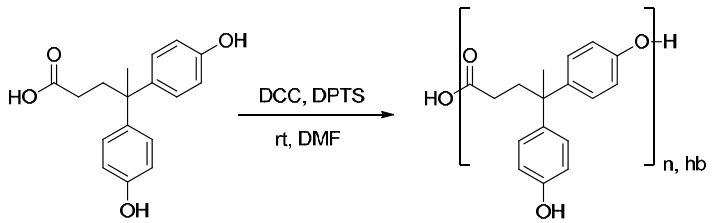

Figure 4.2 Polymerization in solution of bis(4-hydroxyphenyl)pentanoic acid.

The fact that the phenolic groups of the monomer are in two different aromatic rings makes that their reactivity is independent and therefore the DBs obtained are very close to the theoretical value of 0.5 for HBPs. More interesting is the fact that this degree of branching can be tuned. With the use of an AB comonomer, in this case 3-(4-hydroxyphenyl)propionic acid, and controlling the proportion of both comonomers it is possible to obtain DBs going from 0.5 for the case where no AB monomer is present to 0.29 when the proportion is 1:4.

Another way of controlling the DB of this aliphatic-aromatic HB polyesters is the ABB^*/AB_2 approach.[8] In this case, as seen in **Figure 4.3**, the methodology consists in copolymerizing the

---

[6] D. Schmaljohann, H. Komber, B. Voit. *Acta Polym.* **1999**, *50*, 196.
[7] F. Schallausky, M. Erber, H. Komber, A. Lederer. *Macromol. Chem. Phys.* **2008,** *209,* 2331.
[8] A. Khalyavina, F. Schallausky, H. Komber, M. Al Samman, W. Radke, A. Lederer. *Macromolecules* **2010,** *43,* 3268.

AB_2 monomer with another monomer with one of the phenol groups protected with TBDMSiO (ABB*). After the polymerization in solution, the group is deprotected and on that way one can tune the DB without having to different monomers in the final structure of the HBP.

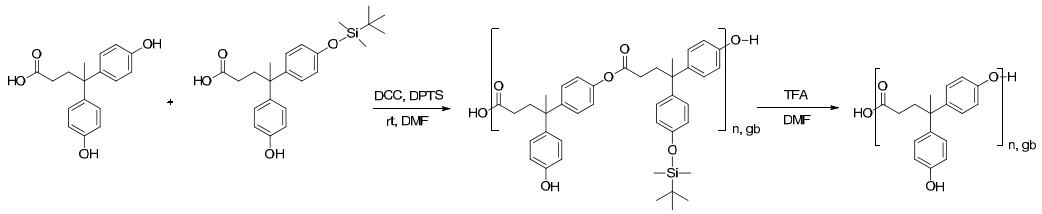

Figure 4.3 Scheme of the ABB*/AB_2 approach for obtaining gradually branched polyesters.

The DB can change dramatically the physical and chemical properties of the resulting polymers. For example the intrinsic viscosity is very influence by the degree of branching since on increasing DB the polymeric structure is more compact.[9]

Also the transitions of a given polymer can change with the DB. For example, the effect of DB on crystallization and melting behaviors of hyperbranched polyethers was studied by Johansson *et al.*[10] It was observed that the crystallinity decreased with increasing DB. Also glass transition temperature is influenced by the DB as demonstrated by Jayakannan *et al.* for HB poly(4-ethyleneoxyl benzoate)s.[11] This changes were attributed to the differences in the free volume of polymers with different DBs. Moreover, the self-assembly, the optoelectric and encapsulation properties among others change dramatically. Having all of this into account, it is evident that the degree of branching must have also influence in the curing process and in the properties of thermosets modified with HBPs.

Epoxy resins cannot be removed from a given substrate after their lifetime is finished. Due to their high chemical and thermal stability, particularly in epoxy resins based on the homopolymerization of DGEBA, it is difficult to eliminate them without damaging the substrate. One strategy to improve reworkability is the introduction of thermal labile groups in the network. Alternatively it also exist the possibility to introduce groups that can be eliminated by chemical reactions. This is the so called "chemical reworkability". There are many different strategies based on this principle. For instance, the introduction of olefinic insaturation in the structure of the resins allows the cleavage of the network oxidation of the double bonds with permanganate. If the groups introduced are carbamates, the cleavage is carried out by strong acid treatment.[12]

Other examples are the resins proposed by Buchwalter *et al.*[13] (**Figure 4.4**). These cycloaliphatic resins contained ketal groups in their structure that can be hydrolyzed after acid treatment.

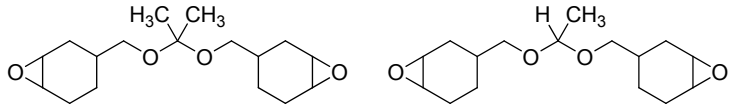

Figure 4.4 Cycloaliphatic epoxy resins containing ketal groups proposed by Buchwalter *et al.*

[9] A. V. Lyulin, D. B. Adolf, G. R. Davies. *Macromolecules* **2001**, *34*, 3783.
[10] H. Magnusson, E. Malström, A. Hult, M. Johansson. *Polymer* **2002**, *43,* 301.
[11] M. Jayakannan, S. Ramakrishnan. *J. Polym. Sci., Part A: Polym. Chem.* **2000**, *38*, 261.
[12] J. R. Griffith. *Epoxy Resin Chemistry.* ACS, Washington DC, **1979**.
[13] S. L. Buchwalter, L. L. Kosbar. *J. Polym. Sci. Part A: Polym. Chem.* **1996**, *34,* 249.

Braun *et al.*[14] proposed a different approach to this "chemical reworkability" concept by reporting the hydrogenolysis of epoxy/anhydride based thermosets and other epoxy based materials.

Finally, another strategy used to improve the chemical reworkability of epoxy resins is the reported by Fernández-Francos *et al.*[15] They proved that the alternate copolymerization of DGEBA with a spirocyclic γ-bislactone initiated by tertiary amines could yield thermosets that could be completely solubilized in 1M ethanolic KOH solutions. However, the main problem of this strategy is the reduction on the T_g of the prepared materials.

This chapter will deal about the use of HB aromatic-aliphatic polyesters to improve the chemical reworkability of systems HBP/DGEBA cured cationically. These esters present the advantage that cannot undergo β-elimination (see Chapter 1), and therefore are thermally stable, but they can be saponified under basic conditions. Also the influence of the DB in the reworkability as well as in the other properties of the resulting thermosets will be discussed. These studies have yielded the articles herein detailed:

4.2 New hyperbranched polyester modified DGEBA thermosets with improved chemical reworkability.

4.3 The effect of the degree of branching in hyperbranched polyesters used as reactive modifiers in epoxy thermosets.

[14] D. Braun, W. von Gentzkow, A. P. Rudolf. *Polym. Degrad. Stab.* **2001,** *74,* 25.
[15] X. Fernández-Francos, J. M. Salla, A. Mantecón, A. Serra, X. Ramis. *Polym. Degrad. Stab.* **2008,** *93,* 760.

4.2 New hyperbranched polyester modified DGEBA thermosets with improved chemical reworkability

D. Foix[1], M. Erber[2], B. Voit[2], X. Ramis[3], A. Mantecón[1], A. Serra[1]

[1] Department of Analytical and Organic Chemistry, University Rovira i Virgili, Marcel.li Domingo s/n, 43007 Tarragona, Spain

[2] Leibniz-Institute of Polymer Research Dresden, Hohe Str. 6, 01069 Dresden, Germany

[3] Laboratory of Thermodynamics, ETSEIB, University Politècnica de Catalunya, Av. Diagonal 647, 08028 Barcelona, Spain

ABSTRACT

The chemical reworkability of epoxy thermosets in alkaline solutions has been increased by adding a hyperbranched polyester (HBPE) as a reactive modifier to the diglycidyl ether of bisphenol A (DGEBA) cured by lanthanide triflates as cationic initiators. The presence of hydroxyl chain-ends in the HBPE allows the modifier to be linked covalently to the epoxy matrix through the monomer activated propagation mechanism, which occurs in cationic polymerizations. $Yb(OTf)_3$ leads to quicker curing than the lanthanum salt and to materials with the highest glass transition temperature (T_g). The addition of HBPE does not affect adversely the thermal stability and leads to a slight reduction of the global shrinkage. The T_g of the materials, the relaxed modulus and the linear thermal expansion coefficients are practically maintained by the addition of HBPE.

INTRODUCTION

Epoxy resins are among the most widely used materials in the coating of electronic devices. This is because they present good properties in terms of electrical insulation, adhesion to various components and thermal stability. However, they are currently lacking in terms of reworkability, meaning the encapsulated or protected material cannot be recovered to be repaired or recycled.

The concept of reworkability is related to the ability of the material to break-down under controlled conditions in order to remove the coatings from the substrate, but it does not mean that the polymeric material can be reused or recycled. The introduction of labile linkages, thermally cleavable over 200 ºC, has been proposed to facilitate the reworking of the thermosets in which they are chemically incorporated.[1-3] The first studies were mainly based on new cycloaliphatic epoxy resins which contained ester groups,[4] but they usually lead to high crosslinking densities, which worsen the mechanical characteristics.

Our research has been focused on increasing the reworkability of epoxy thermosets. In previous papers[5-7] we reported a new route of introducing ester groups in thermosetting materials by the copolymerization of commercial epoxy resins with lactones via ring-opening mechanism. This strategy presents some advantages such as the possible modulation of the properties of the final materials on changing the characteristics of the epoxy resin and the co-monomer, their feed ratio and the initiator used, but it leads to a decrease of the T_g, caused by the aliphatic structure of the comonomer. As a new strategy, the reworkability of modified epoxy thermosets has also been increased on adding hyperbranched polyesters as modifiers.[8,9]

Usually, hyperbranched polymers have been added to epoxy thermosets to improve toughness.[10,11] Moreover, the addition of these modifiers can reduce the shrinkage during curing by reducing the internal stresses, which in turn affects the durability of the coating and its

protection capability.[8] Taking all these improvements into account, the development of these modifiers can be of a great technological importance.[12]

HBPs have some structural advantages such as a large number of functional groups at the end of the branches and a versatile structure depending on the monomeric units selected in their synthesis. Their branched structure leads to a lack of entanglements, which reduce the melt viscosity. In this way, HBPs can be considered as versatile reactive modifiers to improve epoxy coatings.[13]

Since the thermal degradability of polyester moieties involves a β-elimination process, which implies a pericyclic reaction in which a proton in g-position participates,[14] the absence of protons in this position should prevent the thermal degradation from taking place, as is the case with phenyl esters. However, they can be broken down by saponification in alkaline media. Therefore, the presence of phenyl ester moieties in the hyperbranched polymer can increase the chemical reworkability of the modified thermosets without affecting thermal stability. This can be advantageous in the coating of devices working at high temperatures.

In the present article, we report the effect of adding the hyperbranched polyester (HBPE) represented in **Scheme 1** to DGEBA formulations on the curing process and on the characteristics of the materials prepared.

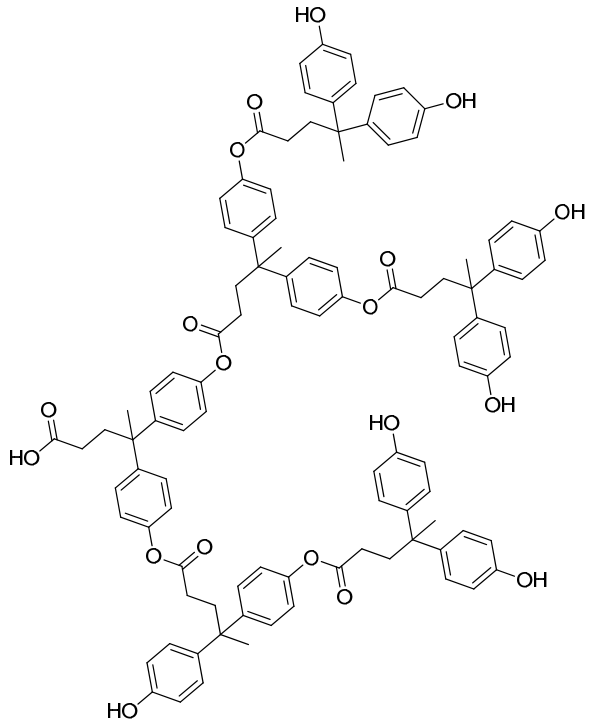

Scheme 1 Idealized chemical structure of HBPE.

The presence of hydroxyl groups at the chain ends in the hyperbranched polymer allows the covalent linkage of this modifier to the epoxy matrix, when lanthanide triflates are used as cationic curing agents. Cationic curing takes place through two propagation mechanisms (activated chain end, ACE, and activated monomer, AM).[15] The occurrence of both mechanisms, represented in **Scheme 2**, influences the kinetics of the process and some characteristics of the

materials, since the AM mechanism leads to chain transfer processes. This mechanism is favoured in the presence of hydroxyl groups. Ytterbium and lanthanum triflates have different Lewis acid characteristics, are stable in humid environments and they are able to act as cationic initiators in the curing of neat epoxy resins and several formulations.[5,6,8,16]

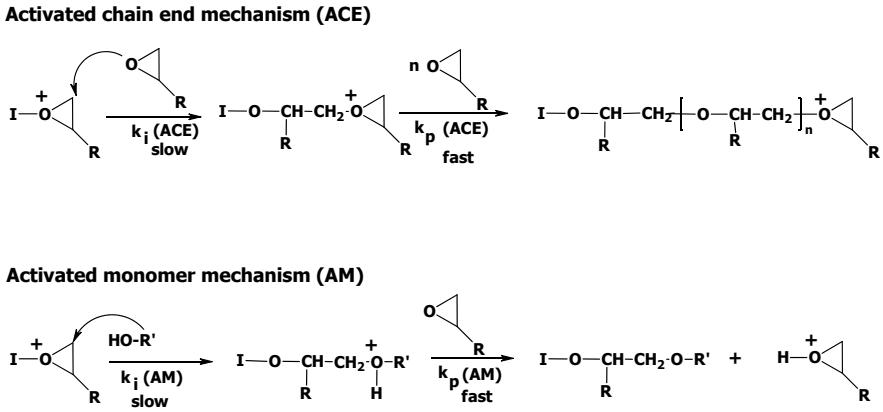

Scheme 2 Propagation mechanisms for the cationic ring opening polymerization of epoxides.

EXPERIMENTAL PART

Materials

4,4'-Bis(4-hydroxyphenyl)valeric acid, N,N'-dicyclohexylcarbodiimide (DCC), methanol and anhydrous N,N-dimethylformamide (DMF), synthesis grade, were purchased from Aldrich or Fluka and used without further purification. 4-(N,N-dimethylamino)pyridinium p-toluenesulfonate (DPTS) was prepared as described in the literature.[17] Diglycidyl ether of Bisphenol A (DGEBA) Epikote Resin 827 was provided by Shell Chemicals with an epoxy equivalent of 182 g/eq and was dried before use. Ytterbium and lanthanum triflates (Aldrich) (99% of purity) were used as received.

Hyperbranched polyester synthesis (HBPE)

The HBPE was synthesized according to a previously described procedure.[18] In a 500 mL two-necked round-bottom flask, 50 g (1 eq) of 4,4-bis(4-hydroxyphenyl) valeric acid and 7.64 g (0.2 eq) of DPTS were dissolved in anhydrous DMF (200 mL). Then, 43.24 g (1.2 eq) of DCC were added in portions and the mixture was kept under argon atmosphere for 24 h at room temperature. Then, the precipitate was filtered off and the solution was poured in methanol (1200 mL) to obtain a white powder after drying in a vacuum oven overnight at 60 ºC. Yield 37 g (conversion: 80%).

The ^{1}H and ^{13}C NMR data are in accordance with those published.[19]

$\bar{M}_n$: 26,000 g/mol, $\bar{M}_w$: 32,000 g/mol.

Sample preparation

All the samples were prepared by mixing the selected proportions of DGEBA and HBPE at 80ºC until a clear solution was obtained. Then, the mixture was allowed to cool down to room temperature and 1 phr (1 part of initiator per 100 parts of the mixture, w/w) of either $Yb(OTf)_3$ or $La(OTf)_3$ was added and mixed thoroughly.

Specimens for density measurements, TGA, DMTA and chemical degradability studies were made in an aluminum mold and cured for 5 hours at 160ºC and 1 hour at 180ºC.

Characterization Techniques

^{1}H NMR and ^{13}C NMR measurements were carried out in sample tubes of 5 mm outer diameter at 500.13 and 125.75 MHz, respectively, using a Bruker DRX 500 NMR spectrometer. DMSO-d_6 was used as a solvent.

Molecular weight and molecular weight distribution was determined by means of a modular build SEC-system coupled with a multi-angle laser light scattering (MALLS) detector DAWN EOS (Wyatt Technologies, USA) and a refractive index (RI) detector (Knauer, Germany) in combination with a PL-GEL 5 μm mixed C column, 300 x 7.5 mm (Polymer Laboratories, UK) using a flow rate of 1 mL/min and THF as eluent.

Calorimetric studies were carried out on a Mettler DSC-821e thermal analyzer in covered Al pans under N_2 at 100 mL/min. The calorimeter was calibrated using an indium standard (heat flow calibration) and an indium-lead-zinc standard (temperature calibration). The samples weighed approximately 7 mg. In the dynamic curing process the degree of conversion by DSC (x_{DSC}) was calculated as follows:

$$x_{DSC} = \frac{\Delta h_T}{\Delta h_{tot}} \quad (1)$$

where Δh_T is the heat released up to a temperature T, obtained by integration of the calorimetric signal up to this temperature, and Δh_{tot} is the total reaction heat associated with the complete conversion of all reactive groups. The kinetic studies were performed at heating rates of 2, 5, 10 and 15 ºC/min in N_2 atmosphere. The precision of the given enthalpies is ± 3%.

The glass transition temperature (T_g) for each material was calculated after a complete dynamic curing, by means of a second scan, as the temperature of the half-way point of the jump in the heat capacity when the material changed from the glassy to the rubbery state. The precision of the determined temperatures is estimated to be ± 1 ºC.

TMA (Mettler TMA40) was used to determine the conversion at the gel point. The samples were supported by two small circular ceramic plates and silanized glass fibers, which were impregnated with the samples. Non-isothermal experiments were performed between 40 and 225 ºC at a heating rate of 5 ºC/min applying a periodic force that change (cycle time = 12s) from 0.0025 to 0.01 N. When the material reaches sufficient mechanical stability (gelation) the TMA measuring probe deforms less the sample and the amplitude of the oscillations is reduced. The gel point was taken in TMA as the temperature at which sudden decrease in the amplitude of the oscillations was observed. The gel conversion, α_{gel}, was determined as the DSC conversion at the temperature gelled in TMA in a non-isothermal experiment.[20]

The linear thermal expansion coefficients in the glassy and rubbery states were measured by thermal mechanical analysis using a Mettler-Toledo TMA40 heating at 10 ºC/min as:

$$\alpha = \frac{1}{L_0}\frac{dL}{dT} = \frac{1}{L_0}\frac{dL/dt}{dT/dt} \quad (2)$$

where, L_o is the initial length.

The global shrinkage was calculated from the densities of the materials before and after curing, which were determined using a Micromeritics AccuPyc 1330 Gas Pycnometer thermostatized at 30 ºC. The densities were measured with a precision of ± 0.001. The precision of the shrinkage calculated values is 0.2%.

Thermogravimetric analyses (TGAs) were carried out in a Mettler TGA/SDTA 851e thermobalance. Pieces of cured sample with an approximate mass of 8 mg were degraded between 30 and 800 ºC at a heating rate of 10 ºC/min in N_2 (100 mL/min measured in normal conditions) in ceramic crucibles.

Chemical degradation was carried out in a solution 1M of KOH in ethanol at reflux temperature. Samples at different saponification times were taken, dried and T_g*s* were measured in a DSC scan from 30 to 200 ºC at 20 ºC/min.

Dynamic mechanical thermal analyses (DMTA) were carried out with a DMTA Rheometrics PL-DMTA MKIII analyser. Single cantilever bending was performed on prismatic rectangular samples (10 × 5 × 1.5 mm^3, approximately). The apparatus operated dynamically at 2 °C/min from 30 to 200 °C at a frequency of 1 Hz.

Kinetic analysis

Integral non-isothermal kinetic analysis was used to determine the kinetic triplet (*A* pre-exponential factor, *E* activation energy and *g(x)* integral function of degree of conversion).

If we accept that the dependence of the rate constant on the temperature follows the Arrhenius equation, non-isothermal kinetic analysis may start with the kinetic equation:

$$\frac{dx}{dt} = \beta \frac{d\alpha}{dT} = Ae^{-\frac{E}{RT}} f(x) \tag{3}$$

where β is the heating rate, *dx/dt* is the rate of conversion, *R* is the universal gas constant, *T* is the temperature and *f (x)* is the differential conversion function.

By integrating eq. (3) and using the Coats-Redfern[21] approximation to resolve the so-called temperature integral and considering that $2RT / E << 1$ the Kissinger-Akahira-Sunose equation (KAS) may be written as:

$$ln\frac{\beta}{T^2} = ln\left[\frac{AR}{g(x)E}\right] - \frac{E}{RT} \tag{4}$$

For each conversion degree, the linear representation of $\ln[\beta / T^2]$ versus T^{-1} enables *E* and $\ln[AR/g(x)E]$ to be determined from the slope and the ordinate in the origin. If the reaction model, *g(x)*, is known, for each conversion the corresponding pre-exponential factor can be calculated for every activation energy.

In this study, we used the reduced master curves procedure of Criado and the Coats-Redfern method to assign a reaction model to the studied systems.[22] By the Coats-Refern method we selected the model which presented the best adjustment and had an activation energy similar to that obtained isoconversionally (considered to be the true). Different kinetic models have been studied: diffusion (D_1, D_2, D_3 and D_4), Avrami-Erofeev (A_2, A_3 and A_4), power law, phase-boundary-controlled reaction (R_2 and R_3), autocatalytic (n+m = 2 and 3) and order n (n = 1, 1.5, 2 and 3). The rate constant, *k*, was calculated with *E* and *A* determined at conversion of 0.5, using the Arrhenius equation.

RESULTS AND DISCUSSION

The use of HBPE as a multifunctional cross linker in the chemical modification of cycloaliphatic epoxy resins photo-cured with triphenylsulfonium hexafluoroantimonate was previously reported.[23] The presence of HBPE increased the curing rate and even the conversion of epoxide groups. The characteristics of the thermosets were also influenced: densities, impact resistance and thermal stability increased but the T_g*s* decreased. However, the used initiator,

the characteristics of the resin and the polymerization procedure can lead to different results. Thus, it seemed interesting to study the cationic thermal curing of DGEBA/HBPE mixtures, with different percentages of HBPE, and the characteristics of the materials obtained. The use of lanthanide triflates as initiators on adding hydroxyl-terminated HBPs to epoxy resins has also been reported only rarely.[8]

Calorimetric studies

The influence of the addition of different amounts of HBPE to DGEBA, initiated by ytterbium or lanthanum triflate, on the curing process was studied by means of DSC. Because of the cationic mechanism adopted in the curing, phenolic groups of the hyperbranched polyester (**Scheme 1**) should react and influence the kinetics of the system, favouring the AM mechanism. When the curing was initiated by $Yb(OTf)_3$ two maxima in the calorimetric curves, registered at 2 °C/min, can be distinguished (**Figure 1**). The peak at low temperature seems to increase on increasing the percentage of hydroxyl groups in the formulation and thus, it could be associated to the propagation taking place by AM mechanism (see **Scheme 2**). In contrast, calorimetric curves of the formulations initiated by $La(OTf)_3$ showed an unimodal shape. In previous calorimetric studies on the copolymerization of DGEBA and lactones, the appearance of a shoulder in the calorimetric curves was also observed. This was more evident when the Lewis acidity increased (from La to Yb)[24,25] Thus, Lewis acidity favours the AM mechanism in this curing process[26] and therefore the covalent linkage of HBPE to the epoxy matrix is more pronounced when using $Yb(OTf)_3$ as the initiator.

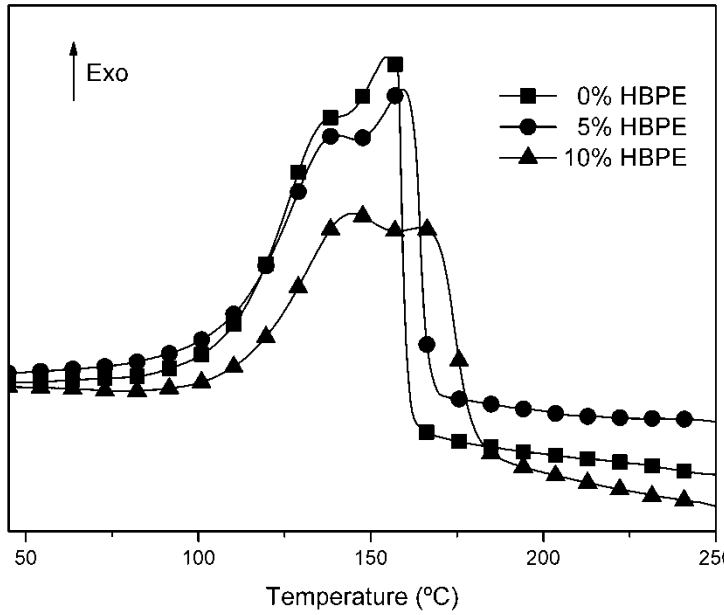

Figure 1 DSC scans recorded at 2 °C/min for the samples of DGEBA containing 0, 5 and 10% of HBPE cured with 1 phr of $Yb(OTf)_3$.

Figure 2 shows the dependence of the activation energy against the degree of conversion, a, between 0.15 and 0.90 for all curing experiments. In the curves, it can be observed that the activation energy remains practically constant in the studied range and the value of $x = 0.5$ has been taken to study the kinetic process.

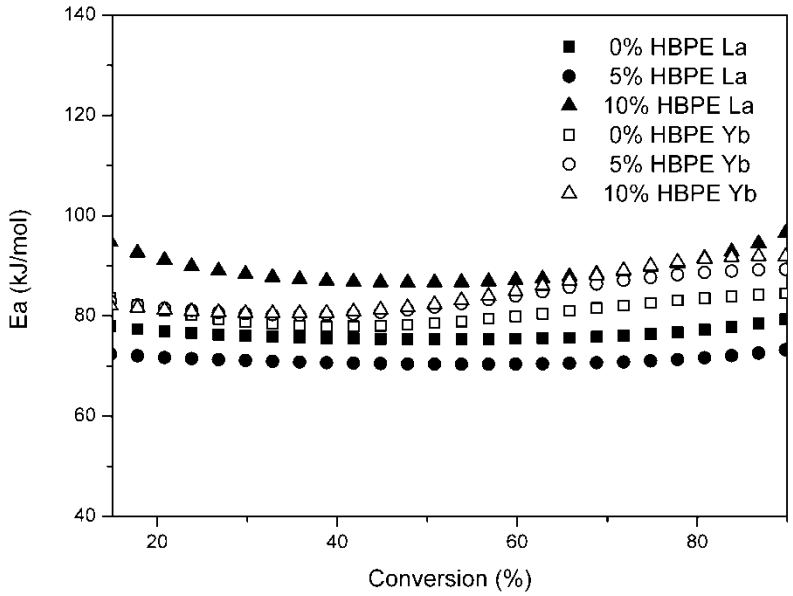

Figure 2 Conversion against activation energy plot for samples of DGEBA with 0, 5 and 10% of HBPE cured with 1 phr of $Yb(OTf)_3$ or $La(OTf)_3$.

In **Table 1** the calorimetric data as well as the kinetic parameters for all the studied formulations are collected. One can see that there is no significant influence on the temperature of the exotherms with the addition of HBPE. However, it is clear that $Yb(OTf)_3$ accelerates the reaction more than $La(OTf)_3$, due to its higher Lewis acidity. This observation is confirmed by calculating the kinetic parameters for these systems using the R_3 theoretical kinetic model, which is the one that fits best with the experimental data and activation energy values. It is apparent that the rate constant is increased when using $Yb(OTf)_3$ and that it is slightly reduced on increasing the proportion of HBPE at 180 °C. This behaviour can be clearly observed in the conversion against temperature curves (**Figure 3**).

Table 1 Calorimetric data and kinetic parameters for the curing of the several DGEBA/HBPE mixtures with 1 phr of the lanthanide triflate selected.

% HBPE	Init.	T_{onset} [a] (°C)	T_{max} [b] (°C)	Δh [c] (J/g)	Δh [c] (kJ/eq)	T_g [d] (°C)	E_a [e] (kJ/mol)	lnA [f] (s^{-1})	k x 10^3 [g] (s^{-1})
0	Yb	132	177	511	93	132	79	16.08	3.27
5	Yb	131	181	480	92	135	82	15.79	2.82
10	Yb	132	181	455	91	138	82	15.64	2.08
0	La	146	188	515	94	118	75	13.60	1.65
5	La	141	190	480	92	111	70	12.11	1.39
10	La	137	194	460	93	115	87	16.38	1.31

a. Onset temperature of the curing exotherm registered at 10 °C/min.
b. Temperature of the maximum of the curing exotherm registered at 10 °C/min.
c. Enthalpy of the curing exotherm registered at 10 °C/min.
d. T_g determined after curing in a dynamic scan registered at 20 °C/min.
e. Values of activation energy at 50% of conversion, evaluated by the isoconversional non-isothermal procedure.
f. Pre-exponential factor for the R_3 kinetic model with $g(x) = [1-(1-x)^{1/3}]$.
g. Values of rate constant at 180 °C using the Arrhenius equation at a conversion of 50%.

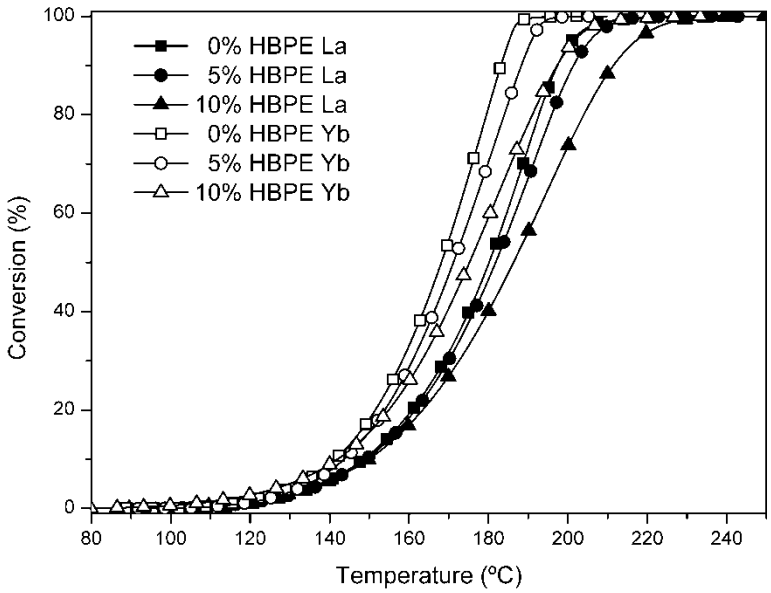

Figure 3 Plot of conversion against temperature for the curing of DGEBA samples containing 0, 5 and 10% of HBPE cured with 1 phr of $Yb(OTf)_3$ or $La(OTf)_3$.

The values of enthalpy released per epoxy equivalent, collected in **Table 1**, confirm that the achieved degree of curing is similar for all the formulations and almost complete,[27] although the addition of HBPE reduces the heat released per gram of the reactive mixture.

Several authors reported that the addition of hyperbranched polymers reduced the T_g of the modified thermosets, but they mainly used hyperbranched polymers with aliphatic moieties.[10,11,28,29] In the present study, the aromatic structure and the covalent linkage of phenolic groups to the epoxy matrix help the T_g of the materials to be practically maintained. As can be seen, the T_g of the $Yb(OTf)_3$ initiated materials is the highest and slightly decreases on adding HBPE, regardless of the proportion. Similar results were observed in a previous study using HBPE/cycloaliphatic epoxides in photo-curing processes.[23] As mentioned before, the AM mechanism seems to be more important for the ytterbium initiator and therefore when $La(OTf)_3$ is used, the HBPE is tethered less to the epoxy matrix, thus T_g is reduced.

As the curing was faster and the T_g of the resulting materials higher when using $Yb(OTf)_3$ we decided to continue the study with the materials obtained with this initiator.

Thermal stability

Some additives used to improve the properties of epoxy resins compromise their good thermal stability. Usually, the introduction of ester groups in the network also decreases it, but as shown in **Table 2**, the addition of the HBPE does not diminish the initial decomposition temperature of these materials. Moreover, the temperature of the maximum degradation rate does not decrease but rather increases slightly and only one degradation process can be observed, as shown in **Figure 4**. The rupture of ester groups usually appears as a small peak at lower temperatures. The high thermal stability can be rationalized on the aromatic structure of the moiety directly linked to the ester group, which prevents the β-elimination reaction to take place,[14] which is the responsible process of the thermal degradation.[5-7] Moreover, the addition of the hyperbranched polymer increases the crosslinking density of the resulting thermosets and therefore the elimination of volatiles becomes more hindered.

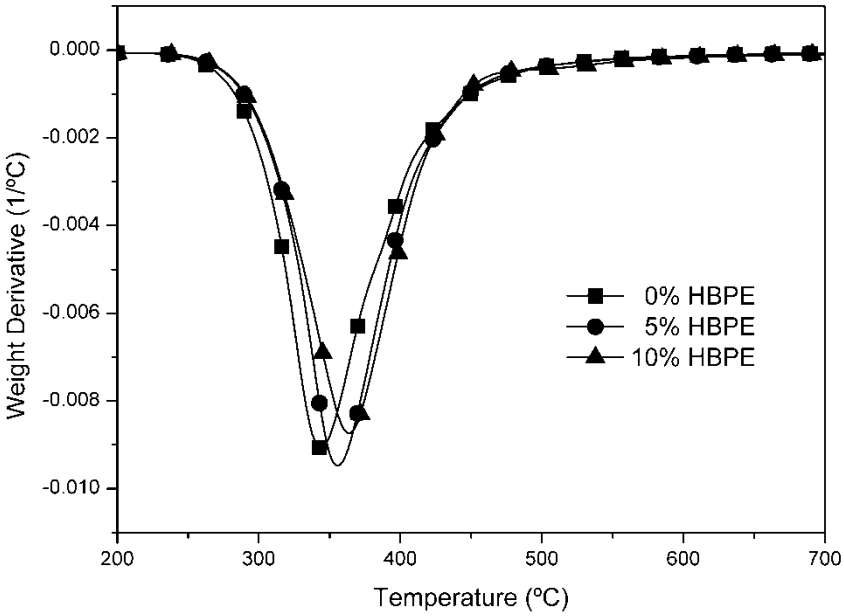

Figure 4 TGA derivative curves for the materials obtained from DGEBA and 0, 5 and 10% of HBPE cured with 1 phr of $Yb(OTf)_3$.

Table 2 Thermogravimetric and thermomechanical data and thermal expansion coefficients measured for the materials obtained from several DGEBA/HBPE mixtures with 1 phr of $Yb(OTf)_3$.

% HBPE	T_{onset} [a] (ºC)	T_{max} [b] (ºC)	Char Yield (%) [c]	α_{gel}	$TEC_{glass} \times 10^6$ (K^{-1})	$TEC_{rubber} \times 10^6$ (K^{-1})	*tan δ* (ºC)	*E'* (MPa)
0	301	344	16	0.33	36	170	150	19.5
5	304	355	16	0.29	40	190	141	20.0
10	304	364	18	0.31	31	174	145	19.8

a. Temperature of the 5% mass loss.
b. Temperature of the peak of the derivative of the thermogram.
c. Measured after a dynamic scan up to 800 ºC.

Chemical degradability

In the literature, there are a lot of contributions devoted to the thermally reworkable thermosets, but only few of them approach the chemically reworkability. Ketal groups are readily cleavable in acidic medium and stable in alkali. Buchwalter *et al.*[30] prepared cycloaliphatic epoxy resins with ketal groups in their structure. These resins were crosslinked by anhydrides and tertiary amines as curing agents and they were reported as chemically reworkable, because they could be degraded by treating them with acetic or phosphoric solutions, but no data on their thermal stability were given.

Ester groups are easy to hydrolyze in both acidic and alkaline conditions and therefore their introduction in epoxy thermosets is a promising way to facilitate the elimination of a coating once its lifetime is over. In some of our previous articles[7,31] new chemically reworkable epoxy thermosets were described. They were prepared by anionic ring-opening copolymerization of stoichiometric mixtures of DGEBA and bis-lactones, since under these conditions an alternating copolymerization occurred and two ester groups were introduced in the network for each bis-

lactone. These thermosets were completely soluble in 1 M ethanolic KOH, but the T_gs were lower than 90 ºC and a decrease in the thermal stability was also observed.

Taken into account these results, we decided to explore the modification of DGEBA with HBPE to solve these limitations. Thus, we evaluated the chemical degradability of the thermosets obtained by treating them with a 1M KOH ethanolic solution under reflux and we followed the degradation process monitoring the T_g of the thermosets. **Table 3** shows the T_gs obtained by DSC in a dynamic scan from 30 to 200 ºC at 20 ºC/min after different saponification times. In neat DGEBA thermosets, after 3 days of reaction still a T_g of 73 ºC was observed. On the contrary, with just a 5% of HBPE in the material, no T_g above room temperature could be detected after less than one day. Moreover, the thermoset ends up being very brittle after this treatment and it is easy to turn it into a powder and therefore to eliminate it from a substrate by brushing. With 10 wt% of HBPE in the formulation the process is even faster and around 10 h are enough to get complete degradation of the coating. **Figure 5** shows the appearance of the materials before and after treatment with 1 M ethanolic KOH under reflux for 10 h. As can be seen, only the material containing HBPE shows an evident degradation to powder.

Table 3 T_gs in ºC of the initial and partially degraded materials subjected to treatment with 1M KOH ethanolic solution for several hours under reflux. The initial materials were obtained by isothermal curing of DGEBA/HBPE formulations with 1 phr of $Yb(OTf)_3$ as initiator.

% HBPE	Saponification time (hours)									
	0	1	3	5	7	12	16	20	48	76
0	148	147	145	140	131	105	95	89	76	73
5	139	136	132	123	85	73	58	-	-	-
10	139	134	114	99	67	-	-	-	-	-

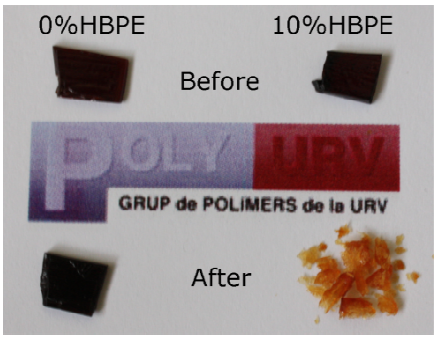

Figure 5 Appearance of the DGEBA and DGEBA/10% HBPE materials before and after treatment with 1M ethanolic KOH under reflux for 10 h.

Thermomechanical Analysis

By TMA in the dynamic oscillatory mode, the conversion at the gel point was determined by curing the formulations in this device as described elsewhere.[20] **Figure 6** shows the calculation method for the sample containing a 5% of HBPE at 5 ºC/min. The materials were cured dynamically in the TMA and DSC and the derivative curves length-T and a-T were overlapped. When the material was observed to gel in the TMA, by a reduction of the amplitude of about

95%, the calorimetric conversion was determined. In **Figure 6** we can see that the critical conversion of gel formation in the formulation with 5 wt% HBPE is calculated to be α = 0.29. **Table 2** collects the conversion at the gelation on adding different proportions of HBPE. As can be seen, the conversion at gelation is practically not influenced by the addition of HBPE. This behaviour differs from the observation made in a previous study[8] in which a hyperbranched aliphatic polyester (Boltorn H30) was used instead of HBPE and the conversion steadily increased. This fact seems to indicate that the low content of hydroxyl groups in HBPE in reference to the epoxides, three times less than in the case of Boltorn H30, reduces the possibility of chemical reaction of HBPE, which affects the gelation process. This can also explain the weak effect observed in the kinetics of the curing process on the addition of HBPE.

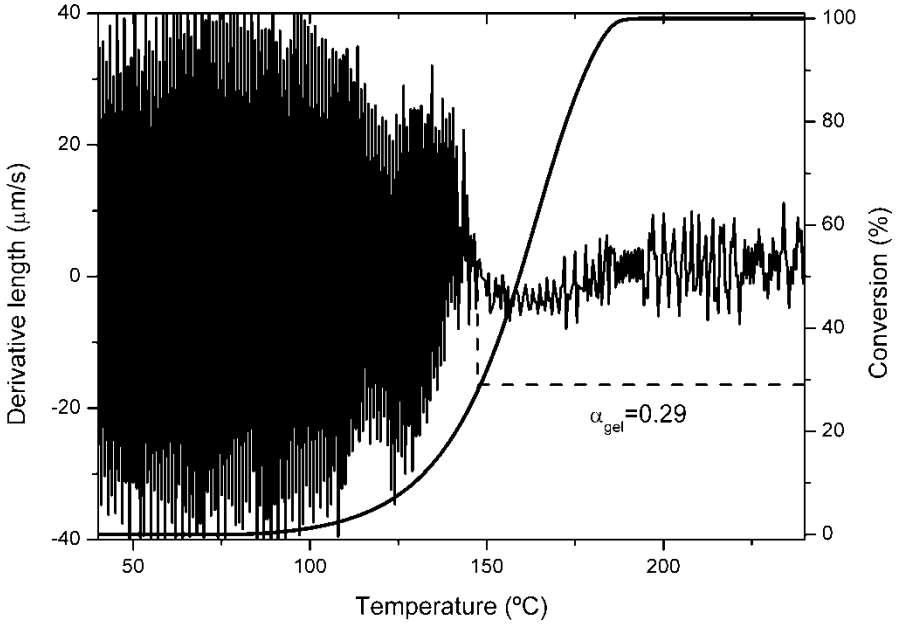

Figure 6 Determination of the gel point by combining DSC and TMA.

TMA also allowed us to measure thermal expansion coefficients, which are also collected in **Table 2**. It should be mentioned that the values of TECs in the glassy and rubbery states are lower than those measured in a previous work.[9] In that study, performed with DGEBA/poly(esteramide) HBP/anhydride systems, values of about 60 and 200 $^{o}C^{-1}$, respectively, were obtained. The lower TECs of the present study account for a higher crosslinking density and a stiffer network. From the values of the table, we can see that the addition of 5 wt% of HBPE slightly increases TECs in the glassy and rubbery state but a further addition of HBPE has no effect. Usually, the modification of epoxy resins with polymer increases this coefficient, whereas in the present case the aromatic nature and the functionality of the HBPE do not lead to a detrimental increase.

Figures 7 and **8** show the plots of *tan* δ and *log E'* against temperature determined by DMTA. The corresponding parameters are collected in **Table 2**. *Tan* δ values are shifted to lower temperatures on adding HBPE, but no relationship between the values and the added proportion of HBPE is found. In addition, the shape of the curves indicates a homogeneous character of the materials. It should be noticed that the small shift of the *tan* δ value is not accompanied by a drop of the relaxed modulus. In our previous study with Boltorn H30,[8] we

could observe a broadening of the tan d curves and a drop of the modulus on increasing the HBP proportion. Thus, the more stiff structure of the HBPE in comparison to the aliphatic Boltorn H30 leads to the maintenance of the storage modulus and the temperature of relaxation.

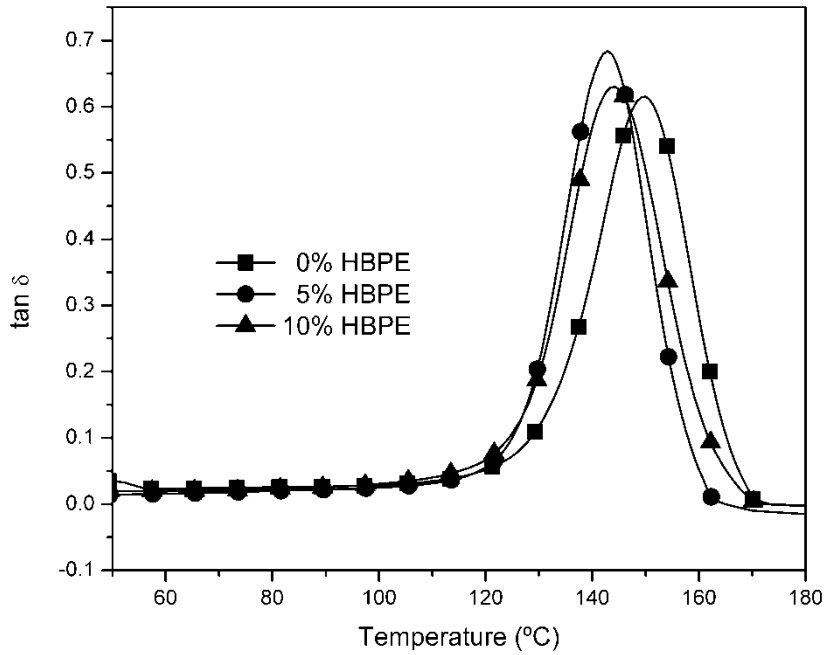

Figure 7 Plot of *tan δ* against temperature for the materials obtained from DGEBA and 0, 5 and 10% of HBPE cured with 1 phr of $Yb(OTf)_3$.

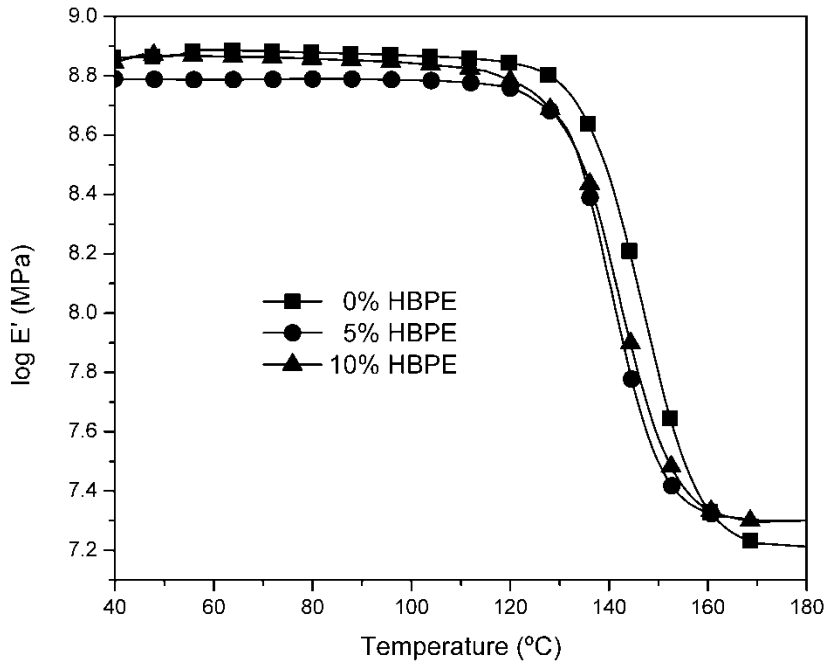

Figure 8 Plot of storage modulus against temperature for the materials obtained from DGEBA and 0, 5 and 10% of HBPE cured with 1 phr of $Yb(OTf)_3$.

Shrinkage

A very important drawback of thermosetting materials used as coatings is the shrinkage they exhibit in their curing process. This shrinkage can cause the formation of bubbles and cracks and the loss of adhesion between the coating and the surface and therefore it is essential to minimize it. In some cases hyperbranched polymers have proved to reduce this shrinkage[8,9] but some other authors described the contrary effect.[32] By looking at the values given in **Table 4** it is apparent that the addition of HBPE slightly decreases the shrinkage going from 3.2% in the case of the neat epoxy resin sample to 2.2% for the material with a 10% of HBPE. One possible explanation for this observation could be that when the reaction takes place the HBP undergoes an expansion as their hydroxyl groups react, as it was reported previously.[33] This reduction of the shrinkage is less evident than that measured when Boltorn H30 was used as modifier,[8] but the lower hydroxyl content and the more rigid structure of HBPE can account for these differences.

Table 4 Densities measured before and after curing of several DGEBA/HBPE mixtures with 1phr of ytterbium triflate and the shrinkage calculated.

% HBPE	ρ_{mon} (g/cm^3)	ρ_{polvm} (g/cm^3)	Shrinkage [a] (%)
0	1.140	1.178	3.2
5	1.139	1.168	2.5
10	1.146	1.172	2.2

a. Calculated as $[(\rho_{polym} - \rho_{mon})/\rho_{polym}] \times 100$.

CONCLUSIONS

It could be shown that the addition of aliphatic-aromatic hyperbranched polyesters (HBPE) as reactive additives to cationic thermally cured DGEBA based epoxy resins results in several advantages. Thus, the addition of HBPE to the epoxy formulation slightly reduces the curing rate at a selected temperature. The use of $Yb(OTf)_3$ as initiator in the curing of DGEBA/HBPE formulations leads to highest curing rates and to higher T_gs in comparison to $La(OTf)_3$ initiated formulations. The presence of hydroxyl chain-ends in the HBPE allows the modifier to be covalently linked through the monomer activated propagation mechanism, which occurs in cationic ring-opening polymerizations. This mechanism is more pronounced in the ytterbium triflate initiated curing systems.

The thermal stability of the modified thermosets is not compromised by the addition of HBPE, but the chemical reworkability of these materials in alkaline solutions is highly enhanced.

The addition of HBPE to DGEBA formulations leads to a slight reduction of the global shrinkage during curing, which can reduce the formation of internal stresses. The TECs and thermo mechanical characteristics of the materials do not change significantly on adding HBPE to the formulation.

ACKNOWLEDGEMENTS

The authors from the Universitat Rovira i Virgili and from Universitat Politècnica de Catalunya would like to thank MICINN (Ministerio de Ciencia e Innovación) and FEDER (Fondo Europeo de Desarrollo Regional) (MAT2008-06284-C03-01 and MAT2008-06284-C03-02), All authors would like to thank the Germany-Spanish DAAD collaboration program (HA2007-0022) for their financial support. D.F. acknowledges the grant FPU-2008 from the Spanish Government.

REFERENCES

1. L. Wang, H. Li, C. P. Wong. J*. Polym. Sci. Part A: Polym. Chem.* **2000,** *38,* 3771.
2. H. Li, C. P. Wong. *IEEE Trans Adv Packaging* **2004,** *27,* 165.
3. J-S. Chen, C. K. Ober, M. D. Poliks, Y. Zhang, U. Wiesner, C. Cohen. *Polymer* **2004,** *45,* 1939.
4. S. Yang, J. S C. hen, H. Körner, T. Breiner, C. K. Ober, M. D. Poliks. *Chem. Mater.* **1998,** *10,* 1475.
5. L. González, X. Ramis, J. M. Salla, A. Mantecón, A. Serra. *Polym. Degrad.. Stab.* **2007,** *92,* 596.
6. M. Arasa, X. Ramis, J. M. Salla, A. Mantecón, A. Serra. *Polym. Degrad. Stab.* **2007,** *92,* 2214.
7. X. Fernández-Francos, J. M. Salla, A. Mantecón, A. Serra, X. Ramis. *Polym. Degrad. Stab.* **2008,** *93,* 760.
8. X. Fernández-Francos, J. M. Salla, A. Cadenato, J. M. Morancho, A. Serra, A. Mantecón, X. Ramis. *J. Appl. Polym. Sci.* **2009,** *111,* 2822.
9. M. Morell, X. Ramis, F. Ferrando, Y. Yu, A. Serra. *Polymer* **2009,** *50,* 5374.
10. R. J. Varley, W. Tian. *Polym. Int.* **2004,** *53,* 69.
11. D. Zhang, D. Jia. *J. Appl. Polym. Sci.* **2006,** *101,* 2504.
12. (a) B. Voit. *J. Polym. Sci. Part A: Polym. Chem.* **2005,** *43,* 2679; (b) C. Gao, D. Yan. *Prog. Polym. Sci.* **2004,** *29,* 183.
13. L. Boogh, B. Pettersson, J. A. E. Månson. *Polymer* **1999,** *40,* 2249.
14. P. Sivasamy, M. Palaniandavar, C. T. Vijayakumar, K. Ledered. *Polym. Degrad. Stab.* **1992,** *38,* 15.
15. P. Kubisa, S. Penczek. *Prog. Polym. Sci.* **1999,** *24,* 1409.
16. P. Castell, M. Galià, A. Serra, J. M. Salla, X. Ramis. *Polymer* **2000,** *41,* 8465.
17. J. S. Moore, S. I. Stupp. *Macromolecules* **1990,** *23,* 65.
18. F. Schallausky, M. Erber, H. Komber, A. Lederer. *Macromol. Chem. Phys.* **2008,** *209,* 2331.
19. D. Schmaljohann, H. Komber, B. Voit. *Acta Polym.* **1999,** *50,* 196.
20. S. González, X. Fernández-Francos, J. M. Salla, A. Serra, A. Mantecón, X. Ramis. *J. Appl. Polym. Sci.* **2007,** *104,* 3406.
21. A. W. Coats, J. P. Redfern. *Nature* **1964,** *201,* 68.
22. X. Ramis, J. M. Salla, A. Cadenato, J. M. Morancho. *J. Therm. Anal. Cal.* **2003,** *72,* 707.
23. M. Sangermano, A. Priola, G. Malucelli, R. Bongiovanni, A. Quaglia, B. Voit, A. Ziemer. *Macromol. Mater. Eng.* **2004,** *289,* 442.
24. C. Mas, A. Mantecón, A. Serra, X. Ramis, J. M. Salla. *J. Polym. Sci. Part A: Polym. Chem.* **2004,** *42,* 3782.
25. L. González, X. Ramis, J. M. Salla, A. Serra, A. Mantecón. *Eur. Polym. J.* **2008,** *44,* 1537.
26. L. Matejka, K. Dusek, P. Chabanne, J. P. Pascault. *J. Polym. Sci. Part A: Polym. Chem.* **1997,** *35,* 665.
27. J. Brandrup, E. H. Immergut, E. A. Grulke. *Polymer Handbook*, 4th ed. Wiley-Interscience, New York, **1999**.
28. G. Cicala, G. Recca, C. Restuccia. *Polym. Eng. Sci.* **2005,** *45,* 225.
29. G. Cicala, G. Recca. *Polym. Eng. Sci.* **2008,** *48,* 2382.
30. S. L. Buchwalter, L. L. Kosbar. *J. Polym. Sci. Part A: Polym. Chem.* **1996,** *34,* 249.
31. M. Arasa, X. Ramis, J. M. Salla, A. Mantecón, A. Serra. *Polymer* **2009,** *50,* 2228.
32. M. Sangermano, G. Malucelli, R. Bongiovanni, A. Priola, A. Harden. *Polym. Int.* **2005,** *54,* 917.
33. A. Lederer, M. Abd Elrehim, F. Schallausky, D. Voigt, B. Voit. *e-Polymers* **2006,** *039,* 1.

4.3 The effect of the degree of branching in hyperbranched polyesters used as reactive modifiers in epoxy thermosets

D. Foix[1], A. Khalyavina[2], M. Morell[1], B. Voit[2], A. Lederer[2], X. Ramis[3], A. Serra[1]

[1] Department of Analytical and Organic Chemistry, University Rovira i Virgili, Marcel.li Domingo s/n, 43007 Tarragona, Spain

[2] Leibniz-Institute of Polymer Research Dresden, Hohe Str. 6, 01069 Dresden, Germany

[3] Laboratory of Thermodynamics, ETSEIB, University Politècnica de Catalunya, Av. Diagonal 647, 08028 Barcelona, Spain

ABSTRACT

The effect of the degree of branching (DB) of a hyperbranched polyester (GBPEX) added as modifier of new thermosets obtained from diglycidylether of bisphenol A has been studied. The use of ytterbium triflate as cationic initiator allows the hydroxyl chain-ends in the GBPEX to become covalently linked to the matrix through the monomer activated propagation mechanism. The curing process has been studied by DSC and rheology. The DB of the modifier does not affect appreciably the thermal stability and the chemical reworkability but shrinkage exhibits a significant reduction on increasing the DB. Thermomechanical characteristics are also improved with increasing the DB of the modifier.

INTRODUCTION

Epoxy resins have a wide acceptance as coatings because of their good characteristics and outstanding formulation versatility. However, the technological application of epoxy thermosets sometimes requires the addition of several additives to improve their properties. In the last years, hyperbranched polymers (HBPs) have been used as reactive modifiers to improve mechanical characteristics of epoxy thermosets.[1-3] The special architecture of the HBPs presents some advantages in comparison to linear polymers: a) their higher reactivity by the presence of a great number of terminal groups and b) the lower entanglement caused by the branching that reduces the viscosity of the mixtures before curing.[4]

Epoxy resins can be cured by stoichiometric curing agents, such as primary amines, anhydrides and isocyanates but also by initiators in catalytic proportions.[5] The use of initiators allows influencing the kinetics of curing and seems to be easier from the point of view of the technological application. However, the reaction mechanism by ring-opening of epoxides leads to a highly compact polyether structure, which usually presents high fragility and brittleness as a drawback. The use of reactive HBPs added to the curing mixture can lead to improvements in toughness and flexibility as well as to other beneficial effects that improve the performance of this type of epoxy coatings.

The use of HBPs can not only improve the mechanical characteristics but also can reduce the shrinkage on curing, as we reported previously.[6,7] When epoxy resins are applied as coatings and adhesives in electrical or electronic devices they show good electrical insulating properties but shrinkage can reduce their durability. This is because of the appearance of stresses that leads to the loss of adhesion and to the formation of voids and cracks allowing corrosion to take place. Moreover, epoxy thermosets cannot be easily eliminated from the coated substrates because of their high chemical and thermal stability, this is they lack in reworkability. This concept is related to the ability of the material to break-down under controlled conditions in order to remove the coatings from the substrate, but it does not mean that the polymeric material can be reused or recycled. To improve the reworkability of epoxy thermosets

ester groups are usually introduced in the network structure. Most of the researchers in this field introduce ester groups in the monomer unit and there are a number of epoxycycloaliphatic structures that lead to reworkable materials thermally degradable at temperatures in the range 200-250 ºC.[8,9] This fact could be a problem in applications in which high thermal stability of the thermoset is required. In a previous paper, we reported the use of a hyperbranched polyester with aromatic ester groups as an alternative to produce chemically reworkable thermosets with high thermal stability.[10]

Although there is some literature on the differences observed by using linear or hyperbranched polymers with similar structure as modifiers in epoxy thermosets,[11] to the best of our knowledge the effect of the degree of branching (DB) of HBPs has not been reported until now. In the present article, we report how the degree of branching of the above mentioned polyesters influences the evolution of the curing process and the characteristics of the thermosets prepared from it.

By polycondensation of AB_2 monomer (4,4-bis(4'-hydroxyphenyl)valeric acid) alone or with AB (3-(4-hydroxyphenyl)propionic acid) in different proportions three HBPs (GBPE50, GBPE40 and GBPE30) with different degrees of branching were synthesized. The structure of these modifiers is represented in **Scheme 1**. These polymers were mixed with DGEBA in different proportions and cured using ytterbium triflate as a cationic initiator. The presence of phenolic hydroxyl groups at the chain ends of the HBPs allows the covalent linkage of these modifiers to the epoxy network, when ytterbium triflate is used as curing agent. Cationic curing takes place through two propagation mechanisms: activated chain end (ACE) and activated monomer (AM).[12] AM mechanism implies hydroxyl groups and therefore their different proportions in the GBPEX structures can influence the curing process because they lead to chain transfer processes. UV initiated cationic curing of epoxy resins with this type of HBP polyesters have been previously reported and the concurrence among these mechanisms studied.[13,14]

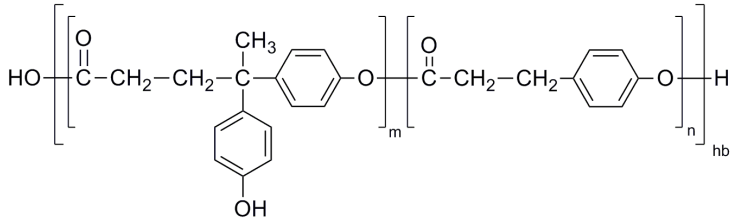

Scheme 1 Schematic structure of the hyperbranched polyesters (GBPEX).

The curing was studied by differential scanning calorimetry (DSC) and rheology and the characteristics of the materials were evaluated by thermogravimetry (TGA), densitometry, thermomechanical analysis (DMTA) and their chemical degradability was tested by saponification tests with 1M ethanolic KOH.

EXPERIMENTAL PART

Materials

4,4-Bis(4-hydroxyphenyl)valeric acid, 3-(4-hydroxyphenyl) propionic acid, N,N'-dicyclohexylcarbodiimide (DCC), methanol and anhydrous N,N-dimethylformamide (DMF), synthesis grade, were purchased from Aldrich or Fluka and used without further purification. 4-(N,N-dimethylamino)pyridinium p-toluenesulfonate (DPTS) was prepared as described in the literature.[15] Diglycidyl ether of Bisphenol A (DGEBA) Epikote Resin 827 was provided by Shell

Chemicals with an epoxy equivalent of 182 g/eq and was dried before use. Ytterbium triflate (Aldrich) (99% of purity) was used as received.

*Polycondensation of AB_2-Monomer (GBPE50) (**Scheme 1**)*

The hyperbranched homopolymer was synthesized according to a previously described procedure.[16] In a 500 mL two-necked round-bottom flask, 50 g (1 eq) of 4,4-bis(4-hydroxyphenyl) valeric acid and 7.64 g (0.2 eq) of DPTS were dissolved in anhydrous DMF (200 mL). Then, 43.24 g (1.2 eq) of DCC were added in portions and the mixture was kept under argon atmosphere for 24 hours at room temperature. Then, the precipitate was filtered off and the solution was poured in methanol (1200 mL) to obtain a white powder after drying in a vacuum oven overnight at 60 °C. Yield 37 g (conversion: 80%).

The ^{1}H and ^{13}C NMR data are in accordance with those published.[17]

$\overline{M}_n$: 26,000 g/mol, $\overline{M}_w$: 32,000 g/mol.

*Copolycondensation of the AB- and AB_2-monomers (GBPEX) (**Scheme 1**)*

For the synthesis of the copolyesters with a degree of branching X, we used the procedure previously described.[16] According to the desired AB2/AB-ratio in the copolyester, 4,4-bis(4-hydroxyphenyl)valeric acid (AB2-monomer), 3-(4-hydroxyphenyl) propionic acid (AB-monomer) and DPTS were dissolved in 15 mL dry DMF. After 30 min, DCC was added and stirred at room temperature for a further 40 hours. The purification was made by precipitation two times in excess of methanol.

The ^{1}H and ^{13}C NMR data are in accordance with those published.[16]

GBPE30 (AB/AB_2-ratio = 3.76) has a DB_{Frey} = 28 ± 3% (determined by ^{13}C-NMR spectroscopy).

$\overline{M}_w$ = 57,800 g/mol, $\overline{M}_n$ = 15,200 g/mol and molecular weight dispersity of 3.8 by SEC in DMAc/LiCl; $R_{found} = X_{AB}/X_{AB2}$ = 3.76.

$\overline{DP}$ = 18 and therefore 18 OH groups in average per polymer molecule.

GBPE40 (AB/AB_2-ratio = 1.74) has a DB_{Frey} = 39 ± 2% (determined by ^{13}C-NMR spectroscopy).

$\overline{M}_w$ = 29,600 g/mol, $\overline{M}_n$ = 12,600 g/mol and molecular weight dispersity of 2.3 by SEC in THF $R_{found} = X_{AB}/X_{AB2}$ = 1.74.

$\overline{DP}$ = 23 and therefore 23 OH groups in average per polymer molecule.

Sample preparation

All samples were prepared by mixing the selected proportions of DGEBA and the hyperbranched polymer at 80 °C until a clear solution was obtained. Then, the mixture was allowed to cool down to room temperature and 1 phr (1 part of initiator per 100 parts of the mixture, w/w) of $Yb(OTf)_3$ was added and mixed thoroughly.

Specimens for density measurements, TGA, DMTA and chemical degradability studies were prepared in an aluminum mould and cured for 5 hours at 160 °C and 1 hour at 180 °C.

Characterization Techniques

^{1}H NMR and ^{13}C NMR measurements were carried out in sample tubes of 5 mm outer diameter at 500.13 and 125.75 MHz, respectively, using a Bruker DRX 500 NMR spectrometer. DMSO-d_6 was used as a solvent.

The determination of molar mass and molar mass distributions was carried out on a modular build SEC-system of analytical pump (Agilent Tech. Series 1200, USA), light scattering (λ= 632 nm) detector (Dawn Tristar or Dawn EOS from Wyatt Tech., USA) and a RI detector (Knauer, Germany) in combination with a Polar Gel 5 mm mixed C column (Polymer Labs, UK) using a flow-rate of 1 mL/min. As eluent were used N,N-dimethyl acetamide (DMAc) with LiCl (3 g/L) or tetrahydrofurane (THF).

Calorimetric studies were carried out on a Mettler DSC-821e thermal analyzer in covered Al pans under N_2 at 100 mL/min. The calorimeter was calibrated using an indium standard (heat flow calibration) and an indium-lead-zinc standard (temperature calibration). The samples weighed approximately 7 mg. In the dynamic curing process the degree of conversion by DSC (x_{DSC}) was calculated as follows:

$$x_{DSC} = \frac{\Delta h_T}{\Delta h_{tot}} \quad (1)$$

where Δh_T is the heat released up to a temperature T, obtained by integration of the calorimetric signal up to this temperature, and Δh_{tot} is the total reaction heat associated with the complete conversion of all reactive groups. The kinetic studies were performed at heating rates of 2, 5, 10 and 15 °C/min in N_2 atmosphere. The precision of the given enthalpies is ± 3%.

The glass transition temperature (T_g) for each material was calculated after a complete dynamic curing, by means of a second scan, as the temperature of the half-way point of the jump in the heat capacity when the material changed from the glassy to the rubbery state. The precision of the determined temperatures is estimated to be 1 °C.

Rheological measurements were carried out in the parallel plates (geometry of 25 mm) mode with an ARG2 rheometer (TA Instruments, UK, equipped with a Peltier system). Experiments were performed isothermally at 110 °C. Because the viscosity of the system changes significantly during the curing process, a control program was used in which the oscillation amplitude diminishes with an increase in the applied stress. By doing so, the cure can be characterized in the whole range of conversion. Gel time was taken as the point where tan δ is independent of frequency.[18] The conversion at the gelation (α_{gel}) was determined by stopping the rheology experiment at gelation and performing a subsequent dynamic DSC scan at 10 °C/min of the gelled sample.

Complex viscosity (η*) of the mixtures without initiator were recorded as function of angular frequency (0.6-10 rad/s) stating a constant deformation of 50% at 110 °C.

The global shrinkage was calculated from the densities of the materials before and after curing, which were determined using a Micromeritics AccuPyc 1330 Gas Pycnometer thermostatized at 30 °C. The densities were measured with a precision of ± 0.001. The precision of the shrinkage calculated values is 0.2%.

Thermogravimetric analyses (TGAs) were carried out in a Mettler TGA/SDTA 851e thermobalance. Pieces of cured sample with an approximate mass of 8 mg were degraded between 30 and 800 °C at a heating rate of 10 °C/min in N_2 (100 mL/min measured in normal conditions) in ceramic crucibles.

Chemical degradation was carried out in a solution 1M of KOH in ethanol at 65 °C. Samples at different saponification times were taken, dried and T_gs were measured in a DSC scan from 30 to 200 °C at 20 °C/min.

Dynamic mechanical thermal analyses (DMTA) were carried out with a TA Instruments DMTA 2980 analyzer. Three point bending was performed on prismatic rectangular samples (10 × 5 × 1.5 mm^3, approximately). The apparatus operated dynamically at 2 °C/min from 30 to 200 °C at a frequency of 1 Hz.

Kinetic analysis

Integral non-isothermal kinetic analysis was used to determine the kinetic triplet (*A* pre-exponential factor, *E* activation energy and *g(x)* integral function of degree of conversion).

If we accept that the dependence of the rate constant on the temperature follows the Arrhenius equation, non-isothermal kinetic analysis may start with the kinetic equation:

$$\frac{dx}{dt} = \beta \frac{dx}{dT} = Ae^{-\frac{E}{RT}} f(x) \tag{2}$$

where β is the heating rate, dx/dt is the rate of conversion, R is the universal gas constant, T is the temperature and $f(x)$ is the differential conversion function.

By integrating eq. (2) and using the Coats-Redfern[19] approximation to resolve the so-called temperature integral and considering that $2RT / E << 1$ the Kissinger-Akahira-Sunose equation (KAS) may be written as:

$$ln\frac{\beta}{T^2} = ln\left[\frac{AR}{g(x)E}\right] - \frac{E}{RT} \tag{3}$$

For each conversion degree, the linear representation of $\ln[\beta/T^2]$ versus T^{-1} enables E and $\ln[AR/g(x)E]$ to be determined from the slope and the ordinate in the origin. If the reaction model, $g(x)$, is known, for each conversion the corresponding pre-exponential factor can be calculated for every activation energy.

In this study, we used the reduced master curves procedure of Criado and the Coats-Redfern method to assign a reaction model to the studied systems.[20] By the Coats-Refern method we selected the model which presented the best adjustment and had an activation energy similar to that obtained isoconversionally (considered to be the true). Different kinetic models have been studied: diffusion (D_1, D_2, D_3 and D_4), Avrami-Erofeev (A_2, A_3 and A_4), power law, phase-boundary-controlled reaction (R_2 and R_3), autocatalytic (n+m = 2 and 3) and order n (n = 1, 1.5, 2 and 3). The rate constant, k, was calculated with E and A determined at conversion of 0.5, using the Arrhenius equation.

RESULTS AND DISCUSSION

Although the modification of epoxy resins with hyperbranched polymers has been extensively reported, the main objective is usually the increase in toughness.[1,2,21] However, few articles describe other improvements such as the reduction of the shrinkage or the increase of reworkability of the final thermosets,[6,7,10,22,23] which are also interesting in thermosets applications. In addition, there are no studies on how the degree of branching can affect these characteristics.

Most of the research papers are based on epoxy/amine systems in which the hyperbranched polymer undergoes phase separation because hydroxyl groups are not reactive in these systems.[21,24,25] On the contrary, cationic curing allows the reaction of hydroxyl-functional hyperbranched polymers with epoxides to take place by means of the AM mechanism. This leads to chain transfer reactions that produce the covalent incorporation of hydroxyl-group

containing structures to the epoxy matrix. Thus, the phase separation is prevented and homogeneous materials can be obtained.

In the present study, we have investigated the influence of the degree of branching of three HBPs (homo and copolymers), obtained from homopolycondensation of AB_2 monomer (4,4-bis(4'-hydroxyphenyl)valeric acid) or by its copolycondensation with (3-(4-hydroxyphenyl) propionic acid) in different proportions, on the cationic curing of DGEBA resins with $Yb(OTf)_3$ as the initiator. These HBPs have been named as GBPEX (**Scheme 1**), with X representing the degree of branching determined by the Frey equations[26,27] which varied from 50% (AB_2 homopolymer) to 40 and 30% (AB_2-AB copolymers). The degree of branching was calculated by ^{13}C-NMR spectroscopy as detailed in a previous publication.[16] The different proportions of hydroxyl and ester functions in the HBP structure and their differences in viscosity should influence the curing evolution and the material characteristics.

Study of the curing process

The effect of adding 5 and 10% of GBPEX (X = 30, 40 and 50) to DGEBA on the curing process initiated by 1 phr of $Yb(OTf)_3$ was studied by means of DSC. Among all lanthanide triflates, we selected the ytterbium salt due to its highest Lewis acidity that favors the AM mechanism,[28,29] allowing a higher chemical incorporation of GBPEX to the material. Although curves registered at higher heating rates showed a unimodal shape, when registering at 2 °C/min two maxima in the calorimetric curves could be distinguished (**Figure 1**). The peak at lower temperature seems to increase on increasing the degree of branching of the modifier. Since the percentage of hydroxyl groups in the formulation increases, this peak could be associated to the propagation taking place by the AM mechanism (see **Scheme 2**). In this way, GBPEX modifiers become covalently linked to the epoxy matrix. The T_g of the resulting thermosets will be influenced by two contradictory effects: on the one hand an increasing covalent bonding of the HBP to the network increases T_g, but on the other hand chain transfer processes lead to a reduction of the crosslinking density and therefore to lower T_g values.

Activated chain end mechanism (ACE)

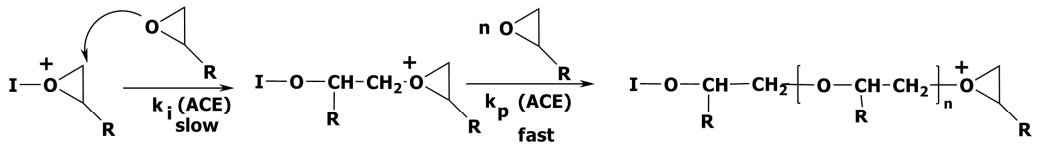

Activated monomer mechanism (AM)

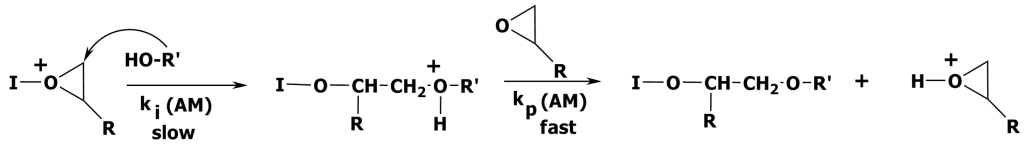

Scheme 2 Competitive propagation mechanisms in cationic ring-opening polymerization of epoxides.

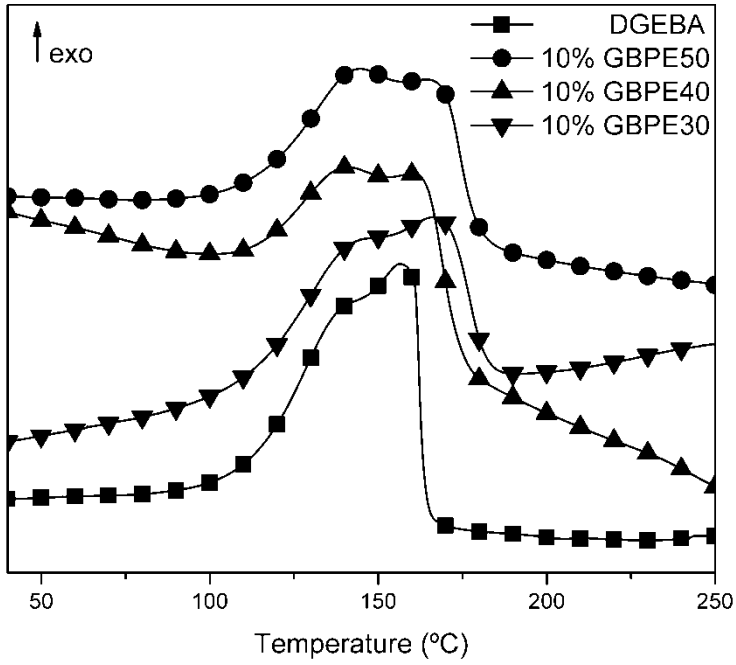

Figure 1 DSC scans recorded at 2 °C· min^{-1} for samples of neat DGEBA and DGEBA formulations containing a 10% of GBPE30, GBPE40, or GBPE50 cured with 1 phr of $Yb(OTf)_3$.

In **Table 1** the calorimetric data for all the studied formulations are collected. The values of enthalpy released per epoxy equivalent confirm that the achieved degree of curing is similar for all the formulations studied and almost complete.[30] However, the addition of GBPEX slightly reduces the heat released per gram of the reactive mixture, due to the lower epoxy content. Several authors reported that the addition of hyperbranched polymers reduced the T_g of the modified thermosets due to the aliphatic nature of the HBPs studied.[1,2,31,32]

Table 1 Composition of the formulations, calorimetric data, and conversion at the gelation of DGEBA mixtures containing different percentages of GBPEXs.

Formulation [a]	eq init: eq epo [b]	eq OH: eq epo [c]	Δh (J/g)	Δh [d] (kJ/ee)	T_g [e] (°C)	α_{gel} [f]
DGEBA / $Yb(OTf)_3$	0.0030	-	498	90.6	137	0.34
5 wt% GBPE50 / DGEBA / $Yb(OTf)_3$	0.0031	0.035	468	89.7	135	0.33
5 wt% GBPE40 / DGEBA / $Yb(OTf)_3$	0.0031	0.017	462	88.5	131	0.31
5 wt% GBPE30 / DGEBA / $Yb(OTf)_3$	0.0031	0.011	455	87.2	130	0.30
10 wt% GBPE50 / DGEBA / $Yb(OTf)_3$	0.0033	0.075	433	87.7	138	0.28
10 wt% GBPE40 / DGEBA / $Yb(OTf)_3$	0.0033	0.037	428	86.6	129	0.27
10 wt% GBPE30 / DGEBA / $Yb(OTf)_3$	0.0033	0.024	430	86.9	122	0.26

a. The amount of initiator ($Yb(OTf)_3$) used in all formulations was 1 phr.
b. Equivalent ratio initiator/epoxy.
c. Equivalent ratio hydroxyl group/epoxy. It has been calculated from the hydroxyl number per molecule of each GBPE. DB50: 97, DB40: 23 and DB30: 18.
d. Enthalpies per equivalent of epoxy group at 10 °C/min
e. Glass transition temperature obtained by DSC, from a second scan after dynamic curing.
f. Conversion at the gelation determined by rheology and DSC at 110 °C.

In the present study, the presence of aromatic structures and the covalent linkage of phenolic groups to the epoxy matrix help the T_g of the materials to be practically maintained, but in general a slight decrease is observed on increasing the proportion of modifier. On decreasing the degree of branching of the GBPEX this value also decreases due to the reduction of covalent bonding of the modifier to the epoxy matrix.

The conversion at the gelation was determined by rheology and calorimetric experiments. As we can see in the table, the addition of HBPs decreases the conversion at the gel point and the influence of the degree of branching is not significant.

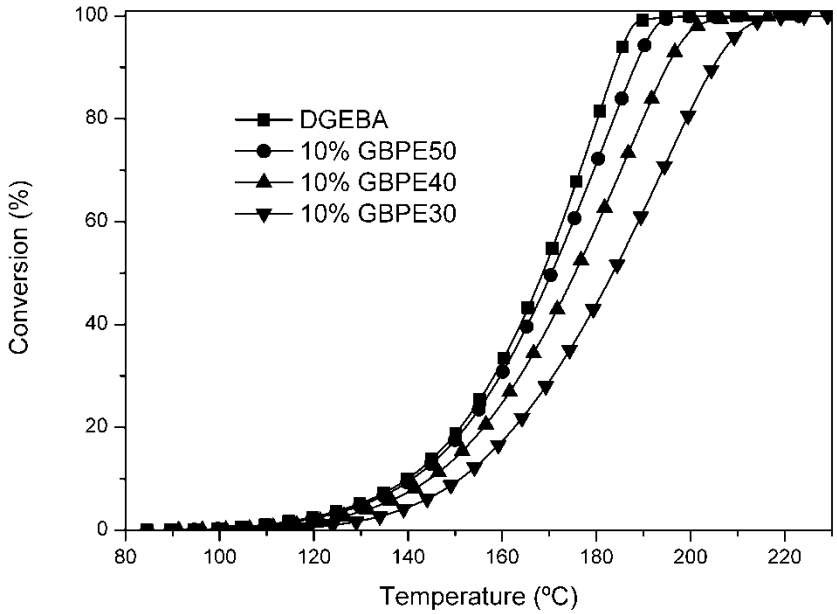

Figure 2 Plot of conversion against temperature for samples of neat DGEBA and DGEBA formulations containing a 10% of GBPE30, GBPE40, or GBPE50 cured with 1 phr of $Yb(OTf)_3$ obtained from a 10 ºC·min^{-1} DSC scan.

Table 2 Kinetic parameters for the curing process of the formulations studied by DSC.

Formulation [a]	*Ea* [b] (kJ/mol)	*ln A* [c] (s^{-1})	*k* x 10^3 [d] (s^{-1})
DGEBA / $Yb(OTf)_3$	79	16.08	3.27
5 wt% GBPE50 / DGEBA / $Yb(OTf)_3$	82	15.92	3.12
5 wt% GBPE40 / DGEBA / $Yb(OTf)_3$	79	15.12	2.21
5 wt% GBPE30 / DGEBA / $Yb(OTf)_3$	84	16.48	2.24
10 wt% GBPE50 / DGEBA / $Yb(OTf)_3$	82	15.34	2.15
10 wt% GBPE40 / DGEBA / $Yb(OTf)_3$	89	17.66	2.09
10 wt% GBPE30 / DGEBA / $Yb(OTf)_3$	74	13.22	1.19

a. The amount of initiator ($Yb(OTf)_3$) used in all formulations was 1 phr.
b. Values of activation energy at 50% of conversion, evaluated by the isoconversional non-isothermal procedure.
c. Pre-exponential factor for the R_3 kinetic model with $g(x) = [1-(1-x)^{1/3}]$.
d. Values of rate constant at 175 ºC using the Arrhenius equation at a conversion of 50%.

The kinetic parameters obtained from DSC experiments are collected in **Table 2** for all the formulations. **Figure 2** represents the plot of conversion against temperature on changing the degree of branching for a 10% of GBPEX content. The kinetic parameters for the curing reaction of all the formulations were calculated using the R_3 theoretical kinetic model, which is the one that better fits with the experimental data and activation energy values. As can be seen, the rate constant is slightly reduced on increasing the proportion of GBPEX and also on decreasing the degree of branching.

Figure 3 collects the plots of complex viscosity against angular frequency for all the formulations studied obtained by rheological measurements. One can see that the Newtonian behaviour for all the mixtures and that the viscosities are higher on increasing the amount of GBPEX in the formulation. Moreover, the higher the DB the lower the formulation's viscosity is. This fact is related to the lower entanglement of highly branched polymers.

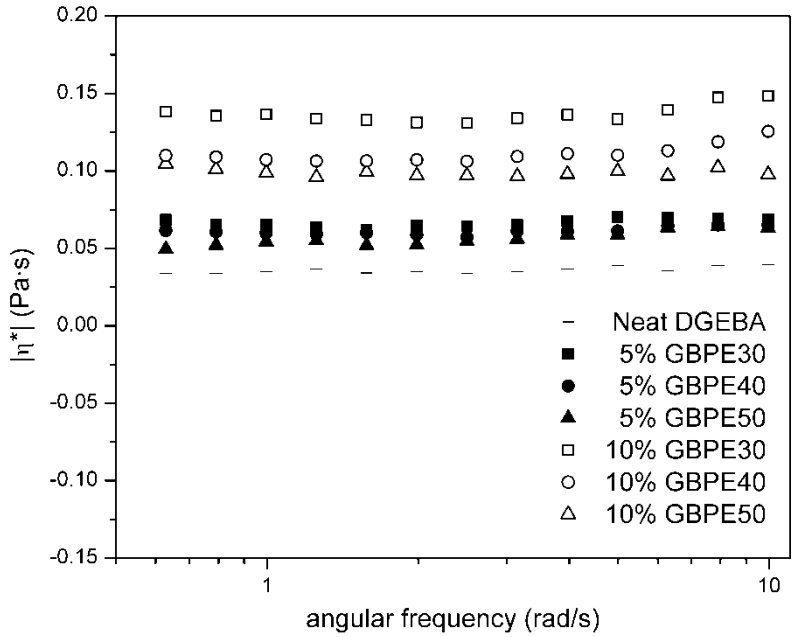

Figure 3 Complex viscosity (/η^*/) against angular frequency (ϖ) at 110 °C for neat DGEBA and DGEBA mixtures containing 5 and 10% of GBPE30, GBPE40, or GBPE50.

Thermal Stability

The introduction of ester groups in linear polymers or thermosets usually decreases the thermal stability, as they can be broken by β-elimination processes which take place at about 200-250 °C. However, when polyesters have no protons in γ-position this process cannot take place and therefore, polyesters derived from phenols are more stable. As we can see in **Table 3**, all the modified materials prepared are more stable than neat DGEBA, due to the introduction of aromatic structures in the network. The thermal stability is much higher when a 10% of GBPEX is included in the formulation. The initial decomposition temperature (T_{onset}) increases on decreasing the degree of branching and, since the hydroxyl content increases with the degree of branching it seems that this reduction in the thermal stability can be related to a possible water elimination from hydroxyl groups formed by the AM mechanism. The degradative process takes place in a single step (see **Figure 4**) which is contrary to what we observed when aliphatic

esters were present in the material, in which a small weight loss at about 250 ºC occurred.[7,23] Finally, it should be commented that the temperature of the maximum degradation rate does not decrease but rather increases slightly as it is shown in the figure.

Table 3 Thermogravimetric, thermomechanical, densities and global shrinkage data of the DGEBA thermosets containing different percentages of GBPEs.

Formulation [a]	T_{onset} [b] (ºC)	T_{max} (ºC)	*tan δ* [c] (ºC)	*E'* [d] (MPa)	*TA* [e] (h x K)	ρ_{mon} (g/cm³)	ρ_{pol} (g/cm³)	Shrinkage [f] (%)
DGEBA / $Yb(OTf)_3$	301	344	154	49	14.33	1.163	1.227	5.2
5% GBPE50/ DGEBA / $Yb(OTf)_3$	304	355	148	42	16.07	1.185	1.214	2.4
5% GBPE40/ DGEBA / $Yb(OTf)_3$	307	356	147	38	15.09	1.171	1.215	3.6
5% GBPE30/ DGEBA / $Yb(OTf)_3$	309	352	147	41	14.99	1.159	1.216	4.7
10% GBPE50/ DGEBA / $Yb(OTf)_3$	304	364	145	38	16.13	1.184	1.208	2.0
10% GBPE40/ DGEBA / $Yb(OTf)_3$	322	368	139	30	17.45	1.179	1.209	2.4
10% GBPE30/ DGEBA / $Yb(OTf)_3$	335	381	129	24	17.04	1.164	1.212	4.0

a. The amount of initiator ($Yb(OTf)_3$) used in all formulations was 1 phr.
b. Temperature of a 5 % of weight loss calculated by TGA.
c. Temperature of the maximum of the *tan δ* curve.
d. Storage modulus of material at the rubbery region at *tan δ* + 50 ºC.
e. *Tan δ* area under the curve of *tan δ* calculated by integration between the maximum of *tan δ* value -50 ºC and +50 ºC
f. Global shrinkage in % determined as $[(\rho_{pol} - \rho_{mon}) / \rho_{pol}] \times 100$.

Thermomechanical Analysis

Figures 5 and **6** show the plots of *E'* and *tan δ* against temperature determined by DMTA for the materials prepared with 10% of the GBPEX. The corresponding parameters for all the formulations are collected in **Table 3**. Although the storage moduli in the rubbery state do not change significantly on adding 5% of GBPEX, the variation is noticed on adding a higher proportion of modifier. The higher the degree of branching of the HBP, the lower is the effect on the relaxation modulus indicating the chemical incorporation of the modifier through the reaction of hydroxyl groups by the AM mechanism that in turn increases the degree of crosslinking achieved. *Tan δ* values are shifted to lower temperatures on adding GBPEX, especially when 10% were added to the formulation, but the maximum reduction observed in this parameter is 25 ºC. The shape of the curves indicates a homogeneous character of all the materials prepared. *Tan δ* is related to properties such as damping of free vibrations and it has been described that there is a relationship between the area under *tan δ* curve (TA) and the height and damping characteristics.[32,33] The value of the area indicates the ability of converting mechanical energy

into heat through molecular motion. Therefore, the materials with a higher value of area have higher damping properties in those selected temperatures and frequency range. As we can see in **Figure 6** and in **Table 3**, the area is higher when GBPEX is present in the formulation, which indicates an increase in the damping ability. However, in reference to the degree of branching the influence is not as significant.

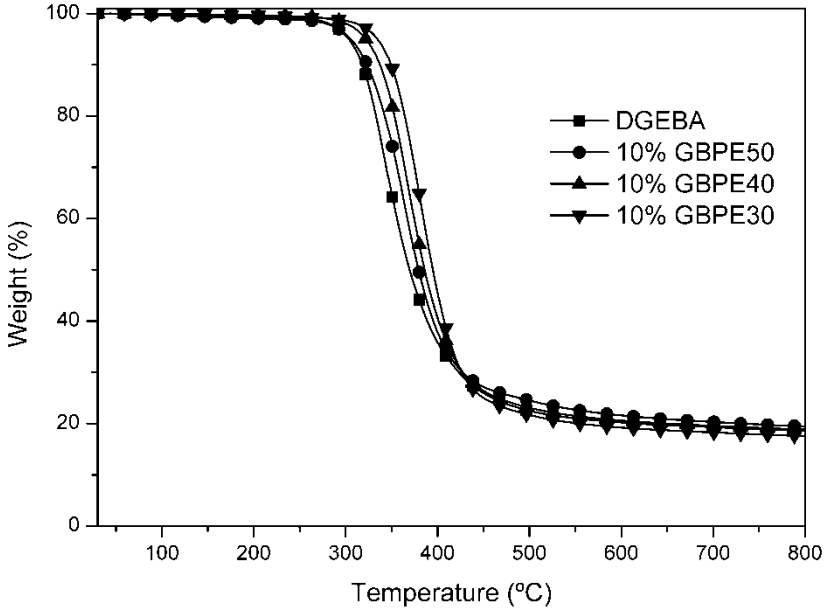

Figure 4 TGA curves for the materials obtained from neat DGEBA and DGEBA formulations containing a 10% of GBPE30, GBPE40, or GBPE50 cured with 1 phr of $Yb(OTf)_3$.

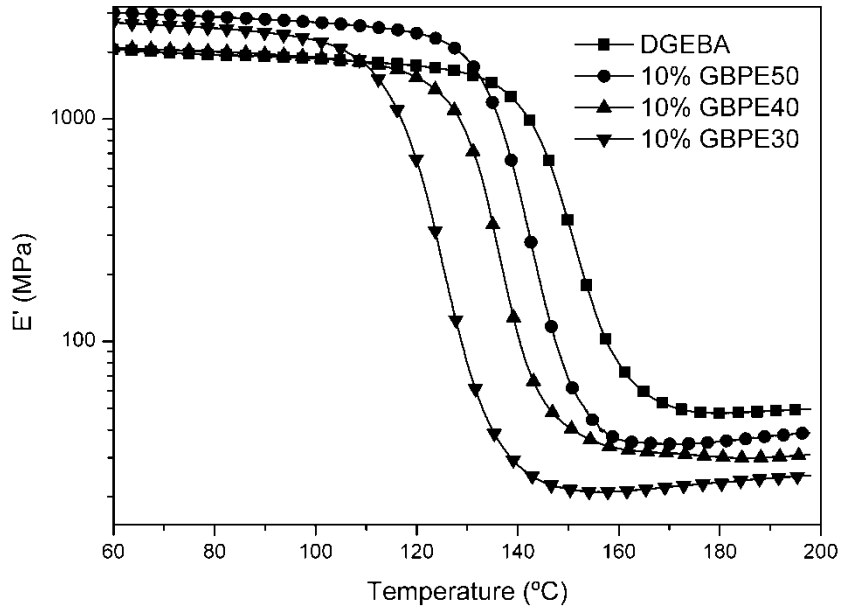

Figure 5 Plot of storage modulus against temperature for the materials obtained from neat DGEBA and DGEBA formulations containing a 10% of GBPE30, GBPE40, or GBPE50 cured with 1 phr of $Yb(OTf)_3$.

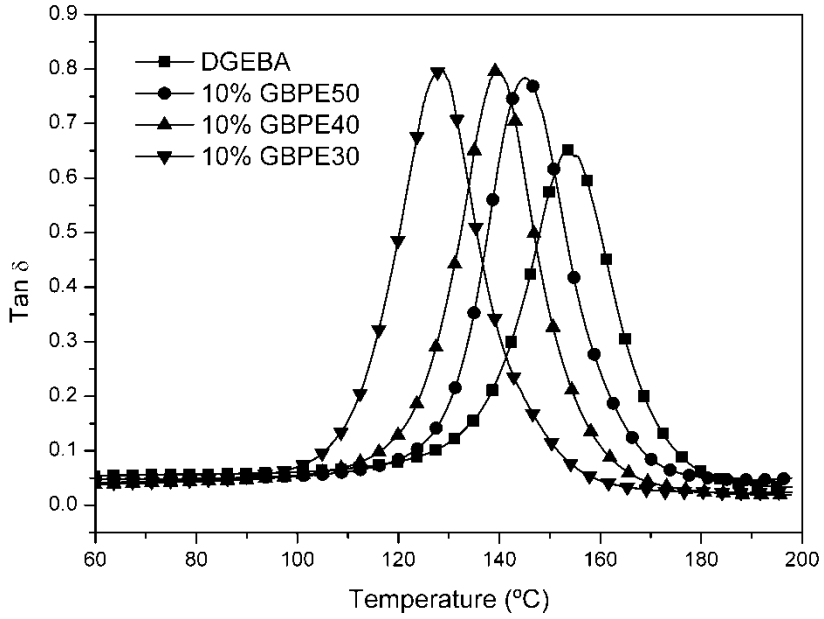

Figure 6 Plot of tan δ against temperature for the materials obtained from neat DGEBA and DGEBA formulations containing a 10% of GBPE30, GBPE40, or GBPE50 cured with 1 phr of $Yb(OTf)_3$.

Shrinkage

One of the main drawbacks of thermosetting materials used as coatings is the shrinkage that occurs during their curing process. This shrinkage can lead to the formation of bubbles and cracks and usually reduces the adhesion between the coating and the surface and, therefore, it is essential to reduce it down to the minimum. From our previous work, we can state that hyperbranched polymers can reduce the shrinkage on curing when hydroxyl groups are present as chain ends and they become covalently linked to the epoxy matrix. [6,7,10,23]

In **Table 3** the densities before and after curing and the shrinkage calculated from them are collected for all the formulations. As can be noticed, the addition of GBPEX decreases the shrinkage down to 2% in reference to the neat DGEBA thermoset (5.2%). The higher the proportion of modifier, the higher is the reduction in shrinkage. It can be assumed that when the HBP is covalently incorporated to the epoxy matrix, the compact HBP partially expands because the intramolecular H-bond interactions decrease. Thus, the density of the cured material decreases as HBP proportion increases. Moreover, the degree of branching also affects the shrinkage measured. GBPE50 led to the highest improvement, which seems to confirm the fact that the compact structure as result from the branching as well as the hydroxyl content of the HBP and its chemical incorporation to the matrix are responsible for the reduction of the shrinkage.

Chemical degradability

In the literature, there is a good number of contributions on thermally reworkable thermosets,[7,9,23] but only few of them are devoted to the chemical reworkability. Buchwalter *et al.*[34] prepared cycloaliphatic epoxy resins with ketalic groups, that could be degraded by treatment in acid solutions. We described the preparation of new chemically reworkable thermosets by anionic copolymerization of DGEBA with spiro- and condensed bislactones.[35,36]

These materials were soluble in ethanolic 1M KOH, but the thermal stability decreased and the T_gs of the materials were lower than 90 ºC.

Table 4 T_g values in ºC determined by DSC of the materials before and after saponification during several times.

Formulation [a]	Saponification time (hours) [b]					
	0	2	6	10	24	72
DGEBA / $Yb(OTf)_3$	135	-	-	136	137	138
5 wt% GBPE50 / DGEBA / $Yb(OTf)_3$	130	124	-	121	73	-
5 wt% GBPE40 / DGEBA / $Yb(OTf)_3$	133	130	-	131	75	-
5 wt% GBPE30 / DGEBA / $Yb(OTf)_3$	129	125	-	129	77	-
10 wt% GBPE50 / DGEBA / $Yb(OTf)_3$	111	103	71	72	73	-
10 wt% GBPE40 / DGEBA / $Yb(OTf)_3$	126	118	74	72	70	-
10 wt% GBPE30 / DGEBA / $Yb(OTf)_3$	130	122	75	74	73	-

a. The amount of initiator ($Yb(OTf)_3$) used in all formulations was 1 phr.
b. Saponification treatment with 1M ethanolic/water 20/80 KOH at 65 ºC during several reaction times.

As we obtained good chemical degradability maintaining the thermal stability in GBPE50 modified DGEBA,[10] we have studied how the degree of branching in GBPEX modifiers influences it by treating thermosets in the same saponification medium and then looking at the evolution of the T_gs of the partially degraded materials. **Table 4** shows the T_gs measured by DSC in a dynamic scan from 30 to 200 ºC at 20 ºC/min after different saponification times. In neat DGEBA thermosets, after 3 days of reaction the T_g remains unchanged. On the contrary, in the GBPEX modified thermosets after several hours this value decreases until reaching a T_g of about 70-75 ºC. As we can see from the table, the degradation is achieved at shorter times when the proportion of GBPEX increases in the formulation, but there is no influence of the degree of branching. Thus, for this type of HBPs we can state that degrees of branching between 30 and 50 are valid to get chemically reworkable thermosets, according to their structure with a similar proportion of ester groups.

CONCLUSIONS

The addition of GBPEXs, with different DB varying from 50 to 30%, as reactive modifiers to cationic thermal curing of DGEBA resins slightly reduces the curing rate at a selected temperature. The presence of hydroxylic chain-ends in the GBPEX allows the modifier to be covalently linked through the monomer activated propagation mechanism, which occurs in cationic ring-opening polymerizations. The contribution of AM mechanism becomes more important when the degree of branching increases, due to the increase in the proportion of hydroxyl groups. Thus, the curing process is slightly decelerated on increasing the proportion of GBPEX or decreasing the DB.

The viscosity of the mixture increases with the proportion of modifier but the higher the DB the lower is the viscosity.

The T_g of the materials slightly decreases on increasing the proportion of modifier. This reduction is lower on increasing the DB of the GBPEX.

The thermal stability is increased when a high proportion of GBPEX is added to the formulation and the initial decomposition temperature increases on decreasing the DB.

Storage moduli in the rubbery state are reduced on adding a higher proportion of modifier. The higher the DB of GBPEX the lower is the effect on the relaxed modulus. The decrease in

tanδ values is only clearly observed when 10% of GBPE30 were added to the formulation. The higher the DB the lower is this decrease. The modified thermosets were completely homogeneous and have better damping characteristics.

The addition of GBPEX to DGEBA formulations leads to a reduction of the global shrinkage during curing. This reduction increases with the proportion of modifier in the formulation and with the DB.

The chemical reworkability of these materials in alkaline solutions is highly enhanced by the addition of GBPEX, but the DB does not affect this characteristics.

Thus, in summary one can state that the best combination of effects of the HBP modifier on the various studied properties can be achieved with the polymers of maximum DB.

ACKNOWLEDGEMENTS

The authors from the Universitat Rovira i Virgili and from Universitat Politècnica de Catalunya would like to thank MICINN (Ministerio de Ciencia e Innovación) and FEDER (Fondo Europeo de Desarrollo Regional) (MAT2008-06284-C03-01 and MAT2008-06284-C03-02), the Generalitat de Catalunya for her financial help (2009-SGR-1512), and the Germany-Spanish DAAD collaboration program (HA2007-0022, DAAD PPP D/07/13493) for their financial support. D.F. acknowledges the grant to the Spanish Government and M.M. to the Generalitat de Catalunya.

REFERENCES

1. R. J. Varley, W. Tian. *Polym. Int.* **2004**, *53*, 69.
2. D. Zhang, D. Jia. *J. Appl. Polym. Sci*. **2006**, *101*, 2504.
3. L. Boogh, B. Pettersson, J. A. E. Månson. *Polymer* **1999**, *40*, 2249.
4. R. A. T. M. van Benthem. *Prog. Org. Coat.* **2000**, *40*, 203.
5. C. A. May. *Epoxy Resins. Chemistry and Technology*, 2ª edition. Marcel Dekker, New York, **1988**.
6. X. Fernández-Francos, J. M. Salla, A. Cadenato, J. M. Morancho, A. Serra, A. Mantecón, X. Ramis. *J. Appl. Polym. Sci.* **2009**, *111*, 2822.
7. M. Morell, X. Ramis, F. Ferrando, Y. Yu, A. Serra. *Polymer* **2009**, *50*, 5374.
8. S. Yang, J. S. Chen, H. Körner, T. Breiner, C. K. Ober, M. D. Poliks. *Chem. Mater.* **1998**, *10*, 1475.
9. L. Wang, H. Li, C.P. Wong. *J. Polym. Sci. Part A: Polym. Chem.* **2000**, *38*, 3771.
10. D. Foix, M. Erber, B. Voit, A. Lederer, X. Ramis, A. Mantecón, A. Serra. *Polym. Degrad. Stab.* **2010**, *95*, 445.
11. J. H. Oh, J. Jang, S. H.Lee. *Polymer* **2001**, *42*, 8339.
12. P. Kubisa, S. Penczek. *Prog. Polym. Sci.* **1999**, *24*, 1409.
13. C. E. Corcione, G. Malucelli, M. Frigione, A. Maffezzoli. *Polym. Test.* **2009**, *28*, 157.
14. M. Sangermano, A. Priola, G. Malucelli, R. Bongiovanni, A. Quaglia, B. Voit, A. Ziemer. *Macromol. Mater. Eng.* **2004**, *289*, 442.
15. J. S. Moore, S. I. Stupp. *Macromolecules* **1990**, *23*, 65.
16. F. Schallausky, M. Erber, H. Komber, A. Lederer. *Macromol. Chem. Phys*. **2008**, *209*, 2331.
17. D. Schmaljohann, H. Komber, B. Voit. *Acta Polym.* **1999**, *50*, 196.
18. J-P. Pascault, H. Sauterau, J. Verdu, R. J. J. Williams. *Thermosetting Polymers*. Marcel Dekker, New York, **2002**.
19. A. W. Coats, J. P. Redfern. *Nature* **1964**, *201*, 68.
20. X. Ramis, J. M. Salla, A. Cadenato, J. M. Morancho. *J. Therm. Anal. Calorim.* **2003**, *72,* 707.
21. G. Cicala, G. Recca, C. Restuccia, *Polym. Eng. Sci.* **2005**, *45*, 225.
22. Y. Eom, L. Boogh, V. Michaud, J. A. E. Månson. *Polym. Compos.* **2002**, *23,* 1044.

23. M. Morell, M. Erber, X. Ramis, F. Ferrando, B. Voit, A. Serra. *Eur. Polym. J.* **2010**, *46*, 1498.
24. G. Xu, W. Shi, M. Gong, F. Yu, J. Feng. *Polym. Adv. Technol.* **2004**, *15*, 639.
25. I. Blanco, G. Cicala, C. Lo Faro, O. Motta, G. Recca. *Polym. Eng. Sci.* **2006**, *46*, 1502.
26. D. Hölter, A. Burgath, H. Frey. *Acta Polymer.* **1997**, *48*, 30.
27. D. Hölter, H. Frey. *Acta Polymer.* **1997**, *48*, 298.
28. C. Mas, A. Mantecón, A. Serra, X. Ramis, J. M. Salla. *J. Polym. Sci. Part A: Polym. Chem.* **2004**, *42*, 3782.
29. L. Matejka, K. Dusek, P. Chabanne, J. P. Pascault. *J. Polym. Sci. Part A: Polym. Chem.* **1997**, *35,* 665.
30. J. Brandrup, E. H. Immergut, E. A. Grulke. *Polymer Handbook*, 4th ed. Wiley-Interscience, New York, **1999**.
31. J-F. Fu, L-Y. Shi, S. Yuan, Q-D. Zhong, D-S. Zhang, Y. Chen, J. Wu. *Polym. Adv. Technol.* **2008**, *19,* 1597.
32. G. Cicala, G. Recca. *Polym. Eng. Sci.* **2008**, *48*, 2382.
33. Y. C. Chern, S. M. Tseng, K. H. Hsieh. *J. Appl. Polym. Sci.* **1999**, *74*, 328
34. S. L. Buchwalter, L. L. Kosbar. *J. Polym. Sci. Part A: Polym. Chem.* **1996**, *34*, 249.
35. M. Arasa, X. Ramis, J. M. Salla, A. Mantecón, A. Serra. *Polymer* **2009**, *50*, 2228.
36. X. Fernández-Francos, J. M. Salla, A. Mantecón, A. Serra, X. Ramis. *Polym. Degrad. Stab*. **2008**, *93*, 760.

Chapter 5

Use of Amphiphilic HBPs in the Modification of Epoxy Resins

5.1 Introduction

Amphiphilic polymers can be defined as macromolecules that are composed by two or more zones (or blocks) with different solubility, being at least one hydrophilic and at least another hydrophobic. If one of these block presents a highly branched nature these polymers are known as amphiphilic hyperbranched polymers. In this work we have selected with two different types of amphiphilic HBPs: multi-arm star polymers and hyperbranched-linear-hyperbranched block copolymers.

Star polymers, containing multiple linear arms connected at a central branched core (multi-arm star polymers), represent one of the simplest nonlinear polymers. The main approaches used in their synthesis are three: "core-first",[1,2] "coupling-onto",[3-5] and "arm-first",[6-8] which differentiate from each other based on the formation sequence of core and arms.

[1] J. S. Wang, D. Greszta, K. Matyjaszewski. *Polym. Mater. Sci. Eng*. **1995,** *73*, 416.
[2] J. Ueda, M. Matsuyama, M. Kamigaito, M. Sawamoto. *Macromolecules* **1998,** *31*, 557.
[3] H. Gao, K. Matyjaszewski. *Macromolecules* **2006,** *39*, 4960.
[4] M. R Whittaker, C. N. Urbani, M. J Monteiro. *J. Am. Chem. Soc.* **2006,** *128*, 11360.
[5] O. Altintas, G. Hizal, U. Tunca. *J. Polym. Sci., Part A: Polym. Chem*. **2006**, *44*, 5699.
[6] J. H. Xia, X. Zhang, K. Matyjaszewski. *Macromolecules* **1999,** *32*, 4482.
[7] K. Y. Baek, M. Kamigaito, M. Sawamoto. *Macromolecules* **2001,***34*, 215.
[8] H. Gao, K.Matyjaszewski. *Macromolecules* **2006,** *39*, 3154.

The core-first method involves the use of a multifunctional initiator (core) that is used to start the polymerization of a monomer. If the functionality is preserved at the end of the linear arms of the star it is also possible to obtain star block copolymers by polymerizing a second monomer[9] (**Figure 5.1**).

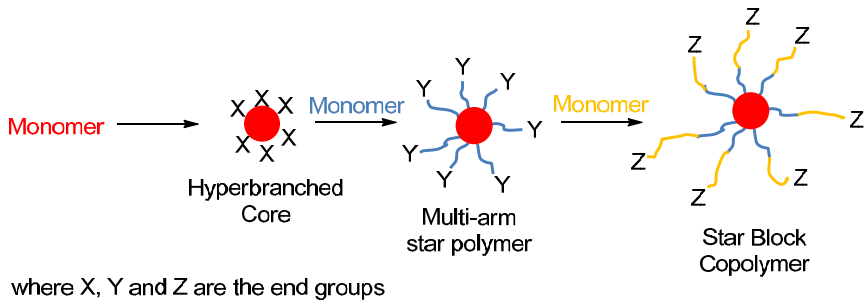

Figure 5.1 Schematic representation of the core-first approach to the synthesis of multi-arm star polymers and copolymers.

In the coupling onto method, a star polymer is synthesized by the coupling reactions between linear polymeric chains (arms) containing a reactive chain end group and a multifunctional coupling agent (core). Due to the slow reaction between the polymer chain end and the multifunctional core, an organic reaction with high coupling efficiency must be employed. For example, the Cu(I)-catalyzed 2 + 3 cycloaddition between an azide and an alkyne,[10] have been used for synthesis of various kinds of star polymers with predetermined structure and high star yield. Moreover, this coupling onto methodology is very useful in the preparation of the so called miktoarm star polymers,[11] by reacting the multifunctional core with two (or more) different linear arms (**Figure 5.2**).

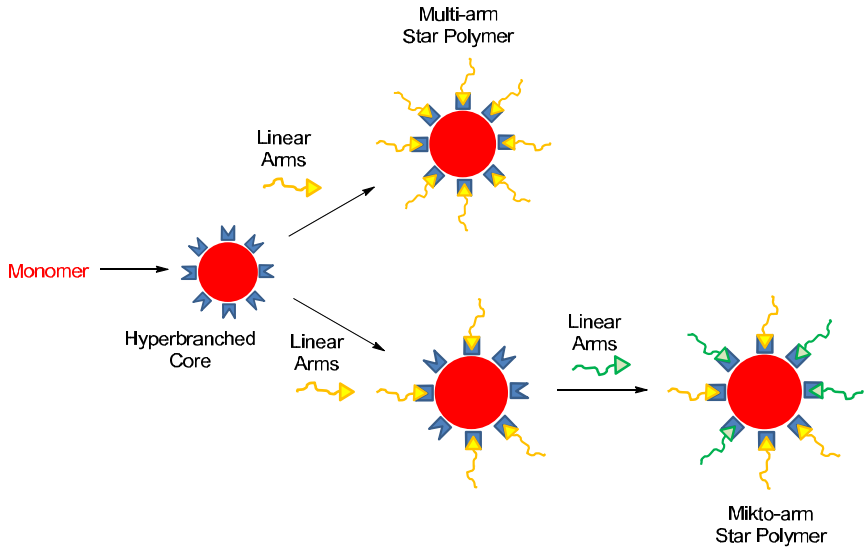

Figure 5.2 Schematic representation of the coupling onto approach to the synthesis of star polymers and miktoarm star polymers.

[9] W. R. Dichtel, K. Y. Baek, J. M. J. Frechet, I. B. Rietveld, S. A. Vinogradov. *J. Polym. Sci. Part A: Polym. Chem.* **2006,** *44*, 4939.
[10] H. C. Kolb, M. G. Finn, K. B. Sharpless. *Angew. Chem. Int. Ed.* **2001,** *40*, 2004.
[11] K. Khanna, S. Varshney, A. Kakkar. *Polym. Chem.* **2010,** *1,* 1171.

Finally, in the arm-first method, the linear arms of the star polymers are synthesized first followed by binding of the arms to form the core (**Figure 5.3**), usually by using a divinyl cross-linker. The resulting star polymers have a statistical distribution of the number of arms and a highly cross-linked core.[12] The preformed arms can be either linear macroinitiators[8] or macromonomers.[13] The unreacted sites of the core can be further employed to initiate the polymerization of another monomer to form miktoarm star copolymers by the "in-out" method.[14]

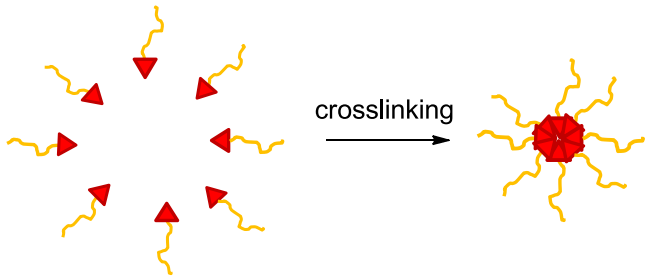

Figure 5.3 Schematic representation of the arm-first approach to the synthesis of star polymers.

Recently, linear-hyperbranched block copolymers (LHBC) have gain increasing interest due to their peculiar properties.[15] Their general structure can be seen in **Figure 5.4**.

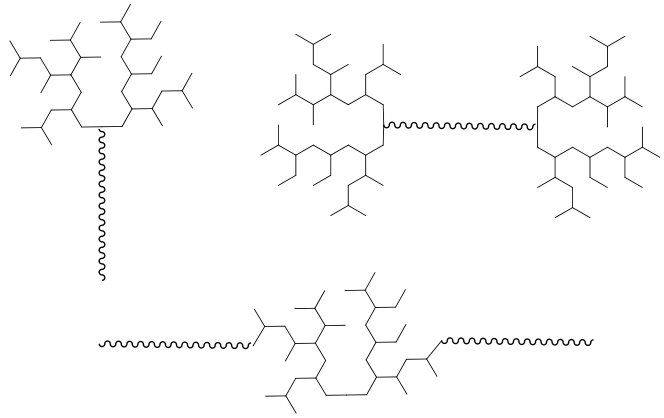

Figure 5.4 Schematic representation of different possible LHBCs.

In the literature one can find different approaches to the synthesis of such structures. Kricheldorf *et al.*[16] reported what can be considered as the first attempt to prepare LHBC, precisely, a hyperbanched-linear-hyperbranched (HLH) copolymer consisting of a linear telechelic oligo(ether ketone) block and two hyperbranched poly(3,5-dihydroxybenzoate) blocks. The synthetic pathway consisted in the polycondensation of an AB_2 monomer in the presence of the linear telechelic block. Lee *et al.*[17,18] have reported the preparation of hyperbranched poly(ether ketone)-*b*-linear poly(ether ketone)-*b*-hyperbranched

[12] K. Y. Baek, M. Kamigaito, M. Sawamoto. *J. Polym. Sci. Part A: Polym. Chem.* **2002,** *40*, 633.
[13] H. Gao, S. Ohno, K. Matyjaszewski. *J. Am. Chem. Soc.* **2006,** *128*, 15111.
[14] J. Z. Du, Y. M. Chen. *Macromolecules* **2004,** *37*, 3588.
[15] F. Wurm, H. Frey. *Prog. Polym. Sci.* **2011,** *36,* 1.
[16] H. R Kricheldorf, T. Stukenbrock. *J. Polym. Sci. Part A: Polym. Chem.* **1998,** *36,* 31.
[17] S. Y. Kwak, D. U. Ahn, J. Choi, H. J. Song, S. H. Lee. *Polymer* **2004,** *45,* 6889.
[18] S. Y. Kwak, C. Q. He, T. Suzuki, S. H. Lee. *J. Polym. Sci. Part A: Polym. Chem.* **2004,** *42,* 3853.

poly(etherketone) triblock copolymers (**Figure 5.5**) by a similar methodology with relatively low molecular weight dispersities (around 2.5).

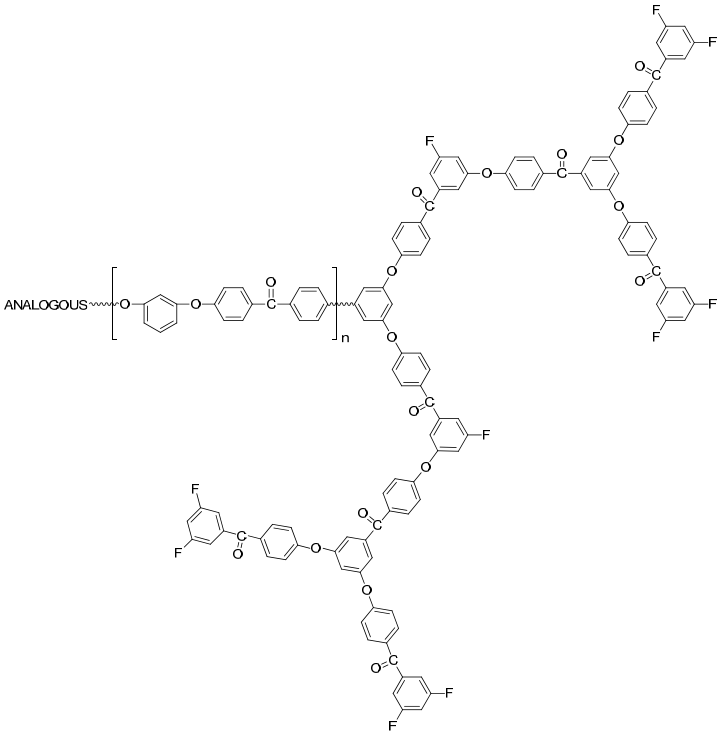

Figure 5.5 Chemical structure of the LHBC prepared by Lee *et al*.

Knauss *et al*.[19] reported the first successful synthesis of well-defined LHBC consisting of an arborescent polystyrene as the hyperbranched block and a linear polystyrene or polyisoprene block via the so-called "convergent living anionic polymerization". The synthetic methodology consists in the preparation of a macroinitiator from the hyperbranched block that initiates the living polymerization of the linear block. With this elegant methodology, quite low dispersities can be achieved (around 1.40).

Cho *et al*.[20] proposed the preparation of dumbbell like LHBCs from the well-known using self-condensing vinyl polymerization (SCVP). A conveniently modified linear poly(ethylene glycol) is used to initiate the SCVP of 4-chloromethylstyrene to obtain the two hyperbranched blocks. An schematic representation of such strategy can be seen in **Figure 5.6**.

Another example of the preparation of such structures is the proposed by Frey *et al*.[21] They reported the first preparation of a well defined amphiphilic block copolymer consisting of a linear polymer chain and a hyperbranched poly(glycerol) segment (**Figure 5.7**). In the first step a commercially available amine terminated linear poly(ethylene oxide)-co-poly(propylene oxide) (Jeffamine®)was bisglycidolized to form a macroinitiator bearing four hydroxyl groups. The hyperbranched poly(glycerol) was grafted onto this linear macroinitiator via ring-opening multibranching polymerization (ROMBP). Using this methodology good polydispersities of around 1.5 can be achieved.

---

[19] H. A. Al-Muallem, D. M. Knauss. *J. Polym. Sci. Part A: Polym. Chem.* **2001,** *39,* 152.
[20] S. G. An, C. G. Cho. *Polym. Bull.* **2004,** *51,* 255.
[21] V. Istratov, H. Kautz, Y. K. Kim, R. Schubert, H. Frey. *Tetrahedron* **2003,** *59,* 4017.

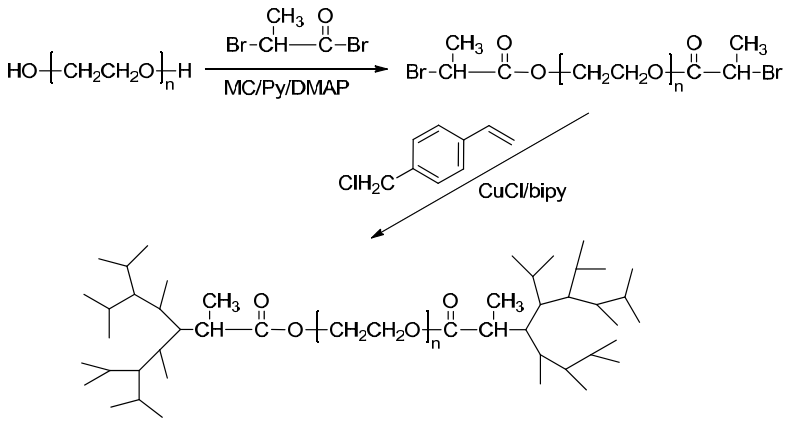

Figure 5.6 Scheme of reaction for the preparation of an amphiphilic LHBC.

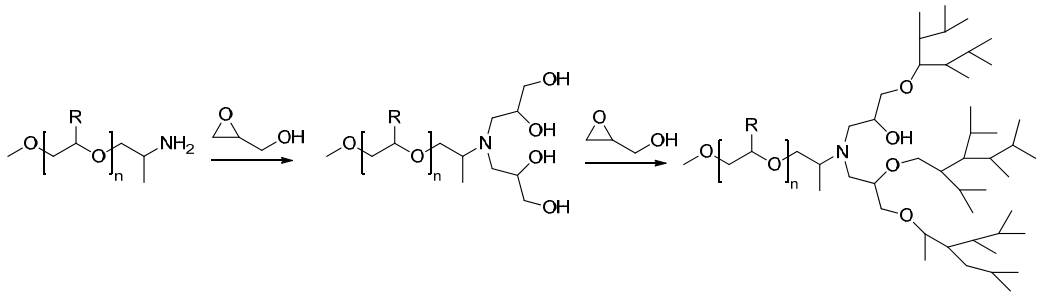

Figure 5.7 Scheme of reaction for the preparation of an amphiphilic LHBCs via ROMBP.

All the strategies to prepare LHBCs mentioned up to now consist in the polymerization of the branched moiety in situ using the linear one as initiator. However there are also some examples of a different approach, consisting in preparing the two blocks separately and linking them via grafting. This approach requires the use of highly efficient linking reactions, as it was the case for the coupling onto approach for the muti-arm star polymer synthesis. For example, in the very first reports on linear-hyperbranched block copolymers a coupling approach with poly(ethylene glycol) monomethyl monoglycidyl ether or poly(ethylene glycol) with one terminal acyl chloride group were employed. Both polymers were subsequently reacted with poly(ethylene imine) ($\bar{M}_w$ = 700 g/mol) and bromoacetic acid to yield poly(ethylene glycol)-b-poly[(N-carboxymethyl) ethyleneimine] (PEG-b-PEIPA, average $\bar{M}_w$ = 3,800 and 6,800 g/mol respectively) as a polymeric analog of EDTA[22]. The main problem of this strategy is the difficulty to find efficient reactions to perform the coupling that results in mixtures of both block copolymers and homopolymers.

The present chapter will deal about the use of two different amphiphilic structures in the modification of epoxy resins: a multi-arm star polymer with an aromatic polyester core and a shell made of poly(ethylene glycol) and a dumbbell like LHBC being the linear block poly(ethylene glycol) and the hyperbranched block an aromatic polyester. Special attention will be paid to the morphology of the prepared thermosets, since nanostructuration is described for the use of amphiphilic polymers in the modification of epoxy resins. As described in Chapter 1,

[22] M. Sedlák, M. Antonietti, H. Cölfen. *Macromol. Chem. Phys.* **1998,** *199,* 247.

one strategy to improve toughness in epoxy resins is the use of polymeric materials that can undergo nanostructuration during the curing process, in the so called “toughening by nanostructure” approach. This study reflects in the following articles:

5.2 New pegylated hyperbranched polyester as chemical modifier of epoxy resins in UV cationic photocuring.

5.3 DGEBA thermosets modified with an amphiphilic star polymer. Study on the effect of the initiator on the curing process and morphology.

5.4 Synthesis of a new hyperbranched-linear-hyperbranched triblock copolymer and its use as a chemical modifier for the cationic photo and thermal curing of epoxy resins.

5.2 New pegylated hyperbranched polyester as chemical modifier of epoxy resins in UV cationic photocuring

D. Foix[1], X. Fernández-Francos[2], X. Ramis[2], A. Serra[1], M. Sangermano[3]

[1] Department of Analytical and Organic Chemistry, University Rovira i Virgili, Marcel.li Domingo s/n, 43007 Tarragona, Spain

[2] Laboratory of Thermodynamics, ETSEIB, University Politècnica de Catalunya, Av. Diagonal 647, 08028 Barcelona, Spain

[3] Department of Material Science and Chemical Engineering, Politecnico di Torino, C.so Duca degli Abruzzi 24, 10129 Torino, Italy

ABSTRACT

A new hyperbranched polymer (HBPpeg) has been obtained via pegylation of an aromatic hyperbranched polyester. This polymer has been used as modifier of a commercially available cycloaliphatic epoxy resin in its cationic UV photocuring, using arylsulfonium salts as photoinitiator. The addition of the HBP slows down the curing as well as reduces the overall conversion achieved at room temperature, due to its interaction with the photoinitiator, but fully cured materials were achieved for formulations containing up to 10 phr of the HBP. The amphiphilic structure of the HBPpeg allows it to phase-separate in the epoxy matrix, which was confirmed by means of FE-SEM. The thermomechanical characteristics and the thermal stability have been also studied.

INTRODUCTION

Epoxy resins are one of the most widely used thermosets in technological applications such as coatings, adhesives, structural applications or electronics due to their mechanical properties, relatively low shrinkage and high chemical and thermal resistance.[1] Moreover, they possess high versatility thanks to the many initiators and hardeners available for their curing. However, one of the main drawbacks that they present is the inherent brittleness. This is caused by the high crosslinking density achieved and it is even more pronounced in cationic systems because of the rigidity of the network and the short distance between crosslinks. There are many approaches in the literature to enhance the toughness of epoxy resins involving the modification of these systems with polymers such as thermoplastics, block-copolymers, liquid rubber or core-shell particles.[2-6] The initially miscible mixture of the epoxy/hardener system with the modifiers becomes immiscible as reaction proceeds due to a growing incompatibility between the developing network and the added polymer, which can phase-separate. This leads to a highly cross-linked and rigid matrix with dispersed polymer particles inside, which are responsible for the toughness enhancement.[7]

Hyperbranched polymers (HBP) belong to a group of macromolecules called dendritic polymers, which have peculiar and often unique properties.[8] They possess a highly branched backbone, which gives access to a large number of reactive groups; their structure gives them excellent flow and processing properties, and they are characterized by lower viscosity than those of linear polymers of comparable molecular weight. This type of polymers has been successfully used as toughening agents that phase-separate during curing.[9-13]

The UV-polymerization of multifunctional monomers is one of the more efficient methods available to generate three-dimensional polymeric networks.[14] Among the advantages of this technology the high cure speed, the reduced energy consumption, and absence of VOC emissions are the most remarkable. It is well known that the UV curing can be performed either

by a radical or a cationic mechanism. The cationic photoinduced process presents some advantages compared to the radical one,[14] in particular lack of inhibition by oxygen, lower shrinkage, good mechanical properties of the UV cured materials, and good adhesion properties to various substrates.

Previously we reported the use of the unmodified polyester HBP in the thermal[15] and UV curing[16] of epoxy resins leading in both cases to homogeneous materials. In the present work, we have studied the effect of adding a hyperbranched polymer that we firstly synthesized, on the photocuring of a commercially available cycloaliphatic resin and on the characteristics of the corresponding thermosets. The new hyperbranched polymer that we synthesized contains a main structure of aromatic polyester with phenol chain ends, which were modified with a linear polyethylene glycol in order to get an amphiphilic structure that can undergo supramolecular assembly during curing, leading to phase-separated thermosets.

EXPERIMENTAL PART

Materials

4,4'-Bis(4-hydroxyphenyl)valeric acid, N,N'-dicyclohexylcarbodiimide (DCC), methanol, anhydrous N,N-dimethylformamide (DMF), monomethyl poly(ethylene glycol) ($\bar{M}_n$ = 550 g/mol), succinic anhydride and pyridine were purchased from Aldrich or Fluka and used without further purification. 4-(N,N-dimethylamino)pyridinium p-toluenesulfonate (DPTS) was prepared as described in the literature.[17]

The bis-cycloaliphatic diepoxy resin 3,4-epoxycyclohexylmethyl-3',4'-epoxycyclohexyl carboxylate (CE, Huntsman) and triphenylsulfonium hexafluoroantimonate (PI, $Ph_3S^+SbF_6^-$, Aldrich) (**Scheme 1**) were used as received.

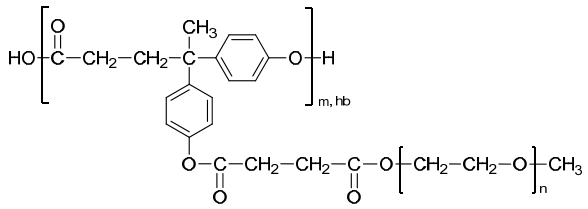

HBPpeg

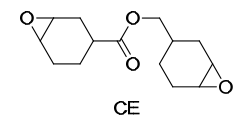

CE

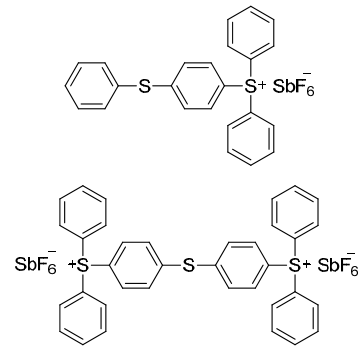

PI

Scheme 1 Components of the curing mixture.

Synthesis of the hyperbranched polyester (HBPE)

HBPE was synthesized according to a previously described procedure.[18] In a 500 mL two-necked round-bottom flask, 50 g (1 eq) of 4,4-bis(4-hydroxyphenyl) valeric acid and 7.64 g (0.2 eq) of DPTS were dissolved in anhydrous DMF (200 mL). Then, 43.24 g (1.2 eq) of DCC were added in portions and the mixture was kept under argon atmosphere for 24 h at room temperature. Then, the precipitate was filtered off and the solution was poured in methanol (1200 mL) to obtain a white powder after drying in a vacuum oven overnight at 60 °C (Yield: 80%). The ^{1}H and ^{13}C NMR data are in accordance with those published.[19]

$\bar{M}_n$: 10,000 g/mol; $\bar{M}_w$: 29,000 g/mol; $Đ_M$: 2.9.
DB_{frey}[20] = 0.50.
T_g = 105 °C.

Synthesis of the acid terminated monomethyl poly(ethyleneglycol)

In a 100 mL two-necked round-bottom flask 10 g (1 eq) of monomethyl poly(ethylene glycol) (CH3OPEG-OH) were dissolved in 150 mL of chloroform. Then, 9 mL of pyridine were added and finally, 9 g (5 eq) of succinic anhydride were added in portions. The mixture was heated up to 60 °C and allowed to react at this temperature for 72 h. After that, the solution was cooled down to room temperature and the solvent eliminated under vacuum. The crude product was dissolved in 15 mL of 1 N HCl, washed with ether and then extracted with chloroform. The solvent was removed under vacuum (Yield: 99%).

^{1}H NMR ($CDCl_3$): δ (in ppm) 4.20 (terminal PEG CH_2); 3.60-3.70 (OCH_2CH_2); 3.30 (OCH_3); 2.50-2.60 (CH_2 succinic).
^{13}C NMR ($CDCl_3$): δ (in ppm) 175.5 (COOH); 172.2 ($COOCH_2$); 71.9, 70.6, 69.0 (OCH_2CH_2); 63.9 (terminal PEG CH2); 59.1 (OCH_3); 29.2, 28.8 (CH_2 succinic).

*Synthesis of the hyperbranched polyester with terminal poly(ethylene glycol) chains (HBPpeg) (**Scheme 1**)*

In a 250 mL round bottom two necked flask provided with a magnetic bar and Ar inlet 3 g (1 eq) of HBP, 0.72 g (0.2 eq) of dimetylaminopyridinium p-toluenesulfonate (DPTS) and 6.9 g (1 eq) of CH_3OPEG-COOH were dissolved in 100 mL of DMF. Then 2.82 g (1.2 eq) of dicyclohexylcarbodiimide (DCC) were added and the mixture allowed to react at room temperature for 48 h. Then the precipitated was filtered off, the volume of DMF reduced to 20 ml and the crude product dialyzed against the same solvent (Yield 80%).

^{1}H NMR ($CDCl_3$): δ (in ppm) 1.50-1.65 (CH_3); 2.33 (CH_2); 2.50-2.60 (CH_2COO); 3.30 (OCH_3); 3.60-3.70 (OCH_2CH_2); 4.20 (terminal PEG CH_2); 6.90-7.15 (aromatics).
^{13}C NMR ($CDCl_3$): δ (in ppm) 172.5, 172.0, 171.0 ($\underline{C}OO$-CH_2); 148.7, 128.4, 121.2 (aromatics); 71.9, 70.5, 69.0 (OCH_2CH_2); 63.9 (terminal PEG CH_2); 59.0 (OCH_3); 45.2 (C); 36.2 (CH_2); 30.3 (CH_2); 29.2, 29.1 (CH_2 succinic); 27.8 (CH_3).
$\bar{M}_n$: 24,000 g/mol; $\bar{M}_w$: 47,000 g/mol; $Đ_M$: 2.0.
T_g = -38 °C and 95 °C.

Film Preparation

To photocurable formulations containing the appropriate amount of HBPpeg (0, 5, 10 and 15 per hundred resin, phr) in the epoxy resin (CE), 2 phr of the photoinitiator were added. The solubility of the HBPpeg in the resin was assessed by visual inspection. The liquid formulations were coated onto a glass substrate or in a polypropylene template (for free-standing films) using

a wirewound applicator. Then the films were exposed to UV radiation with a fusion lamp (H-bulb) in air at a conveyor speed of 5m·min^{-1}, with radiation intensity on the surface of the sample of 280 mW·t·cm^{-2}.

Characterization Techniques

^{1}H NMR 400 MHz and ^{13}C NMR 100.6 MHz measurements were obtained using a Varian Gemini 400 spectrometer with Fourier Transformed. ^{1}H NMR spectra were acquired in 1 min and 16 scans with a 1.0 s relaxation delay (D1). ^{13}C NMR spectra were obtained using a D1 of 0.5 s and an acquisition time of 0.2 s. Five-hundred accumulations were recorded. $CDCl_3$ or DMSO-d_6 were used as solvent and TMS as internal standard.

Size exclusion chromatography (SEC) analysis was carried out with an Agilent 1200 series system with PLgel 3 μm MIXED-E, PLgel 5 μm MIXED-D, and PLgel 20 μm MIXED-A columns in series, and equipped with an Agilent 1100 series refractive-index detector. Calibration curves were based in polystyrene standards having low molecular weight dispersities. THF was used as the eluent at a flow rate of 1.0 mL/min, the sample concentrations were 5-10 mg/mL, and injection volumes of 100 μL were used.

The kinetics of photopolymerization was determined by real time (RT) FT-IR spectroscopy, employing a Thermo-Nicolet 5700 FTIR device. Epoxy group conversion was followed in real-time upon UV exposure, by monitoring the decrease in the absorbance due to epoxy groups in the region 760-780 cm^{-1}. A medium pressure mercury lamp equipped with an optical guide was used to induce the photopolymerization (light intensity on the surface of the sample of about 5 mW/cm^{-2}). Variation in the experimental conditions (light intensity, humidity and temperature) caused slight differences in the kinetic curves. For this reason all the conversion curves contained in the figures were performed on the same day and under the same conditions and thus good reproducibility was obtained. All the polymerization reactions were performed at room temperature at constant humidity (25-30%). The samples were stored for at least 24 h before properties were evaluated.

The conversion ($x_{UV,FTIR}$) was calculated by monitoring the disappearance of the epoxy band (760-780 cm^{-1}) with the time and using the following equation:

$$x_{UV,FTIR} = 1 - \frac{\bar{A}^t}{\bar{A}^0} \quad (1)$$

where $\bar{A}^t$ is the normalized absorbance of the epoxy band at a given time and $\bar{A}^0$ is the initial absorbance.

Photocalorimetric experiments were performed in order to study the effect of temperature on the photocuring kinetics. The various samples were photocured at different temperatures using a Mettler DSC-821e calorimeter appropriately modified to permit irradiation with a Hamamatsu Lightningcure LC5 (Hg-Xe lamp) with two beams, one for the sample side and the other for the reference side. Samples weighing ca. 3 mg were cured in open aluminium pans in a nitrogen atmosphere. Two scans were performed on each sample in order to subtract the thermal effect of the UV irradiation from the photocuring experiment, each one consisting of 4 min of temperature conditioning, 20 min of irradiation and finally 4 more minutes without UV light. A light intensity of 30 mW/cm^2 (calculated by irradiating graphite-filled pans on only the sample side) was employed. Dynamic postcuring experiments were carried out on a Mettler DSC-822e with a TSO801RO robotic arm, from 0 to 200 ºC at 10 ºC/min in nitrogen atmosphere.

The degree of conversion $x_{UV,post}$ during the photocuring stage was calculated based on the residual heat evolved during the postcuring scan as follows:

$$x_{UV,post} = 1 - \frac{\Delta h_{post}}{\Delta h_{theor}} \quad (2)$$

where Δh_{post} is the heat released during the dynamic post-curing process and Δh_{theor} corresponds to the theoretical heat evolved during complete cure of the formulation.

The gel content was determined on the cured films by measuring the weight loss after 24 h extraction with chloroform at room temperature according to the standard test method ASTM D2765-84.

Dynamic mechanical thermal analyses (DMTA) were performed on a MK III Rheometrics Scientific Instrument at 1 Hz frequency in the tensile configuration. The storage modulus, *E'*, and the loss factor, *tan* δ, were measured from -90 ºC to the temperature at which the rubbery state was attained. The T_g value was assumed as the maximum of the loss factor curve (*tan* δ).

Thermogravimetric analysis (TGA) was performed with a METTLER TGA/SDTA 851 instrument between 30 and 800 ºC at a heating rate of 10 ºC/min in air.

The pendulum hardness (Persoz, ASTM D4366) was measured from the damping of the oscillation of the pendulum. Pendulum hardness values are expressed in seconds and are related directly to the softness of the surface of the sample. The shorter the damping time, the lower is the hardness.

SEM analyses were performed on fracture surfaces of the hybrid systems by using a ZEISS SUPRA™ 40 Field Emission Scanning Electron Microscope (FE-SEM) with an acceleration voltage of 10 kV and WD = 2 mm (Nominal resolution: 1.5 nm).

RESULTS AND DISCUSSION

Synthesis and characterization of HBPpeg

To obtain the hyperbranched polymer used in this work (HBPpeg) we firstly synthesized an aromatic hyperbranched polyester with a degree of branching of 50%[19] following a procedure previously reported in literature.[18] Our first approach to pegylation of the aromatic polyester was the conversion of the monomethyl hydroxyl terminated poly(ethylene glycol) into its chlorinated analogue, to be substituted by phenol groups of the polyester. We used different bases (K_2CO_3 and NaH) but it failed because phenolate groups led to transesterification processes and hydrolysis of the ester groups in the HBP structure.

Thus, we carried out a different procedure in which the terminal phenolic groups were esterified with an acid terminated monomethyl poly(ethylene glycol) synthesized in our laboratory, according to a procedure previously described by Fu *et al.*,[21] who functionalized a dihydroxy terminated poly(ethylene glycol) with succinic anhydride to obtain the diacid derivative.

After modification of aromatic polyester with this acid functionalized monomethyl poly(ethylene glycol), we calculated the degree of modification achieved by means of ^{1}H NMR spectroscopy (see **Figure 1**). We integrated the signal corresponding to protons in orto- to the OH groups before and after modification. By comparison, we could calculate the degree of modification that was estimated to be 90%. The remaining 10% of unmodified phenolic groups will allow the covalent linkage of the HBPpeg structure to the epoxy matrix (as it will be

discussed afterwards) and therefore the complete modification was not only unnecessary, but favourable to our interests.

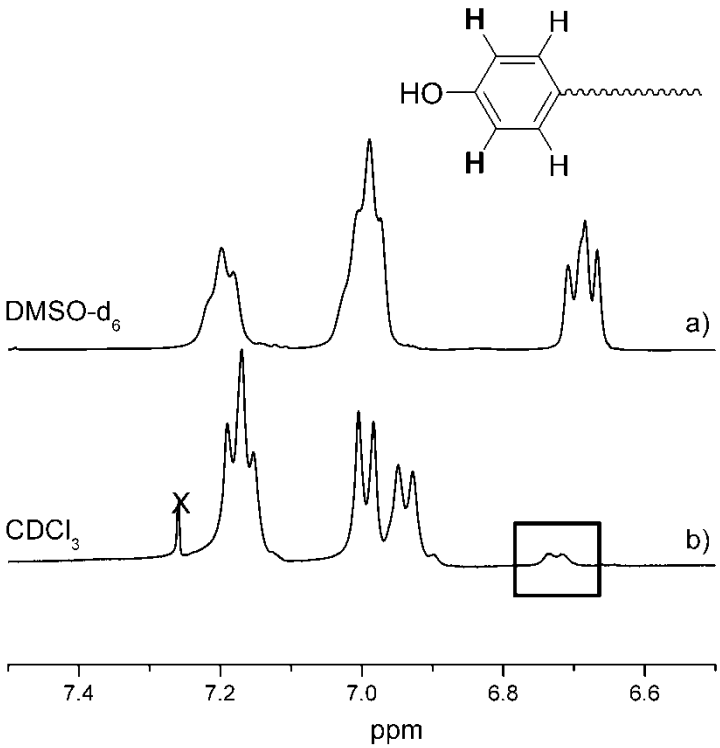

Figure 1 Magnification of the aromatic zone of the ^{1}H NMR spectra of the (a) nonpegylated and (b) pegylated HBP.

Study of the UV photocuring kinetics

Real-time FT-IR analyses were performed on photocurable formulations in order to evaluate the effect of the presence of HBP on UV-curing process. We monitored the disappearance of the epoxy band (760-780 cm^{-1}) with the time and we used Eq. (1) in the experimental part to calculate the conversion.

Figure 2 shows the plot of epoxy conversion as a function of irradiation time for the formulations of CE containing 0, 5, 10 and 15 phr of HBPpeg and 2 phr of PI. As can be appreciated, the addition of this modifier reduces the overall conversion achieved. It is worth noting that in photocuring experiments 100% of conversion is not achieved because the samples vitrify (the ultimate T_g of the materials is much above room temperature). In the case of 15 phr of HBPpeg, however, the sample does not even reach vitrification. For that reason, this formulation was not taken into account for any further experiments performed and we considered the content of 10 phr as the limit of modifier we could use in order to achieve a fully cured material.

A decrease in the curing rate on adding HBPpeg is also appreciated in the first stages of photopolymerization. This decrease in the photocuring rate could be attributed to an increase in the viscosity of the reactive mixture or to the effect of the poly(ethylene glycol) chains on the cationic photoinitaitor. It is well known[22] that ether groups can coordinate cationic active species forming quite stable structures that in that case can reduce the actual number of active species.

It has been reported that interaction of ether groups with the protonated active species formed after photolysis of the photoinitiator leads to inactive complexes that may eventually reactivate with an increase in temperature,[23] and also that ether groups can react with the active chain ends leading to dormant tertiary oxonium cations[24] which may also become active if the temperature is increased. The inability to cure and vitrify of the 15 phr formulation may most likely be related to a depletion of active species by the above explained deactivation mechanisms rather than to a delay caused by viscosity, because there is only a discrete increase in viscosity in respect to the 10 phr formulation, which is able to cure, and the same applies for the general decrease in the curing rate.

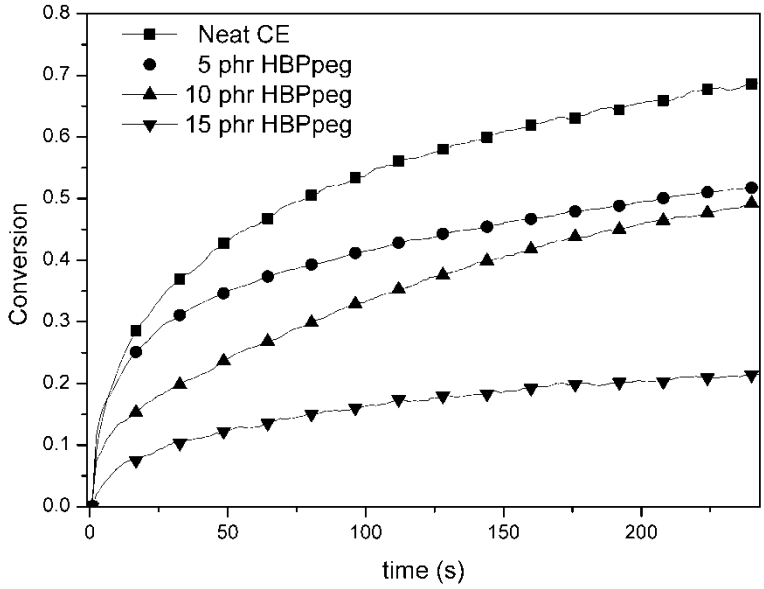

Figure 2 Conversion against irradiation time for the mixtures containing 0, 5, 10 and 15 phr of the HBPpeg calculated by FTIR.

To further investigate the effect of HBPpeg in the kinetics, we performed photo-DSC experiments. By this method we could achieve a better understanding of the effect that the temperature has in the UV-curing process. It was noticed that it was not possible to cure properly the HBPpeg formulations at room temperature in this device because after the photocuring the modified HBPpeg samples were soft and sticky, so it was chosen to work at 50, 70 and 90 °C. Because of the previous FTIR results, it was also decided not to study the formulation with 15 phr of the HBPpeg. **Figure 3** plots the heat evolution of the different formulations at 90 °C.

The photo-DSC measurements are in accordance with the RT-FTIR data. It can be clearly noticed the decelerating effect of HBPpeg additive on the photocuring of CE resin. As pointed out above, this strong effect should be caused by interaction of the HBPpeg ether groups with the protonated active species or the active chain ends. After photocuring at the different temperatures, all samples were able to resume curing in the dynamic dark postcuring at a temperature close to the photocuring temperature, meaning that mixtures with less than 15 phr of modifier were able to photocure up to or very close to vitrification. Therefore, at these temperatures the remaining amount of active species was high enough to sustain the curing process.

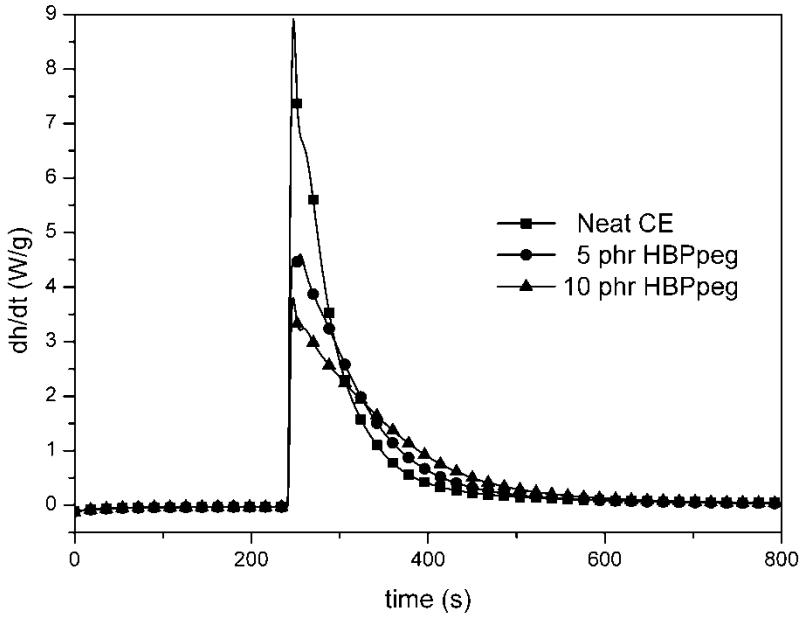

Figure 3 Heat evolution during photocuring at 90 °C of mixtures with different amounts of HBPpeg.

After the dynamic postcuring in the calorimeter, all samples reached complete cure as determined from FTIR spectra. Therefore, the residual heat could be safely used to calculate the degree of conversion after photocuring. **Table 1** shows the calculated degrees of conversion using the residual heat ($x_{UV,post}$) and FTIR spectra after photocuring ($x_{UV,FTIR}$). We can observe a good agreement between the conversions calculated using the two different methodologies and very little influence of the HBPpeg on the achieved degree of conversion, the only appreciable effect is with temperature. Presumably, this plays an important role in the equilibrium between dormant and active species, which limits not only the reaction rate but also the extent of cure at lower temperatures. When the photocuring temperature increases or when a thermal dark postcuring takes place, the dormant species may reactivate thus permitting cure up to vitrification or complete cure.

Table 1 Degree of conversion after photo-DSC calculated from the residual postcuring heat ($x_{UV,post}$) (using a theoretical heat estimated considering 100 kJ/ee for the cycloaliphatic epoxy resin and 126 g/ee) and conversion of epoxy groups from FTIR spectra after photocuring ($x_{UV,FTIR}$).

Sample	$x_{UV,post}$			$x_{UV,FTIR}$		
	50 °C	70 °C	90 °C	50 °C	70 °C	90 °C
Neat CE	0.71	0.80	0.93	0.73	0.86	0.96
5 phr HBPpeg	0.73	0.82	0.94	0.78	0.86	0.96
10 phr HBPpeg	0.60	0.82	0.95	0.67	0.89	0.97

Characterization of the materials

For all the formulations studied (neat CE and CE modified with 5 and 10 phr of HBPpeg) the gel content measured for cured films (see **Table 2**) was quantitative indicating the absence of extractable oligomers, and therefore we can conclude that the modifier is covalently linked to the epoxy network. This is possible because there were still some OH groups present in each

macromolecule that can undergo chain transfer reactions. This behaviour has already been observed when using this type of polymers[17,25] and it has been explained on the basis of the activated monomer mechanism described by Kubisa and Penczek.[26] In this mechanism, OH groups can react with epoxides leading to a different propagation mechanism that competes with the well known active chain-end mechanism. Both mechanisms are depicted in **Scheme 2**. Although it is described that OH groups can accelerate the curing,[27,28] in our case we cannot observe such acceleration effect either because the amount of hydroxyl groups is too little or because the effect of the PEG chains on the propagation is more pronounced.

Table 2 Gel content, thermomechanical data, thermal stability and surface hardness of the materials prepared.

Sample	Gel content (%)	*E'* (MPa)	*Tan δ* (ºC)	$T_{10\%}$ (ºC) [a]	Surface Hardness [b]
Neat CE	99	6.9	178	306	374 ± 17
5 phr HBPpeg	99	7.0	181	325	392 ± 16
10 phr HBPpeg	100	7.2	182	347	422 ± 20

a. Temperature at which the material has lost 10% of its initial weight.
b. Measured as number of oscillations in a Persoz test.

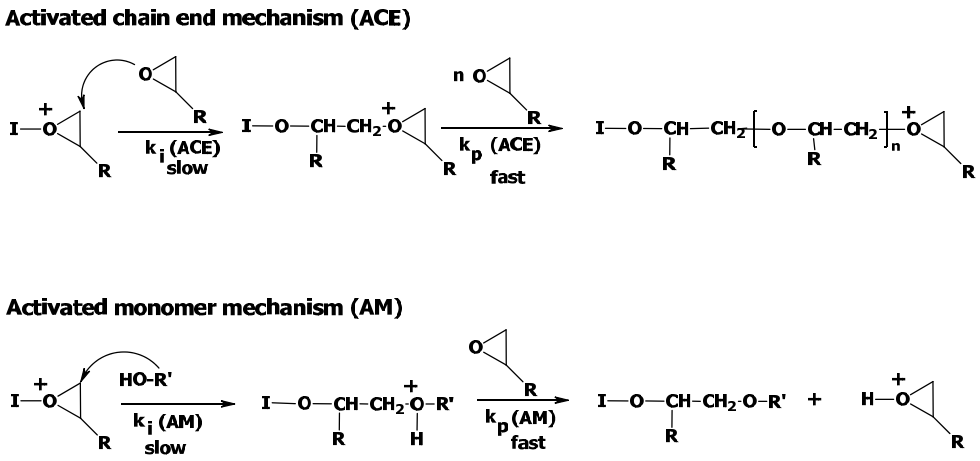

Scheme 2 Propagation mechanisms of epoxide cationic ring opening polymerization.

Dynamic mechanical analysis (DMTA) was performed on cured films. **Figure 4** collects the curves of *tan δ* versus temperature (from -90 to 250 ºC) for all the materials prepared. **Table 2** shows the values of *tan δ* peak (which can be considered as the T_g of the materials) and the values of the relaxed modulus in the rubbery state. It should be mentioned that it was not possible to detect any T_g by DSC, which indicates the rigid characteristics of the prepared thermosets. The temperature of the *tan δ* peak does not change by adding up to 10 phr of HBPpeg to the epoxy resin. This is a typical behaviour of phase separated materials, since the lower T_g of the modifier should decrease the T_g of the material in case of non-separated morphology, as predicted by the Fox equation.[29] We can observe that although the maximum of *tan δ* does not change significantly on increasing the proportion of modifier, there is a decrease in the height and area of the peak indicating a reduction in the flexibility of the network structure and a decrease of its mechanical damping properties.

As seen in **Figure 4** no secondary transition is observed for all the thermosets. Usually, phase separated materials produce a secondary transition, that in our case is expected to be at -38 ºC, which is the T_g of the poly(ethylene glycol) moiety of the HBPpeg. One possible explanation to this fact is the low proportion of pegylated units in the material that leads to a transition of a so low intensity that cannot be detected. The other transition corresponding to the T_g of the HBP at 95 ºC is overlapped with the main peak.

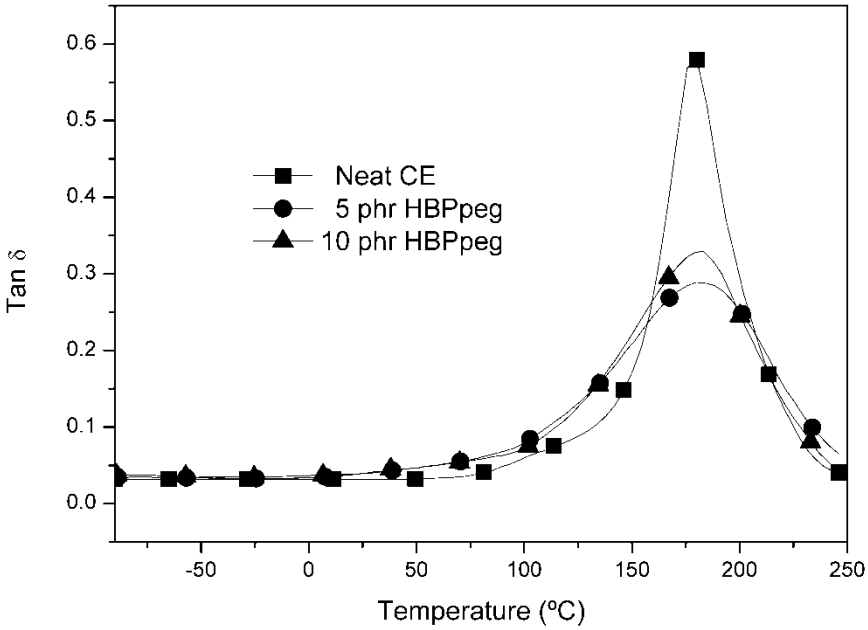

Figure 4 *Tan δ* curves for all the thermosetting materials UV-cured.

It was expected that the amphiphilic character of the polymer, which contains two different parts in its structure with very different solubility (an aromatic hydrophobic part and hydrophilic PEG chains) could lead to self-assembly. For that reason, we decided to observe the morphology of the samples by means of field emission scanning electron microscopy (FE-SEM). We broke under liquid nitrogen free-standing films of each formulation. The FE-SEM observation of the neat CE film showed a completely homogeneous morphology. However, the observation of the films containing 5 or 10 phr of the HBP additive clearly showed the presence of a separated phase, although its dispersion is not homogeneous in the material. As an example **Figure 5** shows the FE-SEM micrographs of the sample with 5 phr of additive. The inherent high speed of the photocuring process and the fact that the modifier becomes covalently linked to the epoxy matrix freeze the particles of the HBPpeg and hinder the adoption of spherical shapes and their homogeneous distribution. This is an interesting result because when phase separation is achieved in epoxy/hyperbranched systems an improvement in mechanical properties can be expected without compromising other thermomechanical properties, as already reported in literature.[30,31]

For some specific applications epoxy materials can be used at high temperatures. Therefore, we decided to investigate the thermal stability of the materials prepared. **Figure 6** shows their thermogravimetric curves obtained under air and **Table 2** collects $T_{10\%}$, defined as the temperature at which the material has lost a 10% of weight. It is evident that the addition of the HBPpeg helps to increase the thermal stability. This can be rationalized on the basis that both

the aromatic rings and the ether bonds present in the structure of the modifier are more thermally resistant than ester groups present in the cycloaliphatic epoxy resin, which can break by a β-elimination process.[32]

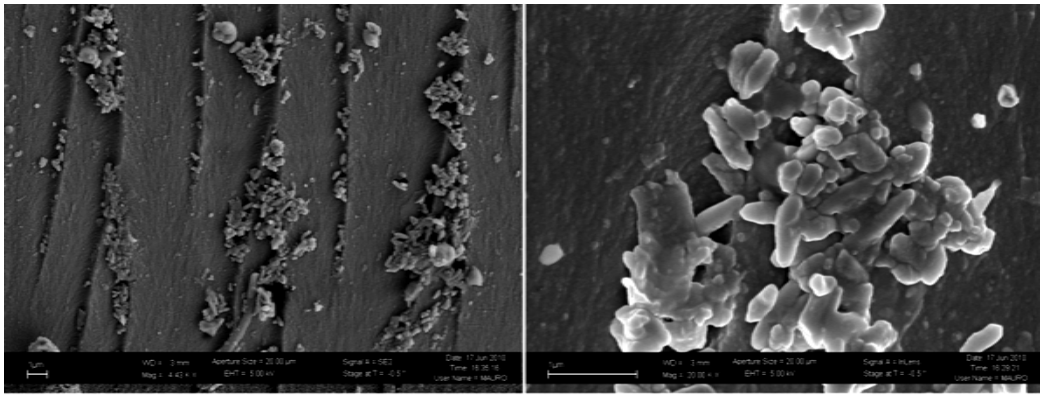

Figure 5 FE-SEM pictures of the breaking of a specimen containing 5 phr of HBPpeg.

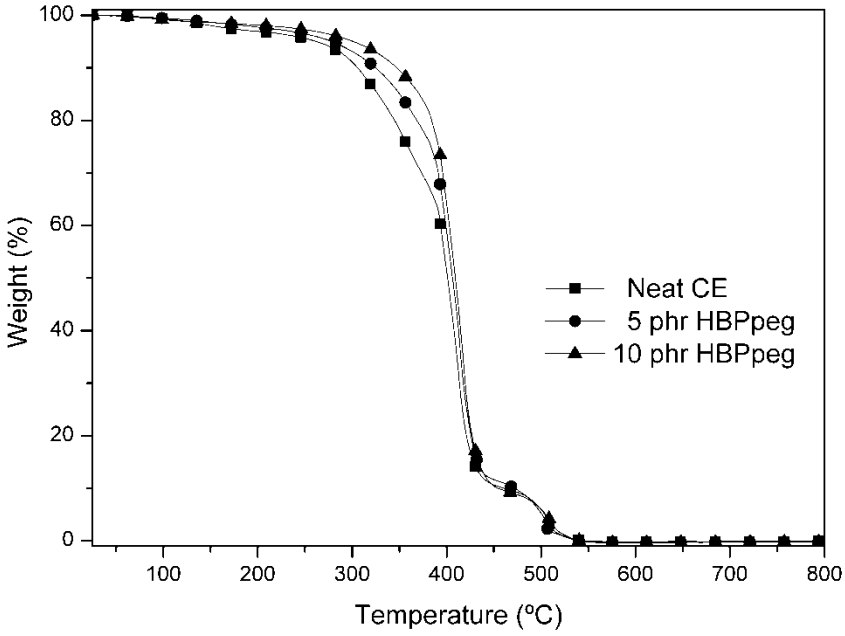

Figure 6 Thermograms obtained under air for all the materials prepared.

Finally, for materials that have to be used as coatings it is important to know their surface resistance. Materials with higher surface hardness can be used for longer and in a wider range of applications. So, to test this property we first coated glass slides with our formulations and then photocured them, and performed a Persoz test. The instrument to perform this test consists of a pendulum which is free to swing on two balls resting on the coated test panel (in our case glass slides). The pendulum hardness test is based on the principle that the amplitude of the pendulum's oscillation will decrease more quickly when supported on a softer surface. In **Table 2** the values obtained in this test (expressed as number of oscillations) together with the uncertainty of the value for all the studied samples are shown. An increase in the surface hardness associated to the addition of the HBPpeg can be observed. This also correlates well

with the increase in the elastic rubbery modulus and the lower height of the *tan* δ peak reported in **Table 2** and **Figure 4**, respectively. A possible explanation is that the presence of some aromatic moieties that can be well ordered help to increase the hardness, especially if they are located in the surface.

CONCLUSIONS

A new pegylated hyperbranched (HBPpeg) could be obtained through a simple methodology consisting in the esterification of a phenol terminated hyperbranched with an acid terminated monomethyl poly(ethylene glycol).

The addition of HBPpeg to a 3,4-epoxycyclohexylmethyl-3',4'-epoxycyclohexyl carboxylate leads to a decrease in the photocuring rate because of the trapping of cationic active species by the poly(ethylene glycol) chains. An increase in the temperature of photocuring allows the mixtures to be fully cured.

The T_g of the materials prepared does not change on adding up to 10 phr of HBPpeg to the formulations significantly, but their mechanical damping properties decrease.

Both the thermal stability and surface hardness were improved on the modified HBPpeg thermosets.

By FE-SEM observation a phase separation in the materials was observed, but the second phase does not lead to an appreciable transition in the dynamomechanical analysis. The presence of a second phase in the micro/nanometric scale can lead to improvements in material's toughness.

ACKNOWLEDGEMENTS

The authors from the Universitat Rovira i Virgili and from Universitat Politècnica de Catalunya would like to thank MICINN (Ministerio de Ciencia e Innovación) and FEDER (Fondo Europeo de Desarrollo Regional) (MAT2008-06284-C03-01 and MAT2008-06284-C03-02) and to the Comissionat per a Universitats i Recerca del DIUE de la Generalitat de Catalunya (2009-SGR-1512). D.F. acknowledges the grant FPU-2008 from the Spanish Government.

REFERENCES

1. C. A. May. *Epoxy Resins. Chemistry and Technology*, 2nd edition. Marcel Dekker, New York, **1988**.

2. Q. Guo, R. Thomann, W. Gronski, T. Thurn-Albrecht. *Macromolecules* **2002,** *35,* 3133.

3. P. M. Lipic, F. S. Bates, M. A. Hillmyer. *J. Am. Chem. Soc.* **1998,** *120,* 8963.

4. J. M. Dean, R. B. Grubbs, W. Saad, R. F. Cook, F. S. Bates. *J. Polym. Sci. Part B: Polym. Phys.* **2003,** *41,* 2444.

5. N. Schroder, L. Konczol, W. Doll, R. Mülhaupt. *J. Appl. Polym. Sci.* **2003,** *88,* 1040.

6. E. Serrano, A. Tercjak, C. Ocando, M. Larrañaga, M. D. Parellada, S. Corona-Galván, D. Mecerreyes, N. E. Zafeiropoulos, M. Stamm, I. Mondragon. *Macromol. Chem. Phys.* **2007,** *208,* 2281.

7. J-P. Pascault, H. Sauterau, J. Verdu, R. J. J. Williams. *Thermosetting Polymers*. Marcel Dekker, New York, **2002**.

8. B. Voit. *J. Polym. Sci. Part A: Polym. Chem.* **2000,** *38,* 2505.

9. I. Blanco, G. Cicala, C. Lo Faro, O. Motta, G. Recca. *Polym. Eng. Sci.* **2006,** *46,* 1502.

10. L. Boogh, B. Pettersson, J. A. E. Månson. *Polymer* **1999,** *40,* 2249.

11. D. Ratna, G.P. Simon. *Polymer* **2001,** *42,* 8833.

12. J. Xu, H. Wu, O.P. Mills, P. A. Heiden. *J. Appl. Polym. Sci*. **1999,** *72,* 1065.

13. X. L. Xie, S. C. Tjong, R. K. Y. Li. *J. Appl. Polym. Sci.* **2000,** *77,* 1975.

14. J. P. Fouassier, J. F. Rabek. *Radiation Curing in Polymer Science and Technology I–IV*, Elsevier, London, **1993**.

15. D. Foix, M. Erber, B. Voit, A. Lederer, X. Ramis, A. Mantecón, A. Serra. *Polym. Degrad. Stab.* **2010,** *95,* 445.

16. M. Sangermano, A. Priola, G. Malucelli, R. Bongiovanni, A. Quaglia, B. Voit, A. Ziemer. *Macromol. Mater. Eng.* **2004,** *289,* 442.

17. J. S. Moore, S. I. Stupp. *Macromolecules* **1990,** *23,* 65.

18. F. Schallausky, M. Erber, H. Komber, A. Lederer. *Macromol. Chem. Phys.* **2008,** *209,* 2331.

19. D. Schmaljohann, H. Komber, B. Voit. *Acta Polym.* **1999,** *50,* 196.

20. D. Hölter, A. Burgath, H. Frey. *Acta Polym.* **1997,** *48,* 30.

21. J. Fu, J. Fiegel, J. Hanes. *Macromolecules* **2004,** *37,* 7174.

22. C. J. Pedersen, H. K. Frensdorff. *Angew. Chem. Int. Ed. Engl.* **1972,** *11,* 16.

23. J. V. Crivello. *J. Polym. Sci. Part A: Polym. Chem.* **2006,** *44,* 3036.

24. L. Matéjka, P. Chabanne, L. Tighzert, J. P. Pascault. *J. Polym. Sci Part A: Polym. Chem.* **1994,** *32,* 1447.

25. M. Sangermano, A. Di Gianni, R. Bongiovanni, A. Priola, B. Voit, D. Pospiech, D. Appelhans. *Macromol. Mater. Eng.* **2005,** *290,* 721.

26. P. Kubisa, S. Penczek. *Prog. Polym. Sci.* **1999,** *24,* 1409.

27. J. V. Crivello, S. Liu. *J. Polym. Sci. Part A: Polym. Chem.* **2000,** *38,* 389.

28. J. M. Morancho, A. Cadenato, X. Ramis, X. Fernández-Francos, J. M. Salla. *Thermochim. Acta* **2010,** *510,* 1.

29. R. Mezzenga, J. A. E. Månson. *J. Mater. Sci.* **2001,** *36,* 4883.

30. J. Zhang, Q. Guo, B. Fox. *J. Polym. Sci. Part B: Polym. Phys.* **2010,** *48,* 417.

31. G. Cicala, A. Recca, C. Restuccia. *Polym. Eng. Sci.* **2005,** *45,* 225.

32. L. Wang, H. Li, C.P. Wong. *J. Polym. Sci. Part A: Polym. Chem.* **2000,** *38,* 3771.

5.3 DGEBA thermosets modified with an amphiphilic star polymer. Study on the effect of the initiator on the curing process and morphology

D. Foix[1], E. Jiménez-Piqué[2], X. Ramis[3], A. Serra[1]

[1] Department of Analytical and Organic Chemistry, University Rovira i Virgili, Marcel.li Domingo s/n, 43007 Tarragona, Spain

[2] Department of Material Science and Metallurgic Engineering, Universitat Politècnica de Catalunya, Av. Diagonal 647, 08028 Barcelona, Spain

[3] Laboratory of Thermodynamics, ETSEIB, University Politècnica de Catalunya, Av. Diagonal 647, 08028 Barcelona, Spain

ABSTRACT

We have studied the preparation of a new class of epoxy thermosets from diglycidyl ether of bisphenol A (DGEBA) modified with an amphiphilic star polymer (SP), initiated either by 1-methyl imidazole or ytterbium triflate, anionic and cationic initiators respectively. The curing process has been characterized by means of DSC, FTIR and rheology. The last technique allowed us to monitor the shrinkage during curing. DMTA provided valuable information about the transitions of the materials, as well as their modulus in the rubbery state. Cationic systems produce monomodal *tan* δ relaxations, whereas anionics presented a shoulder in this peak. By means of electron microscopy we could observe phase separation in the case of cationically initiated systems while in the anionic initiated materials zones with different electronic densities were appreciated. Finally, Young's modulus and hardness of the materials were determined by nanoinentation.

INTRODUCTION

Epoxy resins are one of the most used polymers in the field of coatings. They are versatile materials that present high chemical resistance and good mechanical and thermal properties.[1,2] However, they present some drawbacks such as their lack of reworkability (they cannot be removed after their useful life time is finished), but the main problem they present is that they are inherently fragile, which limits their range of application. During the past decades considerable efforts have been made to improve toughness of epoxy thermosets.[3-6] In most cases, the strategies followed lead to the loss of some of the good properties of the resin, especially in terms of rigidity and glass transition.

Recently, a lot of attention has been paid to the formation of nanostructured epoxy coatings. The final goal of this strategy is the improvement of the toughness of the epoxy thermoset without compromising other properties. In the literature it is possible to find many different approaches. One strategy is the use of linear block copolymers. Lipic *et al.*[7] described the phase separation of a polyethylene oxide/polyethylene-propylene copolymer in an epoxy matrix. Ryan *et al.*[8] have used different block copolymers to induce nano phase separation in epoxy resins. In some cases one block was miscible with the resin while the other not and the separation appears on preparing the reacting mixture. In other copolymers both blocks where miscible but one of them was reactive towards the resin, and then the phase separation occurred during the curing reaction by reaction induced phase separation mechanism. Also Fan *et al.*[9] obtained a nanostructured epoxy resin using a triblock copolymer containing poly(dimethyl siloxane), poly(ε-caprolactone) and poly(styrene) to modify DGEBA.

More recently, Meng *et al.*[10] have used a star-shaped block copolymer and have obtained phase separation in DGEBA matrix, and even increasing the T_g of the resulting thermosets.

Hyperbranched polymers have also been used as a cheaper alternative to obtain phase separation in epoxy. For example, the use of a hyperbranched polyester with terminal long aliphatic chains showed phase separation in the cationic homopolymerization of DGEBA.[11]

However, not only the additive used but also the polymerization procedure seems to be important in the induction of micro/nano phase separation. For example, Ratna *et al.*[12] reported the formation of phase separation in DGEBA/Boltorn H30 formulations cured by diamines, while in $Yb(OTf)_3$ initiated cationic curing no phase separation occurred.[13]

Thus, in the present article we have studied the thermal crosslinking of DGEBA in the presence of an amphiphilic star polymer that have proved to induce phase separation in the UV cationic photopolymerization of a commercially available cycloaliphatic epoxy resin.[14] We have studied both cationic and anionic curing processes, and finally we have observed the difference in the morphology obtained in both cases, as well as the differences on properties such as Young's modulus, hardness or the glass transition temperature.

EXPERIMENTAL PART

Materials

The star polymer (SP) used was synthesized as previously described,[14] and had a molecular weight ($\bar{M}_n$) of 24,000 g/mol, 2.0 of molecular weight dispersion ($Đ_M$) and presented two T_gs at -38 ºC corresponding to the poly(ethylene glycol) arms and at 95 ºC corresponding to the aromatic core. The structure of the SP is depicted in **Scheme 1**. The average number of polyethylene glycol arms per molecule is 90. The calculated remaining amount of hydroxyls groups per molecule is 4.

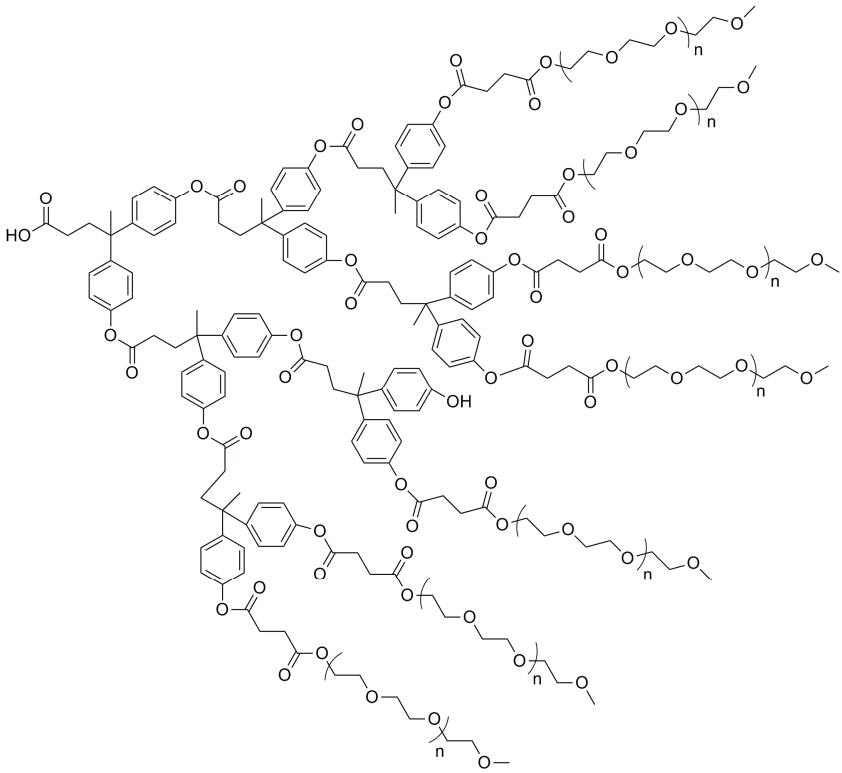

Scheme 1 Idealized chemical structure of the star polymer used.

Diglycidyl ether of Bisphenol A (DGEBA) Epitoke Resin 827 was provided by Shell Chemicals with an epoxy equivalent of 182 g/ee and was dried before use. Ytterbium triflate ($Yb(OTf)_3$) and 1-methyl imidazole (MI) were purchased from Aldrich and used as received.

Sample preparation

The corresponding amount of SP was dissolved in the epoxy resin heating at 80 °C and then was allowed to cool down. In the case of the samples containing MI it was added directly to the mixture at room temperature. For the samples containing $Yb(OTf)_3$ acetone was added to dissolve it and then the mixtures were put under vacuum for 1 hour to eliminate it. Mixtures were stored at -25 °C before using them. **Table 1** shows the proportion of each reactive used in the formulations studied.

The specimens for mechanical testing and thermal and mechanical analyses were cured in metal templates coated with silicon oil to prevent the resin stacking to the mold. The samples containing MI were cured at 120 °C for 2 hours and post-cured at 150 °C for 1 hour whereas the samples containing $Yb(OTf)_3$ were cured 5 hours at 160 °C and post-cured 1 hour at 180 °C. The complete curing was assured by performing a DSC experiment of the cured materials.

Table 1 Quantities in grams used in the preparation and molar amounts of reacting group for all the formulations studied.

Sample	DGEBA		HBP		MI		$Yb(OTf)_3$	
	mmol [a]	g	mmol [b]	g	mmol [c]	g	mmol [c]	g
DGEBA MI	5.5	1	-	-	0.36	0.03	-	-
5 phr SP MI	5.5	1	0.008	0.05	0.36	0.03	-	-
10 phr SP MI	5.5	1	0.016	0.10	0.36	0.03	-	-
DGEBA Yb	5.5	1	-	-	-	-	0.016	0.01
5 phr SP Yb	5.5	1	0.008	0.05	-	-	0.016	0.01
10 phr SP Yb	5.5	1	0.016	0.10	-	-	0.016	0.01

a. mmols of epoxide.
b. mmols of hydroxyl.
c. mmol of initiator.

Characterization Techniques

Calorimetric studies were carried out on a Mettler DSC-821e thermal analyzer in covered Al pans under N_2. The calorimeter was calibrated using an indium standard (heat flow calibration) and an indium-lead-zinc standard (temperature calibration). The samples weighed approximately 7 mg. In the dynamic curing process the degree of conversion by DSC (DSC) was calculated as follows:

$$x_{DSC} = \frac{\Delta h_T}{\Delta h_{tot}} \quad (1)$$

where Δh_T is the heat released up to a temperature T, obtained by integration of the calorimetric signal up to this temperature, and Δh_{tot} is the total reaction heat associated with the complete conversion of all reactive groups. The kinetic studies were performed at heating rates of 2, 5, 10 and 15 °C/min in N_2 atmosphere. The precision of the given enthalpies is ± 3%.

The glass transition temperature for each material (T_g) was calculated after a complete dynamic curing, by means of a second scan, as the temperature of the half-way point of the jump in the heat capacity when the material changed from the glassy to the rubbery state. The precision of the determined temperatures is estimated to be ± 1 °C.

An FTIR spectrophotometer FTIR-680PLUS from Jasco with a resolution of 4 cm^{-1} in the absorbance mode was used to monitor the isothermal curing process at 120, 150 and 180 ºC. This device was equipped with an attenuated total reflection (ATR) accessory with thermal control and a diamond crystal (Golden Gate heated single-reflection diamond ATR, Specac-Teknokroma). The disappearance of the absorbance peak at 915 cm^{-1} was used to monitor the epoxy equivalent conversion. The peak at 1508 cm^{-1} of the phenyl group was chosen as an internal standard. Conversion of the epoxy was determined by the Lambert-Beer law from the normalized change of absorbance at 915 cm^{-1}.

$$x_{IR} = 1 - \frac{\bar{A}^t}{\bar{A}^0} \quad (2)$$

where $\bar{A}^0$ and $\bar{A}^t$ are, respectively, the normalized absorbance of the epoxy group before curing and after a reaction time t.

Rheological measurements were carried out in the parallel plates (geometry of 25 mm) mode with an ARG2 rheometer (TA Instruments, UK, equipped with a Peltier system). The gelation time was determined by setting the device in time sweep and multiwave oscillation mode. Experiments were performed isothermally at 80 ºC (MI) or at 110 ºC (ytterbium triflate). As the viscosity of the system changes significantly during the curing process, a control program was used in which the oscillation amplitude diminishes with an increase in the applied stress. By doing so, the curing process can be characterized in the whole range of conversion. The instrument worked under controlled gap conditions, with a normal force of 0 N and a tolerance of 0.01 N, in order to monitor the shrinkage during the curing process using the following equations:[15]

$$Shrinkage\ (t) = -\left[\left(1 + \frac{1}{3} \times \frac{h_t - h_0}{h_0}\right) - 1\right] \times 100 \quad (3)$$

where h_t is the gap at a certain time and h_0 is the initial gap.

Gel time was taken as the point where δ is independent of frequency.[16] The conversion at the gelation (α_{gel}) was determined by overlapping the *tan* δ curve with a conversion curve obtained from an isothermal DSC experiment at the same temperature of the rheological experiment.

Dynamic mechanical thermal analysis (DMTA) was performed in a TA DMA 2928 dynamic analyzer operating in three point bending mode at 1 Hz. The storage modulus *(E')* and *tan* δ were measured from -90 to 220 ºC at 3 ºC/min on prismatic rectangular specimens (ca. 10 x 5 x 1.5 mm^3).

The cryofracture area of the specimens was observed by scanning electron microscopy (SEM). The samples were metalized with gold and observed with a Jeol JSM 6400 with 3.5 nm resolution.

Transmission electron microscopy (TEM) was performed with a Jeol 1011 microscope. Samples were prepared using an ultramicrotome at room temperature and were observed without staining them.

Thermogravimetric analysis (TGA) was performed with a METTLER TGA/SDTA 851 instrument between 30 and 800 ºC at a heating rate of 10 ºC/min in N_2 (100 cm^3/min measured in normal conditions).

Nanoindentation studies were performed with a Berkovich tip with its function area calibrated against fused silica standard, at a strain rate of 0.05 s^{-1} in an equipment with continuous stiffness measurement at 45 Hz and 2 nm amplitude. The hardness and elastic modulus data presented

are the result of an average of 16 indentation experiments analyzed with the Oliver and Pharr method.[17]

RESULTS AND DISCUSSION

Differential Scanning Calorimetry Studies

We studied all curing formulations by means of DSC. **Table 2** collects the values of enthalpy of the curing exotherm per gram of sample as well as per epoxy equivalent. For the anionic system (the one initiated with MI) while the enthalpy is reduced on adding SP the enthalpy per epoxy equivalent is maintained indicating that the complete curing is reached for all samples. For the $Yb(OTf)_3$ initiated cationic system a slight decrease on this value was observed, but in any case one can consider the samples were completely cured since all values were around 90 kJ/ee.[18]

Table 2 Calorimetric data obtained from DSC for all the studied formulations.

Sample	Tp [a] (ºC)	Δh (J/g)	Δh (kJ/ee)	T_g [b] (ºC)
DGEBA MI	139	503	92	167
5 phr SP MI	137	480	92	159
10 phr SP MI	137	435	89	145
DGEBA Yb	177	511	93	138
5 phr SP Yb	188	462	89	113
10 phr SP Yb	224	418	85	99

a. Temperature of the curing exotherm's peak in a dynamic scan at 10 ºC/min.
b. Glass transition temperature determined after a second scan at 20 ºC/min.

By performing a second scan at 20 ºC/min from 30 to 200 ºC of the cured samples the T_g of the resulting polymers was determined. The first thing one can see is that the T_g*s* are higher for the thermosets initiated by MI. This result has been observed in previous works[20] and may be related with the fact that lanthanide triflates could induce the formation of macrocyclic structures by back-biting processes that reduce the crosslinking density of the network and lead to plasticization of the thermoset.[20] Regardless of the initiation mechanism (cationic or anionic) the addition of the SP results in a decrease in the T_g, although this is less pronounced in the case of MI initiated systems.

Using equation 1 we plotted the conversion against the temperature for all the formulations (see **Figure 1**). First of all, it is evident that the anionic initiator allows curing faster and at lower temperatures in comparison to $Yb(OTf)_3$. The addition of SP in the case of MI shows a slight increase in the curing rate which can be attributed to the presence of some OH groups in the structure of the additive, which have demonstrated to speed up the anionic curing.[21]

A similar accelerative effect of the OH groups has also been described in cationic systems[22] and has been explained because of the concurrence of AM mechanism.[23] However, in the cationic curing we observed a clear decelerative effect in the presence of the additive. This can be related to the oxophilicity of the ytterbium salt, which can strongly coordinate with the ether groups of the poly(oxyethylene) arms and therefore reducing the effective proportion of the initiator. Therefore, as seen in the figure, on increasing the amount of SP this effect is more pronounced and it is difficult to cure formulations with more than 10 phr of SP with this initiator. In previous studies with this SP in the UV cationic photocuring of a cycloaliphatic epoxy resin we observed a similar behavior[14] although in that case the initiator was an aryl alkyl sulfonium salt. In general, we can anticipate that this SP will show this effect in most cationic systems, since they are usually initiated by Lewis acids, which are well known for coordinating with oxygen.

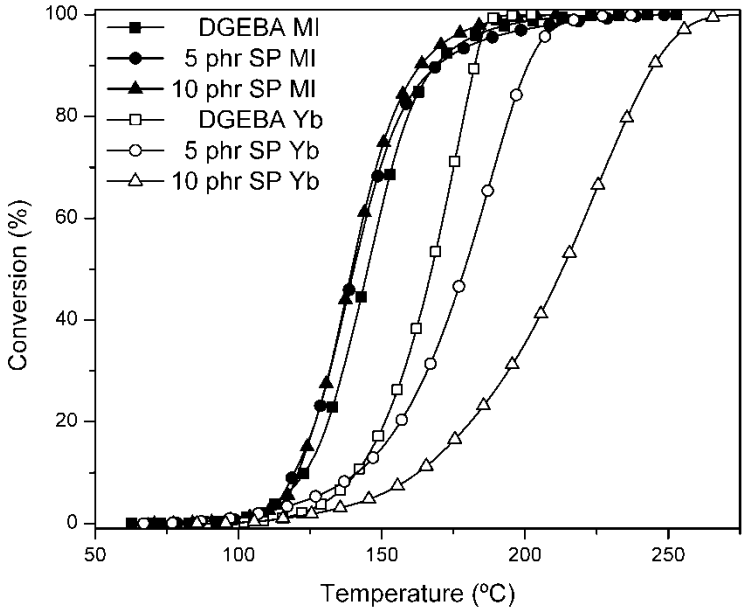

Figure 1 Conversion against temperature plots for all the studied formulations.

By working at different heating rates we were able to determine the activation energy of the curing process. **Figure 2** shows the plot of activation energy against conversion for all of them. The first noticeable fact of the plot is the higher activation energies required for the reaction in the case of using ytterbium triflate. In the 10 phr SP Yb formulation not only is the *Ea* higher, but also it increases with the conversion. This indicates that the decelerative effect is more pronounced at higher conversions. For the anionic MI system no significant differences can be appreciated for all the studied formulations. These results are essentially in agreement the reaction rates shown in **Figure 1**.

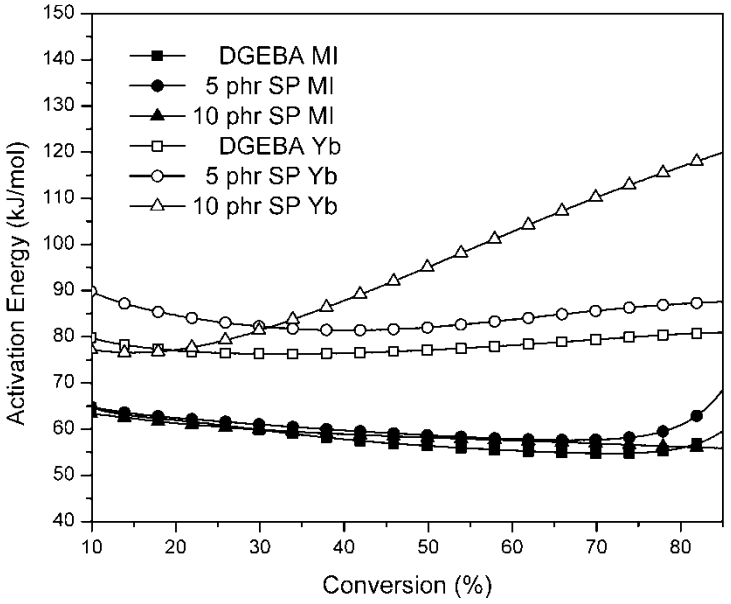

Figure 2 Activation energy against conversion plots for all the studied formulations.

Infrared Spectroscopy Studies

The isothermal study of the curing systems was performed by FTIR. Samples were cured at different temperatures and the disappearance of the band at 910 cm^{-1} corresponding to the epoxy group was monitored. The temperatures selected are higher for the curing with $Yb(OTf)_3$ as initiator according to what is observed in the dynamic DSC measurements.

Figure 3 shows the conversion against time plots for the MI initiated systems. It can be seen that when working at 120 °C the curing rate is nearly the same in all cases but only for the sample with 10 phr of SP the complete curing is reached. One explanation to this fact is that for the neat and 5 phr SP samples vitrification takes place and the curing cannot finish while it is not the case for the 10 phr sample since it has a lower T_g. On increasing the temperature up to 150 °C the curing was obviously quicker but the quantitative curing was reached in all cases, confirming the fact that at lower temperatures the materials vitrify.

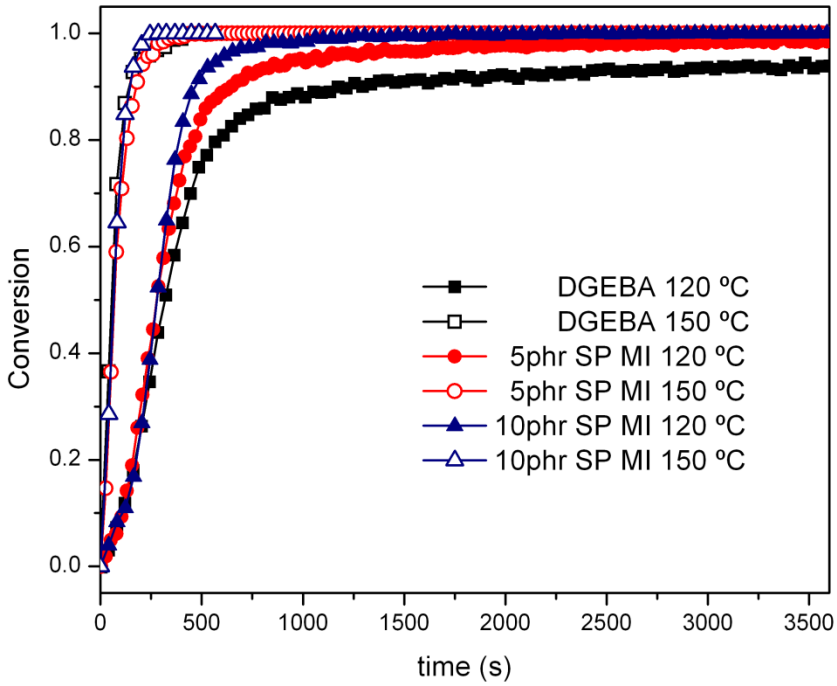

Figure 3. Conversion against time plots at 120 and 150 °C for the formulations initiated with MI.

Figure 4 plots the conversion against time for the $Yb(OTf)_3$ initiated curings. In that case, the only difference between curing at 150 or at 180 °C is the time required to achieve the completion since both temperatures are above the final T_g of the materials and therefore no vitrification takes place during curing. Similarly to that observed by DSC in the dynamic experiments, the formulations containing SP cure slower than the neat system since the amount of effective initiator is reduced due to the coordination of the ytterbium salt with the ether groups of the additive. The decrease in the curing rate is proportional to the amount of SP. For the case of the sample containing 10 phr of SP around 2 hours are required to complete the curing even working at 180 °C.

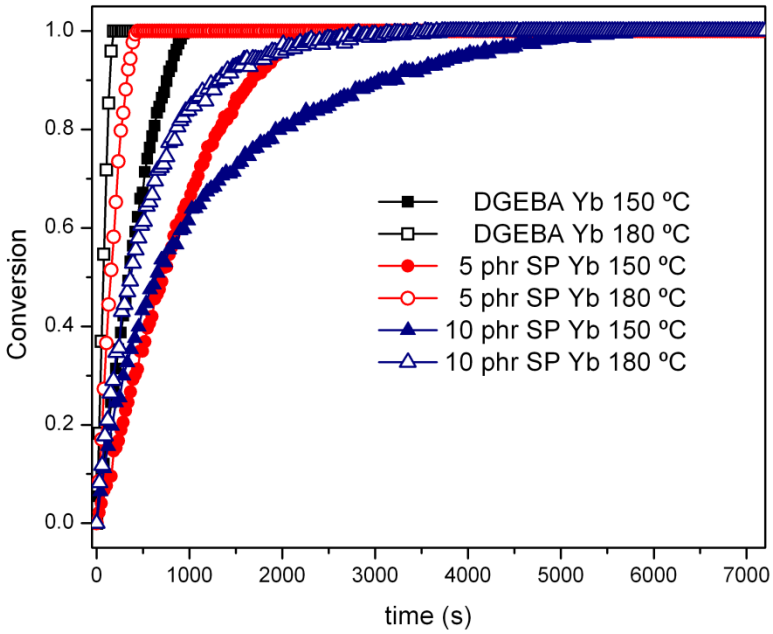

Figure 4. Conversion against time plots at 150 and 180 °C for the formulations initiated with $Yb(OTf)_3$.

Rheology

Rheology is a very powerful technique that can provide a lot of information about the starting mixture as well as of the curing process. **Figure 5** shows the plot of complex viscosity against frequency for mixtures of DGEBA containing 0, 5 or 10 phr of SP at 80 °C. We did not add the initiator to avoid the curing reaction during the viscosity measurements.

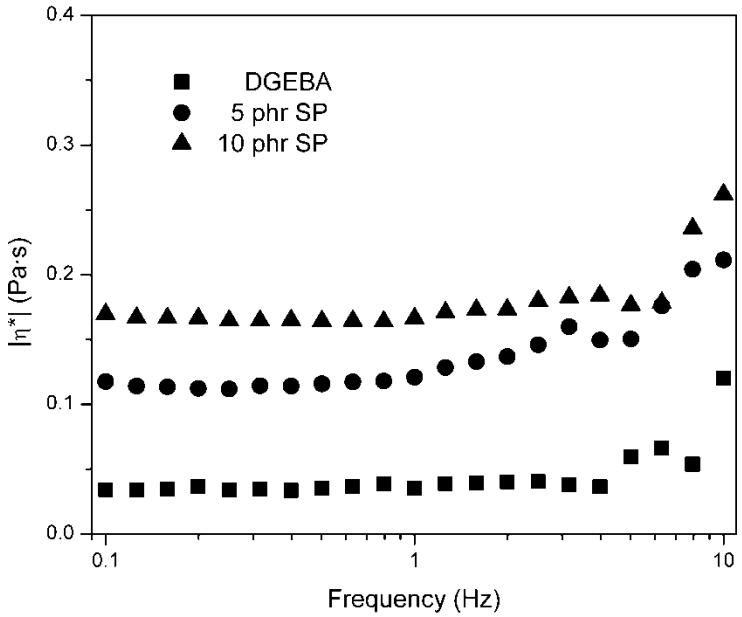

Figure 5 Complex viscosity against frequency plots for mixtures of 0, 5 and 10 phr of SP in DGEBA.

First of all one can see that the measured viscosity is independent of the frequency within the linear viscoelasticity range for all the formulations, indicating that they all behave like Newtonian liquids. This evidences that the SP is perfectly dissolved in the resin since if there were dispersed particles in the mixture could yield to the loss of this behavior. One can also appreciate an increase in the viscosity with the addition of SP although this is not very pronounced up to 10 phr (see **Table 3**). We would like to point out that since the viscosity is proportional to the complex viscosity according to the Cox-Merz rule[24] it is possible to do this comparison to evaluate the processability.

Table 3 Complex viscosity, gel time, gel conversion an shrinkage data for all the studied formulations.

Sample	|η*| (Pa·s)	Gel time (min)	α_{gel} (%)	A [a]
DGEBA MI	0.047	27.1	32	0.092
5 phr SP MI	0.121	34.2	43	0.115
10 phr SP MI	0.166	43.0	54	0.151
DGEBA Yb	0.047	28.5	27	0.055
5 phr SP Yb	0.121	40.2	25	0.081
10 phr SP Yb	0.166	70.8	24	0.113

a. Slope of the straight line of the shrinkage versus conversion plot.

By means of this technique, we also investigated the gelation process which is very important for the understanding of the curing process. The gel point is defined as the point at which the first thermoset network is formed ($\bar{M}_w \rightarrow \infty$).[16] The values of gelation time and conversion at the gel point are collected in **Table 3**. In the case of MI initiated curing the addition of SP retards the gelation process. This is an advantage for the applicability of the resin. Consequently, as the gelation is retarded and the curing rate is very similar for the three systems (as demonstrated by DSC and FTIR); the conversion at gelation is also increased (going from 32% to 54%). For the cationic system the gelation time is also increased but the conversion achieved at that point remains unaltered. In this case, as the curing rate is reduced so much with the addition of the SP, it takes more time to reach the conversion required to gel, but this conversion is the same regardless of the proportion of SP in the formulation.

Shrinkage during curing is also a very important parameter in thermosetting coatings. There are many cases in the literature where the addition of dendritic polymers to epoxy resins results in a reduction of the global shrinkage.[13,25] In the present study, we investigated this phenomenon by means of rheology. By controlling the gap distance between plates during the curing process and using equation 3 it is possible to obtain graphics of shrinkage against time.[26] However, the values of shrinkage after gelation obtained are not comparable since the gelation time and conversions, and the values of the T_gs are very different between systems. For that reason, we decided to plot the shrinkage against conversion,[27] obtained in a DSC isothermal scan. **Figure 6** is an example of this plot for the neat DGEBA MI and 10 phr SP MI systems. Due to experimental limitations the shrinkage cannot be monitored before gelation. One can appreciate that right after gelation starts, a straight line appears. Estimating the slope of this curve allowed us comparing all the systems. These values are collected in **Table 3**. Comparing the values of the neat systems one can say that the shrinkage is more pronounced in the case of MI initiated materials. The differences cannot be attributed to the different temperatures used since, as

described in the literature, the value of the slope is independent of the curing temperature.[27] The addition of SP increases the slope value, this is the shrinkage after gelation, in both cases but in $Yb(OTf)_3$ initiated thermosets the value with 10 phr of SP is more than twice as much as the neat system.

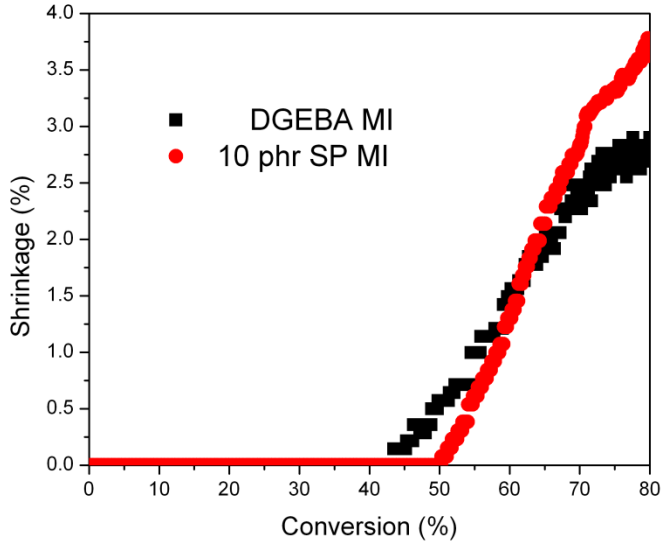

Figure 6 Shrinkage versus conversion curves for the DGEBA MI and 10 phr SP MI samples.

In previous studies, we demonstrated that the presence of OH terminal groups in dendrimeric molecules used as epoxy modifiers led to a reduction of the global shrinkage.[13] The explanation to this fact is that, on reacting, the intramolecular hydrogen bonding association is reduced and these molecules expand. The SP used in the current study has a very small amount of OH in its structure and therefore no expansion takes place.

Dynamic thermal mechanical analysis

DMTA can provide us with information about the transitions of the cured material. The *tan δ* plots of the samples containing MI as curing initiator are shown in **Figure 7a**. The biggest peak is associated to the T_g of the materials, and the values of these maxima are collected in **Table 4**.

Table 4 Dynamic mechanic and thermal data for all the studied thermosets.

Sample	*tan δ* [a] (ºC)	*E'* [b] (MPa)	*TA* [c] (a.u.)	$T_{5\%}$ [d] (ºC)	T_{max} [e] (ºC)	Char yield [f] (%)
DGEBA MI	176	77	14.72	387	430	11.8
5 phr SP MI	174	76	16.69	393	432	12.1
10 phr SP MI	158	70	21.33	391	435	11.7
DGEBA Yb	155	42	18.62	301	335	16.8
5 phr SP Yb	135	37	23.13	315	352	14.3
10 phr SP Yb	115	28	28.19	319	367	14.6

a. Maximum of the *tan δ* main peak at 3 ºC/min.
b. *E'* at *tan δ* + 50 ºC.
c. Normalized area of the *tan δ* main peak.
d. Temperature of the loss of 5% of weight in a TGA under nitrogen at 10 ºC/min.
e. Temperature of the maximum weight loss rate in a TGA under nitrogen at 10 ºC/min.
f. Residue at 800 ºC in a TGA under nitrogen at 10 ºC/min.

On can see how on adding SP the T_g slightly decreases. All the curves also present a peak below -50 °C which has been attributed to a β-transition associated to the aromatic rings of the resin.[16] In the case of adding SP a shoulder in the α transition appears at around 90 °C and becomes bigger on increasing the proportion. This could be related to the presence of zones with different degrees of crosslinking, promoted by the presence of the SP or to a possible phase separation of the SP within the epoxy matrix. To go deeper in the study of the morphology, we performed electron microscopy analysis and the results are discussed into detail in the next section.

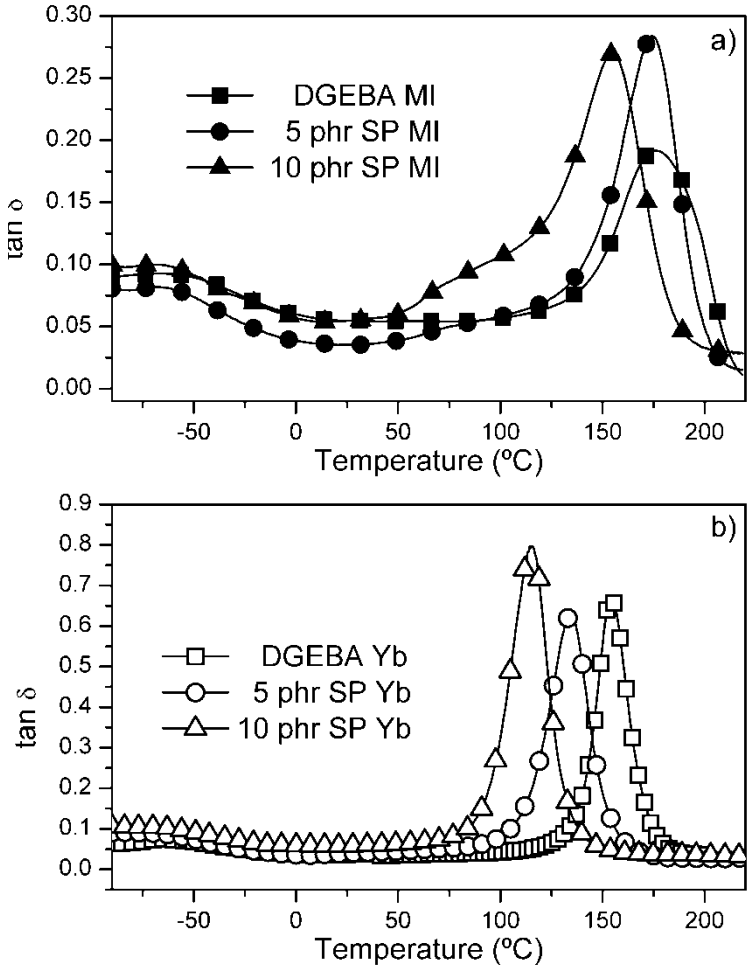

Figure 7 DMTA curves for the samples initiated by MI (a) and by $Yb(OTf)_3$ (b).

In the case of using $Yb(OTf)_3$ as initiator, as can be seen in **Figure 7b**, only two peaks are appreciated: the one at low temperature corresponding to the β-transition and the main peak due to the T_g of the thermoset. This could indicate that no phase separation occurs but it is also possible that the T_g of the resulting thermoset overlaps with the T_g of the SP. What can be clearly appreciated is that the addition of SP reduces the T_g (see **Table 4**).

The area of the *tan δ* is related to the damping properties. An increase in the area is related to an improvement of them. So, as seen in **Table 4**, the addition of SP increases the area of the peak in both systems (anionic and cationic).

By means of DMTA we could also determine the modulus of the materials in the rubbery state. **Table 4** shows the values for all the thermosets. We can see how the addition of the SP reduces this modulus due to the flexible structure of the PEG moiety introduced and the reduction of the crosslinking density. On comparing the values between the anionic and cationic materials, the use of MI as initiator allows obtaining higher values of E', maybe as result of a more crosslinked structure derived from a more efficient initiation.

Morphology

The amphiphilic character of the SP, with an aromatic core (hydrophobic) and branches of polyethylene glycol in the surface (hydrophilic) has proved to yield a phase separated morphology in similar systems, when working in the UV cationic curing of a cycloaliphatic epoxy resin.[14] In our case, the curing system is different since we are working in thermal conditions, inherently slower if compared to UV initiated polymerization. By means of Scanning Electron Microscopy (SEM) of cryofractured specimens, we observed the morphology of the thermosets. **Figure 8** shows the SEM pictures of the a) DGEBA MI and b) 10 phr SP MI samples at 20000 magnifications. The neat sample presents a globular morphology already described for these materials[28,29] and the addition of SP allows eliminating it and no phase separation could be appreciated. Thus, we decided to use Transmission Electron Microscopy (TEM), a more sensitive technique, in order to observe different zones within the material that could explain the shoulder in the *tan* δ peak observed by DMTA. **Figure 9** shows the TEM micrograph of the sample 10 phr SP MI. The morphology is non homogeneous, probably due to the presence of zones with different degree of crosslinking, promoted by the presence of the SP. In the surrounding of SP molecules the concentration of epoxy groups is lower and this can cause the differences observed.

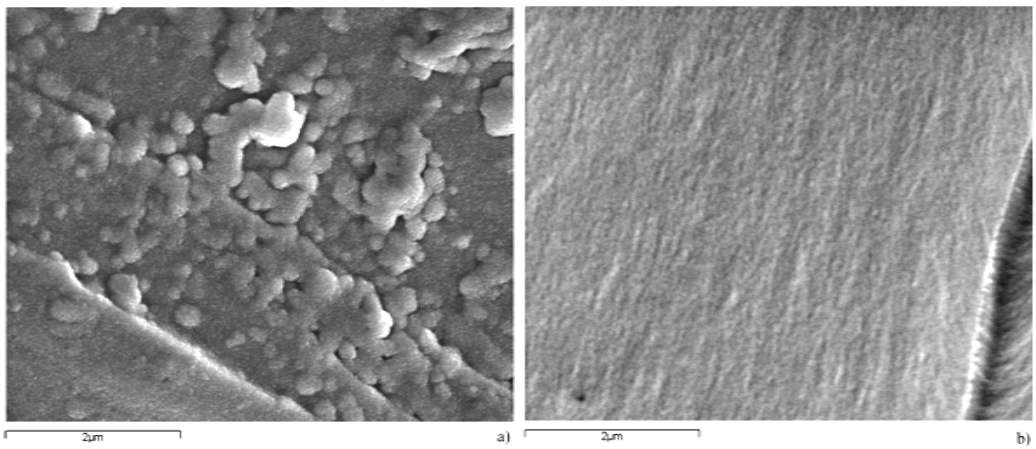

Figure 8 SEM pictures at 20000 magnifications for the DGEBA MI (a) and 10 phr SP MI (b) samples.

Figure 10 shows the SEM pictures of samples DGEBA Yb and 10 phr SP Yb at 20000 magnifications. One can see how on adding SP a second phase within the epoxy matrix appears which is a nanograined morphology. The domains of the SP are globular and at the same time are composed of smaller spheres of the material. It should be commented that only a certain proportion of the SP in the formulation undergoes phase separation. Lower proportions are dissolved in the epoxy matrix leading to a reduction of the T_g as observed by DMTA (**Table 4**).

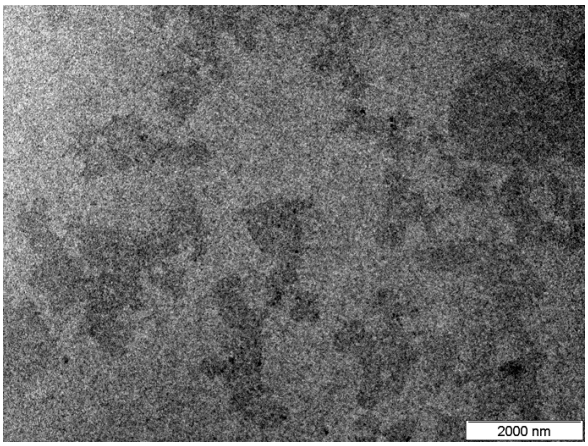

Figure 9 TEM picture of the 10 phr SP MI sample at 12000 magnifications.

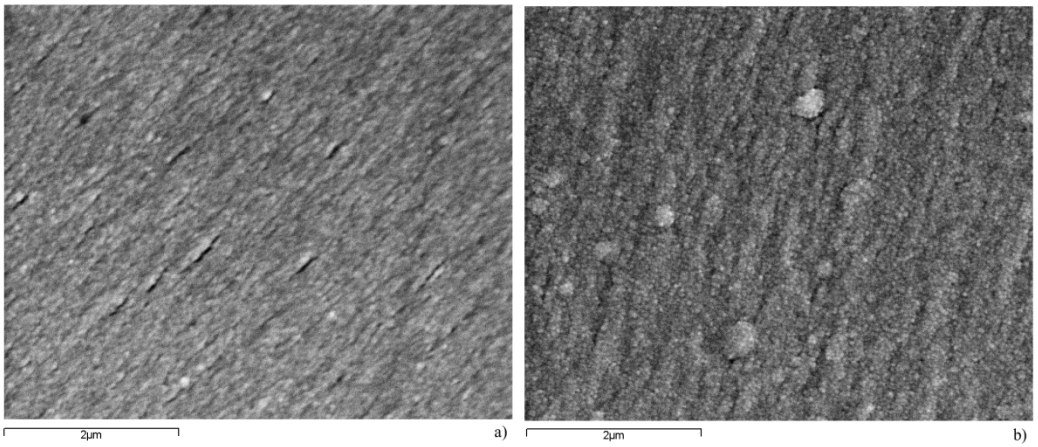

Figure 10. SEM pictures at 20000 magnifications for the DGEBA Yb (a) and 10 phr SP Yb (b) samples

Thus, it is quite evident that the curing mechanism is very important on the formation of phase separation in epoxy systems. It seems that cationic systems, the one herein studied and the one presented before in UV curing,[14] allow obtaining phase separation for this amphiphilic SP while anionics do not. Moreover, the phase separation obtained in thermal conditions is structurally better defined, probably because it is a slower process in comparison to the UV and during the curing the regions rich in SP can reorder themselves in a more organized structure. However, the proportion of SP that phase separates is lower in thermal conditions, since its solubility in the DGEBA increases with the temperature.

Thermogravimetric analysis

Figure 11 shows the thermograms under nitrogen atmosphere for all the studied formulations and Table 4 shows the values of the initial degradation temperature, the temperature of the maximum degradation rate and the char yield. Comparing both type of materials it is evident that the $Yb(OTf)_3$ initiated thermosets degrade at lower temperatures. It has been established that lanthanide triflates can promote the thermal degradation due to its Lewis acidity[30] which can improve the reworkability of the resulting thermosets.[31]

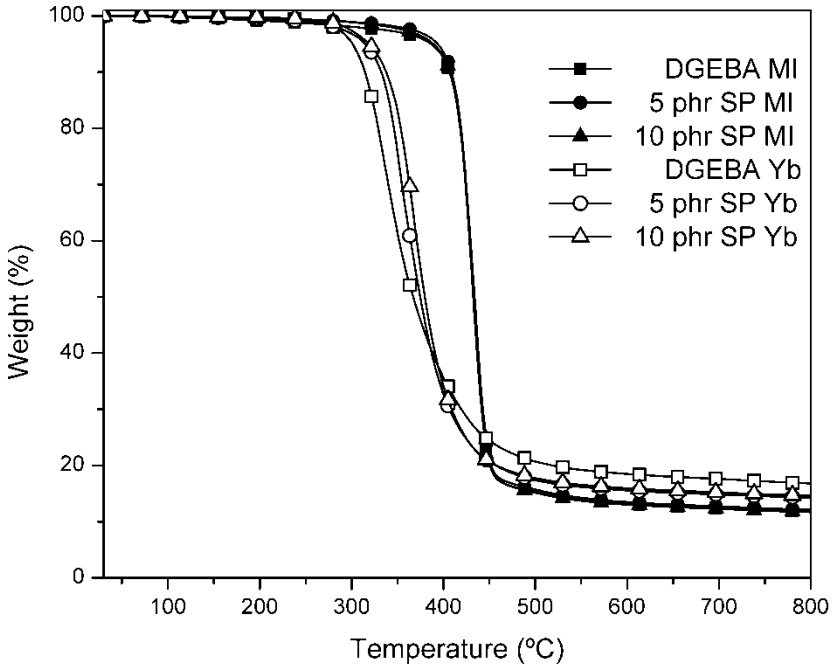

Figure 11 TGA curves for all the studied systems at 10 ºC/min under N_2.

The addition of SP increases the stability of the resulting thermosets, especially in the case of $Yb(OTf)_3$ cured materials since its thermal stability is lower and therefore the effect is more evident. The high thermal stability shown in all the thermosets can be attributed to the structure of the SP which contains aromatic esters that cannot undergo the β-elimination process responsible for the ester degradation[32] and ether groups well known for its thermal stability.

The char yield observed after degradation is higher for the systems cured with ytterbium triflate, but practically no influence on the addition of SP is observed.

Nanoindentation tests

Nanoindentation is a technique that recently has turn out to be very interesting in the characterization of mechanical properties such as Young's modulus or hardness[33] especially in the field of plastics.[34,35] Due to its "nano" scale it allows performing a great amount of tests within a small specimen and give reliable information. **Table 5** shows the values of the Young's modulus and the hardness determined for all the studied materials. The first noticeable fact is that neat MI cured thermosets present higher values of Young's modulus than the thermosets cured cationically, indicating a higher cohesive energy density of those materials, leading to more rigid thermosets. However, the addition of SP to ytterbium triflate initiated materials leads to an increase on the Young's modulus. Thus, the addition of the SP to these cationic initiated materials allows obtaining thermosets with similar rigidity than the ones obtained anionically.

The hardness of the final thermoset is slightly affected either by the addition of the SP or by the initiation system used in the curing. In all cases the values are around 0.25 GPa, presenting a slight increase for the samples with SP and initiated cationically. On that way, the addition of the SP allows obtaining thermosets with improved Young's modulus without compromising other properties such as hardness, very important in the field of coating applications.

Table 5 Mechanical properties measured in a nanoindentation test for all the studied thermosets

Sample	Young's Modulus (GPa)	Hardness (GPa)
DGEBA MI	3.66 ± 0.12	0.25 ± 0.02
5 phr SP MI	3.66 ± 0.22	0.24 ± 0.02
10 phr SP MI	3.78 ± 0.23	0.25 ± 0.03
DGEBA Yb	3.03 ± 0.14	0.25 ± 0.02
5 phr SP Yb	3.83 ± 0.15	0.27 ± 0.02
10 phr SP Yb	3.70 ± 0.09	0.27 ± 0.01

CONCLUSIONS

A new type of epoxy thermosets, modified with an amphiphilic star polymer was obtained by two different initiating systems: anionic (1-methyl imidazole) and cationic (ytterbium triflate).

While in the anionic system (MI) a slight increase in the curing rate was observed on increasing the amount of SP due to the presence of some hydroxyl groups in its structure, in the cationic $Yb(OTf)_3$ initiated systems an important decelerative effect occurred. This observation was attributed to the coordination of the catalyst with the polyethylene glycol arms that strongly reduced the effective amount of the ytterbium salt in the curing mixture.

The more flexible structure of the star in comparison to the epoxy matrix resulted in a decrease in the T_g of the resulting thermosets. The T_g*s* of the MI initiated materials were higher, due to a more crosslinked structure.

The gelation was delayed with the addition of the SP for both systems. In the case of MI initiated systems this resulted in an increase on the conversion at the gel point.

Ytterbium triflate initiated thermosets presented less shrinkage after gelation than MI initiated ones, but the addition of the SP caused an increase in this value for both systems.

By means of SEM we could observe a phase separated morphology for the cationically initiated thermosets containing SP. TEM demonstrated the presence of zones with different degree of crosslinking in anionically cured thermosets, in accordance to the observed by DMTA.

The thermal stability of the thermosets mainly depended on the inititator. MI yielded thermosets with higher thermal stability. No influence on the addition of the SP could be observed.

The Young's modulus of the materials was improved with the addition of SP in the case of cationic initiated materials, while the hardness remained practically unaffected in all the studied materials.

ACKNOWLEDGEMENTS

The authors from the Universitat Rovira i Virgili and from Universitat Politècnica de Catalunya would like to thank MICINN (Ministerio de Ciencia e Innovación) and FEDER (Fondo Europeo de Desarrollo Regional) (MAT2008-06284-C03-01 and MAT2008-06284-C03-02) and to the Comissionat per a Universitats i Recerca del DIUE de la Generalitat de Catalunya (2009-SGR-1512). D.F. acknowledges the grant FPU-2008 from the Spanish Government.

REFERENCES

1. E. M. Petrie. *Epoxy adhesive formulations.* McGraw-Hill, New York, **2006**.
2. J-P. Pascault, R. J. J. Williams. *Epoxy Polymers*. Wiley-VCH, Weinheim, **2010**.
3. T. J. Kemp, A. Wilford, O. W. Howarth, T. C. P. Lee. *Polymer* **1992,** *33,* 1860.

4. A. H. Gilbert, C. B. Bucknall. Macromol. *Chem. Phys. Macromol. Symp.* **1991,** *45,* 289.
5. C. K. Riew. *Adv. Chem. Ser. Vol. 222.* American Chemical Society, Washington DC, **1989**.
6. T. Iijima, T. Tochimoto, M. Tomoi. *J. Appl. Polym. Sci.* **1991,** *43,* 1685.
7. P. M. Lipic, F. S Bates, M. A. Hillmyer. *J. Am. Chem. Soc.* **1998,** *120,* 8963.
8. L. Ruiz-Pérez, G. J. Royston, J. P. A. Fairclough, A. J. Ryan. *Polymer* **2008,** *49,* 4475.
9. W. Fan, L. Wang, S. Zheng. *Macromolecules* **2009,** *42,* 327.
10. Y. Meng, X-H. Zhang, B-Y. Du, B-X. Zhou, X. Zhou, G-R. Qi. *Polymer* **2011,** *52,* 391.
11. X. Fernández-Francos, D. Foix, A. Serra, J. M. Salla, X. Ramis. *React Funct Polym* **2010,** *70,* 798.
12. D. Ratna, G. P. Simon. *Polymer* **2001,** *42,* 8833.
13. X. Fernández-Francos, J. M. Salla, A. Cadenato, J. M. Morancho, A. Serra, A. Mantecón, X. Ramis. *J. Appl. Polym. Sci.* **2009,** *111,* 2822.
14. D. Foix, X. Fernández-Francos, X. Ramis, A. Serra, M. Sangermano. *React. Funct. Polym.* **2011,** *71,* 417.
15. D. U. Shah, P. J. Schubel. *Polym. Test* **2010,** *29,* 629.
16. J-P. Pascault, H. Sauterau, J. Verdu, R. J. J. Williams. *Thermosetting Polymers*. Marcel Dekker, New York, **2002**.
17. W. C. Oliver, G. M. Pharr. *J. Mater. Res.* **1992,** *7,* 1564.
18. J. Brandrup, E. H. Immergut, E. A. Grulke. *Polymer Handbook*, 4th ed. Wiley-Interscience, New York, **1999**.
19. X. Fernández-Francos, J. M. Salla, G. Pérez, A. Mantecón, A. Serra, X. Ramis. *Macromol. Chem. Phys.* **2009,** *210,* 1450.
20. H. C. Aspinall, J. L. M. Dwyer, N. Greeves, E. G. McIver, J. C. Wooley. *Organometallics* **1998,** *17,* 1884.
21. X. Fernández-Francos, W. D. Cook, J. M. Salla, A. Serra, X. Ramis. *Polym. Int.* **2009,** *58,* 1401.
22. M. Sangermano, A. Priola, G. Malucelli, R. Bongiovanni, A. Quaglia, B. Voit, A. Ziemer. *Macromol. Mater. Eng.* **2004,** *289,* 442.
23. P. Kubisa, S. Penczek. *Prog. Polym. Sci.* **2000,** *24,* 1409.
24. W. G. Cox, E. H. Merz. *J. Polym. Sci.* **1958,** *28,* 619.
25. D. Foix, M. Erber, B. Voit, A. Lederer, X. Ramis, A. Mantecón, A. Serra. *Polym. Degrad. Stab.* **2010,** *95,* 445.
26. M. Haider, P. Hubert, L. Lessard. *Composites: Part A* **2007,** *38,* 994.
27. L. Khoun, P. Hubert. *Polym. Composites* **2010,** *31,* 1603.
28. C. A. May. *Epoxy Resins. Chemistry and Technology*, 2nd edition. Marcel Dekker, New York, **1988**.
29. R. Mezzenga, C. J. G. Plummer, L. Boogh, J. A. E. Månson. *Polymer* **2001,** *42,* 305.
30. L. González, X. Ramis, J. M. Salla, A. Mantecón, A. Serra. *Polym. Degrad. Stab.* **2007,** *92,* 596.
31. J. S. Chen, C. K. Ober, M. D. Poliks. *Polymer* **2002,** *43,* 131.
32. P. Sivasamy, M. Palaniandavar, C. T. Vijayakumar, K. Ledered. *Polym. Degrad. Stab.* **1992,** *38,* 15.
33. A. C. Fischer-Cripps. *Nanoindentation*. Springer, New York, **2004**.
34. L. Shen, Y. I. Phang, L. Chen, T. Liu, K. Zeng. *Polymer* **2004,** *45,* 3341.
35. J. A. Ramos, M. Blanco, I. Zalakain, I. Mondragón. *J. Colloid. Interf. Sci.* **2009,** *336,* 431.

5.4 Synthesis of a new hyperbranched-linear-hyperbranched triblock copolymer and its use as a chemical modifier for the cationic photo and thermal curing of epoxy resins

D. Foix[1], X. Ramis[2], M. Sangermano[3], A. Serra[1]

[1] Department of Analytical and Organic Chemistry, University Rovira i Virgili, Marcel.li Domingo s/n, 43007 Tarragona, Spain

[2] Laboratory of Thermodynamics, ETSEIB, University Politècnica de Catalunya, Av. Diagonal 647, 08028 Barcelona, Spain

[3] Department of Material Science and Chemical Engineering, Politecnico di Torino, C.so Duca degli Abruzzi 24, 10129 Torino, Italy

ABSTRACT

A new hyperbranched-linear-hyperbranched polymer was prepared in a one pot process by reaction of 4,4-bis(4-hydroxyphenyl)valeric acid and poly(ethylene glycol) (HPH). After characterization by ^{1}H and ^{13}C NMR, SEC, DSC and TGA, this polymer was used, in proportions of 5, 10 and 15 phr, as a chemical modifier in the UV and thermal cationic curing of 3,4-epoxycyclohexylmethyl-3',4'-epoxycyclohexyl carboxylate epoxy resin. The curing process was studied by calorimetry, demonstrating the accelerating effect of the hydroxyl groups present in HPH's structure. The morphology of the resulting thermosets depended on the curing system used, as demonstrated by FE-SEM microscopy, but in both cases phase separation occurred. Thermosets obtained by thermal curing presented lower thermal stability than UV cured materials.

INTRODUCTION

Epoxy resins are among the most used thermosets in the field of coatings. They are versatile materials that posses unique properties in terms of chemical resistance, thermal stability, transparency and good overall mechanical properties. However, one of their main disadvantages is the poor performance in terms of toughness which limits their range of application.[1,2] In order to overcome this drawback many strategies have been used. For example, it is well known that the addition of rubbers or thermoplastics to the epoxy matrix improve its impact resistance.[3-6] However, this strategy sacrifices other properties such as T_g or the processability. Recently, more complex polymer topologies such as hyperbranched polymers,[7] star polymers[8] or block copolymers[9,10] have been used in order to improve toughness without compromising other peculiar properties of the epoxy thermosets such as high modulus and mechanical properties. In some cases, even other characteristics have also been improved. For example star polymers are well known for improving the processability of the resin[11] or the use of some hyperbranched polyesters have demonstrated to improve the chemical reworkability of the resulting thermosets.[12]

In general, the most used strategy for improving the toughness of epoxy resins when using the above mentioned topologies is the formation of nanostructured materials.[13] One of the first examples was the use of hyperbranched polymers. For instance, Månson *et al.*[14] reported the use of commercially available hyperbranched polyesters with terminal epoxy groups to obtain phase separation within DGEBA epoxy matrix and this led to improvements of around 300% in toughness. Fröhlich *et al.*[15] investigated the use of a hyperbranched polyglicidol with epoxide end groups as DGEBA toughener, and could also observe fracture toughness improvements.

Another strategy recently applied to enhance toughness is the use of block copolymers. Lipic *et al.*[16] described the phase separation of a polyethylene oxide/polyethylene-propylene copolymer in an epoxy matrix. Ryan *et al.*[17] used different block copolymers to induce nanophase separation in epoxy resins. In some cases, one block was miscible with the resin while the other not and the separation appears on preparing the reacting mixture. In other copolymers both blocks where miscible, but only one of them was reactive towards the resin, and then the phase separation occurred during the curing reaction by reaction induced phase separation mechanism (RIPS). In recent years a growing interest has aroused for the preparation and use of linear-hyperbranched block copolymers as polymeric modifiers.[18]

To obtain phase separated morphologies, not only is the polymeric additive used of the main importance, but also the curing procedure. For example, Ratna *et al.*[19] reported the preparation of phase separated thermosets when working with DGEBA/Boltorn H30 mixtures and curing with diamines. On the contrary, phase separation was not observed in DGEBA/Boltorn H30 mixtures using $Yb(OTf)_3$ as cationic thermal initiator[20] or curing with anhydrides.[21]

Having all of this into account, in the current work we present the use of a novel hyperbranched-linear-hyperbranched triblock copolymer as a chemical modifier for a commercially available cycloaliphatic epoxy resin. The polymer consists in two blocks of an aromatic-aliphatic hyperbranched polyester connected by a linear central block of poly(ethylene glycol) (**Scheme 1**). The different solubility of the blocks confers the structure an amphiphilic character. UV and thermal curing initiated cationically have been investigated. Differences both in the evolution of the curing and in the morphology and properties of the thermosets prepared by the two methodologies have been appreciated.

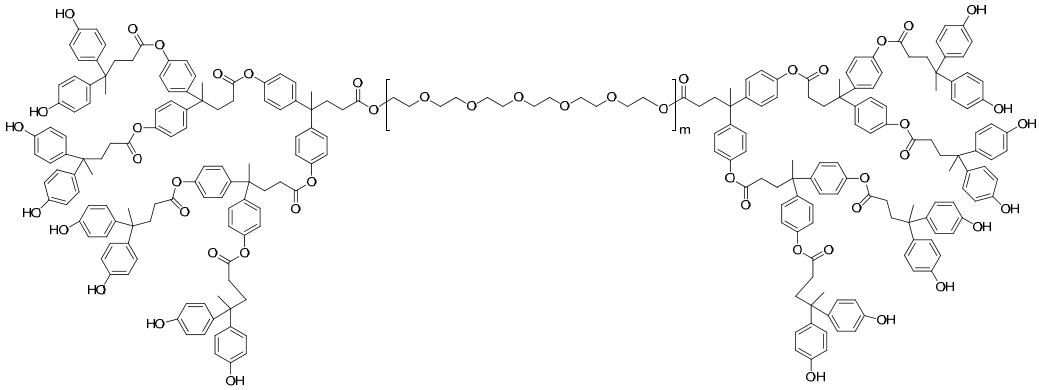

Scheme 1 Idealized chemical structure of the prepared Hyperbranched-Linear-Hyperbranched block copolymer.

EXPERIMENTAL PART

Materials

4,4-Bis(4-hydroxyphenyl)valeric acid, 3-(4-hydroxyphenyl) propionic acid, N,N'-dicyclohexylcarbodiimide (DCC), poly(ethylene glycol) ($\bar{M}_n$ = 2,000 g/mol), methanol and anhydrous N,N-dimethylformamide (DMF), synthesis grade, were purchased from Aldrich or Fluka and used without further purification. 4-(N,N-dimethylamino)pyridinium p-toluenesulfonate (DPTS) was prepared as described in the literature.[22]

Biscycloaliphatic diepoxy resin 3,4-epoxycyclohexylmethyl-3',4'-epoxycyclohexyl carboxylate (CE, Huntsman), lanthanum triflate (Aldrich, 99% of purity) and triphenylsulfonium

hexafluoroantimonate (PI, $Ph_3S^+SbF_6^-$, Aldrich 50% in weight solution in propylene carbonate) were used as received.

*Polymer Synthesis (HPH) (**Scheme 1**)*

In a 500 mL round-bottomed flask provided with Ar inlet and magnetic stirring, 10 g (35 mmol) of 4,4-bis(4-hydroxyphenyl)valeric acid, 2.80 g (1.4 mmol) of poly(ethylene glycol), and 2.06 g (7 mmol) of DPTS were dissolved in 250 ml of anhydrous DMF. Then, 8.67 g (42 mmol) of DCC were introduced in portions and the flask was sealed and the mixture was kept under stirring for 24 hours. Then, the crude product was filtered to eliminate the urea formed and it was precipitated first in 1 L of methanol, redissolved in THF and reprecipitated in 1 L of water. The solid product was dried in a vacuum oven at 50 ºC for 3 days. (Yield 68%).

^{1}H NMR ($CDCl_3$): δ (in ppm) 1.52, 1.57, and 1.62 (CH_3); 2.30, 2.35, 2.41 and 2.45 (CH_2); 3.51 (CH_2-O); 6.66, 6.97, 7.18 (aromatic protons); 9.20, 9.23 (OH)
^{13}C NMR ($CDCl_3$): δ (in ppm) 27.06, 27.24, 27.42 (CH_3); 30.0 ($\underline{C}H_2$-CO); 35.72, 35.95, 36.13 ($\underline{C}H_2$-C); 43.94, 44.42, 44.89 (C quaternary); 69.85 (CH_2-O); 114.83, 114.99, 121.26, 121.45, 127.92, 128.01, 138.14, 139.19, 145.70, 146.76, 148.32, 148.51, 155.16, 155.38 (aromatics); 171.6-172.2 (C=O)
$\bar{M}_n$: 10,000 g/mol
$\bar{M}_w$: 16,000 g/mol
$Đ_M$: 1.63
T_g: 120 ºC

Sample preparation for UV curing

The appropriate amount of HPH (0, 5, 10 or 15 phr) was dissolved in the cycloaliphatic epoxy resin (CE) at 80 ºC. Then the mixtures were allowed to cool down and 4 phr of the solution in propylene carbonate of the photoinitiator (PI) were added. Formulations were kept at -25 ºC in the dark before use.

To prepare free standing films the liquid formulations were coated on a poly(propylene) substrate using a wirewound applicator and were exposed to UV radiation with a fusion lamp (H-bulb) in air at a conveyor speed of 5 m·min^{-1}, with radiation intensity on the surface of the sample of 280 mW·cm^{-2}.

Sample preparation for thermal curing

The appropriate amount of HPH (0, 5, 10 or 15 phr) was dissolved in the cycloaliphatic epoxy resin (CE) at 80 ºC. Then the mixture was allowed to cool down and 1 phr of $La(OTf)_3$ (dissolved in one drop of propylene carbonate) was added. Formulations were kept at -25 ºC before use.

To prepare specimens the liquid formulations were poured into a metal mold coated with silicon oil to prevent the attachment and cured at 140 ºC for 5 hours and post-cured at 180 ºC for 1 hour in an oven.

Characterization Techniques

^{1}H NMR 400 MHz and ^{13}C NMR 100.6 MHz NMR spectra were obtained using a Varian Gemini 400 spectrometer with Fourier Transformed. ^{1}H NMR spectra were acquired in 1 min and 16 scans with a 1.0 s relaxation delay (D1).

Size exclusion chromatography (SEC) analysis was carried out with an Agilent 1200 series system with PLgel 3 m MIXED-E, PLgel 5 m MIXED-D, and PLgel 20 μm MIXED-A columns in series, and equipped with an Agilent 1100 series refractive-index detector. Calibration curves

were based in polystyrene standards having low molecular weight dispersities. THF was used as the eluent at a flow rate of 1.0 ml/min, the sample concentrations were 5-10 mg/ml, and injection volumes of 100 μl were used.

The kinetics of photopolymerization was determined by real time (RT) FT-IR spectroscopy, employing a Thermo-Nicolet 5700 FTIR device. Epoxy group conversion was followed in real-time upon UV exposure, by monitoring the decrease in the absorbance due to epoxy groups in the region 760-780 cm^{-1}. A medium pressure mercury lamp equipped with an optical guide was used to induce the photopolymerization (light intensity on the surface of the sample of about 5 mW/cm^{-2}). Variation in the experimental conditions (light intensity, humidity and temperature) caused slight differences in the kinetic curves. For this reason all the conversion curves contained in the figures were performed on the same day and under the same conditions and thus good reproducibility was obtained. All the polymerization reactions were performed at room temperature at constant humidity (25-30%).

To determine the kinetics of the thermal polymerization an FTIR spectrophotometer FTIR-680PLUS from Jasco with a resolution of 4 cm^{-1} in the absorbance mode was used. This device was equipped with an attenuated total reflection (ATR) accessory with thermal control and a diamond crystal (Golden Gate heated single-reflection diamond ATR, Specac-Teknokroma). The curing temperature was 130 ºC.

The conversion ($x_{UV,FTIR}$) was calculated by monitoring the disappearance of the epoxy band (760-780 cm^{-1}) with the time and using the following equation:

$$x_{UV,FTIR} = 1 - \frac{\bar{A}^t}{\bar{A}^0} \quad (1)$$

where $\bar{A}^t$ is the normalized absorbance of the epoxy band at a given time and $\bar{A}^0$ is the initial absorbance.

Photocalorimetric experiments were performed in order to study the effect of temperature on the photocuring kinetics. The various samples were photocured at different temperatures using a Mettler DSC-821e calorimeter appropriately modified to permit irradiation with a Hamamatsu Lightningcure LC5 (Hg-Xe lamp) with two beams, one for the sample side and the other for the reference side. Samples weighing ca. 3 mg were cured in open aluminium pans in a nitrogen atmosphere. Two scans were performed on each sample in order to subtract the thermal effect of the UV irradiation from the photocuring experiment, each one consisting of 4 min of temperature conditioning, 20 min of irradiation and finally 4 more minutes without UV light. A light intensity of 30 mW/cm^2 (calculated by irradiating graphite-filled pans on only the sample side) was employed. Dynamic postcuring experiments were carried out on a Mettler DSC-822e with a TSO801RO robotic arm, from 0 to 200 ºC at 10 ºC/min in nitrogen atmosphere. The degree of conversion x_{UV} during the photocuring stage was calculated based on the residual heat evolved during the postcuring scan as follows:

$$x_{UV} = 1 - \frac{\Delta h_{post}}{\Delta h_{theor}} \quad (2)$$

where Δh_{post} is the heat released during the dynamic post-curing process and Δh_{theor} corresponds to the theoretical heat evolved during complete cure of the formulation.

In the thermal dynamic curing process the degree of conversion by DSC (x_{DSC}) was calculated as follows:

$$x_{DSC} = \frac{\Delta h_T}{\Delta h_{tot}} \quad (3)$$

where Δh_T is the heat released up to a temperature T, obtained by integration of the calorimetric signal up to this temperature, and Δh_{tot} is the total reaction heat associated with the complete conversion of all reactive groups.

The gel content was determined on the cured films by measuring the weight loss after 24 h extraction with chloroform at room temperature according to the standard test method ASTM D2765-84.

Dynamic-mechanical thermal analyses (DMTA) were performed on a MK III Rheometrics Scientific Instrument at 1 Hz frequency in the tensile configuration. The storage modulus, *E'*, and the loss factor, *tan* δ, were measured from -90 ºC to the temperature at which the rubbery state was attained. The T_g value was assumed as the maximum of the loss factor curve *(tan* δ*)*.

Thermogravimetric analysis (TGA) was performed with a METTLER TGA/SDTA 851 instrument between 30 and 800 ºC at a heating rate of 10 ºC/min under air (100 mL/min).

SEM analyses were performed on fracture surfaces of the hybrid systems by using a ZEISS SUPRA™ 40 Field Emission Scanning Electron Microscope (FE-SEM) with an acceleration voltage of 10 kV and WD = 2 mm (Nominal resolution: 1.5 nm).

Transmission electron microscopy (TEM) was performed with a Jeol 1011 microscope and the samples were prepared by dissolving the polymer in acetone in a concentration of 1 mg/mL.

RESULTS AND DISCUSSION

HPH Synthesis

The block copolymer used in this work (HPH) was synthesized in a one pot process as seen in **Scheme 2**. Linear poly(ethylene glycol) with terminal hydroxyl groups and a molecular weight $\bar{M}_n$) of 2,000 was used as the cental block from where 4,4-bis(4-hydroxyphenyl)valeric acid was polymerized to form the other two blocks. The polymerization of this monomer has been extensively studied,[23] and the methodology herein used consisted in a polycondensation reaction using DCC as coupling agent and DPTS as catalyst.[24]

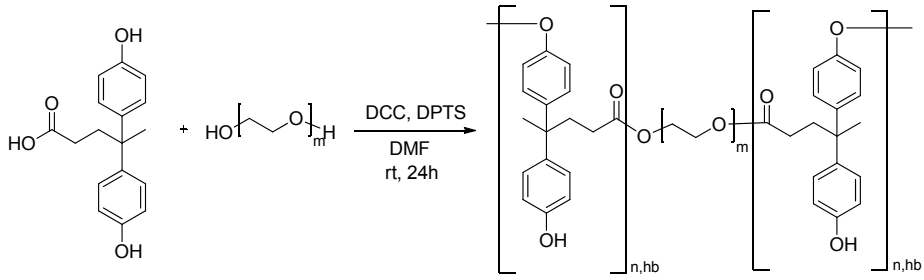

Scheme 2 Scheme of reaction for the synthesis of HPH.

Figure 1 shows the ^{1}H NMR spectra of the copolymer. One can see that together with the signals of the hyperbranched aromatic aliphatic polyester, a signal near 3.5 ppm appears. This is attributed to the poly(ethylene glycol) block. The signals corresponding to the CH_2OCO group of the linkage between blocks could not be detected due to the considerable small proportion in respect to the other signals and to the different relaxation times of the blocks.

The degree of branching of the hyperbranched block was calculated using the ^{13}C NMR signals between 43.94 and 44.89 ppm which correspond to the quaternary carbon of the

terminal, linear and dendritic units, using Frey's equation.[25] The value of 0.50 obtained confirmed the hyperbranched nature of the block.

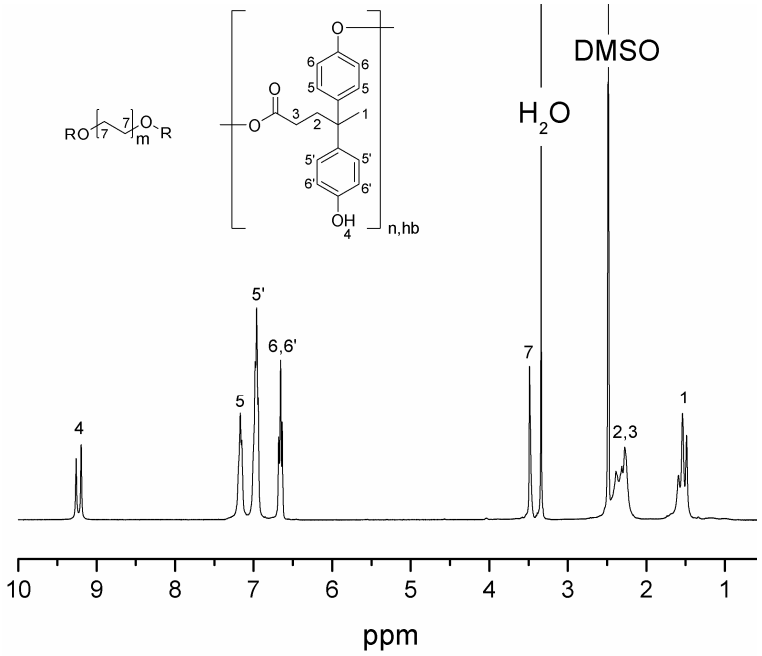

Figure 1 ^{1}H-NMR spectra of the prepared HPH.

The molecular weight of the synthesized block copolymer was measured by SEC analysis obtaining a value of $\overline{M}_n$ of 10,000 g/mol. The molecular weight dispersity of the resulting polymer was 1.63, indicating a quite narrow distribution probably due to the fractionation that takes places in the precipitation in methanol. It should be pointed out that the SEC curve obtained was unimodal, which confirms that the poly(ethylene glycol) block is linked to both hyperbranched blocks.

Using Transmission Electron Microscopy (TEM) we could observe that the block copolymer, in solution of acetone, was able to form spherical phases of around 100 nm (**Figure 2**). It indicates the capacity of the block copolymer synthesized to reorder itself in solution in spherical particles. Therefore, it is reasonable to think that it would behave in a similar way when dissolved into DGEBA in order to obtain nanostructured materials.

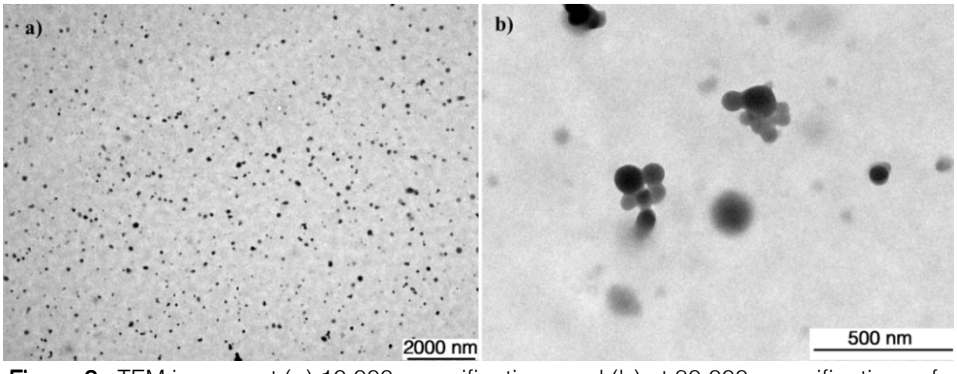

Figure 2 TEM images at (a) 10,000 magnifications and (b) at 80,000 magnifications of 1 mg/mL solutions in acetone of the prepared HPH.

By means of a dynamic DSC scan between 30 and 250 ºC at 20 ºC/min we could determine the T_g of the polymer, 120 ºC. The value is quite high due to the aromatic character of the polymer. No T_g corresponding to the poly(ethylene glycol) moiety could be appreciated probably because of the lower proportion of this part in respect to the aromatic part and of a limitation in the mobility for being incorporated in the copolymer.

The thermal stability of the synthesized block copolymer was evaluated by means of TGA. **Figure 3** shows the thermogram obtained as well as the derivative curve of the same. HPH is stable up to a temperature of 315 ºC (temperature of 5% loss), and presents two maxima of degradation one at 370 ºC corresponding to the first degradative process and another at 530 ºC, corresponding to the second one. As expected, no residue is observed at 800 ºC when the experiment is carried out under air.

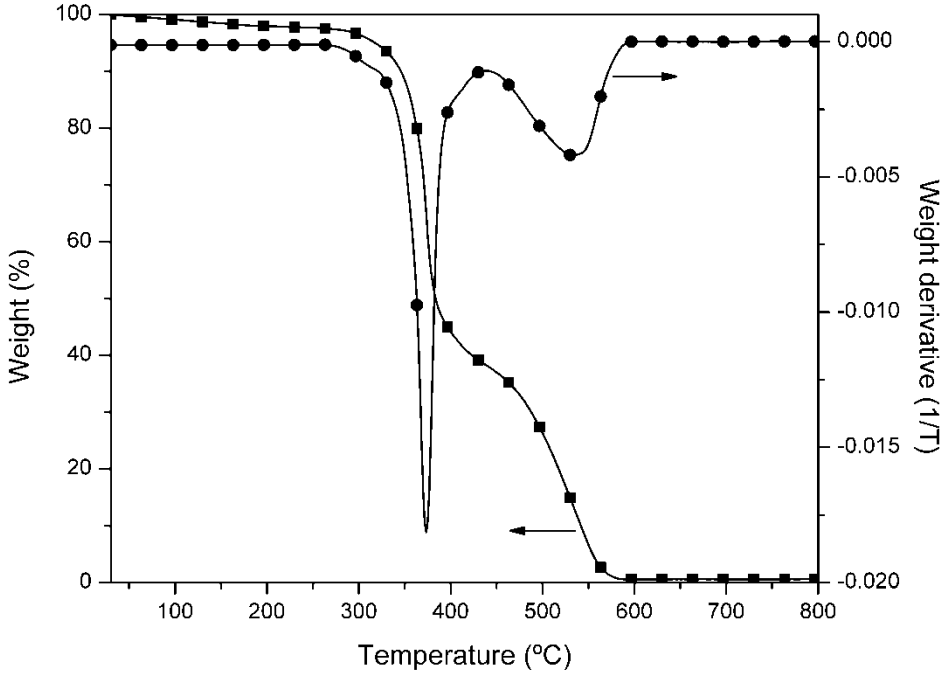

Figure 3 TGA thermogram and derivative TGA (dTGA) curves of the prepared HPH.

DSC Studies

Once synthesized and characterized the block copolymer (HPH), it was blended in different proportions with a commercially available cycloaliphatic epoxy resin (CE) and the curing process was studied both in thermal and UV conditions.

By means of differential scanning calorimetry we investigated the thermal curing process in dynamic conditions. **Table 1** shows the calorimetric data for all the thermally cured systems and **Figure 4** shows the conversion against temperature plots. One can see that there is not a big influence in the kinetics of the curing on adding the block copolymer. The temperature of the maximum of the curing exotherm remains similar in all cases and only a slight decelerative effect can be appreciated in the curves of conversion, with the addition of HPH, being more pronounced at lower temperatures.

Table 1 Calorimetric data obtained from DSC and photo-DSC experiments.

Sample	Thermal-DSC [a]			Photo-DSC [b]			
	T_p (ºC)	Δh (J/g)	$x_{thermal}$ (%)	Δh_{40} (J/g)	$x_{UV,40}$ (%)	Δh_{120} (J/g)	$x_{UV,120}$ (%)
CE	133	623	100	367	59	618	98
5 phr HPH	136	592	100	362	61	586	99
10 phr HPH	138	561	100	369	66	554	99
15 phr HPH	137	528	99	356	67	524	99

a. cured with $La(OTf)_3$

b. cured with $Ph_3S^+SbF_6^-$

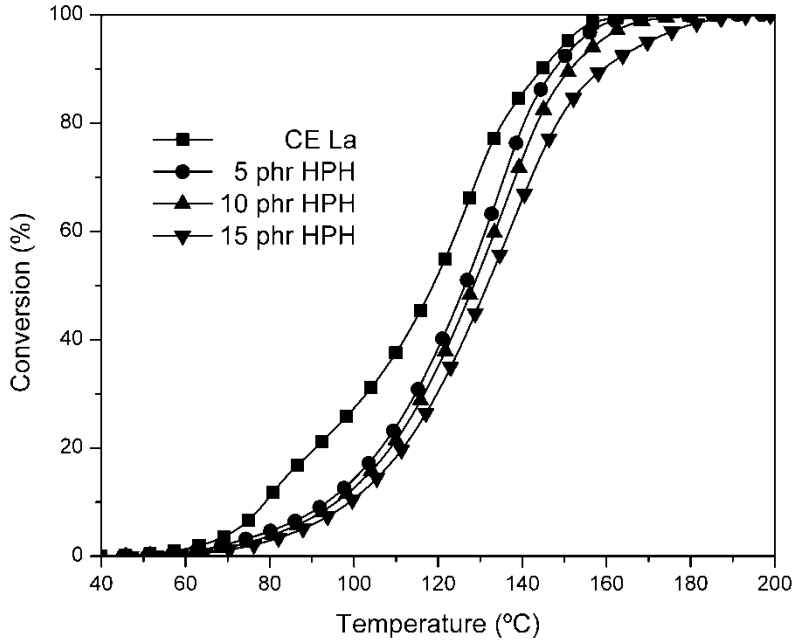

Figure 4 Conversion curves obtained at 10 ºC/min for all the studied formulations.

There are examples in the literature that describe an accelerative effect in the cationic thermal curing of epoxy resins when HBPs with hydroxyl groups are present in the mixture.[26] This is a consequence of the activated monomer propagation mechanism (**Scheme 3**) described by Kubisa and Penczek.[27] However, in this system that was not the case. The decelerative effect could be attributed to an increase in the viscosity (**Table 2**) of the mixtures that reduces the mobility of the reacting groups, competing with the acceleration produced by the OH groups.

The enthalpy released per gram decreases with the addition of HPH, as predictable, since the content of epoxy groups is reduced. However in all thermally cured systems the conversion of epoxy groups achieved was quantitative.

Using a DSC equipped with an irradiating lamp we were able to study the UV curing of these mixtures. An aryl sulfonium antimoniate salt was chosen as photo initiator and two different temperatures (40 and 120 ºC) were selected. **Table 1** shows the values of enthalpy obtained for all UV cured systems as well as the conversion achieved. The values of heat released were determined from the difference between the theoretical value (it was used the value obtained in

the thermal dynamic curing since it was quantitative) and the dynamic postcuring of the UV irradiated samples since the UV curing is very fast and it is difficult to measure the whole heat released. At 40 °C the conversion achieved increases with the addition of HPH increasing from 59% for the neat system to 67% for the mixture containing 15 phr of HPH. This can be explained either by an increase in the curing rate promoted by the hydroxyl groups of the polymer[28] or by a retardation of the vitrification that would allow curing up to higher conversions. At 120 °C vitrification did not take place in any case and all formulations regardless of the amount of additive were able to cure quantitatively.

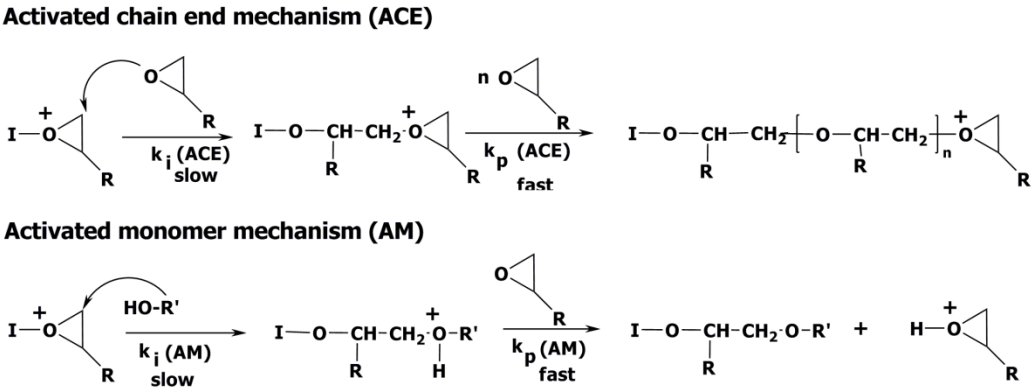

Scheme 3 Propagation mechanism for the cationic polymerization of epoxides.

DSC is also the most recognized technique to determine the glass transition temperature. However in our case, the rigidity of the network is too high and it was not possible to determine the T_g on that way.[29]

FTIR Studies

In order to study the curing process in isothermal conditions we used FTIR. For the thermal system a normal FTIR equipped with an ATR with heating control was used. We selected 130 °C since the curing did not take place too quickly and we were able to monitor it. **Figure 5** shows the evolution of the conversion against time for all the thermal cured systems. One can see that the conversion achieved in all cases is nearly quantitative and approximately the same in all cases. The inset in the figure shows the beginning of the curing. It shows a deceleration on the addition of HPH as already demonstrated in the thermal dynamic DSC measurements.

In the case of UV curing, it was necessary to use real-time FT-IR analysis since UV curing takes place in a matter of minutes. **Figure 6** shows the conversion curves as a function of the irradiation time for all the UV cured formulations. In this case, the formulations cure up to around 60% without any clear tendency with the addition of HPH. This indicates that vitrification takes place. However, as seen in the inset of the figure, at the beginning of the polymerization there is an accelerative effect on adding the block copolymer. This is in contrast to what is observed in thermal conditions. In the case of UV curing, the effect of the hydroxyls present in HPH that can promote the quicker AM mechanism seems to be more important than the effect of the increasing viscosity. This can be rationalized on the basis that the higher acidity of the "superacid" generated by UV irradiation to the photoinitiator confers more importance to the AM mechanism in comparison to the case of using $La(OTf)_3$. This is in accordance with the problems experimented when preparing curing mixtures with $Yb(OTf)_3$, since its higher acidity favors the AM mechanism compared to $La(OTf)_3$ increasing the curing rate.[30]

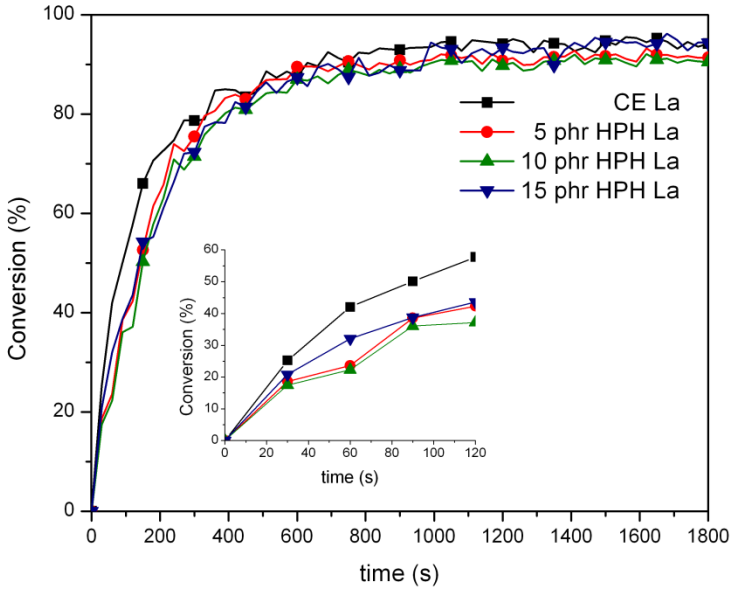

Figure 5 Conversion plots obtained by FTIR for the samples cured with $La(OTf)_3$.

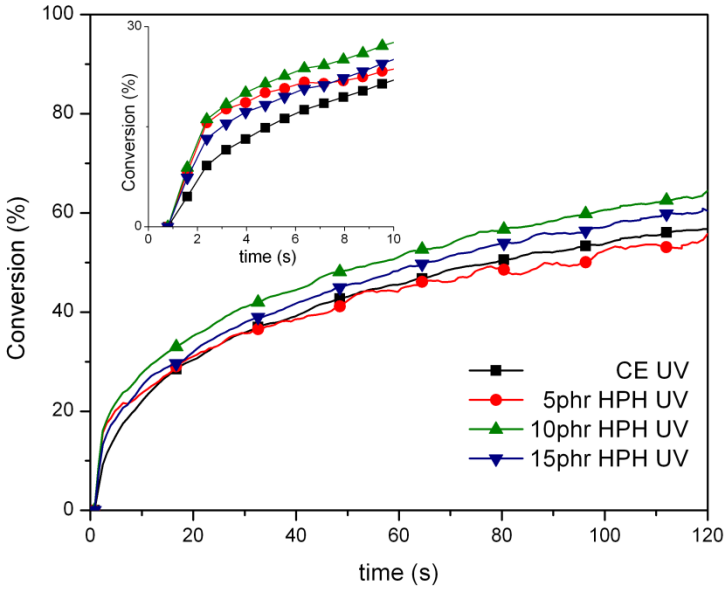

Figure 6 Conversion plots obtained by FTIR for the samples cured with $Ph_3S^+SbF_6^-$

Gel Content

Once understood the curing process, specimens of all the formulations were prepared in order to characterize the resulting thermosets.

First of all, it is important to know whether the block copolymer is chemically linked to the epoxy matrix or not. Even if the additive was phase separated from the matrix there are many cases in which there is at least a small amount of chemical linkages between phases.[29] For that reason we measured the gel content of all the cured formulations. As seen in **Table 2** both thermal and UV initiated thermosets presented quantitative gel content, indicating that the HPH is chemically linked to the network. The incorporation of the additive can be explained on the

basis of the hydroxyl groups present in the hyperbranched block. Both thermal and UV systems are performed via a cationic mechanism and therefore, due to the concurrence of the AM mechanism, hydroxyl groups react with the activated epoxy monomer leading to its chemical incorporation.[27]

Table 2 Viscosity of the formulations, and gel content and thermal mechanical data of the prepared thermosets.

Sample	|η*| (Pa·s)	Gel content (%)	*tan δ* (ºC)	*E'* (MPa) [a]	$T_{5\%}$ [b] (ºC)	T_{max} [c] (ºC)
CE La	0.176	100	206	18.5	256	280
5 phr HPH La	0.795	100	205	18.2	260	288
10 phr HPH La	1.635	99	206	18.3	265	293
15 phr HPH La	1.889	100	198	17.9	267	295
CE PI	0.176	99	178	10.2	262	403
5 phr HPH PI	0.795	99	180	13.1	267	406
10 phr HPH PI	1.635	100	179	14.0	268	408
15 phr HPH PI	1.889	99	179	14.4	279	411

a. Measured at the maximum of *tan δ* + 50 ºC.
b. Temperature of the lost of a 5% in weight in TGA experiment under air at 10 ºC/min.
c. Temperature of the maximum degradation rate in TGA experiment under air at 10 ºC/min.

DMTA Analysis

Dynamic Mechanical Thermal Analysis is a very powerful technique in the viscoelastic characterization of thermosets. For example the loss factor curve can provide us not only with information about the transitions of the material but also can be related to its morphology. **Figure 7** shows the *tan δ* against temperature curves for the thermosets obtained by cationic thermal and UV curing with 0 and 15 phr of HPH, and the values of the maximum of *tan δ* for all the studied thermosets are collected in **Table 2**. In the case of UV cured materials, only one transition at around 190 ºC appears. However, no influence on the addition of HPH can be appreciated for these maxima, which can be related to the T_g of the material. This led us to the conclusion that phase separation is taking place since if the material were homogeneous the T_g of the resulting thermoset should decrease as predicted by the Fox equation.[31] However, the transition of the block copolymer (approximately 120 ºC by DSC) is not appreciated in any case, but this may be due to the relative small content of HPH in respect to the resin or because it is partially overlapped with the main transition of the resin.

As seen in **Figure 7** and **Table 2**, the use of $La(OTf)_3$ as thermal cationic initiator allows obtaining T_g*s* of around 200 ºC, 20 ºC higher than for the case of UV cured thermosets. Again, the addition of HPH does not drop down the maximum of *tan δ*, indicating a possible phase separation.

From DMTA, it is possible to obtain information about the modulus *E'* modulus at the rubbery state, which is related to the crosslinking density of the material. As seen in the values collected in **Table 2**, thermally cured thermosets present higher values of *E'* than UV cured ones, indicating a higher crosslinking density. This can be rationalized on the basis of the AM mechanism. In the case UV curing, the presence of protons generated by the photoinitiator, promotes up to a higher extent the AM mechanism, which leads to chain transfer reactions,

lowering the crosslinking density, and the temperature of the maximum of *tan δ*. On the other hand, the addition of HPH only has a noticeable effect on UV cured thermosets, yielding a slight increase of *E'* (around 4 MPa for the case with the highest amount of HPH).

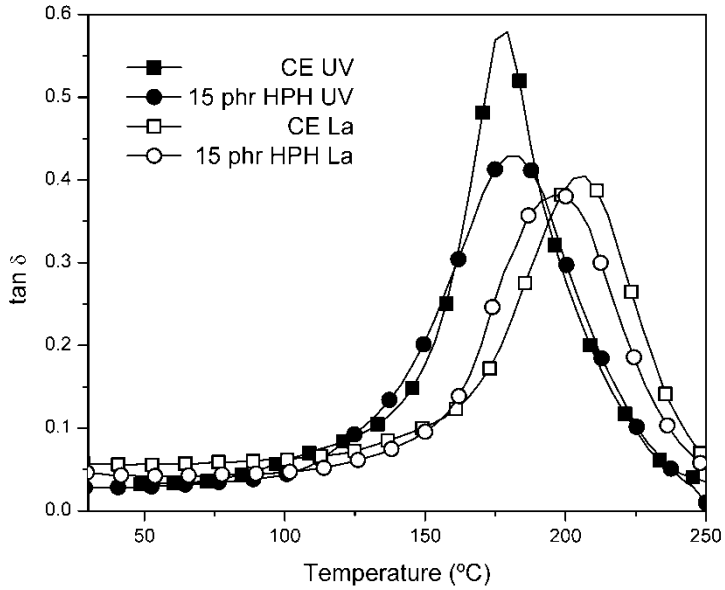

Figure 7 DMTA curves for some of the studied thermosets.

Morphology

In order to confirm the observations of the DMTA analysis we used Field Emision Scanning Electron Microscopy (FE-SEM) to observe the morphology in cryofractured specimens. This type of electron microscopy is well known to have higher resolution than conventional SEM and therefore, allows observing more clearly phases that can have a size in the nanoscale. **Figure 8a** shows the micrograph obtained for the sample 15 phr HPH UV at 50,000 magnifications. For the other UV cured thermosets containing HPH similar pictures were obtained. One can appreciate the presence of spherical particles homogeneously dispersed within all the material. Although some bigger particles product of agglomeration appear, most of them are in a size comprised between 50 and 100 nm.

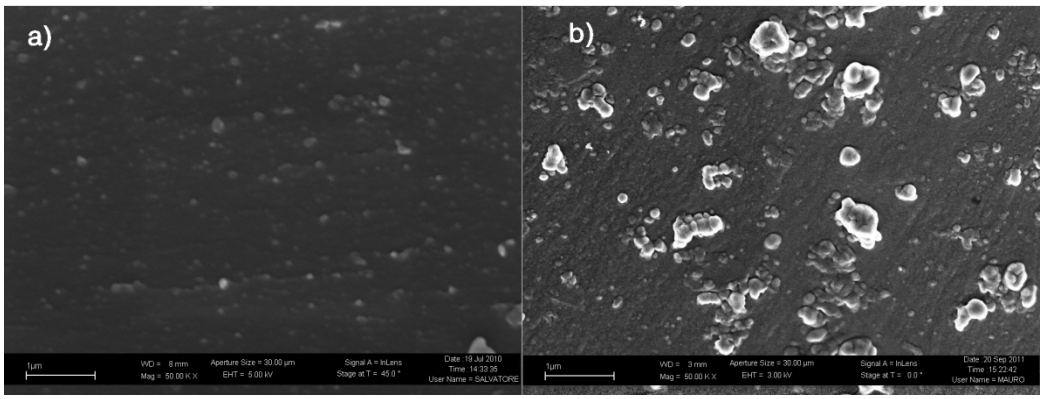

Figure 8 FE-SEM images at 50,000 magnifications of the samples (a) 15 phr HPH UV and (b) 15 phr HPH La.

Figure 8b shows the micrograph obtained for the sample cured thermally containing 15 phr of HPH at 50,000 magnifications. One can appreciate that more agglomeration takes place than in UV cured materials, yielding bigger and irregular particles with sizes around 500 nm. Assuming that in this system phase separation occurs through a reaction induced phase separation mechanism and that the temperature increases the solubility of HPH, it is reasonable that the particles obtained in thermal curing are bigger, since particles remain solubilized in the resin up to a bigger size at high curing temperatures.

TGA Analysis

Another key feature in the characterization of thermosets is the understanding of its thermal stability. The cycloaliphatic epoxy resin used in this work degrades at low temperatures since the presence of an ester linkage in its structure allows the degradation via a β-elimination process typical of aliphatic esters.[32] **Figure 9** shows the thermograms for the UV and thermal cured thermosets. In **Table 2** the values of the temperatures of initial degradation and maximum degradation rate are collected. One can state that the presence of aromatic moieties in HPH allows obtaining thermosets with higher thermal stability regardless of the curing mechanism. We have to point out that, as demonstrated in previous articles,[12] the aromatic ester bonds of the hyperbranched block cannot undergo the aforementioned β-elimination process and therefore the thermal stability increases.

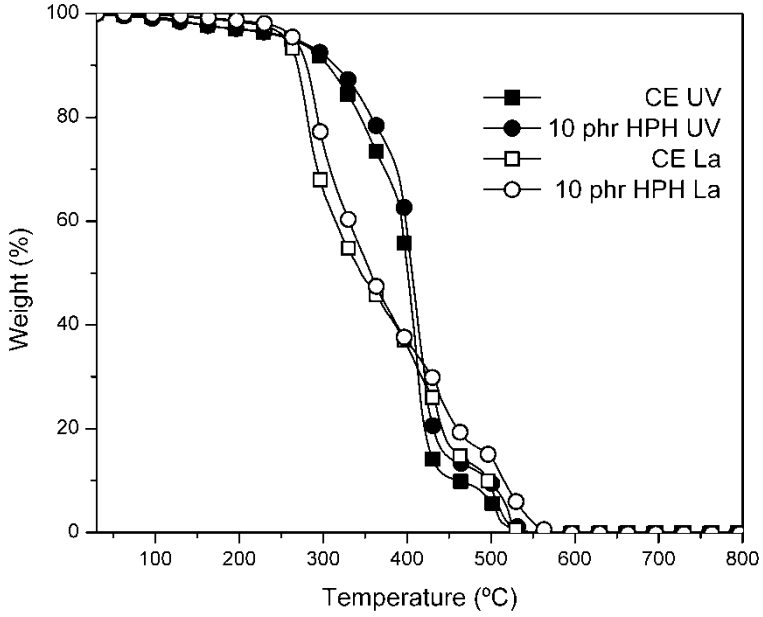

Figure 9 Thermograms obtained at 10 ºC/min for some of the prepared thermosets.

On comparing thermal and UV initiated thermosets one can see that UV ones are more stable as seen in the initial degradation temperature ($T_{5\%}$) but specially in the temperature of the maximum degradation (T_{max}), which is shifted more than 100 ºC. In previous studies that we performed with rare earth triflates as cationic curing agents of DGEBA/Meldrum's acid mixtures, we demonstrated that they can catalyze the β-elimination of esters due to its Lewis acidity.[33] In our case, using a cycloaliphatic resin which also yields ester groups in the thermosetting network, $La(OTf)_3$ promotes the elimination at lower temperatures and therefore the thermal stability falls down.

As expected on degrading under air atmosphere, the char yield was 0% for all the studied thermosets, since all moieties present were organic.

CONCLUSIONS

A new block copolymer has been synthesized in an easy one pot process, and it has been characterized by means of NMR, SEC, TEM, DSC and TGA.

The synthesized block copolymer HPH has been used as an additive to prepare epoxy thermosets by UV and thermal cationic curing. The curing rate is determined by the viscosity of the curing mixture and the concurrence of the AM mechanism. In the case of UV curing, due to the higher acidity of the photo-generated species, the accelerative effect of AM mechanism is more important than the decelerative effect of the increasing viscosity. On that way, the presence of HPH in the formulation increases the curing rate. On the contrary, in thermal conditions using $La(OTf)_3$ AM mechanism becomes less important and the viscosity effect results in a retarding of the curing on adding HPH.

Thermally initiated thermosets presented higher values of *tan* δ, which is related to the T_g of the material. The addition of HPH did not affect the T_g of the resulting thermosets for both cases (UV and thermal), suggesting phase separated morphologies.

By FE-SEM microscopy it was possible to confirm the presence of phase separation of the HPH in the epoxy resin for the UV cured samples. The particle size observed was in the range of 50 to 100 nm with a defined spherical shape. In the case of thermally cured materials the particle size is bigger as a consequence of aggregation, yielding irregular particles of around 500 nm.

Due to the introduction of aromatic moieties in the mixture, the thermal stability of the thermosets containing HPH increases in respect to the neat systems regardless of the initiator used. The presence of $La(OTf)_3$ in thermally cured thermosets promotes the degradative process of esters at lower temperatures.

ACKNOWLEDGEMENTS

The authors from the Universitat Rovira i Virgili and from Universitat Politècnica de Catalunya would like to thank MICINN (Ministerio de Ciencia e Innovación) and FEDER (Fondo Europeo de Desarrollo Regional) (MAT2011-27039-C03-01 and MAT2011-27039-C03-02) and to the Comissionat per a Universitats i Recerca del DIUE de la Generalitat de Catalunya (2009-SGR-1512). D.F. acknowledges the grant FPU-2008 from the Spanish Government.

REFERENCES

1. E. M. Petrie. *Epoxy adhesive formulations.* McGraw-Hill, New York, **2006**.
2. C. A. May. *Epoxy Resins. Chemistry and Technology*, 2nd edition. Marcel Dekker, New York, **1988**.
3. R. S. Bauer, *Advances in Chemistry,* ACS Symposium Series, vol. 114. ACS, Washington DC, **1979**.
4. H. S-Y. Hisich. *Polym. Eng. Sci.* **1990,** *30,* 493.
5. S. C. Kunz, J. A. Sayre, R. Assink. *Polymer* **1973,** *23,* 1897.
6. P. Bussi, H. Ishida. *J. Appl. Polym. Sci.* **1994,** *53,* 441.
7. R. Mezzenga, L. Boogh, J. A. E. Månson. *Compos. Sci. Technol.* **2001,** *61,* 787.
8. Y. Meng, X-H. Zhang, B-Y. Du, B-X. Zhou, X. Zhou, G-R. Qi. *Polymer* **2011,** *52,* 391.
9. U. Buchholz, R. Mülhaupt. *Polymer Prepr.* **1992,** *33,* 205.
10. L. Könczöl, W. Döll, U. Buchholz, R. Mülhaupt. *J. Appl. Polym. Sci.* **1994,** *54,* 815.

11. M. Morell, A. Lederer, X. Ramis, B. Voit, A. Serra. *J. Polym Sci Part A: Polym Chem.* **2001,** *49,* 2395.
12. D. Foix, M. Erber, B. Voit, A. Lederer, X. Ramis, A. Mantecón, A. Serra. Polym. Degrad. Stab. **2010,** *95,* 445.
13. J-P. Pascault, R. J. J. Williams. *Epoxy Polymers*. Wiley-VCH, Weinheim, **2010**.
14. L. Boogh, B. Pettersson, J. A. E. Månson. *Polymer* **1999,** *40,* 2249.
15. J. Fröhlich, H. Kautz, R. Thomann, H. Frey, R. Mülhaupt, *Polymer* **2004,** *45,* 2155.
16. P. M. Lipic, F. S. Bates, M. A. Hillmyer. *J. Am. Chem. Soc.* **1998,** *120,* 8963.
17. L. Ruiz-Pérez, G. J. Royston, J. P. A. Fairclough, A. J. Ryan. *Polymer* **2008,** *49,* 4475.
18. F. Wurm, H. Frey. *Prog. Polym. Sci.* **2011,** *36,* 1.
19. D. Ratna, G. P. Simon. *Polymer* **2001,** *42,* 8833.
20. X. Fernández-Francos, J. M. Salla, A. Cadenato, J. M. Morancho, A. Serra, A. Mantecón, X. Ramis. *J. Appl. Polym. Sci.* **2009,** *111,* 2822.
21. D. Foix, Y. Yu, A. Serra, X. Ramis, J. M. Salla. *Eur. Polym. J.* **2009,** *45,* 1454.
22. J. S. Moore, S. I. Stupp. *Macromolecules* **1990**, *23*, 65.
23. D. Schmaljohann, H. Komber, B.Voit. *Acta Polym* **1999,** *50,* 196.
24. F. Schallausky, M. Erber, H. Komber, A. Lederer. *Macromol. Chem. Phys.* **2008,** *209,* 2331.
25. D. Hölter, A. Burgath, H. Frey. *Acta Polym.* **1997,** *48,* 30.
26. J. M. Morancho, A. Cadenato, X. Ramis, X. Fernández-Francos, J. M. Salla. *Thermochim. Acta.* **2010,** *510,* 1.
27. P. Kubisa, S. Penczek. *Prog. Polym. Sci.* **2000,** *24,* 1409.
28. M. Sangermano, A. Priola, G. Malucelli, R. Bongiovanni, A. Quaglia, B. Voit, A. Ziemer. *Macromol. Mater. Eng.* **2004,** *289,* 442.
29. D. Foix, X. Fernández-Francos, X. Ramis, A. Serra, M. Sangermano. *React. Funct. Polym.* **2011,** *71,* 417.
30. C. Mas, A. Mantecón, A. Serra, X. Ramis, J. M. Salla. *J. Polym. Sci. Part A: Polym. Chem.* **2004,** *42,* 3782.
31. T. G. Fox, P. J. Flory. *J. Appl. Phys.* **1950,** *21,* 581.
32. P. Sivasamy, M. Palaniandavar, C. T. Vijayakumar, K. Ledered. *Polym. Degrad. Stab.* **1992,** *38,* 15.
33. L. González, X. Ramis, J. M. Salla, A. Mantecón, A. Serra. *Polym. Degrad. Stab.* **2007,** *92,* 596.

Chapter 6

Thiol-ene Based HBPs in the Modification of Epoxy Resins

6.1 Introduction

"Click Chemistry" is a term that was introduced by Sharpless *et al.*[1] in 2001 to describe a new concept for conducting organic reactions, based upon the premise that organic synthesis should focus its attention on highly selective, simple orthogonal reactions that do not yield side products and that give heteroatom-linked molecular systems with high efficiency under a variety of mild conditions. Several efficient reactions, which are capable of producing a wide catalogue of functional synthetic molecules and organic substrates, have been grouped accordingly under the term click reactions. Characteristics of modular click reactions include a) high yields with by-products (if any) that are removable by non-chromatographic processes, b) regiospecificity and stereospecificity, c) insensitivity to oxygen or water, d) mild, solventless (or aqueous) reaction conditions, e) orthogonality with other common organic synthesis reactions, and f) amenability to a wide variety of readily available starting compounds.

Among the molecular processes considered to fit all or most of these criteria, the metal catalyzed azide/alkyne 'click' reaction stands out. It is a variation of the Huisgen 1,3-dipolar cycloaddition reaction between terminal acetylenes and azides that have find many applications up to now.[2-4] However, there are many other reactions that may be considered as "click

[1] H. C. Kolb, M. G. Finn, K. B. Sharpless. *Angew. Chem. Int. Ed.* **2001,** *40,* 2004.
[2] H.C. Kolb, K.B. Sharpless. *Drug Discovery Today* **2003,** *8,* 1128.
[3] C. J. Hawker, K. L. Wooley. *Science* **2005,** *309,* 1200.
[4] D. Fournier, R. Hoogenboom, U. S. Schubert. *Chem. Soc. Rev.* **2007,** *36,* 1369.

reactions" as for example: Diels-Alder cycloaddition, nucleophilic ring opening reactions of epoxides and aziridines, the thiol-ene and thiol-yne reactions or Michael additions among others.[5,6] **Figure 6.1** shows some examples of those reactions.

In recent years the reaction between thiols and double bonds has developed a growing interest as a very useful "click reaction".[7] The relatively weakness of the sulfur-hydrogen bond of thiols results in a plethora of chemical reactions with nearly quantitative yields and an ability to initiate these reactions by a variety of methods under mild conditions. It presents some advantages in respect to the classic alkyne-azide reaction such as the fact that no metal catalyst is required that results in the reduction of the citotoxicity of the synthesized products. Also the fact that in many cases it can be carried out without solvent represents a clear advantage of this methodology.

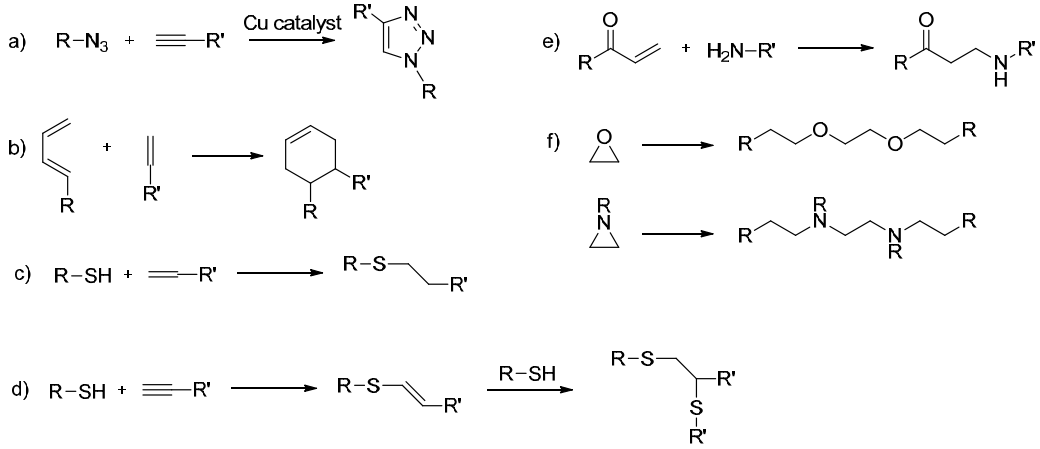

Figure 6.1 Examples of "click reactions".

During the last century, two thiol reactions emerged: thiol-ene free-radical addition to electron-rich/electron-poor carbon-carbon double bonds, and the catalyzed thiol Michael addition to electron-deficient carbon-carbon double bonds. Regardless of the reaction mechanism, the reactivity is certainly influenced by the basic structure of the thiol. Four prominent thiol types typically encountered in literature reports include alkyl thiols, thiophenols, thiol propionates, and thiol glycolates (**Figure 6.2**).

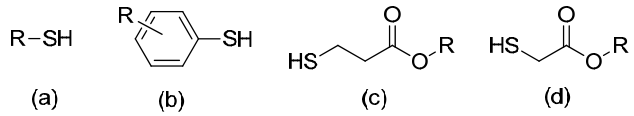

Figure 6.2 Chemical structure of (a) alkyl thiols; (b) thiophenols; (c) thiol propionates and (d) thiol glycolates.

Radical addition has been well known to be an efficient reaction for several decades in the field of material science.[8,9] Crosslinked polymers formed from thiol-ene radical systems are the

[5] C. R. Becer, R. Hoogenboom, U. S. Schubert. *Angew. Chem. Int. Ed.* **2009,** *48,* 4900.
[6] W. H. Binder, R. Sachsenhofer. *Macromol. Rapid Commun.* **2007,** *28,* 15.
[7] C. E. Hoyle, C. N. Bowman. *Angew. Chem. Int. Ed.* **2010,** *49,* 1540.
[8] M. S. Kharasch, A. T. Read, F. R. Mayo. *Chem. Ind.* **1938,** *57,* 752.
[9] C. R. Morgan, F. Magnotta, A. D. Ketley. *J. Polym. Sci. Polym. Chem. Ed.* **1977,** *15,* 627.

most ideal homogeneous network structures ever formed by free-radical polymerization, with narrow glass transitions[10] and low polymerization shrinkage stresses.[11]

The mechanism of radical thiol-ene reaction is depicted in **Figure 6.3**. The ideal thiol-ene radical reaction promoted by a photoinitiator (PI) is based in the alternation between the reaction of a thiyl radical with an ene functional group followed by a chain-transfer reaction, which involves the abstraction of a hydrogen radical from the thiol by the carbon-centered radical. In the ideal purely step-growth thiol-ene reaction no homopolymerization in which the carbon-centered radical propagates through the ene moiety occurs.

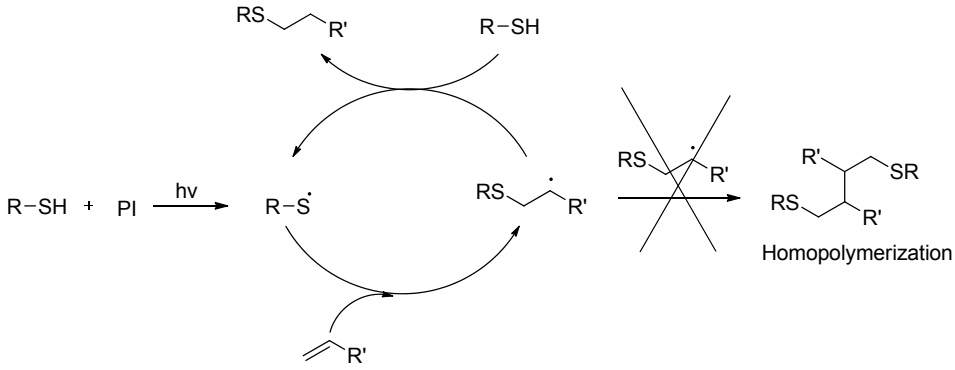

Figure 6.3 Idealized mechanism of radical thiol-ene coupling.

Apart from the traditional thiol-ene free-radical reaction, thiol-vinyl reactions between a thiol and an electron-deficient "ene" also occur readily. Depending on the substrate the reaction may have different names but, in general, one can refer to this click reaction as a thiol-Michael addition reaction, providing that the "ene" functionality is electron deficient, such as (meth)acrylates, maleimides, α,β-unsaturated ketones, fumarate esters, acrylonitrile, cinnamates or crotonates.

Traditionally, a wide variety of catalysts have been used to initiate the thiol-Michael addition reaction, including strong bases, metals, organometallics, and Lewis acids.[12] During the last few years, a strategy of using primary or secondary amines[13-15] or even more powerful and efficient nucleophilic alkyl phosphine catalysts[16] has emerged as a model for extremely efficient thiol-Michael addition reactions between electron-deficient "enes" and several types of thiols.

The reaction proceed with high conversion by an extremely efficient anionic chain process that is analogous to the mechanism for the radical reaction, except that instead of radicals there are anions and that the mechanism for generation of the initial thiolate anion involves the addition of the nucleophilic catalyst to the electron-deficient alkene, followed by a subsequent proton abstraction of the thiol (**Figure 6.4**).

---

[10] J. D. Fouassier, J. F. Rabek. *Radiation Curing in Polymer Science and Technology III*, Elsevier, London, **1993**
[11] C. E. Hoyle, T. Y. Lee, T. Roper. *J. Polym. Sci. Part A: Polym. Chem.* **2004,** *42,* 5301.
[12] B. D. Mather, K. Viswanathan, K. V. Miller, T. E. Long. *Prog. Polym. Sci.* **2006,** *31,* 487.
[13] T. Y. Lee, W. Kaung, E. S. Jonsson, K. Lowery, C. A. Guymon, C. E. Hoyle. *J. Polym. Sci. Part A: Polym. Chem.* **2004,** *42,* 4424.
[14] X.-P. Qiu, F. Winnik. *Macromol. Rapid Commun.* **2006,** *27,* 1648.
[15] V. S. Khire, T. Y. Lee, C. N. Bowman. *Macromolecules* **2007,** *40,* 5669.
[16] J. W. Chan, B. Yu, C. E. Hoyle, A. B. Lowe. *Chem. Commun.* **2008,** 4959.

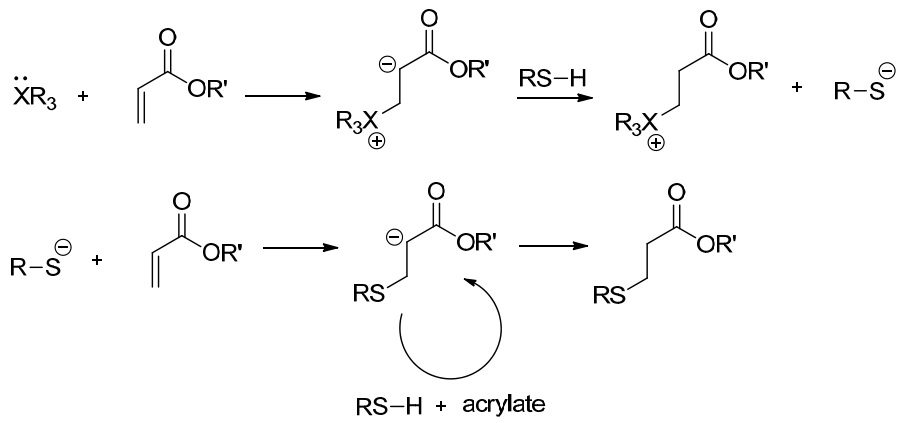

Figure 6.4 Mechanism of the thiol-Michael addition.

In the field of hyperbranched polymers the most extended application of "click reactions" is in the middle-upon approach for HBP synthesis. There are many examples of previously synthesized HBPs whose end groups have been modified via click chemistry. Carefully choosing these end groups one can use different click reactions for the modification. In the literature one can find polymers with azide, double or triple bonds, or thiol end groups that have been modified with different click chemistry reactions.

One can find also some examples of hyperbranched polymers synthesized from a bottom-up approach using "click reactions". For instance, Voit *et al.*[17] and in parallel Smet *et al.*[18] described the use of the methodology of self-coupling of azido and acetylenic building blocks to generate hyperbranched polymers. The monomers proposed are depicted in **Figure 6.5**.

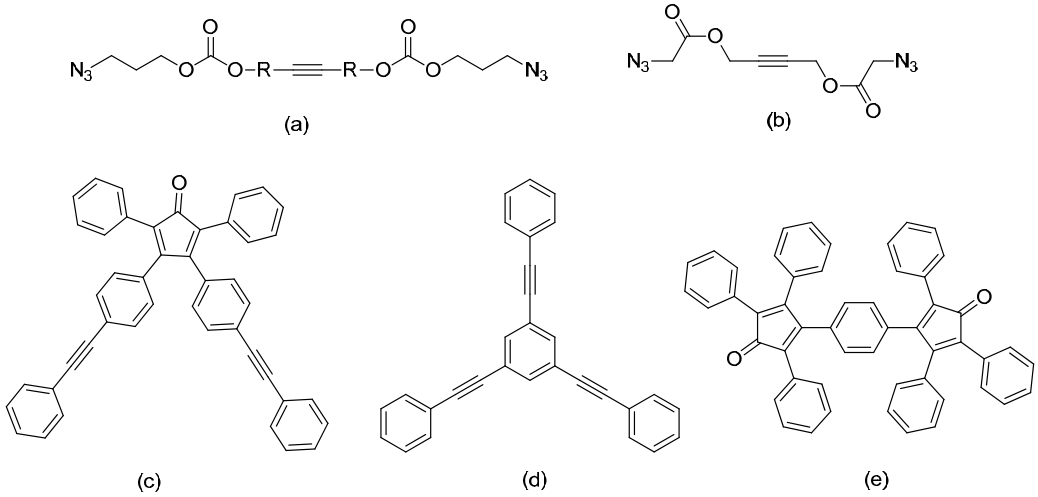

Figure 6.5 AB_2 monomers for the Huisgen cycloaddition (a) and (b); AB_2 monomer for the Diels-Alder reaction (c) and A_2 and B_3 monomers for the Diels-Alder reaction (d) and (e).

[17] A. Scheel, H. Komber, B. I. Voit. *Macromol. Rapid Commun.* **2004,** *25,* 1175.
[18] M. Smet, K. Metten, W. Dehaen. *Coll. Czech. Chem. Commun.* **2004,** *69,* 1097.

Another example is the preparation of HBP using the Diels-Alder cycloaddition. Müllen *et al.*[19] reported the Diels-Alder reaction of an AB_2 monomer to prepare hyperbranched polyphenylenes. Later, Voit *et al.*[20] proposed an alternative route based on the $A_2 + B_3$ approach to prepare this polymer. These monomers are depicted in **Figure 6.5**. Harrison and Feast[21] reported the preparation of highly soluble hyperbranched polyarylimides also using the Diels-Alder cycloaddition reaction but employing AB_2 monomers with maleimide and cyclopentadienone moieties.

Recently also UV induced thiol-yne coupling have emerged as a powerful strategy for the preparation of HBPs. Since the reaction allows the simple addition of two thiols to an alkyne, it appears to be perfectly suited to create multifunctional polymer structures. For example, Perrier and co-workers[22] exploited the branching power of thiol-yne chemistry to generate hyperbranched polymers (**Figure 6.6**). Bifunctional thiol-alkynes were used as AB_2 type monomers where the thiol is the A unit and a single alkyne represents the two B units. The most striking result is the fact that the DB of the HBPs prepared with that methodology is close to one, the expected value for dendrimers.

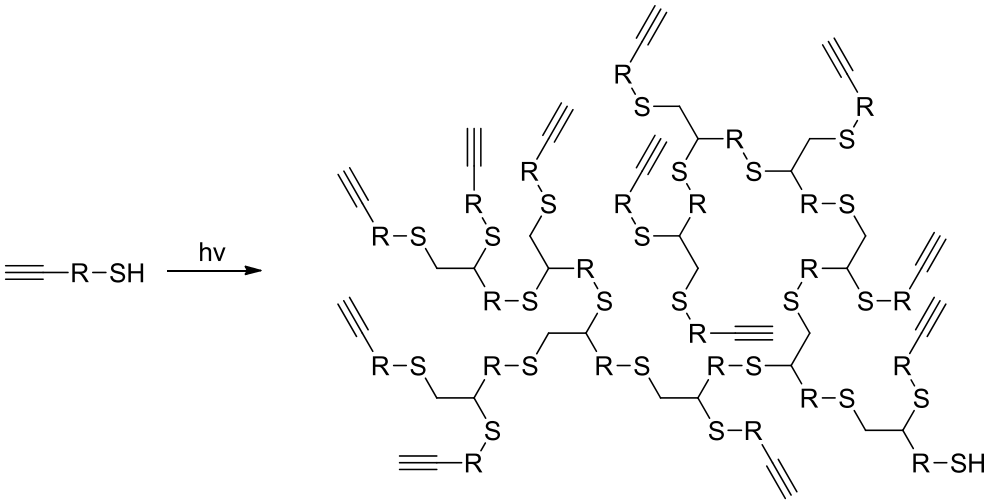

Figure 6.6 One-pot thiol-yne mediated synthesis of highly functional hyperbranched polymers.

Another example of the use of this thyol-ene/yne UV induced reaction in the synthesis of HBPs is the proposed by Gao et al.[23] They used of a sequential thiol-ene and thiol-yne click pathway via the $A_2 + CB_2$, as depicted in **Figure 6.7**. The first reaction is selective towards the double bond and therefore an AB_2 monomer is generated *in situ*. This, in turn, photopolymerizes with UV light, using a photoinducer such as AIBN, and yielding the desired HBP without the risk of gelation, and with convenient molecular weights and narrow dispersites.

[19] F. Morgenroth, M. Müllen. *Tetrahedron* **1997**, *53*, 15349.
[20] K. Stumpe, H. Komber, B. Voit. *Macromol. Chem. Phys.* **2006**, *207*, 1825.
[21] R. M. Harrison, W. J. Feast. *PMSE Prepr. (ACS)* **1997**, *77*, 162.
[22] D. Konkolewicz, A. Gray-Weale, S. Perrier. *J. Am. Chem. Soc.* **2009,** *131,* 18075.
[23] J. Han, B. Zhao, Y. Gao, A. Tang, C. Gao. *Polym Chem.* **2011,** DOI: 10.1039/c1py00235j

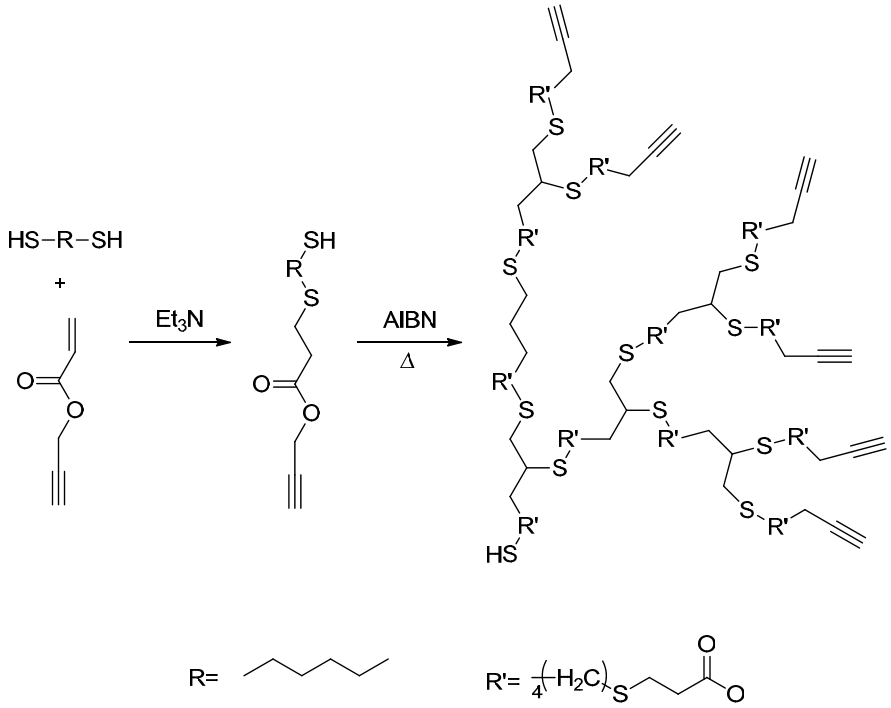

Figure 6.7 Reaction proposed by Gao *et al.*

This chapter will deal about the use of a hyperbranched polymer synthesized from a bottom-up approach using the thiol-ene coupling reaction in the field of epoxy resins used as coatings. On the one hand, the utility of the thiol-ether functionality introduced by this reaction in the structure of the polymer will be demonstrated in a latent dual UV-thermal curing process; and on the other the anionic thermal curing process of DGEBA modified with the HBP and the properties of the final materials will be studied.

The work herein presented has been published in the following articles that compose this chapter:

6.2 UV generation of a multifunctional hyperbranched thermal crosslinker to cure epoxy resins.

6.3 DGEBA thermosets modified with an amphiphilic star polymer. Study on the effect of the initiator on the curing process and morphology.

6.2 UV generation of a mutifunctional hyperbranched thermal crosslinker to cure epoxy resins

D. Foix[1], X. Ramis[2], A. Serra[1], M. Sangermano[3]

[1] Department of Analytical and Organic Chemistry, University Rovira i Virgili, Marcel.li Domingo s/n, 43007 Tarragona, Spain

[2] Laboratory of Thermodynamics, ETSEIB, University Politècnica de Catalunya, Av. Diagonal 647, 08028 Barcelona, Spain

[3] Dept. of Material Science and Chemical Engineering, Politecnico di Torino, C.so Duca degli Abruzzi 24, 10129 Torino, Italy

ABSTRACT

A new hyperbranched polymer (HBP) was obtained via an iterative synthetic procedure that consists of esterification and thiol-ene click reaction. This polymer was used as a latent multifunctional macroinitiator for the dual curing of a commercially available cycloaliphatic epoxy resin and this process was studied by photo-DSC and FTIR. The presence of thioether groups in the HBP structure leads, by photoirradiation, to the formation of sulfonium salts, which are thermal cationic initiating species. The materials obtained were characterized by DMTA, TGA, gel content and FESEM. By means of the last technique domains of HBP as a second phase within the epoxy matrix were observed.

INTRODUCTION

Epoxy resins are widely used as thermosets in technological applications such as coatings, adhesives, structural applications or electronics but they lack of good toughness characteristics for some specific applications. This is due to their high crosslinking character and rigid structure, which leads to a poor resistance to crack formation and its growth.[1]

Toughening of epoxy thermosets can be done by the reduction of the crosslinking density or by the addition of polymeric rubber particles that leads to phase separated morphologies, but the deterioration of other characteristics, such as the T_g and stiffness are common side effects accompanying these solutions.[2] Recently, Le et al.[3] reported that the addition of rubber particles of nanometer size doubled the fracture toughness of the modified epoxy without observing loss of strength, modulus and glass transition temperature. Also H-J. Sue *et al.*[4] reported the use of block copolymers in epoxy thermosets to improve the fracture toughness in a 300% without compromising its modulus by a nanocavitation mechanism of fracture. Another approach to increase toughness in epoxy resin has been the addition of hyperbranched polymers (HBPs). The possibility to tailor their structure and the presence of a great number of reactive or non-reactive groups as chain ends can lead to homogeneous or phase separated epoxy thermosets with improved characteristics.[5,6] The use of HBPs as reactive modifiers does not affect substantially the T_g and stiffness if their structure is efficiently tailored[7,8] and even can present some other advantages, such as the reduction of the shrinkage on curing[9] and increased reworkability.[7,10] In addition, the curing process can be accelerated in reference to the curing of the neat resin and the conversion at the gelation can be increased.[9]

A multitude of high-tech and electronic applications, such as coatings in electronic fibers, microelectronics and printed circuit boards use UV curable formulations. This is because the formation of the film is a very quick process with low energy consumption and absence of VOC emissions. Cationic photopolymerization is a very advisable technique because the lack of

inhibition by oxygen and the good characteristics of the thermosets obtained. The photocrosslinking of HBP-epoxy formulations has been extensively reported in the literature.[11,12]

Thiol-ene photocurable coatings present advantages such as inherently rapid reaction rate, low shrinkage, reduced oxygen inhibition, photoinitiator-free polymerization and formation of homogeneous polymer structures. However, they present odor problems, low surface hardness and poor mechanical properties.[13] To increase mechanical characteristics it seemed interesting to incorporate epoxy resins into these systems to be polymerized by a cationic UV-induced process. However, it was demonstrated that when cationic and thiol-ene photocurable systems were photopolymerized, the interactions between the components of the formulation inhibit the cationic polymerization.[14,15] It was reported that thiol groups reacted with oxirane rings of the protonated epoxy monomers to form new sulfide bonds between the thiols and the epoxy groups. Once the sulfide groups were formed, they reacted with the oxonium terminated growing chains to form trialkyl sulfonium salts. These salts promoted the thermal curing of the unreacted epoxy monomer, which allowed obtaining hard and homogeneous materials.[14] This process was considered to be an UV-thermal dual-curing.

The aim of the present work was the study of one-pot curing mixtures containing cycloaliphatic epoxy resin, a poly(ester-sulfide) hyperbranched polymer and a photoinitiator, triphenylsulfonium hexafluoroantimoniate. By effect of the UV irradiation on the mixture a thermal latent multifunctional macroinitiator was generated from the HBP.

The poly(ester-sulfide) hyperbranched polymer tested in the present work was synthesized by esterification and thiol-ene click reaction following an iterative procedure.[16] The structure of the HBP, with a flexible aliphatic structure, was tailored to produce a phase separation on curing and has hydroxyl chain ends, which can become covalently linked to the epoxy matrix in cationic curing by the well-known monomer activated mechanism.[17,18] The thioethers in the HBP structure allow the formation of trialkyl sulfonium salts by reaction with the oxonium groups formed during irradiation. The macroinitiator having sulfonium salts in the structure leads to the complete curing of the mixture in thermal conditions avoiding vitrification that often occurs in UV curing.

Latent curing agents show no activity under normal conditions but become active by external stimulation, in our case UV irradiation, and therefore they can simplify the technological curing process.[19]

EXPERIMENTAL PART

Materials

Triethylamine (TEA), 1,1,1-tris(hydroxymethyl) propane (TMP), 10-undecenoyl chloride, 2,2-dimethoxy-2-phenylacetophenone (DMPA) and 1-thioglycerol were purchased from Aldrich and used as received. Tetrahydrofurane was purchased from Panreac and dried over Na/benzophenone before using it. Diethylether, $NaHCO_3$, HCl and $MgSO_4$ were purchased from Panreac and used without further purification.

The bis-cycloaliphatic diepoxy resin 3,4-epoxycyclohexylmethyl-3',4'-epoxycyclohexyl carboxylate, (CE, Huntsman, 126 g/ee) and triphenylsulfonium hexafluoroantimonate (PI, $Ph_3S^+SbF_6^-$, Aldrich) were used as received.

HBP synthesis

In a 100 ml two-necked round bottomed flask provided with magnetic stirring and Ar atmosphere, 1 g (7.45 mmol) of TMP was dissolved in 50 ml of anhydrous THF and 3.6 ml (25.8 mmol) of TEA were added and kept the mixture under stirring for 30 minutes. Then 4.8 ml (25.8

mmol) of 10-undecenoyl chloride were added drop by drop and the mixture was allowed to react overnight. Then the precipitate was filtered off and the solvent was eliminated under vacuum. The crude product was dissolved in diethyl ether, and extracted three times with $NaHCO_3$ (sat), HCl (0.1 N) and finally with brine. The organic layer was dried with anhydrous $MgSO_4$ and concentrated under vacuum. The product was used without further purification.

The crude product was added in a vial together with 1.9 ml (21.9 mmol) of 1-thioglycerol and 3 mg (0.06% mol) of DMPA, and 2 ml of THF were added to help dissolve the catalyst. Then the mixture was irradiated for 3 hours with 365 nm UV light at room temperature under stirring. The product was precipitated in diethyl ether.

The product obtained was again reacted twice iteratively by the same procedure described before (esterification followed by thiol-ene coupling) yielding the final hyperbranched polymer (HBP). The synthetic pathway is depicted in **Scheme 1**.

^{1}HNMR ($CDCl_3$): δ (in ppm) 0.85 (CH_3 core); 1.15-1.30 (CH_2); 1.45-1.60 ($\underline{CH_2}$-CH_2-S, $\underline{CH_2}$-CH_2-CO); 2.20-2.30 (CH_2-S, CH_2-CO); 2.45-2.65 (CH_2-S), 3.55-3.95 (CH_2-OH, CH-OH); 4.00 (CH_2 core); 4.10-4.40 (CH_2-O-CO); 5.15-5.20 (CH-O-CO).

$\bar{M}_{n,theoretic}$ (g/mol): 5,288
$\bar{M}_{n,NMR}$ (g/mol): 4,063
$\bar{M}_{n,GPC}$ (g/mol): 4,000
$Đ_M$: 1.35 (calculated by GPC)

Samples Preparation

To formulations containing the appropriate amount of HBP (5, 10 and 15 parts per hundred parts of resin, phr) in the epoxy resin (CE), 2 phr of the photoinitiator were added in reference to the CE resin. The solubility of the HBP in the resin was assessed by visual inspection. To obtain the specimens, the liquid formulations were coated onto an aluminum template (for free-standing films). Then the samples were exposed to UV radiation with a fusion lamp (H-bulb) in air at a conveyor speed of 5 $m \cdot min^{-1}$, with radiation intensity on the surface of the sample of 280 $mW \cdot cm^{-2}$. After that, they were placed in an oven for 4 hours at 150 °C.

Characterization

^{1}H NMR 400 MHz and ^{13}C NMR 100.6 MHz NMR spectra were obtained using a Varian Gemini 400 spectrometer with Fourier Transformed. ^{1}H NMR spectra were acquired in 1 min and 16 scans with a 1.0 s relaxation delay (D1).

Size exclusion chromatography (SEC) analysis was carried out with an Agilent 1200 series system with PLgel 3 μm MIXED-E, PLgel 5 μm MIXED-D, and PLgel 20 μm MIXED-A columns in series, and equipped with an Agilent 1100 series refractive-index detector. Calibration curves were based in polystyrene standards having low molecular weight dispersities. THF was used as the eluent at a flow rate of 1.0 mL/min, the sample concentrations were 5-10 mg/mL, and injection volumes of 100 μL were used.

FTIR measurements were performed in a Thermo-Nicolet 5700 FTIR device. All the measurements were performed at room temperature at constant humidity (25-30%).

Photocalorimetric experiments were performed in order to study UV part of the dual curing. The various samples were photocured at different temperatures using a Mettler DSC-821e calorimeter appropriately modified to permit irradiation with a Hamamatsu Lightningcure LC5 (Hg-Xe lamp) with two beams, one for the sample side and the other for the reference side. Samples weighing *ca.* 3 mg were cured in open aluminium pans in a nitrogen atmosphere. Two

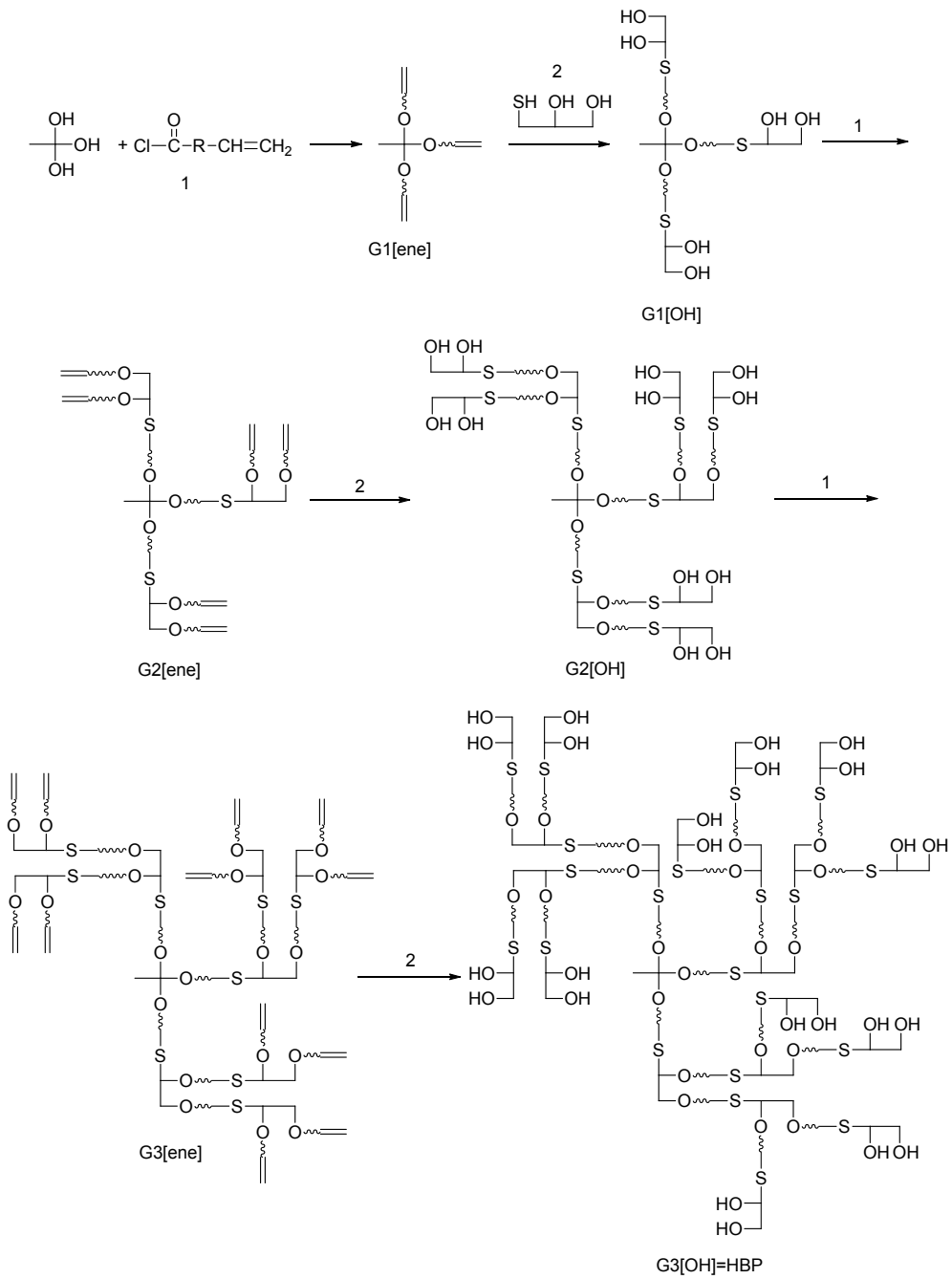

Scheme 1 Synthetic pathway for the preparation of the hyperbranched polymer.

scans were performed on each sample in order to substract the thermal effect of the UV irradiation from the photocuring experiment, each one consisting of 4 minutes of temperature conditioning, 20 minutes of irradiation and finally 4 more minutes without UV light. A light intensity of 30 mW/cm^2 (calculated by irradiating graphite-filled pans on only the sample side) was employed. Dynamic postcuring experiments were carried out on a Mettler DSC-822e with a TSO801RO robotic arm, from 0 to 300 ºC at 10 ºC/min in nitrogen atmosphere. The degree of

conversion x_{UV} during the photocuring stage was calculated based on the heat evolved during the postcuring as follows:

$$x_{UV} = 1 - \frac{\Delta h_{post}}{\Delta h_{theor}} \quad (1)$$

where Δh_{post} is the heat released during the postcuring process and Δh_{theor} corresponds to the theoretical heat evolved during complete cure of the formulation which was assumed to be 100 kJ/ee.[20]

The kinetic studies were performed in a DSC-822e with a TSO801RO robotic arm, from 30 to 300 ºC at heating rates of 2, 5, 10 and 15 ºC/min in N_2 atmosphere and the activation energy of the process was calculated using the STARe software.

The gel content was determined on the cured films by measuring the weight loss after 24 h extraction with chloroform at room temperature according to the standard test method ASTM D2765-84.

Dynamic-mechanical thermal analyses (DMTA) were performed on a MK III Rheometrics Scientific Instrument at 1 Hz frequency in the tensile configuration. The storage modulus, E', and the loss factor, *tan* δ, were measured from -90 ºC to the temperature at which the rubbery state was attained. Specimens of 10 x 7.5 x 1 mm^3 were used.

Thermogravimetric analysis (TGA) was performed with a METTLER TGA/SDTA 851 instrument between 30 and 800 ºC at a heating rate of 10 ºC/min in nitrogen.

SEM analyses were performed on fracture surfaces of the hybrid systems by using a ZEISS SUPRA™ 40 Field Emission Scanning Electron Microscope (FE-SEM) with an acceleration voltage of 10 KV and WD= 2 mm (Nominal resolution: 1.5 nm).

RESULTS AND DISCUSSION

HBP synthesis

The approach we followed to obtain the HBP used in this work was based in the work of C. J. Hawker *et al.*[16] They obtained a dendrimer, making sure that a complete reaction took place after every step and purifications were performed after each generation. In technological applications the perfect shape of a dendrimer is not required and therefore the synthesis of HBP was performed by iterative methodology but without thorough purification between steps. The synthetic pathway is shown in **Scheme 1** and the structure of HBP is represented in **Scheme 2**.

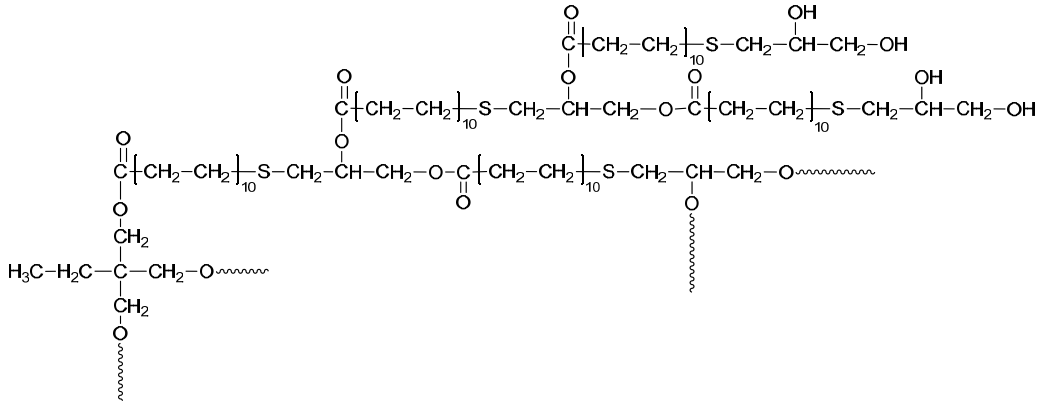

Scheme 2 Chemical structure of the synthesized hyperbranched polymer.

We selected TMP as the core molecule, which contains three reacting hydroxyl groups, which were esterified with 10-undecenoyl chloride. This yielded a molecule with three terminal double bonds that were reacted with thioglycerol using UV light to promote it. This reaction is very advantageous because is quick, needs very little solvent, is nearly quantitative and takes place in the presence of other functional groups.[21,22] The hydroxyl groups of the resulting molecule were again esterified with 10-undecenoyl chloride and this was iterated until obtaining a third generation HBP. Due to the different reactivity of primary and secondary hydroxyls present in thioglycerol and the sterical hindrance of the long chains on increasing the generation number, the esterification was not complete and therefore, we obtained a molecular weight-dispersed hyperbranched polymer.

We calculated the average molecular weight in number ($\bar{M}_n$) by ^{1}H-NMR spectroscopy using the signals corresponding to the methyl of the core molecule (signal CH_3 core) and the signal that includes methylene in β-position to carbonyl and sulfur (signal $\underline{CH_2}$-CH_2-S, $\underline{CH_2}$-CH_2-CO) (**Figure 1**). One can see that the $\bar{M}_n$ obtained in this way is in agreement with the one obtained by GPC ($\bar{M}_{n,NMR}$: 4,063 g/mol; $\bar{M}_{n,GPC}$: 4,000 g/mol). They differ slightly from the theoretical one ($\bar{M}_{n,theoretic}$: 5,288 g/mol) because, as we have mentioned, we could not achieve the full esterification. However, the value calculated for the molecular weight dispersity ($Đ_M$) is quite low, 1.35, indicating a narrow molecular weight distribution. This was something expected considering the methodology we have used to synthesize the HBP, more similar to the one used for dendrimers.

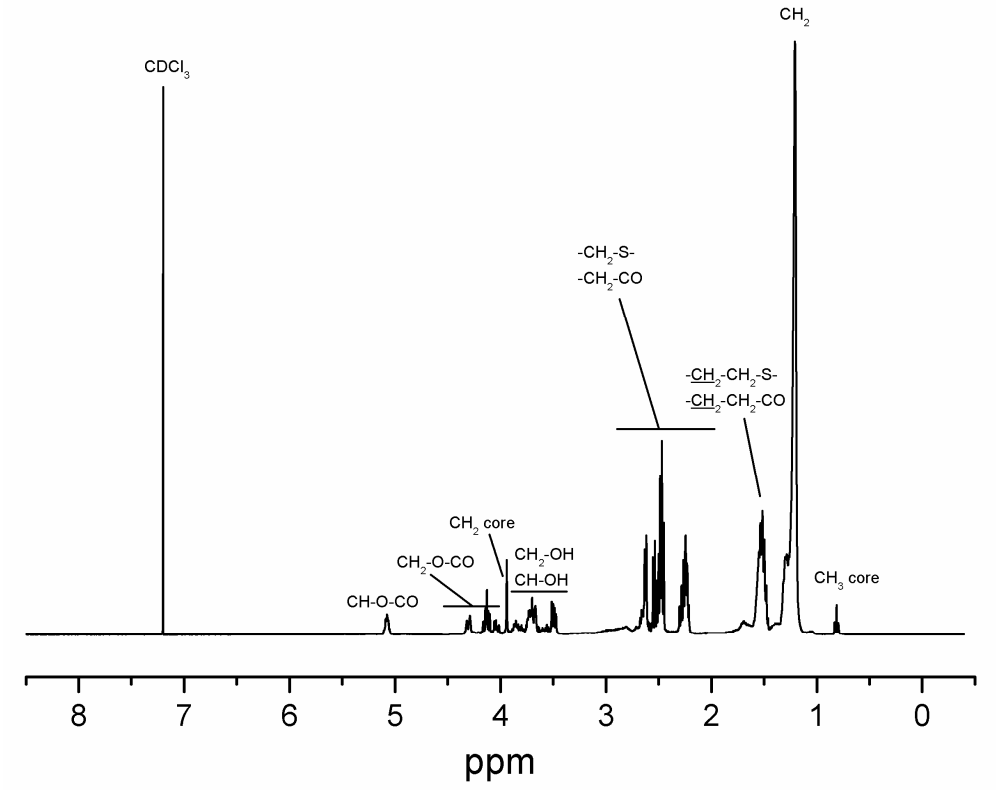

Figure 1 ^{1}H-NMR spectra of the HBP in $CDCl_3$.

The polymer obtained was also characterized by differential scanning calorimetry (DSC). **Figure 2a** shows the curve obtained and the values of the glass transition and melting

endotherms. As one can see, there is a glass transition at low temperatures typical of a polymer with such a low molecular weight and flexible structure. Also two broad melting endotherms can be observed at higher temperatures (25 and 38 °C), due to the presence of long chains that probably can crystallize in different size and shapes.

Thermogravimetric analysis (**Figure 2b**) shows that there is a main process of degradation which starts at around 300 °C. This initial loss of weight can be attributed to the presence of ester groups that experiments a β-elimination process leading to the formation of small fragments.

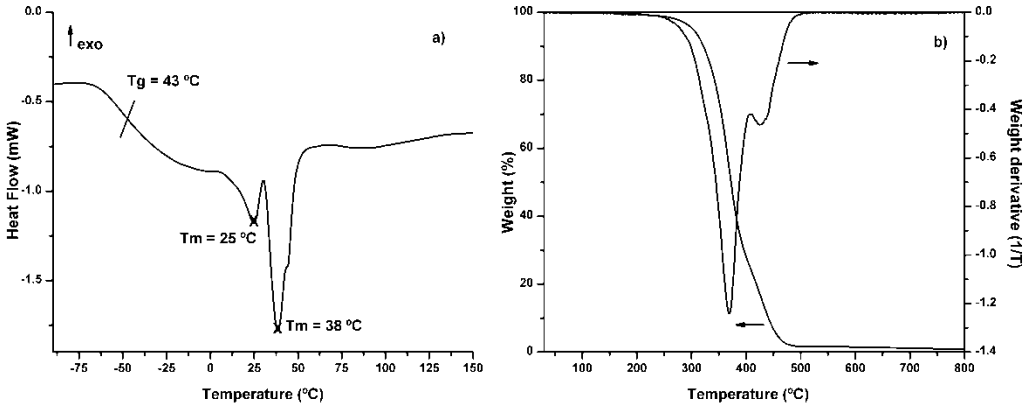

Figure 2 (a) DSC curve of the HBP obtained in a 20 °C/min scan under N_2 (b) TGA and dTGA curves of the HBP obtained at 10 °C/min under N_2.

Study of the dual curing

As we mentioned in the introduction, the presence of sulfides in the HBP structure allows the formation of trialkyl sulfonium salts from oxonium groups formed during irradiation as depicted in **Scheme 3**. The HBP becomes a multifunctional macroinitiator with sulfonium salts in the structure, which can promote the cationic thermal curing.[23]

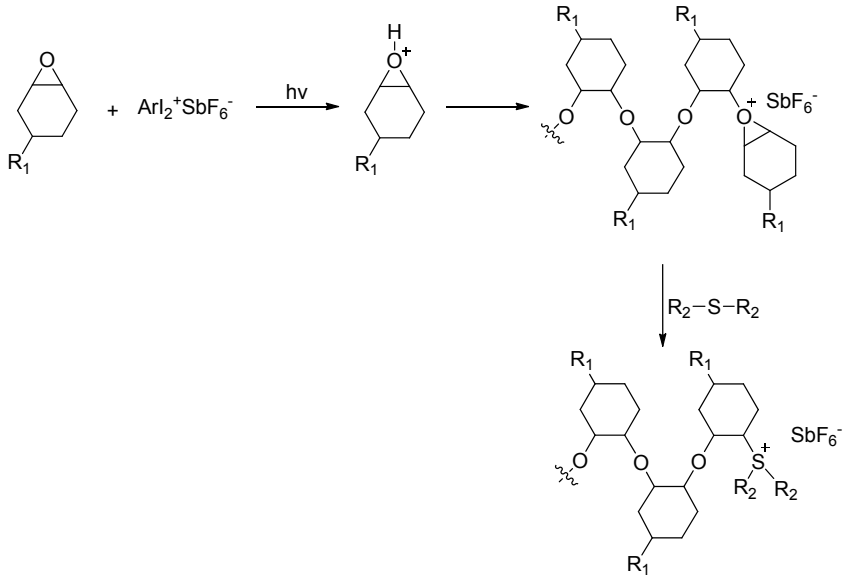

Scheme 3 Mechanism of trialkylsulfonium salt formation.

As the curing takes place in two stages, we studied both separately. By means of photo-DSC we irradiated the sample with UV light at different temperatures and registered the enthalpy of the process. The same sample was scanned in a DSC at 10 ºC/min to measure the enthalpy of the thermal process and to be able to calculate the percentage of curing that takes place in each step. **Table 1** shows the measured enthalpy values of both processes for all the formulations studied as well as the conversion determined for the UV part (x_{UV}). FTIR spectra were recorded after each curing step and the epoxy band at 740 cm^{-1} was monitored. After photoirradiation this absorption decreases in a similar extent than the calculated from DSC experiments. After thermal curing the band completely disappears implying that the complete curing was reached.

Scheme 3 shows the mechanism proposed for the formation of the alkylsulfonium salt[14] that is the real initiating specie in the thermal step of epoxy crosslinking. In this mechanism, a thioether interacts with a propagating chain stopping its growth and generating the above mentioned latent macroinitiator. In the sample containing 5 phr of HBP, the thioether concentration is lower (**Table 2**) and therefore more time is needed to react with all the growing chains and thus the enthalpy of photocuring is higher (**Table 1**). Consequently, the sample containing 15 phr of HBP has a higher concentration of thioether groups and the UV curing is stopped very quickly (conversion of the UV part less than a 25% of the overall process at 40 ºC). **Figure 3** shows the decrease on the curing enthalpy more clearly. As we can see, the higher the proportion of HBP the lower the height of the photocuring exotherm is. In no case by UV irradiation the gelation was reached, since the materials were viscous liquids and fully soluble in chloroform.

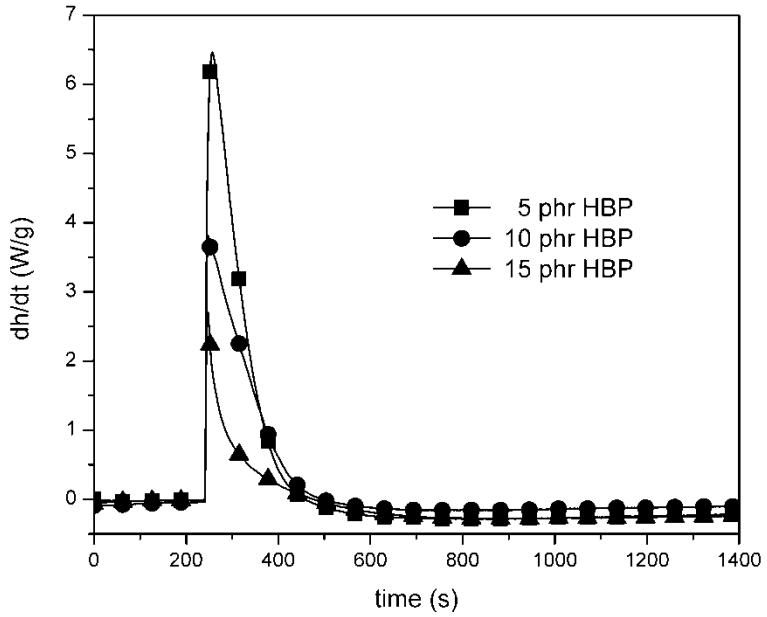

Figure 3 Photo-DSC curves obtained at 40 ºC for the formulations containing 5, 10 and 15 phr of HBP.

By working at different temperatures (see **Table 1**) we can appreciate that at higher temperatures the conversions achieved in the photocuring step are higher for all the formulations studied. However, the tendency observed at 40 ºC is the same as the one observed for all the temperatures, this is the decrease of x_{uv} on increasing the amount of HBP.

Table 1 Values for the enthalpies of the UV and the thermal processes, and calculated conversion for the UV irradiation part.

HBP content (phr)	40 °C			80 °C			120 °C		
	Δh_{UV} (kJ/ee)	Δh_T (kJ/ee)	x_{UV}	Δh_{UV} (kJ/ee)	Δh_T (kJ/ee)	x_{UV}	Δh_{UV} (kJ/ee)	Δh_T (kJ/ee)	x_{UV}
5	17	67	0.33	24	63	0.37	28	53	0.47
10	14	69	0.31	15	67	0.33	18	65	0.35
15	8	76	0.24	10	73	0.27	13	70	0.30

Once understood the UV part of the process we performed a study on the thermal part. We irradiated samples with a 300 nm UV light source at room temperature and then cured in a DSC. **Figure 4** shows the exotherms obtained for all the studied formulations. First of all we can appreciate no enthalpy evolution until high temperatures (around 159 °C). This indicates that no vitrification took place during the UV irradiation, because if that was the case the exotherm would begin at lower temperatures (about the T_g of the material after irradiation). Thus, the second step is a real thermal curing process initiated by the generated macroinitiator.

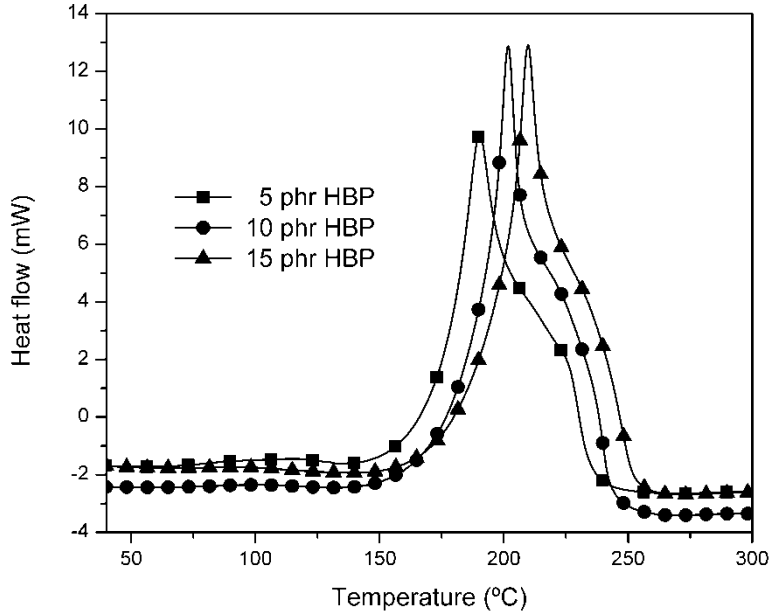

Figure 4 DSC curves of the thermal step of curing of samples containing 5, 10 and 15 phr of HBP.

The shape of the curves presents a main peak attributed to the thermal initiation by the effect of the UV generated multifunctional macroinitiator. Also a shoulder at higher temperatures appears which could account for the uninitiated thermal curing that usually takes place at this range of temperatures. In **Table 2** the temperatures of the maximum of the exotherms are collected. It can be seen that on increasing the amount of HBP in the formulation the temperature increases. The generation of sulfonium active points in the macroinitiator is limited by the amount of photoinitiator added to the formulation. Thus, a higher proportion of HBP does not imply an increase in the amount of thermal initiator sites since all formulations contain enough sulfides to react with all the growing chains generated by UV irradiation (see **Table 2**). One explanation to the observed decelerative effect is the increase on the viscosity of the

samples on adding HBP. Moreover, the addition of HBP reduces the concentration of epoxy groups in the mixture that also leads to the deceleration of the curing. The increase in the proportion of OH:epoxy groups on increasing the amount of HBP in the reactive mixture that usually accelerates the curing by the AM mechanism in this case does not produce any observable effect.

Table 2 Proportion of sulfide and hydroxyls in respect to the photoinitiator and epoxy groups and kinetic data for all the studied systems.

HBP content (phr)	eq S : eq PI	eq S : eq epox	eq OH : eq epox	*Tp* [a] (ºC)	*Ea* [b] (kJ/mol)
5	16.31	0.033	0.038	190	130
10	32.62	0.066	0.076	202	138
15	48.93	0.099	0.114	210	120

a. Temperature of the maximum of a dynamic DSC curve performed at 10 ºC/min.
b. Activation energy calculated for a conversion of 0.5.

In order to obtain the activation energy of the thermal process we registered DSC curves at different rates (2, 5, 10 and 15 ºC/min). The calculated values are collected in **Table 2**. We can state that all of them are of the same order and typical of thermal curing systems, much higher than the ones usually obtained in UV cured systems.[24,25]

Characterization of the materials

First of all we assured the chemical incorporation of the HBP into the epoxy matrix by determining the gel content (see **Table 3**) of all the materials obtained. In all cases it was quantitative. This indicates that the polymer is chemically linked to the epoxy matrix, due to the fact that the HBP act as a multifunctional macroinitiator. Moreover, hydroxyl groups can become covalently linked to the epoxy matrix by the AM mechanism of cationic ring opening as observed in similar systems.[26]

Table 3 Gel content, DMTA and TGA data for all the studied formulations.

HBP content (phr)	Gel content (%)	*Tan δ* (ºC)	*E'* [a] (MPa)	$T_{10\%}$ [b] (ºC)	Char Yield [c] (%)
5	99	221	19	358	1.9
10	100	209	23	356	1.8
15	99	204	29	355	2.9

a. Moduli were measured at *tan δ* + 50 ºC.
b. Temperature at which the material has lost a 10% weight.
c. Residue at 800 ºC in the TGA performed under nitrogen atmosphere.

Dynamic mechanical thermal analysis (DMTA) is a technique that allows knowing, among other characteristics, the T_g of the materials, relating this to the maximum of the loss factor curve. T_g can also be determined by DSC but in our case the rigidity of the network was too high and no appreciable transitions were observed by this technique. **Figure 5** shows the *tan δ* plot of the different thermosets prepared together with the curve of the cycloaliphatic resin cured by UV from -90 to 250 ºC. As one can see, the rigidity of the network is much higher in the case of using the HBP (the height of the main transition is much lower). This can be rationalized in the basis that the HBP, although having a very flexible structure, acts as a multifunctional initiator leading to highly crosslinked networks. In **Table 3** the values of the maximum of *tan δ* peak are collected. In all cases we were able to obtain materials with very high T_gs (all of them above 200 ºC). The sample with the highest T_g was the one containing 5 phr of HBP. It should be pointed

out that the thermal curing of CE with 1 phr of lanthanum triflate as cationic initiator led to a thermoset with a *tan δ* value of 164 °C,[27] lower than the one of the photocured analogous thermoset.

The fact that the T_gs were so high could lead to the conclusion that a partial phase separation of the HBP from the epoxy matrix can occur. In case of homogeneous materials, the calculation of the T_gs by the Fox equation will give much lower values, according to the fact that the HBP has a lower T_g than the neat epoxy thermoset.[17]

We also performed the DMTA analysis at low temperature in order to observe if a transition associated to the HBP appeared. As we can see in the inset of **Figure 5**, a broad transition at around -50 °C can be appreciated. This can be related to the T_g of the hyperbranched polymer (as determined by DSC was -43 °C). One can also appreciate how on increasing the proportion of HBP this transition becomes more evident. This behavior is typical of materials with phase separation, where the T_gs of the two polymers can be appreciated separately.

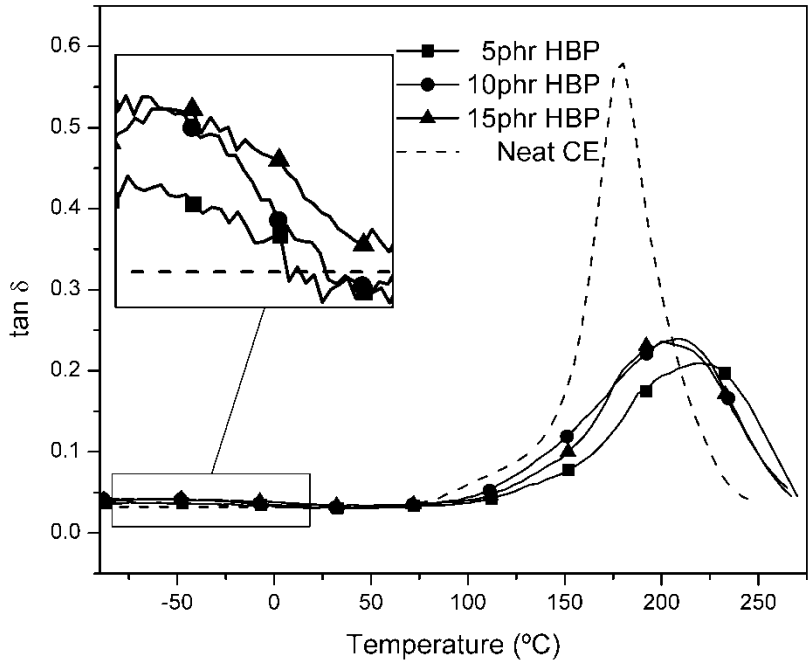

Figure 5 DMTA curves obtained for the materials containing 5, 10 and 15 phr of HBP.

DMTA can also provide us with information about the storage modulus of the thermosets in the rubbery state. In our case, the higher the proportion of HBP in the formulation the higher is the modulus after relaxation. This fact accounts for the macroinitiator function of the HBP together with the presence of OH groups that can become covalently linked to the epoxy matrix by the AM mechanism, increasing the rigidity of the materials.

In order to find a confirmation of the presence of phases of HBP within the epoxy matrix, as we have detected in the *tan δ* curves we performed scanning electron microscopy of cryofractured materials. Actually, we used field emission SEM which is a technique that allows obtaining higher resolutions than classical SEM, very adequate in case of nanophase separations. **Figure 6** shows two pictures at different magnifications for the sample containing 15 phr of HBP. This material is the one with a higher content of HBP and therefore is easier to see

the phase separation, but similar pictures were obtained for the samples with lower content of HBP. At lower magnification (**Figure 6a**) only the cracks of the breaking of the samples can be observed but, on increasing the magnifications (**Figure 6b**) one can see the presence of phases of around 50 nm which can be attributed to HBP domains. They show spherical-like morphology, although in some regions agglomerations can be appreciated. It should be pointed out, that the presence of phase separation especially in the nanometric scale can lead to improvements on the toughness characteristics of epoxy resins without compromising other properties such as transparency, T_g or thermal stability among others.[28,29]

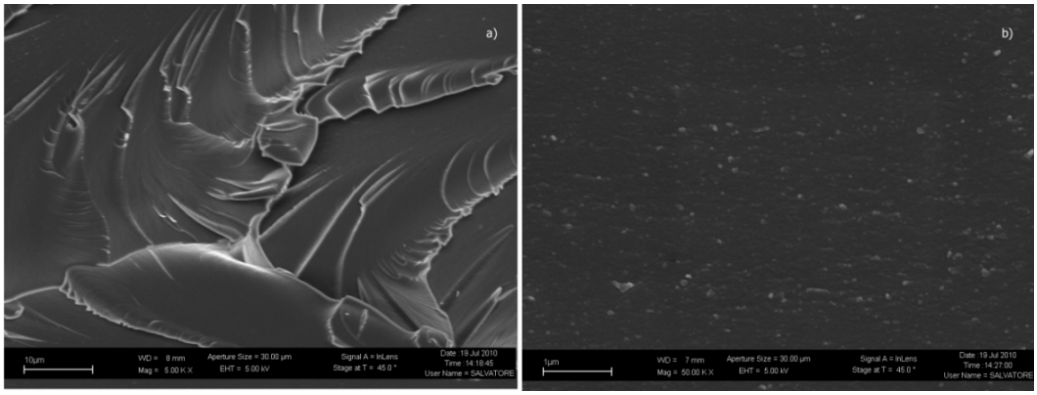

Figure 6 FE-SEM pictures at magnification of 5000 (a) and 50000 (b) of the sample containing 15 phr of HBP

To evaluate the thermal stability of this series of materials prepared we carried out thermogravimetric analysis under nitrogen atmosphere. The values obtained for the different parameters and the curves are presented in **Table 3** and **Figure 7** respectively. We could observe that regardless of the amount of HBP the stability was practically the same. In all cases we obtained high $T_{10\%}$ values (around 350 ºC), which is interesting for materials that have to be used at high temperatures. Also the residue obtained was unaffected by the amount of HBP. The high thermal stability of the thermosets accounts for a high density of crosslinking of the materials.

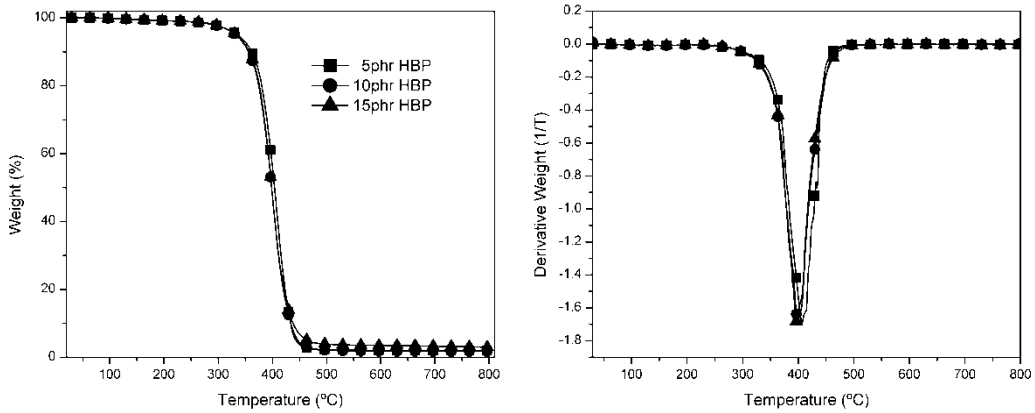

Figure 7 TGA thermograms obtained at 10 ºC/min under N_2 for the materials containing 5, 10 and 15 phr of HBP

CONCLUSIONS

We synthesized and characterized a new hyperbranched polymer with thioether and esters in the structure with hydroxyl groups as chain ends. Its preparation followed an iterative methodology based on thiol-ene click reaction and esterification processes.

The HBP synthesized was used as a dual latent macroinitiator for the curing of a commercially available cycloaliphatic epoxy resin. In a first step, promoted by UV irradiation, the thioether groups of the HBP reacted with the photoinitiator (a triaryl sulfonium salt), leading to the formation of a thermal macroinitiator containing several trialkyl sulfonium groups. In the second step, the thermal curing of the epoxy resin can take place, leading to highly crosslinked networks in all the mixtures studied containing different proportions of HBP.

The T_g of the resulting thermosets were higher than those determined for the neat epoxy material photo or thermally cured. However, on increasing the amount of HBP in the formulation the T_g*s* of the final thermosets decreased, although in all cases they were higher than 200 ºC.

Electron microscopy allowed us to confirm the nanophase separation of the HBP dispersed within the epoxy matrix.

The storage modulus in the rubbery state increased with the proportion of HBP in the formulation. The higher rigidity of the materials could be related to the multifunctionality of the HBP that becomes covalently linked to the epoxy matrix.

No decrease in the thermal stability of the materials was observed on using up to 15 phr of HBP in the formulation.

ACKNOWLEDGEMENTS

The authors from the Universitat Rovira i Virgili and from Universitat Politècnica de Catalunya would like to thank MICINN (Ministerio de Ciencia e Innovación) and FEDER (Fondo Europeo de Desarrollo Regional) (MAT2008-06284-C03-01 and MAT2008-06284-C03-02) and to the Comissionat per a Universitats i Recerca del DIUE de la Generalitat de Catalunya (2009-SGR-1512). D.F. acknowledges the grant FPU-2007 from the Spanish Government.

REFERENCES

1. C. A. May. *Epoxy Resins. Chemistry and Technology*, 2nd edition. Marcel Dekker, New York, **1988**.

2. J-P. Pascault, H. Sauterau, J. Verdu, R. J. J. Williams. *Thermosetting Polymers*. Marcel Dekker, New York, **2002**.

3. Q-H. Le, H-C. Kuan, J-B. Dai, I. Zaman, L. Luong, J. Ma. *Polymer* **2010,** *51,* 4867.

4. J. Liu, H-J. Sue, Z. J. Thompson, F.S. Bates, M. Dettloff, G. Jacob, N. Verghese, H. Pham. *Macromolecules* **2008,** *41,* 7616.

5. L. Boogh, B. Pettersson, J. A. E. Månson. *Polymer* **1999,** *40,* 2249.

6. J. Zhang, Q. Guo, B. Fox. *J. Polym. Sci. Part B: Polym. Phys.* **2010,** *48,* 417.

7. D. Foix, M. Erber, B. Voit, A. Lederer, X. Ramis, A. Mantecón, A. Serra. *Polym. Degrad. Stab.* **2010,** *95,* 445.

8. M. Sangermano, A. Priola, G. Malucelli, R. Bongiovanni, A. Quaglia, B. Voit, A. Ziemer. *Macromol. Mater. Eng.* **2004,** *289,* 442.

9. X. Fernández-Francos, J. M. Salla, A. Cadenato, J. M. Morancho, A. Serra, A. Mantecón, X. Ramis. *J. Appl. Polym. Sci.* **2009,** *111,* 2822.

10. M. Morell, X. Fernández-Francos, X. Ramis, A. Serra. *Macromol. Chem. Phys.* **2010,** *211,* 1879.

11. A. Di Gianni, M. Sangermano, G. Malucelli, B. Voit. *Macromol. Mater. Eng.* **2006,** *291,* 1004.
12. Z. Chen, D. C. Webster. *Polym. Int.* **2007,** *56,* 754.
13. M. Sangermano, G. Colucci, M. Fragale, G. Rizza. *React. Funct. Polym.* **2009,** *69,* 719.
14. R. Acosta Ortiz, B. A. Puente Urbina, L. V. Cabello Valdez, L. Berlanga Duarte, R. Guerrero Santos, A. E. Garcia Valdez, M. D. Soucek. *J. Polym. Sci. Part A: Polym. Chem.* **2007,** *45,* 4829.
15. M. Sangermano, M. Cerrone, G. Colucci, I. Roppolo, R. Acosta Ortiz. *Polym. Int.* **2010,** *59,* 1046.
16. K. L. Killops, L. M. Campos, C. J. Hawker. *J. Am. Chem. Soc.* **2008,** *130,* 5062.
17. X. Fernández-Francos, D. Foix, A. Serra, J. M. Salla, X. Ramis. *React. Funct. Polym.* **2010,** *70,* 798.
18. P. Kubisa, S. Penczek. *Prog. Polym. Sci.* **1999,** *24,* 1409.
19. T. Endo, F. Sanda. *Macromol. Symp.* **1996,** *107,* 237.
20. J. Brandrup, E. H. Immergut, E. A. Grulke. *Polymer Handbook*, 4th ed. Wiley-Interscience, New York, **1999**.
21. C. R. Becer, R. Hoogenboom, U. S. Schubert. *Angew. Chem. Int. Ed.* **2009,** *48,* 4900.
22. A. Dondoni. *Angew. Chem. Int. Ed.* **2008,** *47,* 8995.
23. D. J. Brunelle. *Ring-Opening Polymerization, Mechanisms, Catalysis, Structure and Utility.* Hanser Publishers, Munich, Vienna, New York, Barcelona, **1993**.
24. M. J. M. Abadie, N. K. Chia, F. Boey. *J. Appl. Polym. Sci.* **2002,** *86,* 1587.
25. X. Fernández-Francos, X. Ramis, J. M. Salla. *Thermochim. Acta* **2005,** *438,* 144.
26. D. Foix, X. Fernández-Francos, X. Ramis, A. Serra, M. Sangermano. *React. Funct. Polym.* **2011,** *71,* 417.
27. X. Fernández-Francos, J. M. Salla, A. Serra, A. Mantecón, X. Ramis. *J. Polym. Sci. Part A: Polym. Chem.* **2005,** *43,* 3421.
28. L. H. Sperling. *Introduction to Physical Polymer Science*, 4th ed. Wiley-Interscience, Hoboken, **2006**.
29. J. Karger-Kocsis, J. Fröhlich, O. Gryshchuk, H. Kautz, H. Frey, R. Mülhaupt. *Polymer* **2004,** *45,* 1185.

6.3 Improvement of epoxy thermosets using a thiol-ene based polyester hyperbranched polymer as modifier

D. Foix[1], X. Ramis[2], F. Ferrando[3], A. Serra[1]

[1] Department of Analytical and Organic Chemistry, University Rovira i Virgili, Marcel.li Domingo s/n, 43007 Tarragona, Spain

[2] Laboratory of Thermodynamics, ETSEIB, University Politècnica de Catalunya, Av. Diagonal 647, 08028 Barcelona, Spain

[3] Department of Mechanical Engineering, University Rovira i Virgili, Països Catalans 26, 43007 Tarragona, Spain

ABSTRACT

The anionic curing initiated by 1-methyl imidazole of diglycidyl ether of bisphenol A (DGEBA) with a hyperbranched polyester containing long aliphatic chains in the structure were studied. The hydroxyl groups present as chain ends in the HBP structure played an important role in the curing kinetics, as demonstrated by DSC, FTIR and rheological studies. Properties such as shrinkage on curing or thermomechanical characteristics were also investigated. The structure of the HBP, which contains long aliphatic chains and reactive hydroxyl groups as chain ends, flexibilize the network significantly improving the impact resistance without affecting notably neither T_g nor the microhardness of the modified thermosets.

INTRODUCTION

Epoxy resins are one of the most used polymers in the coatings industry due to their excellent properties in terms of thermal and chemical resistance, price and versatility. They present one main drawback which is their poor impact resistance, which comes from the fact that they are highly crosslinked thermosets inherently rigid.[1]

Toughening of epoxy thermosets can be achieved mainly through two different strategies. The first one consists in the reduction of the crosslinking density and the second is the addition of polymer particles that leads to microphase separated morphologies. However, both approaches lead to the loss of some other good characteristics such as the T_g or the stiffness among others.[2] The use of rubbers as additives has been extensively applied, but they are characterized by a low compatibility with the resin that makes difficult the mixing process and the preparation of epoxy matrices with homogeneously distributed particles. As an alternative to rubbers, thermoplastic polymers have been used to increase the fracture resistance leading to lower reductions of Young's modulus and the thermal stability.[3]

Hyperbranched polymers (HBPs) are a special type of dendritic polymers and have as a common feature a very high branching density with the potential of branching in each repeating unit. They are usually prepared in a one-pot synthesis, which limits the control on molar mass and branching accuracy and leads to "heterogeneous" products with a distribution in molar mass and branching. This distinguishes hyperbranched polymers from perfectly branched and monodisperse dendrimers. There are many synthetic methods to obtain these polymers such as polycondensation or ring opening polymerization but recently "click chemistry" methodologies have been studied.[4] Reactions such as Huisgen's cycloaddition,[5] Diels-Alder,[6] thiol-ene[7] or thiol-yne[8] reactions have been used to obtain HBPs. All of them present advantages such as high yields, chemoselectivity and mild reaction conditions that leads to better defined structures.

Taking all this into account, the use of hyperbranched polymers (HBPs) with reactive groups as chain ends that can react with the epoxy matrix could be considered as a good way to

increase toughness in epoxy thermosets.[9,10] The use of HBPs as reactive modifiers does not affect substantially the T_g and stiffness if their structure is efficiently tailored[11,12] and even some other advantages, such as reduction of the shrinkage on curing[13] and increase in the reworkability[11,13] can be accomplished. In addition, the curing process can be accelerated[14] and the conversion at the gelation can be increased.[13] Reduction of the shrinkage on curing and increasing conversion at the gel point are of the main importance, because both lead to a reduction of the internal stresses which appear during curing, improving the performance of these materials. In the present paper the use of a hyperbranched polyester with hydroxyl chain ends in order to improve epoxy toughness is reported. This HBP is particularly interesting as its synthesis is based on the efficient thiol-ene coupling reaction, which has allowed obtaining the HBP in an easy way.[15]

EXPERIMENTAL PART

Materials

Diglycidyl ether of Bisphenol A (DGEBA) Epitoke Resin 827 was provided by Shell Chemicals with an epoxy equivalent of 182 g/eq and was dried before use. Triethylamine (TEA), 1,1,1-tris(hydroxymethyl) propane (TMP), 10-undecenoyl chloride, 2,2-dimethoxy-2-phenylacetophenone (DMPA), 1-thioglycerol and 1-methyl imidazole (1-MI) were purchased from Aldrich and used as received. Tetrahydrofurane was purchased from Panreac and dried over Na/benzophenone before using it. Diethylether, $NaHCO_3$, HCl and $MgSO_4$ were purchased from Panreac and used without further purification. The hyperbranched polyester used in this work, whose structure is depicted in **Scheme 1**, was synthesized as described before using an iterative methodology.[15] The polymer had a molecular weight ($\bar{M}_n$) of 4,000 g/mol, 1.35 of molecular weight dispersion ($Đ_M$) and presented a T_g at -43 ºC and two melting processes at 25 and 38 ºC.

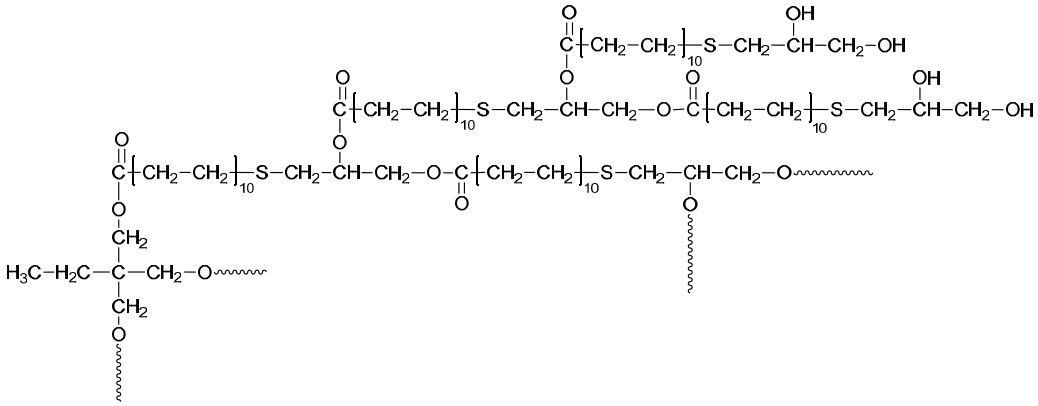

Scheme 1 Chemical structure of the synthesized hyperbranched polymer.

Sample preparation

The samples were prepared by mixing the selected proportions of DGEBA and HBP (0, 5, 10 and 15 phr) at 80 ºC until a clear solution was obtained. Then the mixture was allowed to cool down to room temperature and 3 phr of 1-MI in respect to the epoxy resin were added. After that, the mixture was milky but homogeneous and becomes transparent on heating. To obtain specimens the formulations were placed in aluminum templates (previously coated with silicone) with the corresponding dimensions and cured for 2 hours at 120 ºC and then post-cured at 150 ºC for 1 hour in an oven.

Characterization

Calorimetric studies were carried out on a Mettler DSC-821e thermal analyzer in covered Al pans under N_2. The calorimeter was calibrated using an indium standard (heat flow calibration) and an indium-lead-zinc standard (temperature calibration). The samples weighed approximately 7 mg. In the dynamic curing process the degree of conversion by DSC (x_{DSC}) was calculated as follows:

$$x_{DSC} = \frac{\Delta h_T}{\Delta h_{tot}} \quad (1)$$

where Δh_T is the heat released up to a temperature T, obtained by integration of the calorimetric signal up to this temperature, and Δh_{tot} is the total reaction heat associated with the complete conversion of all reactive groups. The kinetic studies were performed at heating rates of 2, 5, 10 and 15 °C/min in N_2 atmosphere. The precision of the given enthalpies is ± 3%.

The glass transition temperature for each material (T_g) was calculated after a complete dynamic curing, by means of a second scan, as the temperature of the half-way point of the jump in the heat capacity when the material changed from the glassy to the rubbery state. The precision of the determined temperatures is estimated to be ± 1 °C. The Fox equation was used to obtain the theoretical values of the T_gs of the resulting thermosets:

$$\frac{1}{Tg_{Fox}} = \frac{X_{HBP}}{Tg_{HBP}} + \frac{X_{DGEBA}}{Tg_{DGEBA}} \quad (2)$$

where X_{HBP} and X_{DGEBA} are the weight fractions of HBP and DGEBA in the formulation and $T_{g,\,HBP}$ and $T_{g,\,DGEBA}$ are the glass transition temperatures of pure HBP and the neat crosslinked DGEBA resin.

An FTIR spectrophotometer FTIR-680PLUS from Jasco with a resolution of 4 cm^{-1} in the absorbance mode was used to monitor the isothermal curing process at 100, 120 and 150 °C. This device was equipped with an attenuated total reflection (ATR) accessory with thermal control and a diamond crystal (Golden Gate heated single-reflection diamond ATR, Specac-Teknokroma). The disappearance of the absorbance peak at 915 cm^{-1} was used to monitor the epoxy equivalent conversion. The peak at 1508 cm^{-1} of the phenyl group was chosen as an internal standard. Conversion of the epoxy was determined by the Lambert-Beer law from the normalized change of absorbance at 915 cm^{-1}.

$$x_{IR} = 1 - \frac{\bar{A}^t}{\bar{A}^0} \quad (3)$$

where $\bar{A}^0$ and $\bar{A}^t$ are, respectively, the normalized absorbance of the epoxy group before curing and after a reaction time t.

Rheological measurements were carried out in the parallel plates (geometry of 25 mm) mode with an ARG2 rheometer (TA Instruments, UK, equipped with a Peltier system). The gelation time was determined by setting the device in time sweep and multiwave oscillation mode. Experiments were performed isothermally at 100 °C. Because the viscosity of the system changes significantly during the curing process, a control program was used in which the oscillation amplitude diminishes with an increase in the applied stress. By doing so, the curing process can be characterized in the whole range of conversion. Gel time was taken as the point where δ is independent of frequency. The conversion at the gelation (α_{gel}) was determined by stopping the rheometry experiment at gelation and performing a subsequent dynamic DSC scan of the gelled sample and comparing it with the initial one.

The gel content was determined on the cured films by measuring the weight loss after 24 h extraction with chloroform at room temperature according to the standard test method ASTM D2765-84.

Dynamic mechanical thermal analysis (DMTA) was performed in a TA DMA 2928 dynamic analyzer operating in three point bending mode at 1 Hz. The storage modulus (*E'*) and *tanδ* were measured from -90 to 220 ºC at 3 ºC/min on prismatic rectangular specimens (ca. 10 x 5 x 1.5 mm^3).

The cryofracture area of the specimens was observed by scanning electron microscopy (SEM). The samples were metalized with gold and observed with a Jeol JSM 6400 with 3.5 nm resolution.

Thermogravimetric analyses (TGAs) were carried out in a Mettler TGA/SDTA 851e thermobalance. Cured samples with an approximate mass of 8 mg were degraded between 30 and 800 ºC at a heating rate of 10 ºC/min in N_2 (100 cm^3/min measured in normal conditions).

The global shrinkage was calculated from the densities of the materials before and after curing, which were determined using a Micromeritics AccuPyc 1330 Gas Pycnometer thermostatized at 30 ºC. The densities were measured with a precision of ± 0.001. The precision of the shrinkage calculated values is 0.2%.

The impact test was performed at 23 ºC by means of an Zwick 5110 impact tester, according to ASTM D 4508-05 (2008) using prismatic rectangular specimens (ca. 20 x 11 x 2.5 mm^3). The pendulum employed had a kinetic energy of 1 J.

Microhardness was measured with a Wilson Wolpert (MicroKnoop 401MAV) device following the ASTM D1474-98 (2002) standard procedure. For each material 10 determinations were made with a confidence level of 95%. The Knoop microhardness (HKN) was calculated from the following equation:

$$HKN = \frac{L}{A_p} = \frac{L}{l^2 \times C_p} \quad (4)$$

where, *L* is the load applied to the indenter (0.025 Kg), A_p is the projected area of indentation in mm^2, *l* is the measured length of the long diagonal of indentation in mm, C_p is the indenter constant (7.028×10^{-2}) relating l^2 to A_p.

Kinetic analysis

Integral non-isothermal kinetic analysis was used to determine the kinetic triplet (*A* is the pre-exponential factor, *E* is the activation energy and *g(x)* is the integral function of degree of conversion).

If we accept that the dependence of the rate constant on the temperature follows the Arrhenius equation, non-isothermal kinetic analysis may start with the kinetic equation:

$$\frac{dx}{dt} = \beta \frac{dx}{dT} = Ae^{-\frac{E}{RT}} f(x) \quad (5)$$

where β is the heating rate, *dx/dt* is the rate of conversion, *R* is the universal gas constant, *T* is the temperature and *f(x)* is the differential conversion function.

By integrating eq(5) and using the Coats-Redfern[24] approximation to resolve the so-called temperature integral and considering that $2RT / E << 1$ the Kissinger-Akahira-Sunose equation (KAS) may be written as:

$$ln\frac{\beta}{T^2} = \ln\left[\frac{AR}{g(x)E}\right] - \frac{E}{RT} \quad (6)$$

For each conversion degree, the linear representation of $ln[\beta/T^2]$ versus T^{-1} enables E and $ln[AR/g(x)E]$ to be determined from the slope and the ordinate in the origin. If the reaction model, $g(x)$, is known, for each conversion the corresponding pre-exponential factor can be calculated for every activation energy.

In this study, we used the reduced master curves procedure of Criado[25] and the Coats-Redfern method to assign a reaction model to the systems studied.[26] By the Coats-Redfern method we selected the model which presented the best adjustment and had an activation energy similar to that obtained isoconversionally (considered to be the true). Different kinetic models have been studied: diffusion (D_1, D_2, D_3 and D_4), Avrami-Erofeev (A_2, A_3 and A_4), power law, phase-boundary-controlled reaction (R_2 and R_3), autocatalytic (n + m = 2 and 3) and order n (n = 1, 1.5, 2 and 3). The rate constant, k, was calculated with E and A determined at conversion of 0.5, using the Arrhenius equation.

RESULTS AND DISCUSSION

Recently, we reported the use of the hyperbranched polymer prepared in the present work on the dual curing of a cycloaliphatic epoxy resin. In that case, the polymer acted as a precursor of a multifunctional thermal crosslinker that was activated by UV light.[15] The presence of a phase separated morphology in that materials encouraged us to study the behavior of this HBP in other epoxy systems. We chose the well known anionic thermal DGEBA/1-methyl imidazole system because of the good results obtained in previous works[14,18] and the possibility to chemically incorporate the HBP to the epoxy network by the presence of OH groups in its structure. The mechanism, depicted in **Scheme 2**, is based in the nucleophilic attack of the tertiary amine to the oxirane ring and the proton exchange between the hydroxyl groups of the HBP and the alkoxide formed. Thus, the two types of alkoxides formed are able to attack the epoxide groups and initiate the homopolymerization process, leading to the chemical linkage of the HBP to the epoxy matrix.

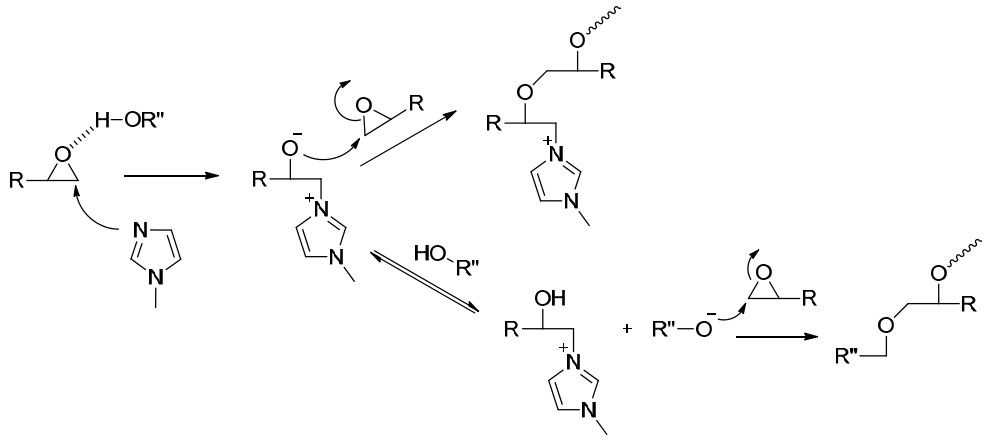

Scheme 2 Possible mechanisms of initiation of the anionic ring opening polymerization of epoxides in the presence of reactive hydroxyl groups.

Study of the curing process

Differential scanning calorimetry is a very useful technique for the evaluation of the curing kinetics. We cured samples containing from 0 to 15 phr of HBP in the calorimeter at 10 °C/min

and then we evaluated the enthalpy of the process. As one can see in **Table 1**, the enthalpy of the curing exotherm decreases on increasing the proportion of HBP modifier. However, if we look at the enthalpy per epoxy equivalent all the formulations present similar values, around 90 kJ/mol, indicating that the complete curing was achieved.[19]

Table 1 Calorimetric data obtained for all the studied formulations.

Content of HBP (phr)	Δh (J/g)	Δh [a] (kJ/ee)	Ea [b] (kJ/mol)	lnA [c] (s^{-1})	k [d] x 10^3 (s^{-1})	T_g [e] (ºC)	$T_{g,Fox}$ [f] (ºC)
0	503	92	56	13.67	28.05	167	167
5	468	90	61	15.27	37.78	151	149
10	445	90	62	15.84	44.14	133	133
15	412	89	64	16.42	45.61	126	120

a. Enthalpies per equivalent of epoxy group at 10 ºC/min.
b. Values of activation energy at 50 % of conversion, evaluated by the isoconversional non-isothermal procedure.
c. Pre-exponential factor for the n = 1.5; m = 0.5 kinetic model at a conversion of 50%.
d. Values of rate constant at 120 ºC using the Arrhenius equation at a conversion of 50%.
e. Glass transition temperature obtained by DSC, from a second scan after dynamic curing.
f. Glass transition temperature estimated by the Fox equation.

From the values of the curing exotherm we evaluated the conversion by means of eq(1). **Figure 1** shows the plot of conversion against temperature for all the studied formulations. It is clear that the curing goes faster on increasing the amount of HBP in the mixture, although proportions higher than 10 phr HBP do not further accelerate. This acceleration can be rationalized on the basis of the hydroxyl groups present in the HBP. It has been established that in the anionic ring opening polymerization of DGEBA initiated by tertiary amines, hydroxyl groups can coordinate via H-bonding to the epoxy groups, favoring the nucleophilic attack of the tertiary amine to the epoxide and thus accelerating the curing process.[20]

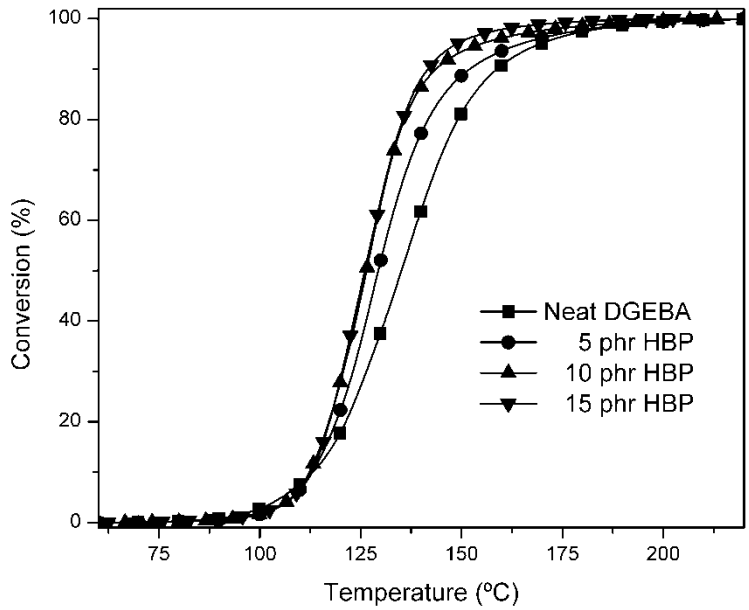

Figure 1 Plot of conversion against temperature for all the studied formulations obtained by DSC at 10 ºC/min.

Moreover, the exchange of protons depicted in **Scheme 2** should also influence the kinetics of the curing process. It is worth to note that the ratio of epoxy equivalent to 1-MI is the same for all the formulations. Therefore, the acceleration must be only attributed to the hydroxyl content. Although not so pronounced, acceleration was observed in a previous study based on DGEBA with hyperbranched polyester amines with hydroxyl groups as chain ends.[14] In the present study, the proportion of hydroxyl groups in the HBP structure is higher, which leads to a more significant effect.

On adding HBP to the formulation the viscosity is increased as we have evaluated by rheological measurements (see **Table 2**). Thus, in the sample with 15 phr of HBP the acceleration produced by the OH groups competes with the increase in viscosity of the formulation and no significant improvement on the curing rate in reference to the 10 phr HBP formulation can be appreciated

Table 2 Rheological and thermomechanical data of all the studied formulations.

Content of HBP (phr)	Gel time (min)	α_{gel} [a] (%)	$\|\eta\|$ [b] (Pa·s)	Gel content (%)	*Tan δ* (ºC)	*E'* [c] (MPa)
0	27.1	34	0.047	99	179	106
5	23.3	42	0.071	99	170	77
10	24.6	41	0.086	100	162	69
15	25.5	41	0.116	99	136	38

a. Conversion at the gelation determined by rheometry and DSC at 80 ºC.
b. Measured at the temperature of 100 ºC.
c. Measured at the maximum of *tan* δ + 50 ºC.

By performing the DSC experiments at different heating rates we were able to evaluate the activation energies of the studied systems. These activation energies (see **Table 1**) increase slightly on increasing the proportion of HBP, but all of them remain constant during all the process allowing us to consider the activation energy at α = 0.5 as the mean *Ea*. As the activation energy is not enough to describe the kinetics of a system we calculated the preexponential factor *(lnA)* and the kinetic constant *(k)* for all the formulations. We firstly adjusted our data to an n = 1.5; m = 0.5 model and with that we obtained the values shown in **Table 1** for α = 0.5 and a temperature of 120 ºC. It is evident how on increasing the percentage of HBP the pre-exponential factor and the kinetic constant increase, confirming the fact that the HBP accelerates the curing reaction.

We also evaluated the T_g*s* of the thermosets in a second dynamic scan at 20 ºC/min. The presence of the HBP leads to a decrease on this value, but in all cases the materials obtained presented T_g*s* above 100 ºC, which is an important factor in case of materials that can be used at high temperatures. As seen in **Table 1**, the values of T_g*s* obtained fit quite well with the ones predicted by the Fox equation. This is an indication that the HBP added is homogeneously incorporated into the network.

In order to go deeply on the curing kinetics we decided to cure all formulations in an ATR-FTIR with thermal control at different curing temperatures. We chose 100, 120 and 150 ºC as the curing temperatures and we monitored the disappearance of the epoxy band at 915 cm^{-1}. Using eq(3) we obtained the plots of conversion against time for all the studied formulations. **Figure 2** shows the conversion plots of the sample containing 10 phr of HBP at the selected temperatures. As predictable, the increase on the temperature allowed us to cure the samples quicker and we could also see that only by working at high temperatures the curing was

quantitative. We took profit of that information to establish the curing schedule of the thermosets whose characterization will be discussed in detail afterwards.

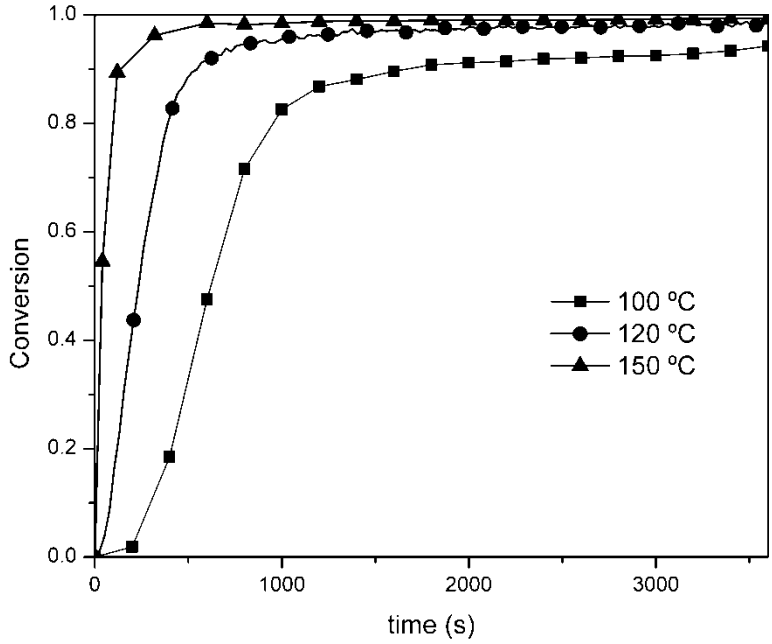

Figure 2 Conversion against time at different temperatures for the formulation containing 10 phr of HBP determined by FTIR-ATR.

Figure 3 shows the conversion plot at 120 ºC for all the studied formulations. The results obtained are in accordance to those previously observed by DSC working in dynamic conditions. This is, the HBP accelerates the curing reaction. By FTIR we could also prove that the conversion of epoxy groups achieved was higher in the presence of OH groups as we could observe in a previous study.[18] In this previous study, on increasing the proportion of OH groups the final conversion increased. In the figure we can see that the maximum of conversion is reached for the formulation with a 10% of HBP. This can be explained by the topological hindrances in the epoxy reaction by the high viscosity of the mixture and the reduced concentration of reactive groups, when the proportion of HBP is higher.

It should be noticed that only formulations containing 10 and 15 phr of HBP can reach the complete curing, since their $T_g s^{\infty}$ are lower and therefore vitrification is avoided.

By rheometric experiments we evaluated first of all the viscosity of the samples. As seen in **Table 2** the addition of the HBP, although not critically, increases the viscosity of the resulting mixture going from 0.047 for the neat sample to 0.116 Pa·s for the formulation with 15 phr of HBP.

When dealing with the curing of a thermoset a very important process to study is the gelation process. The gel point is defined as the point at which the first infinite network is formed ($\bar{M}_w \rightarrow \infty$) and after it the resin cannot be further processed. In rheology, the gel point can be determined as the moment where the value of $tan\ \delta$ is independent of the frequency.[2] However, for the sake of clarity we have represented δ instead, which is equivalent. **Figure 4** shows the determination of this gel point for the neat and 10 phr HBP formulations as an example.

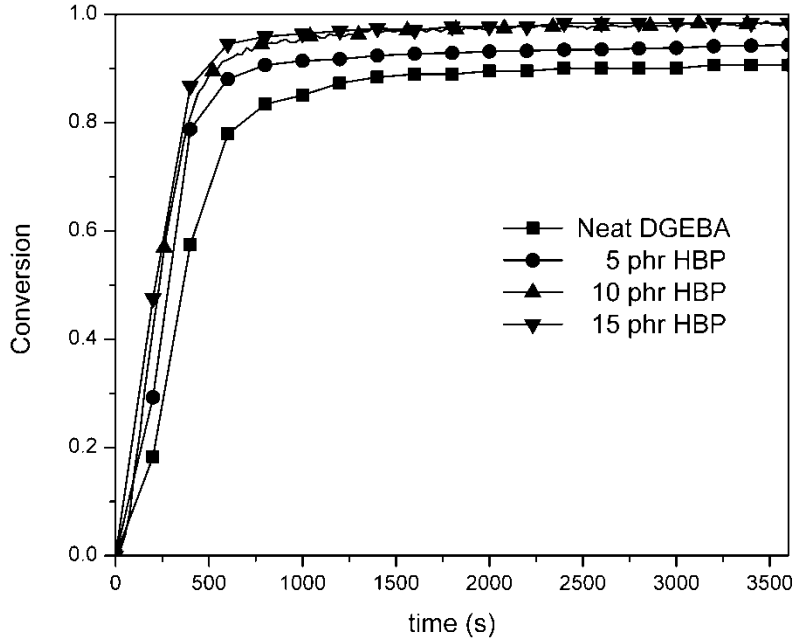

Figure 3 Conversion against time for all the studied formulations at 120 °C determined by FTIR-ATR.

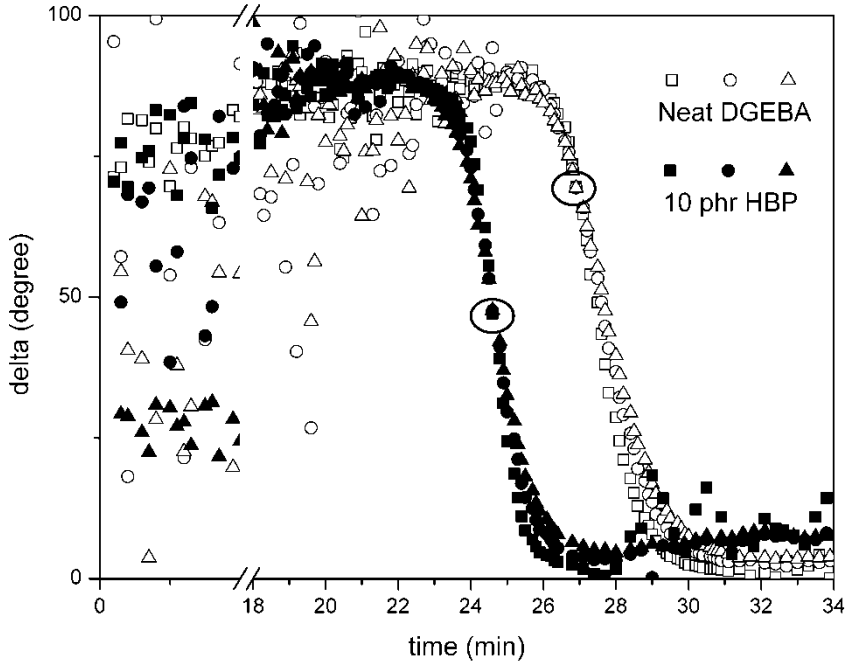

Figure 4 delta against time plots for the neat and 10 phr HBP formulations in a rheological experiment to determine gelation times.

Table 2 collects the values of gel time of all the formulations as well as the conversion at the gel point (α_{gel}) determined by taking a sample from the rheometer in the moment at which the gelation occurs, quenching it, performing a dynamic DSC scan at 10 °C/min and comparing the

enthalpy released with the global one. The α_{gel} is increased on adding HBP to the formulations, going from 0.34 for the neat sample to around 0.40 for all the others. This is an interesting result, because after gelation the material losses its mobility ant the stresses originated by the shrinkage inherent to the curing of epoxy cannot be dissipated. Therefore, on delaying the gelation to higher conversions fewer tensions within the matrix are generated. Those tensions are responsible for the generations of microcracks and microvoids that can appear in a coating, ruining it.

Also the gel time is influenced by the presence of HBP. As we have mentioned before the HBP can accelerate the curing process, resulting in a decrease on the gel time. However this decrease is more pronounced for the sample with 5 phr of HBP (23.3 min). This is a confirmation that the increase on the viscosity of the formulations competes with the accelerative effect of the hydroxyl groups in those systems.

A way to ensure the chemical incorporation of the HBP is the measurement of the gel content of the samples. In all cases it was quantitative (see **Table 2**), indicating that the HBP is chemically linked to the matrix. The mechanism through which it becomes incorporated is depicted in **Scheme 2**. The hydroxyl groups of the HBP can not only interact via hydrogen bonding with epoxides and favoring its ring opening but also undergo an intermolecular acid/base equilibrium that leads to the formation of an alkoxylate end group that can attack the epoxy ring opening it, and therefore a chemical bonding is formed between the HBP and the epoxy network.

Characterization of the thermosets

The dynamic mechanical properties of the thermosets were investigated. **Figure 5** shows the tan δ plot from -90 to 220 ºC for all the prepared materials. Two relative maxima can be appreciated. The maximum at higher temperature can be related to the T_g of the material. As one can see (see also **Table 2**) on increasing the amount of HBP in the thermoset a decrease on the T_g value is appreciated. The variation in the T_g indicates that, as seen for the T_g*s* obtained by DSC, there is a compatibility of the HBP in the epoxy matrix. From the area of this peak we can also anticipate an increase in the damping properties of the material, on increasing the amount of HBP. The peak at lower temperatures can be attributed to a β transition due to the aromatic rings in the epoxy resin structure.[2]

The loss modulus of the thermosets in the rubbery state was also evaluated and as we can see in **Table 2**, there is a decrease in this value on increasing the amount of HBP. This is an indication of the flexibilization effect induced by the presence of the more flexible structure of the HBP, which is incorporated to the epoxy matrix.

To observe the morphology of the materials we performed scanning electron microscopy (SEM) of the cryofractured samples containing HBP. As one can see in **Figure 6a**, the fracture pattern of the sample is plastic with filaments, some of them completely separated from the main fracture surface. This can derivate in an increase in the fracture toughness. **Figure 6b** shows the pure morphology of the sample at high magnifications in a zone where no fracture lines appear. It is quite evident that the material is homogeneous confirming the miscibility of the HBP within the epoxy matrix. **Figure 6c** shows the morphology of the neat material which presents a non homogeneous surface (even at lower magnification than the previous micrograph, **6b**) with abundant globular micelles. These micelles can arise from crosslinking reactions that proceed most rapidly at specific points in the resin. This structural inhomogeneity is characterized by regions of higher and lower crosslinking density.[21] It should be taken into account that chainwise

polymerizations are intrinsically inhomogeneous, since the increase of molecular weight of the polymer chains is not as regular as in polycondensations. In thermosets, the inhomogeneities become fixed by the crosslinks. In our case, the addition of the HBP increments the homogeneity of the material possibly due to the reaction transfer processes that leads to more homogeneous crosslinking process.

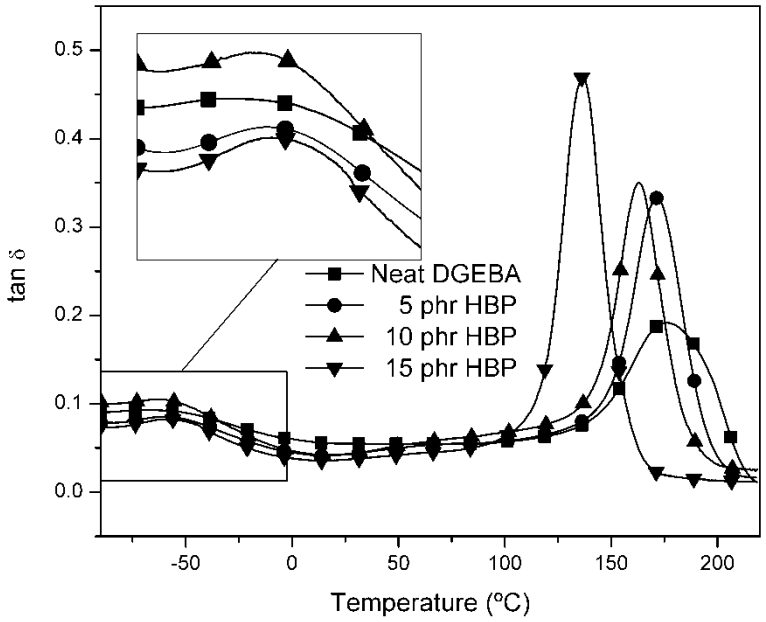

Figure 5 Plots of *tan δ* against temperature for all the studied formulations determined by DMTA.

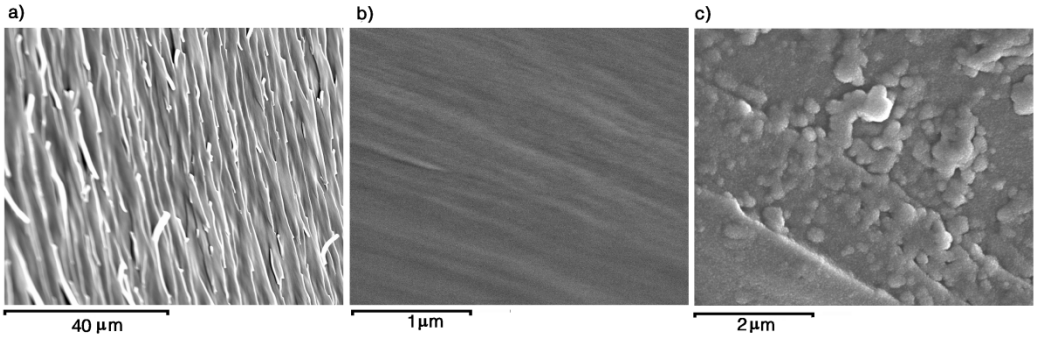

Figure 6 SEM pictures of the cryofractured material containing 10 phr of HBP at 1,400 magnifications (a) and at 40,000 magnifications (b) and the neat material at 20,000 magnifications (c).

The use of anionic initiators in the curing of epoxy resins usually leads to materials with high thermal stability.[22] By TGA we evaluated this characteristic and the data obtained are collected in **Table 3**. On adding HBP the thermal stability is slightly reduced (around 20 ºC in the $T_{10\%}$ and T_{max} for the case with a higher proportion of additive) despite of the presence of ester groups that usually reduces this parameter up to a higher degree. The presence of the HBP in the thermoset also influences the percentage of char yield reducing it, because of its aliphatic structure.

A very important characteristic to determine in thermosetting materials to be used as coatings is the shrinkage on curing. It is established that the shrinkage produced during the curing of a resin comes from the fact that the molecules in the initial mixture go from a Van der Waals distance to a covalent bonding distance after reaction.[23]

Table 3 Thermal data, densities and shrinkage of all the studied thermosets.

Content of HBP (phr)	$T_{10\%}$ [a] (ºC)	T_{max} (ºC)	Char Yield [b] (%)	ρ_{mon} (g/cm³)	ρ_{polym} (g/cm³)	Shrinkage [c] (%)
0	408	433	10.4	1.157	1.177	1.7
5	400	427	10.2	1.157	1.173	1.4
10	397	418	9.8	1.156	1.170	1.2
15	391	412	9.6	1.156	1.168	1.0

a. Temperature of loss of a 10% of mass in a TGA analysis at 10 ºC/min under N_2.
b. Measured at 800 ºC.
c. Measured as $[(\rho_{polym} - \rho_{mon})./\rho_{polym}] \times 100$

Among many strategies proposed for overcoming this drawback, the addition of HBP as chemical modifiers of epoxy resins has turn out to be one of the most successful.[13] From the data collected in **Table 3**, it is evident that the addition of the studied HBP can reduce the global shrinkage of the resin. Although the shrinkage in curing by ring-opening homopolymerization is quite low even in the neat material the addition of HBP reduces it. A possible explanation to this is the reduction of the internal interactions in the HBP by reaction of OH groups with the DGEBA that leads to expansion. In addition, a lower number of covalent bonds are formed during the curing process when a prepolymer HBP is added to the formulation.

Mechanical Properties

One of the objectives of introducing an HBP with such a flexible structure as an additive in an epoxy system is toughness improvement. There are many publications which show how on adding HBPs to epoxy formulations, whether there is phase separation or not, an improvement in fracture toughness is observed.[24,25]

To evaluate the toughness of the samples we performed impact strength tests. We impacted samples with a pendulum and recorded the energy lost in the impact. As we can see in the data collected in **Table 4**, adding up to 15 phr of HBP leads to an increase of 113 % in respect to the neat formulation. In previous studies we observed that toughness reached a maximum value in formulations with a 5-10% of HBP and then dropped down.[26] In contrast, the thermosets here discussed show a regular increase up to 15 phr. From the point of view of toughness higher proportions of HBP could be advisable but they can be detrimental for the T_g or modulus characteristics. So, it is quite evident that the flexible structure of HBP chemically incorporated to the rigid epoxy matrix promotes the dissipation of the energy of an impact and hinders the propagation of the cracks generated, resulting in tougher materials.

Table 4 Mechanical properties for all the studied thermosets.

Content of HBP (phr)	Impact Strength (kJ/m²)	HKN (kg/mm²)
0	1.5 ± 0.4	15.6 ± 0.5
5	2.4 ± 0.2	13.3 ± 0.4
10	2.8 ± 0.5	14.2 ± 0.6
15	3.2 ± 0.5	13.5 ± 0.5

The microhardness of the materials was investigated by means of microindentation. The values obtained, shown in **Table 4**, indicate that the hardness of the system is only slightly affected by the addition of the HBP. This is a very interesting result since we were able to improve toughness of the resulting thermosets without compromising other important mechanical properties such as hardness, a milestone in coating applications.

CONCLUSIONS

A series of new epoxy thermosets with different proportions of a hyperbranched polyester obtained via click thiol-ene chemistry as modifier were obtained by using 1-methylimidazole as anionic initiator.

The hydroxyl end groups of the HBP accelerated the curing reaction as demonstrated by DSC and FTIR experiments. However, on increasing the amount of HBP this accelerative effect competes with the increase in viscosity of the samples. The addition of HBP influences the gelation process, reducing the gelation time and increasing the conversion at the gelation. The chemical incorporation of the HBP was demonstrated by measuring the gel content, which was quantitative in all cases.

The addition of the HBP produces a flexibilization effect, slightly reducing the value of the glass transition temperature and improving the damping properties. By means of SEM we observed that the modified materials were more homogeneous than the neat one.

The shrinkage produced during the curing process was reduced with the increased proportion of the HBP, which in addition to the higher conversion at the gelation achieved can reduce the apparition of internal stresses on curing.

The toughness of the materials was improved using the HBP as demonstrated by impact tests, without compromising other mechanical properties such as microhardness.

ACKNOWLEDGEMENTS

Authors would like to thank MICINN (Ministerio de Ciencia e Innovación) and FEDER (Fondo Europeo de Desarrollo Regional) (MAT2008-06284-C03-01 and MAT2008-06284- C03-02) and the Generalitat de Catalunya (2009-SGR-1512) for their financial help. D.F. acknowledges the grant FPU-2008 from the Spanish Government.

REFERENCES

1. J-P. Pascault, R. J. J. Williams. *Epoxy Polymers*. Wiley-VCH, Weinheim, **2010**.
2. J-P. Pascault, H. Sauterau, J. Verdu, R. J. J. Williams. *Thermosetting Polymers*. Marcel Dekker, New York, **2002**.
3. R. D. Brooker, A. J. Kinloch, A. C. Taylor. *J. Adhesion* **2010,** *86,* 726.
4. B. Voit, A. Lederer. *Chem. Rev.* **2009,** *109,* 5924.
5. C. Li, M. G. Finn. *J. Polym. Sci. Part A: Polym. Chem.* **2006,** *44,* 5513.
6. F. Morgenroth, M. Müllen. *Tetrahedron* **1997,** *53,* 15349.
7. K. L. Killops, L. M. Campos, C. J. Hawker. *J. Am. Chem. Soc.* **2008,** *130,* 5062.
8. D. Konkolewicz, D. A. Gray-Weale, S. Perrier. *J. Am. Chem. Soc.* **2009,** *131,* 18075.
9. L. Boogh, B. Pettersson. J. A. E. Månson. *Polymer* **1999,** *40,* 2249.
10. J. Zhang, Q. Guo, B. Fox. *J. Polym. Sci. Part B: Polym. Phys.* **2010,** *48,* 417.
11. D. Foix, M. Erber, B. Voit, A. Lederer, X. Ramis, A. Mantecón, A. Serra. *Polym. Degrad. Stab.* **2010,** *95,* 445.
12. M. Sangermano, A. Priola, G. Malucelli, R. Bongiovanni, A. Quaglia, B. Voit, A. Ziemer. *Macromol. Mater. Eng.* **2004,** *289,* 442.

13. X. Fernández-Francos, J. M. Salla, A. Cadenato, J. M. Morancho, A. Serra, A. Mantecón, X. Ramis. *J. Appl. Polym. Sci.* **2009,** *111,* 2822.
14. M. Morell, X. Fernández-Francos, X. Ramis, A. Serra. *Macromol. Chem. Phys.* **2010,** *211,* 1879.
15. D. Foix, X. Ramis, A. Serra, M. Sangermano. *Polymer* **2011,** *52,* 3269.
16. A. W. Coats, J. P. Redfern. *Nature* **1964,** *201,* 68.
17. X. Ramis, J. M. Salla, A. Cadenato, J. M. Morancho. *J. Therm. Anal. Cal.* **2003,** *72,* 707.
18. X. Fernández-Francos, W. D. Cook, A. Serra, X. Ramis, G. G. Liang, J. M. Salla. *Polymer* **2010,** *51,* 26.
19. J. Brandrup, E. H. Immergut, E. A. Grulke. *Polymer Handbook*, 4th ed. Wiley-Interscience, New York, **1999**.
20. B. A. Rozenberg. *Adv. Polym. Sci.* **1986,** *75,* 113.
21. C. A. May. *Epoxy Resins. Chemistry and Technology*, 2nd edition. Marcel Dekker, New York, **1988**.
22. M. Arasa, X. Ramis, J. M. Salla, A. Mantecón, A. Serra. *Polymer* **2009,** *50,* 2228.
23. R. K. Sadhir, M. R. Luck. *Expanding monomers. Synthesis, characterization and applications.* CRC Press, Boca Raton, **1992**.
24. M. Sangermano, G. Malucelli, R. Bongiovanni, A. Priola, A. Harden. *Polym. Int.* **2005,** *54,* 917.
25. J. P. Yang, Z. K. Chen, G. Yang, S. Y. Fu, L. Ye. *Polymer* **2008,** *48,* 3168.
26. M. Morell, M. Erber, X. Ramis, F. Ferrando, B. Voit, A. Serra. *Eur. Polym. J.* **2010,** *46,* 1498.

Chapter 7

Conclusions

As demonstrated during this thesis, hyperbranched polymers are extremely versatile modifiers to tune the properties of epoxy resin based thermosets. The most remarkable conclusions that can be inferred from this thesis are listed below:

- The addition of Boltorn H30 hyperbranched polyester to DGEBA/tetrahydrophtalic anhydride formulations leads to a slight increase in toughness, which is enhanced by the addition of a small proportion of sepiolite, without reducing the T_g of the materials. Regarding the thermal stability, while sepiolite have barely no effect on it the addition of Boltorn H30 can slightly reduce it, allowing obtaining reworkable thermosets when added in a 10% in weight or more.
- In the curing of DGEBA initiated by ytterbium triflate with end-capped Boltorn H30, the characteristics of the terminal groups of the HBP play an important role. Whereas the addition of unmodified or silylated Boltorn H30 yields homogeneous materials, the addition of benzoylated Boltorn H30 leads to phase separated morphologies, which can be explained by the Π-Π stacking of the benzoyl rings.
- The curing kinetics of DGEBA with Boltorn H30 type HBPs is controlled by the amount of remaining OH groups and the viscosity of the curing formulation. Whereas the former accelerates the curing the latter has the opposite effect.

- The addition of an aliphatic-aromatic hyperbranched polyester to DGEBA/lanthanide triflate formulations improves the chemical reworkability without compromising thermal stability and T_g.
- The increase in the degree of branching of the aliphatic-aromatic hyperbranched polyester used as reactive modifier of DGEBA/ytterbium triflate formulations reduces the viscosity of the mixture, increases the curing rate due to the enhancement of the AM propagation mechanism and reduces the shrinkage during curing.
- Amphiphilic dendritic polymers with multi-arm star and linear-hyperbranched topologies combining poly(ethylene glycol) and aromatic-aliphatic hyperbranched polyester moieties have been successfully synthesized.
- The morphology of the thermosets obtained by using the multi-arm star amphiphilic topology is strongly affected by the curing system chosen. While 1-methylimidazole thermal initiated curing yield thermosets with heterogeneous crosslinking density, cationic initiated systems produce phase separated morphologies. In the case of UV cationic curing phase separation occurs up to a higher extent than in thermal initiated conditions, but the phase separated morphology is better defined in the latter.
- The linear-hyperbranched morphology of the modifier leads to phase separated morphologies in cationic photocuring with size between 50 and 100 nm, whereas the size in cationic thermal curing was around 500 nm, due to increase in solubility promoted by the temperature.
- By thiol-ene coupling reaction and following an iterative synthetic procedure, a thioether-HBP with hydroxyl terminal groups has been obtained. The presence of sulfur in the structure allows generating a latent multifunctional thermal crosslinker by UV irradiation. The thermosets obtained by this methodology present higher T_g*s* than the conventional UV cured cycloaliphatic epoxy resins.
- The thioether HBP has also been used as modifier of anionically initiated systems. This additive allows reducing the shrinkage during curing and increasing the conversion at the gelation, which leads to a potential reduction of the internal stresses in the final thermosets. Moreover, due to the flexibility introduced by the HBP structure, the toughness of the resulting thermosets increases.

APPENDIXES

APPENDIX A List of Abbreviations

α_{gel}	Conversion at gelation
A	Pre-exponential factor
BDMA	N, N, N-benzyldimethylamine
CE	3,4-epoxycyclohexylmethyl-3',4'-epoxycyclohexyl carboxylate
Δh_t	Heat released
DB	Degree of branching
DCC	N,N'-Dicyclohexylcarbodiimide
DGEBA	Diglycidyl ether of bisphenol A
$Đ_M$	Molecular weight dispersity
DMF	N, N-dimethylformamide
DMTA	Dynamic mechanical thermal analysis
$\overline{DP}$	Degree of polymerization
DPTS	4-(N,N-dimethylamino)pyridinium p-toluene sulfonate
E'	Storage modulus
E''	Loss modulus
E_a	Apparent activation energy
ee	Epoxy equivalent
FTIR	Fourier-transformed infrared spectroscopy
GBPE	Gradually branched poly(ester)
HBP	Hyperbranched polymer
HBPE	Hyperbranched poly(ester)
HKN	Hardness Knoop Number
k	Rate constant
MI	1-methyl imidazole

$\bar{M}_n$	Number average molecular weight
$\bar{M}_w$	Weight average molecular weight
$\|\eta^*\|$	Complex viscosity
NMR	Nuclear magnetic resonance spectroscopy
phr	Parts per hundred of resin
PI	Photo-initiator
PEG	Poly(ethylene glycol)
SEC	Size exclusion chromatography
SEM	Scanning electron microscopy
SP	Star polymer
$tan\ \delta$	Loss factor
TEC	Thermal expansion coefficient
TEM	Transmission electron microscopy
T_g	Glass transition temperature
TGA	Thermogravimetric analysis
THF	Tetrahydrofurane
THPA	1,2,3,6-Tetrahydrophthalic anhydride
TMA	Thermal mechanical analysis
T_{max}	Temperature of the maximum degradation rate
TMS	Tetramethyl silane
T_p	Temperature of the peak of the curing exotherm
Triflate	Trifluoromethanesulfonate
$T_{x\%}$	Temperature of the lost of x% of weight
UV	Ultra violet

APPENDIX B List of Publications

PUBLICATIONS FROM THE THESIS

D. Foix, Y. Yu, A. Serra, X. Ramis, J. M. Salla. Study on the chemical modification of epoxy/anhydride thermosets using a hydroxyl terminated hyperbranched polymer. *European Polymer Journal,* **2009,** *45,* 1454.

D. Foix, M. Erber, B. Voit, A. Lederer, X. Ramis, A. Mantecón, A. Serra. New hyperbranched polyester modified DGEBA thermosets with improved chemical reworkability. *Polymer Degradation and Stability,* **2009,** *95,* 445.

D. Foix, X. Fernández-Francos, J. M. Salla, A. Serra, J. M. Morancho, X. Ramis. New thermosets obtained from DGEBA and hydroxyl ended hyperbranched polymers partially blocked with benzoyl and trimethyl silyl groups. *Polymer International,* **2010,** *60,* 389.

D. Foix, X. Fernández-Francos, X. Ramis, A. Serra, M. Sangermano. New pegylated hyperbranched polyester as chemical modifier of epoxy resins in UV cationic photocuring. *Reactive and Functional Polymers,* **2011,** *71,* 417.

D. Foix, X. Ramis, A. Serra, M. Sangermano. UV generation of a multifunctional hyperbranched thermal crosslinker to cure epoxy resins. *Polymer,* **2011,** *52,* 3269.

D. Foix, A. Khalyavina, M. Morell, B. Voit, A. Lederer, X. Ramis, A. Serra. The Effect of the Degree of Branching in Hyperbranched Polyesters Used as Reactive Modifiers in Epoxy Thermosets. *Macromolecular Materials and Engineering,* **2011,** *In press*. DOI: 10.1002/mame.201100078

D. Foix, E. Jiménez-Piqué, X. Ramis, A. Serra. DGEBA Thermosets Modified with an Amphiphilic Star Polymer. Study on the Effect of the Initiator on the Curing Process and Morphology. *Polymer,* **2011,** *52,* 5009.

D. Foix, X. Ramis, F. Ferrando, A. Serra. Improvement of epoxy thermosets using a thiol-ene based polyester hyperbranched polymer as modifier. *Polymer International*, **2011.** *In press*

D. Foix, M. T. Rodríguez-Blasco, X. Ramis, F. Ferrando, A. Serra. Combined use of sepiolite and a hyperbranched polyester in the modification of epoxy/anhydride thermosets. A study of the curing process and the final properties. *Polymer Testing.* Submitted

D. Foix, X. Ramis, M. Sangermano, A. Serra. Synthesis of a new hyperbranched-linear-hyperbranched triblock copolymer and its use as a chemical modifier for the cationic photo and thermal curing of epoxy resins. *Journal of Polymer Science Part A: Polymer Chemistry.* Submitted

COLLABORATIONS IN OTHER PUBLICATIONS

X. Fernández-Francos, D. Foix, A. Serra, J. M. Salla, X. Ramis. Novel thermosets based on DGEBA and hyperbranched polymers modified with vinyl and epoxy end groups. *Reactive and Functional Polymers,* **2010,** *70,* 798.

M. Morell, D. Foix, A. Lederer, X. Ramis, B. Voit, A. Serra. Synthesis of a New Multiarm Star Polymer based on Hyperbranched Poly(styrene) Core and Poly(ε-caprolactone) Arms and Its Use as Reactive Modifier of Epoxy Thermosets. *Journal of Polymer Science Part A: Polymer Chemistry,* **2011,** *49,* 4639.

M. Flores, X. Fernández-Francos, E. Jiménez-Piqué, D. Foix, A. Serra, X. Ramis. New epoxy thermosets obtained from DGEBA and modified hyperbranched polyesters with long aliphatic chains cured by diisocyanates. *Polymer Engineering and Science*. Submitted

APPENDIX C Stages and Meeting Contributions

D. Foix, A. Mantecón, A. Serra.
"Modificación y Caracterización Estructural de Polímeros Hiperramificados Hidroxilados con Cadenas Lineales Insaturadas"
X Meeting of the Specialized Group of Polymers (GEP). Sevilla, September 2007. Poster Presentation.

D. Foix, X. Ramis, A. Serra.
"Polímers Hiperramificats Derivats de Fonts Renovables com a Agents Modificants de Reïnes Epoxi"
Workshop of Sustainable Chemistry (URV). Tarragona, May 2009. Poster Presentation.

D. Foix, A. Mantecón, X. Ramis, A. Serra.
"Nuevos Copolímeros Amfifílicos Hiperramificado-Lineal-Hiperramificado como Modificantes Reactivos de Resinas Epoxi"
XI Meeting of the Specialized Group of Polymers (GEP), Valladolid, September 2009. Poster Presentation.

X. Ramis, D. Serrano, X. Fernández-Francos, J. M. Morancho, A. Cadenato, J. M. Salla, D. Foix, A. Serra.
"Nuevos Termoestables con Propiedades Mejoradas a Base de Resinas Epoxi y Polímeros Hiperramificados con Grupos Terminales Hidroxilo, Benzoilo o Trimetilsililo"
XI Meeting of the Specialized Group of Polymers (GEP), Valladolid, September 2009. Poster Presentation.

X. Fernández-Francos, X. Ramis, A. Arauz, J.M. Morancho, A. Cadenato, J.M. Salla, D. Foix, A. Serra.
"Nuevos Termoestables con Propiedades Mejoradas a Base de Resinas Epoxi y Polímeros Hiperramificados con Grupos Vinilo y Epoxi"
XI Meeting of the Specialized Group of Polymers (GEP), Valladolid, September 2009. Poster Presentation.

D. Foix, M. Erber, B. Voit, X. Ramis, Y. Yu, A. Mantecón, A. Serra.
"New Hyperbranched Polyester Modified DGEBA Thermosets with Improved Chemical Reworkability"
8th International Conference on Advanced Polymers via Macromolecular Engineering (APME), Dresden, October 2009. Poster Presentation.

D. Foix, A. Khalyavina, M. Morell, B. Voit, A. Lederer, X. Ramis, A. Serra.
"New Chemically Reworkable Epoxy Thermosets by Modification of DGEBA with Hyperbranched Polyesters. Study on the Influence of the Degree of Branching"
Macro 2010, 43rd IUPAC World Polymer Congress. Glasgow, July 2010. Poster Presentation.

D. Foix, X. Ramis, A. Serra, M. Sangermano.
"New Pegylated Hyperbranched Polyesters as Modifiers for the UV Cationic Photocuring of Cycloaliphatic Epoxy Resins"
Baltic Polymer Symposium. Palanga, September 2010. Poster Presentation.

D. Foix, X. Ramis, A. Serra, M. Sangermano.
"New Thio-Click Hyperbranched Polymers as Macroinititators for the Dual Curing of Cycloaliphatic Epoxy Resins"
European Polymer Congress (EPF). Granada, June 2011. Poster Presentation.

A. Serra, M. Morell, D. Foix, A. Lederer, X. Ramis, B. Voit.
"Synthesis of a New Multiarm Star Polymer based on Hyperbranched Poly(styrene) Core and Poly(ε-caprolactone) Arms and its Use as Reactive Modifier of Epoxy Thermosets"
9th International Conference on Advanced Polymers via Macromolecular Engineering (APME), Cappadocia, September 2011. Poster Presentation.

Stays Abroad

Organization: Leibniz-Insitute für Polymerforschung
Department: Institute of Macromolecular Chemistry (Prof. Voit)
City: Dresden **Country:** Germany
Length: 1 month **Year:** 2008

Organization: Politecnico di Torino
Department: Dept. of Material Science and Chemical Engineering (Dr. Sangermano)
City: Turin **Country:** Italy
Length: 4 months **Year:** 2010